The thesis of Committee for Erdi AYDIN

Certifies that this is the approved version of the following thesis:

Numerical Simulation and History Matching of Steam-Foam Process to Enhance Heavy Oil Recovery

Approved by

Committee:

Kamy Sepehrnoori, Supervisor

Hamid Reza Lashgari

.

Numerical Simulation and History Matching of Steam-Foam Process to Enhance Heavy Oil Recovery

by

Erdi AYDIN

Thesis

Presented to the Faculty of the Graduate School of

The University of Texas at Austin

in Partial Fulfillment

of the Requirements

for the Degree of

Master of Science in Engineering

The University of Texas at Austin

May 2018

Dedication

To
My parents

for their unconditional support

Acknowledgements

I would like to thank my advisor Kamy Sepehrnoori for his guidance and for the practical research question addressed in the thesis. He has been a great support throughout my time in The University of Texas at Austin. I would also like to thank faculty members at The University of Texas at Austin who have facilitated my learning in reservoir and petroleum engineering. In particular, I would like to thank the professors who have taught me during my time here: Dr. Paul Bommer, Dr. Eric DeRouffignac, Dr. Kishore Mohanty, and Dr. Hugh C. Daigle. I would also like to thank Dr. Hamid Reza Lashgari at The University of Texas at Austin for giving me such a solid foundation in engineering and lending an aptitude for constant learning that I will cherish my entire life. Last but not least, I would like to thank my parents for their unconditional love and for being patient with me.

I would like to acknowledge the staff of the Petroleum and Geosystems Engineering Department at The University of Texas at Austin: Frankie Hart, John Cassibry, Mary Pettengill, Glen Baum, and Gary Miscoe for their technical and administrative support. Finally, I would like to extend my appreciation to all of my close friends for their love, support, understanding, and encouragement.

Abstract

Numerical Simulation and History Matching of Steam-Foam Process to Enhance Heavy Oil Recovery

Erdi AYDIN, MSE

The University of Texas at Austin, 2018

Supervisor: Kamy SEPEHRNOORI

Thermal enhanced oil recovery techniques have been considered as the best approach to produce heavy oil; however, hybrid methods, which are combinations of different oil recovery methods, reveal more promise in enhancing oil production from heavy and viscose reservoirs. In this research, we investigate improving recovery from heavy oil reservoirs, considering steam foam method to control the mobility of steam and oil in such reservoirs, and delivering proper amount of heat to reservoir in order to reduce oil viscosity.

In this thesis, a compositional K-value based reservoir simulator, CMG-STARS, was used to build simulation models for all case studies. Steam table is used to calculate the phase change during steam injection and to capture latent heat effect on energy balance and mass balance equations. CMG-STARS empirical foam model is used to

capture mobility of steam in the presence of surfactant. Simulation models are tuned with experimental core data and field history data.

Simulation results illustrated that a considerable increase in oil recovery is obtained when steam foam is used. It is also observed that foam parameters, which was used in modeling, affects oil recovery, reservoir average temperature, average pressure and gas saturation. Optimized foam parameters were determined considering oil recovery, average reservoir temperature, and average reservoir pressure. Finally, simulations revealed that field and simulation results were in good agreement with field data, and that steam foam oil recovery method has the potential to become a promising oil recovery method for heavy oil reservoirs.

Table of Contents

List of Tables

List of Figures

Chapter 1: Introduction

This chapter briefly describes heavy oil reserves and exhibits proven heavy oil resources all over the world, technology challenges, and relevant problems in heavy oil production. Moreover, here we explain the purpose of the thesis; an overview of the chapters has been presented.

1.1 BACKGROUND

Heavy oil is defined as oil which has API (American Petroleum Institute) gravity less than 20° API (Briggs et al., 1998). Farouq Ali (1976) states that heavy oil deposits are important resources in the world, which is around several trillion barrels. However, since mobility ratio of the water phase to oil phase is not favorable, water flood and primary production can only produce 5 to 10 percent of original oil in place (Liu et al., 2006). According to Das (1988), in heavy oil reservoirs mostly thermal recovery methods are used to reduce viscosity by heating the reservoir, since high viscosity decreases primary production. Steam injection, such as steam flooding, cyclic steam stimulation, steam assisted gravity drainage (SAGD), is included in thermal methods, and some hybrid methods in which thermal methods used together with other methods are often used for heavy oil recovery.

Table 1-1 Classifications of Heavy oil based on API (Farouq Ali, 1976)

Classification	API
Light	>31.1
Medium	22.3 - 31.1
Heavy	10 - 22.3
Extra Heavy	<10
Bitumen	<10

According to Farouq Ali (1976), the non-thermal methods that are other ways to produce oil from heavy oil reservoirs are water flooding, prior gas injection, polymer flooding, surfactant and wettability alteration flooding, carbon dioxide (CO2) and carbonated water flooding, inert gas injection and cyclic well stimulation, caustic and emulsion flooding, and solvent stimulation.

This thesis proposes modeling and simulation of a hybrid method by combining cyclic steam injection (continuous steam injection) in the presence of surfactant, changing interfacial tension (IFT) between oil and water, to maximize oil production. Surfactant flood is considered to generate foam for the steam mobility control as well as to reduce slightly IFT between viscous oil and water phases.

1.2 PROBLEM DESCRIPTION

The main problem in steam injection is the unfavorable mobility which leads to a poor control of steam in reservoir. Adding surfactants to control the steam mobility and can also potentially stabilize the emulsion viscosity. Aforementioned issues might be potentially resolved adding high temperature stable surfactants or even alkaline. In the literature, there is no sophisticated and general numerical model exhibited for this type of

process which can accurately capture underlying mechanisms. Heavy oil industry, working on several technologies to enhance heavy oil and bitumen recovery intensively, needs such models to understand how and what operations involve during steam foam injection. Parameter optimization, economic analysis, reservoir behavior and characterization, process efficiency are all required for such a simulation model to well understand before starting to launch a EOR project for heavy oil reservoirs. Having said that, industry expertise can investigate different steam foam aspects. Steam foam is a promising EOR technology based on pilot testing in Southern Californian heavy oil fields according to Patzek and Koinis (1990).

1.3 RESEARCH OBJECTIVE

The main focus of this thesis is to investigate how to improve oil recovery from heavy oil reservoirs using steam foam method to control the mobility of steam in such reservoirs and deliver heat to reservoir properly to reduce oil viscosity.

1.4 REVIEW OF CHAPTERS

This thesis describes the application of coupled thermal chemical models with emphasis on physical mechanisms and optimizing parameters using history match with core and field data from literature.

Chapter 2 is a summary of literature review on the work done on heavy oil reservoirs. It elaborates the most popular stimulation techniques used for enhancing oil recovery. Since steam foam injection process is a major topic of interest in the thesis, it details the working of the process. It clearly discusses the physics of cold production, water flooding, solvent injection, thermal methods and hybrid methods.

Chapter 3 presents the two main models in foam modeling area which are population balance and implicit texture models along with their mathematical model expressions. UT model, CMG Stars model and Vassenden-Holt model are briefly illustrated in the section of implicit texture models. Then, in population balance models section, Kovscek et al. (basis of population balance model) that were modified by Chen et al. in 2010, Kam et al. (2007) model and Kam model (2008) are briefly discussed.

Chapter 4 describes a history matching study on CMG-STARS for alkaline steam foam experiment conducted by H. C. Lau (2012). The experiment was conducted on a core and we tried to model the same experiment using CMG-STARS and we compare results. Steam foam effect on cumulative oil recovery was attempted to be observed in simulation program. Additionally, since relative permeability tables were not given in the paper, using Brooks - Corey model we tried to history match in order to obtain proper relative permeability tables for this simulation study.

Chapter 5 introduces a parameter optimization study by changing foam parameters for a reservoir. Based on CMG-STARS foam model, some parameters were changed, and oil recovery, reservoir pressure, reservoir temperature, and average gas saturation were observed carefully for each case. Results analyzed and interpreted for each case, and subsequently influence of foam model on reservoir response was detected. Optimized foam parameters obtained in this chapter were used for the next steam foam simulation case.

In Chapter 6, production history data are matched for Mecca Lease, which is located in Kern River in Southern California by using similar reservoir geology given in

Patzek and Koinis' work demonstrated in 1989 to construct the numerical simulation model in order to evaluate steam foam process efficiency. Given geological properties from the reference paper were used to capture all model parameters. Same rock and reservoir properties including the same volume of the field were applied to build the reservoir model through CMG-STARS. Also, oil recovery for each step was matched with minor differences. In this work steam-foam parameters obtained in chapter 5 were used accordingly.

Chapter 7 presents a summary and conclusions of this research based on the simulation case studies and provides recommendations for future studies.

Chapter 2: Background and Literature Review

In this chapter, we concisely present the overview and summary of recovery methods used for heavy oil reservoirs. These methods include cold production, water flooding, thermal flooding, and chemical flooding. Screening criteria for each method will also be discussed.

2.1 LITERATURE REVIEW

Heavy oil, bitumen deposits, and extra heavy oil reservoirs are mostly shallow reservoirs. After they had formed in deep formations as conventional oil, they migrated through surface region, where they degraded by bacteria and weathering, by leaving the lightest hydrocarbons behind. Heavy oil, bitumen deposits, and extra heavy oil comprise low hydrogen content, while showing high sulfur, heavy metal, and carbon content (Clark, Graves, Lopez-de-Cardenas, Gurfinkel, & Peats, 2007). During heavy oil recovery, to choose and optimize the method, fluid characterization was made based on mobility and mobility deviation of oil under different extraction conditions (Memon et al., 2010).

2.2 COLD PRODUCTION

Cold production is a method which is used to increase primary production from heavy oil reservoirs. Sand is produced with heavy oil in cold production and this process increases oil production rate through boosted permeability wormholes. This process seems to the most important thing on formation and flow of foamy oil through wormholes. This increases the accessibility of reservoirs. Figure 2.1 demonstrates a schematic of cold heavy oil production with sand.

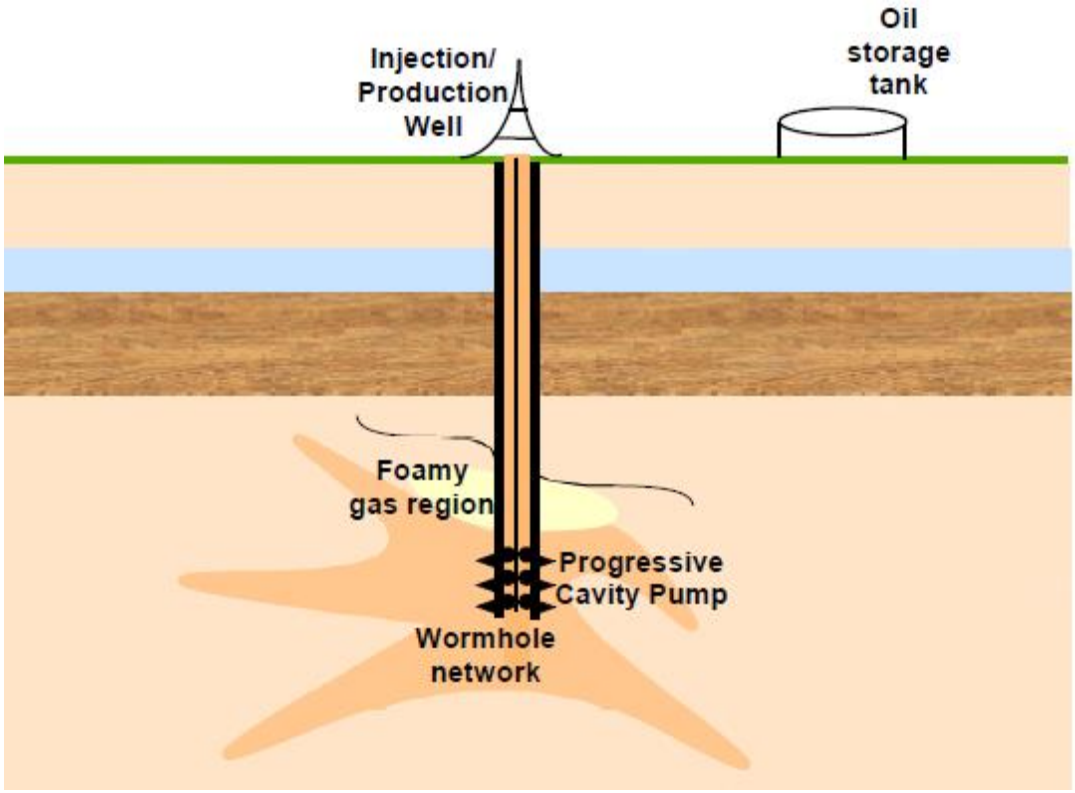

Figure 2.1 Cold heavy oil production with sand schematic (Karajgikar, 2015).

According to production Table 2-1, heavy oil production is roughly 37000 m^3/day. Using cold production technology in western Canada from a producing well, it is produced nearly 6000 m^3/day. Table 2-2 indicates oil recovery with surfactant floods.

Table 2-1 Cold production figures (daily production and well count) for the four blocks within the cold production belt surrounding Lloydminster at November (Thomas, Ali, Scoular, & Verkoczy, 2001).

Block	Producing Well Count #	Oil Production (m^3/day)
Llyodminster	3367	21757
Lindbergh	1322	8348
Cold Lake	600	4486
SW Saskatchewan	306	2220
TOTALS	5895	36811

Table 2-2 Oil recovery by surfactant floods (Thomas, Ali, Scoular, & Verkoczy, 2001).

Process Description	Original Oil in Place Recovery (%)
Base cold waterflood	36.7
Base hot waterflood	47.7
Surfactant Floods	
Cold, after waterflood	7
Hot, after cold surfactant flood	21
Hot, after cold surfactant flood, following cold waterflood	22
Hot, after cold waterflood	33
Hot, after hot waterflood	10

For this process, key reservoir conditions include unconsolidated, clean sands (very low fines content); a minimum oil viscosity; mobile oil; and a minimum initial gas-oil ratio (GOR). Measuring is the key operating practice to prevent down hole sanding problems during the early production when sand cuts tend to be high (e.g. annular

injection of crude or lighter heavy oil while pumping and cleaning of perforations) and aggressive fluid withdrawal even when bottom hole fluid levels are very low. Important field issues are pool exploitation strategies like step-out patterns, timing, well spacing, infill locations, production profile guesses, reserves estimates and issues in well operations such as bottom hole pressure effect, gas production, stimulation of poor producers and the extension of well life.

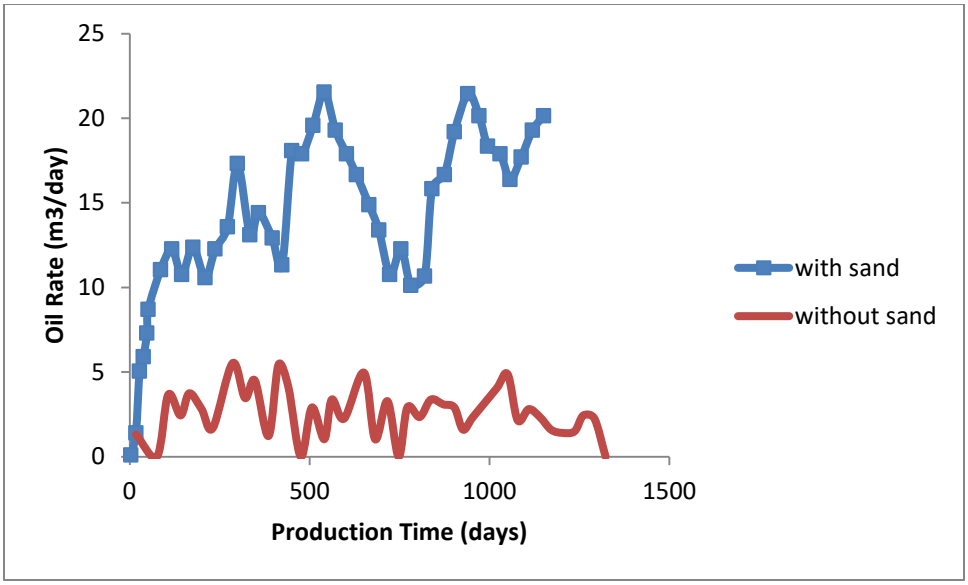

Figure 2.2 Comparison of oil production rates for two wells in the same Edam pool one with sand production and one without (Sawatzky, et al., 2002).

Cold production recovery factors are higher than primary production factors without substantial sand production. Ultimate cold production recovery factors usually fall within a range of about 8-15% of the initial oil in place. Recovery factors for primary production without sand production are reported to be somewhat lower. Figure 2.2 shows a comparison of oil production between sand production and without sand production in the same pool. Although mechanisms behind this process still not understood completely, generally accepted idea is that foamy oil flow and sand production induced reservoir

access are the dominant mechanisms involved in cold production. Sawatzky et al. stated that, based on their laboratory and field studies, the key recovery mechanisms for cold production are the foamy oil behavior generated drive, and wormhole network growth generated reservoir access. Heavy oil depressurization is involved in cold production process, which causes the dissolved gases to rise as bubbles in oil. Fluid volume is increased by gas bubbles forcing both oil and gas to the well. The gas bubbles are long-lived and stay distributed throughout the oil phase in high viscosity heavy oils. This dispersion is called as 'foamy oil.' Presence and behavior of foamy oil effects are felt in two ways:

- Suppressed gas rise
- Restricted gas mobility.

Foamy oil is not at equilibrium. With time, the gas bubbles will coalesce to form a continuous gas phase at equilibrium with the oil phase. This is why foam itself is not a thermodynamic phase and is never stable over time. The time required to reach equilibrium depends on many factors, including shear rate, the containment environment, interfacial properties, and oil viscosity. Sand is produced with heavy oil during cold production. They are bound together intimately in the process. Dramatic pressure gradients are generated in the reservoir as mobile heavy oil flows toward the production well. This results in failure of the unconsolidated sand matrix.

The failed sand is pulled to the well by the high viscosity oil. Produced sand volume during cold production is substantial and persistent. Sand production from an unconsolidated heavy oil reservoir creates a network of high permeability channels – wormholes – that grow into the reservoir. The network of wormholes is usually extensive and can grow to great distances which connect wells. It tends to grow predominantly in

preferred layers within the producing formation. Figure 2.3 exhibits a schematic of wormhole.

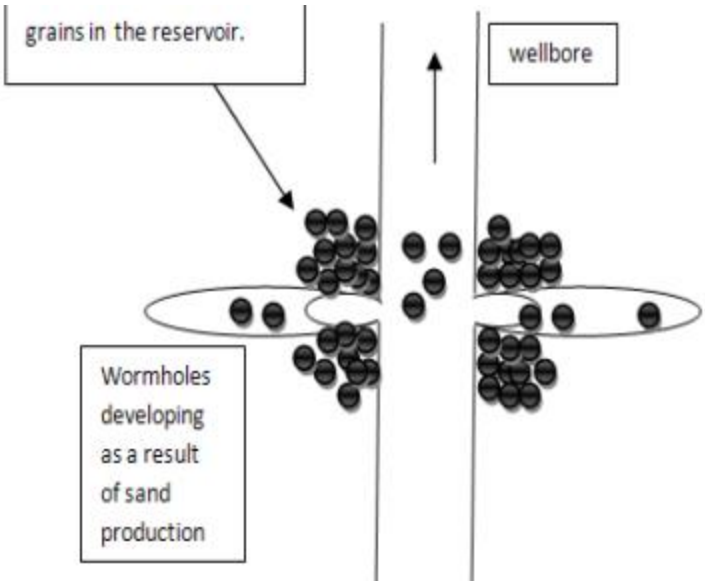

Figure 2.3 Wormhole schematic. Adapted from University of Calgary Reservoir Simulation by W. Naeem, (n.d.), Retrieved from http://ucalgaryreservoirsimulation.ca/modeling-sand-production-and-wormhole-growth-using-pressure-and-stress/.

Thus, in the cold production drainage distances are very short. Weak cohesive strength existence in unconsolidated heavy oil reservoirs is critical to the development of wormholes during cold production. It would be hard to cause the sand to fail if the cohesive strength were too high, as in the case where cementation exists. It is not likely to produce big amounts of sand. On the contrary, if the cohesive strength were too low wormholes would not likely be able to grow forward very far. They would tend to collapse. When sand is produced from excessively weak sand packs, such as water-saturated sands or loosely packed sands, rather than wormholes cavities will generally form. As the pressure gradient increases, wormholes tend to grow faster. Their diameter boosts with the size of the area they drain. Experimental results indicate that wormholes will usually be steady in the field during the cold production. Wormholes will tend to

grow in the weakest sand, and toward the highest pressure gradient. Mostly, in these layers porosity and oil saturation are highest, which allows a higher flow rate toward the wormhole tip. Finally, wormholes can be divided into two distinct categories: those that are filled completely with loose sand and those in which a channel has been eroded at the top of the loose sand by the influx of oil. (Sawatzky et al., 2002). Progressive-cavity (PC) pump can be used for primary heavy oil production by letting formation sand to come out of well with formation fluids. Which is called cold production since heat is not applied to reservoir to extract heavy oil (Journal of Petroleum Technology [JPT], 1997). According to this journal, generally a cold-production well produces around 30 to 40% and it decreases to 1 to 5% in a year of production. Two accepted theories for production mechanisms are: (1) wormholes that are created by sand production, which increases effective permeability and well bore radius and (2) foamy oil phenomenon that is a reservoir drive mechanism that includes retention of solution gas by the viscous oil. Other factors that might be considered increases drainage radius, gas expansion, and opening pores.

2.3 WATER FLOODING

In order to supply pressure to move oil through producing wells water flooding is generally used together with primary or after primary recovery technique in heavy oil reservoirs (Mai and Kantzas, 2009). They reported that although water flooding is a well-known way to improve oil recovery after primary production in conventional oil reservoirs with the assumption of similar oil and water viscosity, when dealing with heavy oil reservoirs that is not the case. Oil/water relative permeability concept is

different in heavy oil reservoirs where the flow area for oil and water might be different. Figure 2.4 shows a schematic representation of water flooding process.

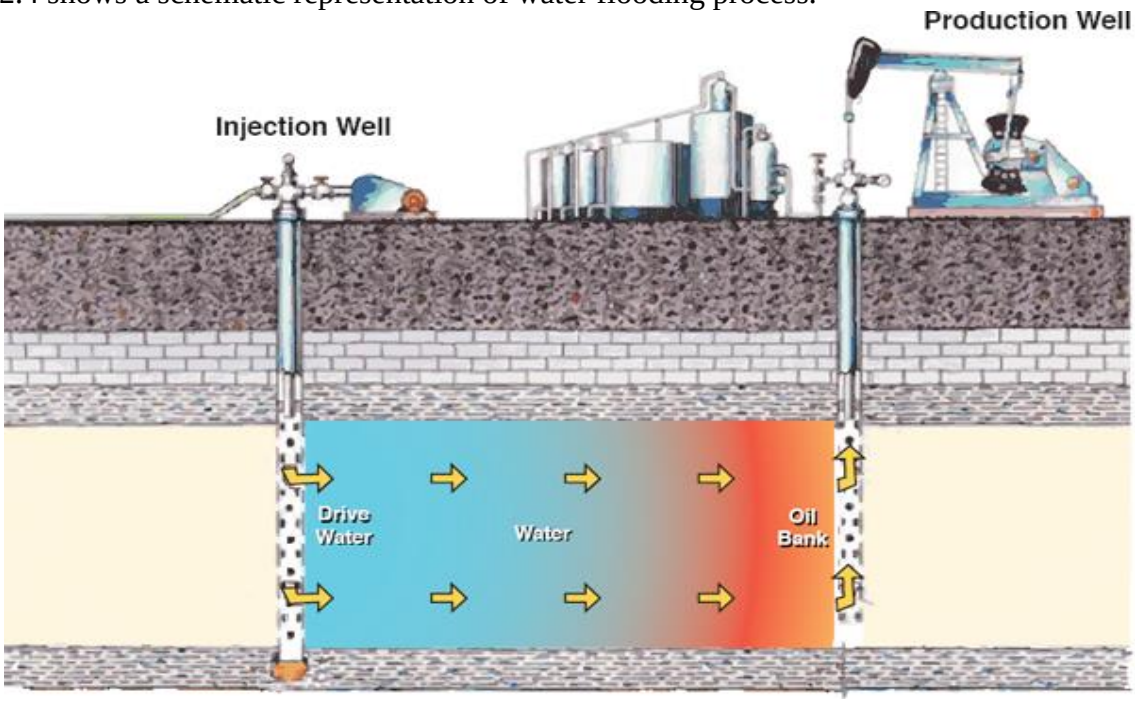

Figure 2.4 Schematically representation of water flooding process. Adapted from *NAP* by National Academy of Sciences, 2013. Retrieved from https://www.nap.edu/read/13355/chapter/6.

2.4 SOLVENT INJECTION

Mass transfer and gravity drainage are the essential mechanisms in heavy oil recovery in solvent based methods. Although injecting hydrocarbon solvent causes lower carbon footprints comparing to thermal recovery methods, the limitation for solvent based methods is low diffusivity in heavy oil reservoirs under low temperature condition (Immai et al., 2003). They also reported that in heavy oil reservoirs, using solvent injection method without thermal methods is not as effective as using it with thermal methods since without thermal methods mixing take place at colder situation. Declining steam oil ratio is the main mechanism during steam assisted methods. Figure 2.5 illustrates the cyclic solvent injection process.

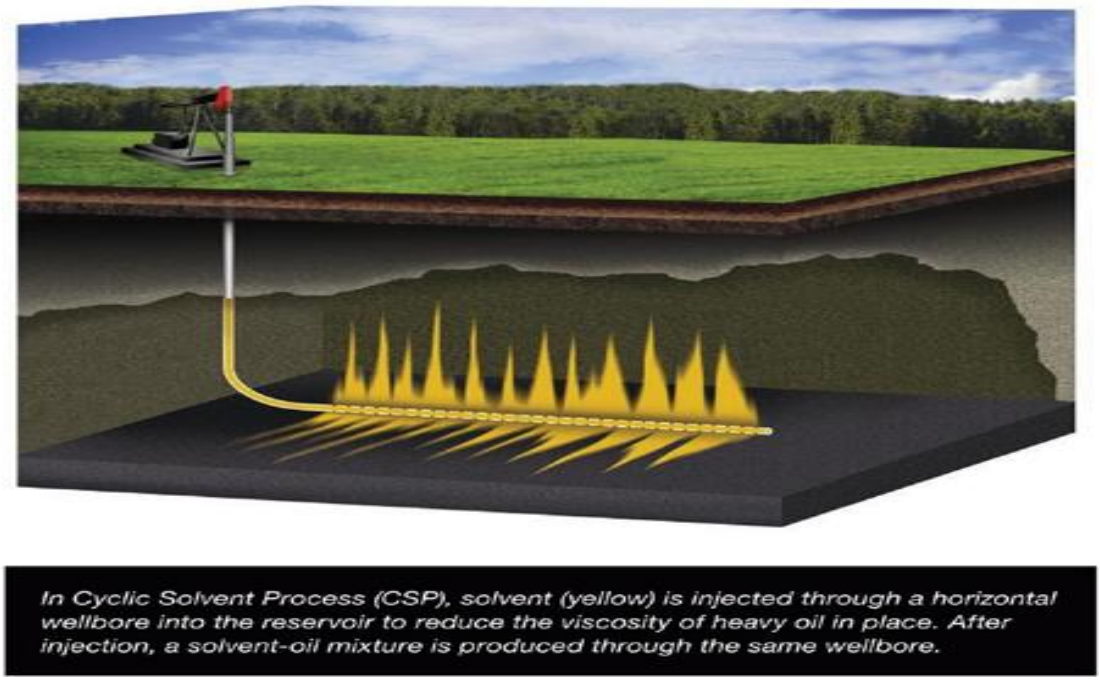

Figure 2.5 Cyclic solvent injection process. Adapted from *Exxon Mobil*, (2010), Retrieved from https://www.sec.gov/Archives/edgar/data/34088/000095012311031215/d80379exv99.htm.

2.5 THERMAL OIL RECOVERY

Szasz and Berry Jr. (1963) noted that minimizing reservoir non homogeneities effects, supplying viscosity reduction, scavenging by vaporization can cause a better and quicker oil recovery which can be reached by heating reservoirs. Thermal recovery methods can be categorized as four methods based on their way to supply heat to reservoir. These methods are hot fluid injection, forward combustion, reverse combustion, and conduction heating. Since heat reduces viscosity of oil, it increase the production rate and improves mobility ratio between oil and displacing fluid which decrease produced gas oil ratio or water oil ratio. Heat is not affected by reservoir heterogeneities and goes to tighter parts by conduction, which increases volumetric sweep efficiency. Heat may also reduce interfacial tension and change the wettability character of reservoir (pp. 1 - 2).

2.5.1 Steam Injection

Steam injection is a thermal drive process in which extra heat is added to the reservoir. Steam injection is conducted in order to reduce viscosity of oil-in-place by expanding the oil-in-place. Also, injected steam serves as extra drive energy to the reservoir energy. As a result it is aimed to increase the recovery factor of oil-in-place. Figure 2.6 shows a schematic representation of steam flooding process. According to Sarathi and Olsen (1992) in 1990 in United States recovery amount of steam flooding reached to 520000 barrels of oil per day and this production data was 73 % of all conducted EOR processes in United States in 1990. It is worth to notice that its high heat content per pound of steam makes it an ideal fluid in order to supply extra energy to the reservoir. For instance, saturated steam at 400°F contains 1201 Btu/lb of energy while water contains 375 Btu/lb of energy at 400°F (Sarathi & Olsen, 1992).

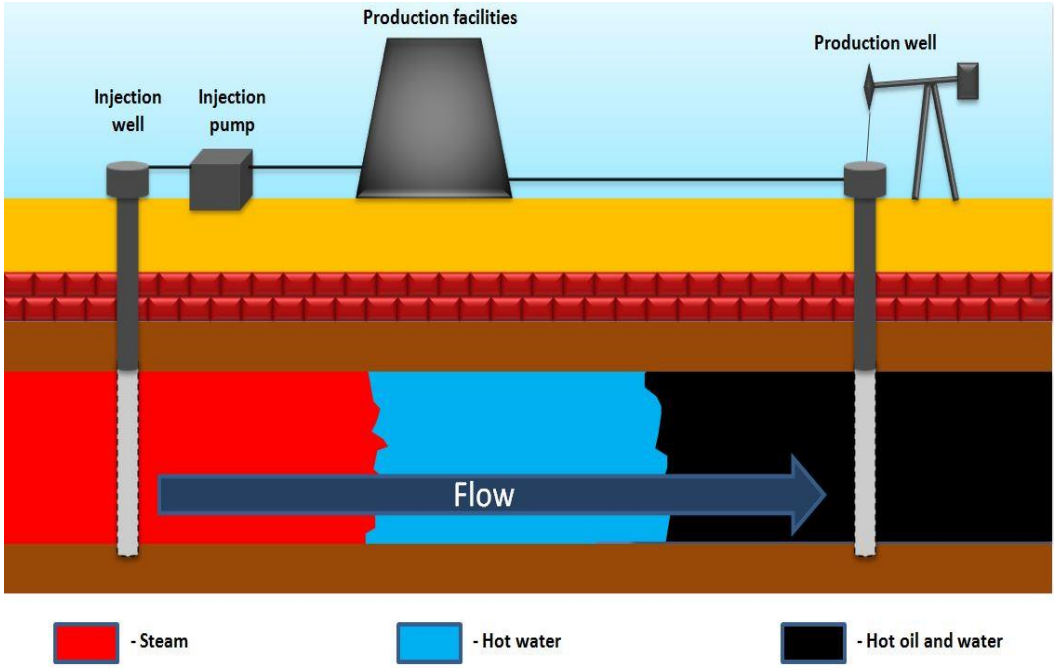

Figure 2.6 Schematically representation of steam flooding process. Adapted from *Stanford University* by G. Zerkalov, (2015). Retrieved from http://large.stanford.edu/courses/2015/ph240/zerkalov2/.

The method which is explained is a continuous method for steam injection. There is also a method in which steam is injected after the first injected steam is allowed to give its energy to reservoir. Cyclic steam injection process is conducted in order to decrease the viscosity of oil-in-place (OIP), thereby increase producing capacity of the well. Therefore, it can be concluded that in one manner cyclic steam injection process is similar to hydraulic fracturing process. In hydraulic fracturing process permeability of reservoir is increased in order to increase producing capacity of the well whereas in cyclic steam injection process viscosity of oil is reduced in order to increase producing capacity of the well. Cyclic steam injection process, as Sarathi and Olsen (1992) mentioned, is able to increase recovery by additional 3 to 5 % OIP by reducing viscosity of oil and by cleaning wellbore effects up. In "huff-'n-puff", also known as steam soak, cyclic steam injection process steam is injected into the producing well for a short time.

Then this injected production well is shut in for several days in order to soak the reservoir with steam. Later the production well is opened for production. Figure 2.7 shows a schematic of "Huff-n-Puff" cyclic steam injection process.

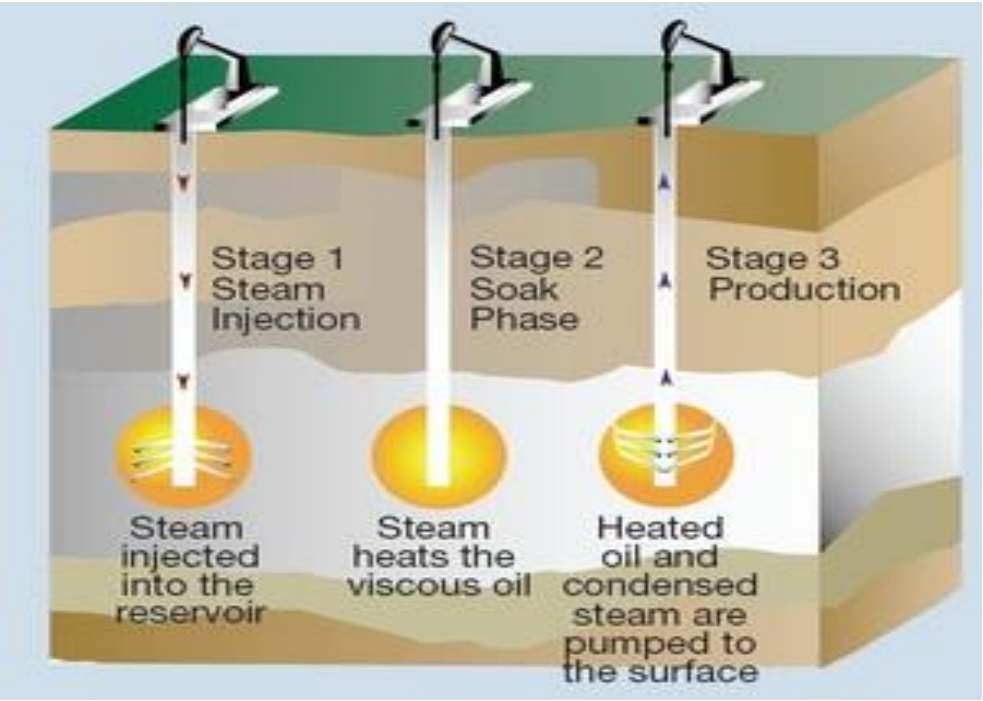

Figure 2.7 Schematic of "Huff-n-Puff " cyclic steam injection process. Adapted from *Saskoil* by E. Eaton, (n.d.), Retrieved from http://www.saskoil.org/extraction/.

On the other hand, in "push-pull" cyclic steam injection process steam is circulated around a packer. That is, steam is injected down to the reservoir from annulus and is allowed to flow in to the formation above the packer of production well. Then injected steam heats the oil by reducing its viscosity and displaces it toward the bottom of the tubing. From the tubing the oil is pumped up to the surface. Since in this method well is not shut-down, it is more advantageous than the previous method. However, in order to apply this cyclic steam injection process, the reservoir needs to be thick and

homogeneous. Also, good vertical permeability is required. Figure 2.8 exhibits a schematic of “push-pull” cyclic steam injection process.

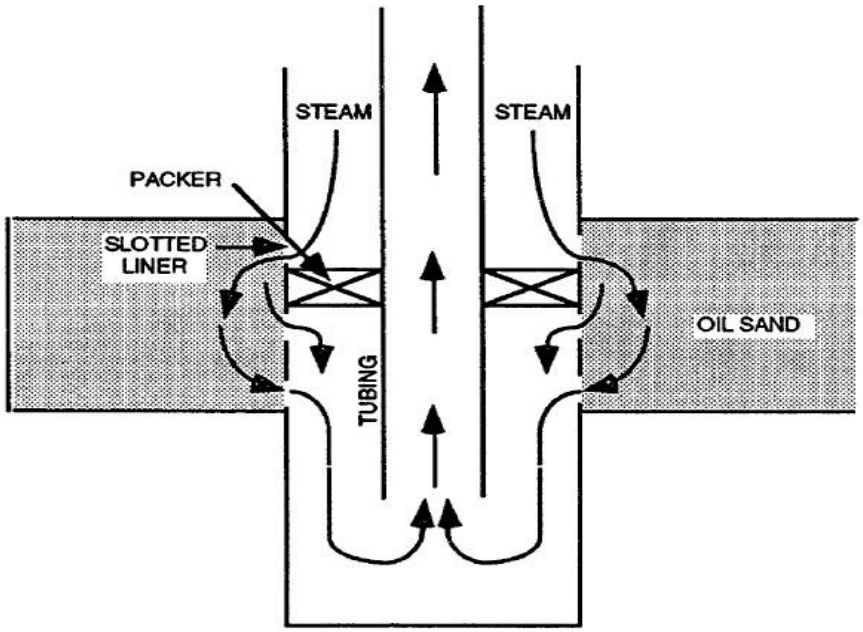

Figure 2.8 Schematic of “push-pull” cyclic steam injection process (Sarathi & Olsen, 1992).

2.5.2 In Situ Combustion

As Prats (1982) explained in in-situ combustion processes, firstly oxygen is injected into a reservoir and then crude oil in-situ reservoir is ignited; some of this in-situ reservoir crude oil is burned and as a result of this processes heat is generated in-situ reservoir. The most widespread way is air injection which includes oxygen. Primary concern of the method is generating heat in in-situ reservoir or injecting heat down to the reservoir. In order to deal with this situation in ISC thermal recovery method, heat is generated within the reservoir by injecting a gas that contains oxygen, such as air. With the help of injected gas, heavy hydrocarbons in place is burned generating heat and producing carbon oxides and water. This in-situ combustion process produces a

combustion front. As an in-situ combustion continues combustion front moves forward from injection well to the production well. When combustion zone moves, the burning front pushes ahead a mixture of hot combustion steam and hot water gases. Hot combustion steam and hot water gases, by reducing oil viscosity, displace oil toward production wells (Karimi and Samimi, 2010). Figure 2.9 shows in-situ combustion process.

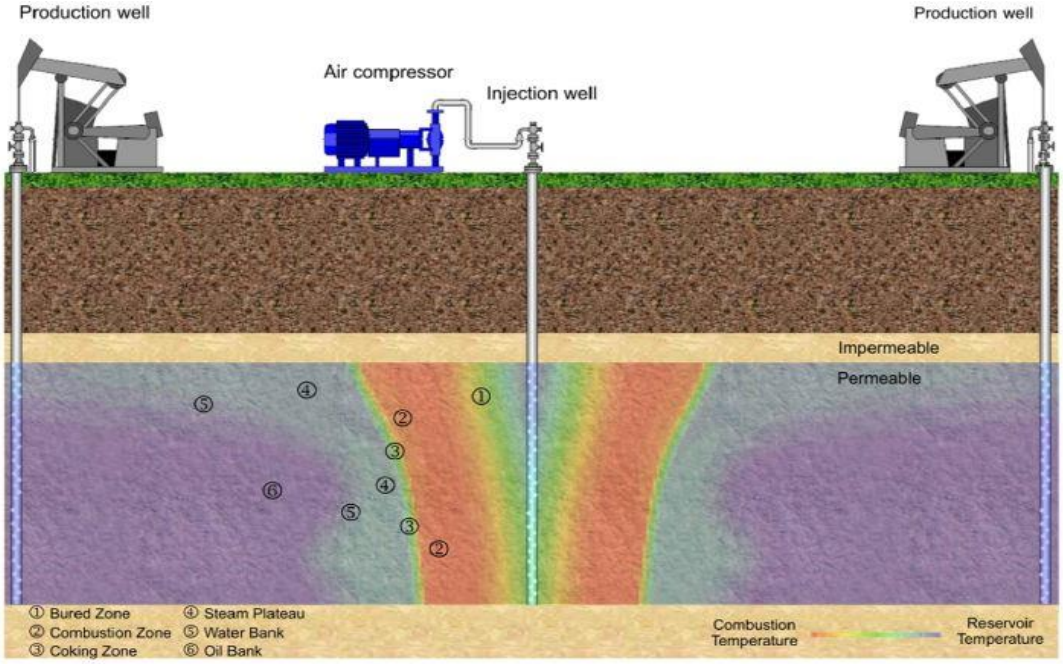

Figure 2.9 In-situ combustion (Cınar, 2011).

2.6 HYBRID PROCESSES

In these processes different methods are combined together to make heavy oil recovery economic and more efficient. There are several hybrid methods applied to reservoirs already and several methods yet not applied but under research. Chemical-thermal methods, gas or solvent with steam in steam assisted gravity drainage (SAGD) process and hot water with surfactant injection will be explained in this part.

2.6.1 Chemical-thermal method Steam-foam-surfactant CSS

A simulation is conducted by Taghavifar *et al*. (2014) with real data from Peace field, in which a hybrid method is used. Hybrid method used in this simulation is combined with thermal and chemical methods. Same horizontal wells are used for both fluid and heat injection to reservoir. Alkali-Co-solvent-Polymer (ACP) flooding is used as chemical enhanced oil recovery method and Electrical heating is used to pre-heat reservoir. Alkali-Co-solvent-Polymer (ACP) is a method recently developed in The University of Texas at Austin. In this method alkali reacts with acids in heavy oil to form soap and reduces the interfacial tension. Water viscosity is increased by polymer to control mobility ratio. Preventing the formation of highly viscous emulsions and optimizing the phase behavior is the purpose of using co-solvent. Low frequency electrical resistive heating (ERH) method is used to heat reservoir, in which horizontal wells are used as injectors, producers and electrodes. Current is forced through reservoir in this method by applying a potential gradient between horizontal wells (McGee and Vermeulen, 2007). The enhanced oil recovery method is applied in 3 stages in this study. First stage is heating reservoir with electricity to create conditions for fluid injection, which increases the pressure and the energy of the formation prior to production, and results in higher recovery. At the second stage, after injection conditions are achieved, hot water at high flow rate and high pressure is injected and thereby heat increase in reservoir is accelerated at the same time production started. Water injection takes energy from hot sand near wells and transports that energy to deeper parts of reservoir and sweeps oil through producers. Recovery mechanisms for this process are oil expansion, viscosity reduction, and oil sweeping by water. Subsequently, potential recovery factors are increased 5 to 25 percent original oil in place. At the third stage, since oil viscosity is

low enough after hot water injection, chemical flood can be performed where oil can be mobilized and swept by low pressure gradients. ACP is inexpensive, robust, and fully adjustable to each reservoir and can produce oil as much as surfactant based methods. Electrical properties are important in this study because they affect the magnitude and distribution of resistive heating. Electrical part of this study is performed by CMG CMG-STARS and chemical flooding part is performed by UTCHEM. In this study injectors were planted near bottom of reservoir and producers were near the top, which causes a vertical upward sweep. An economic optimization made in this study with Net Present Value calculation method and MATLAB is used for optimization.

2.6.2 Solvent with steam in SAGD process Alkaline-Surfactant–Polymer Flooding

Nasr et al. stated a paper (2001) based on development of ES-SAGD which is a combination of SAGD process and an expanding solvent. Figure 2.10 shows a schematic cartoon of ES-SAGD process.

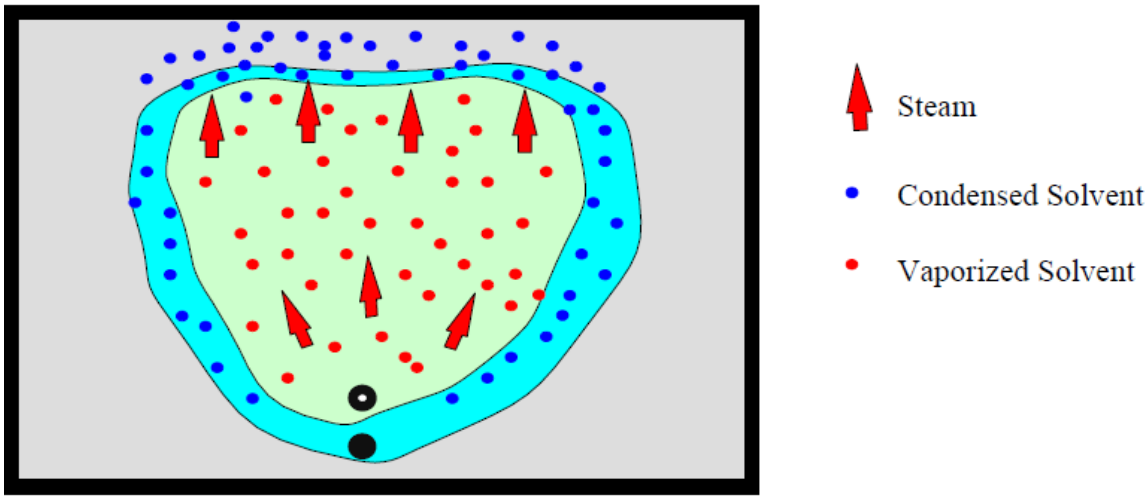

Figure 2.10 Schematic cartoon of ES-SAGD process (Nasr & Ayodele, 2005).

That method was successfully field tested with increased oil rates, oil steam ratios (OSR), and lower steam requirements compared to SAGD. The recovery mechanism is heat transfer for SAGD and diffusion/ dispersion control for solvent. This process makes expansion of steam chamber faster and supplies reflux at interface between steam and transition zone. Most of injected solvent was recovered with production in this method and the produced oil viscosity is low; also this method requires low net solvent to oil ratio.

2.7 FOAM

Foam is gas dispersion in water stabilized by surfactants. By reducing gas mobility and supplying a stable displacement front, foam can solve the problems related with gas injection. Foam improves oil recovery based on the following mechanisms:

1) Displacement front stabilization
2) High permeable swept zone block

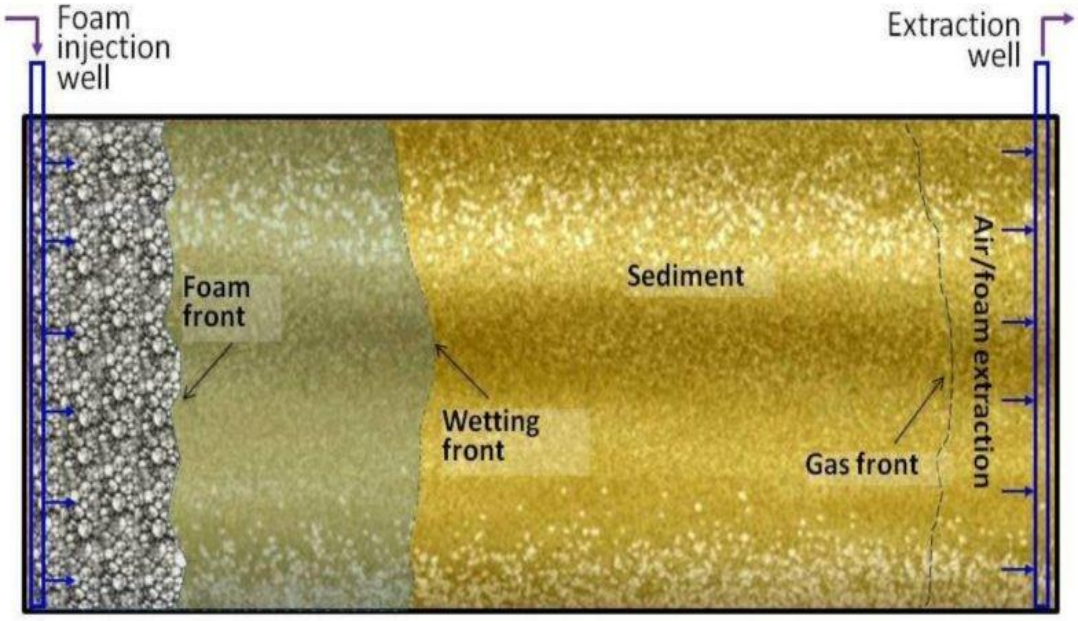

Figure 2.11 Foam injection schematic. Adapted from "Foam Delivery of Amendments for Vadose Zone Remediation," by Z. Lirong et al., (2010), *Vadose Zone Journal,* 9, p. 760.

Viscosity of displacing fluid, which is gas or foam, is increased by foam and mobility is reduced. The ratio of gas volumetric flow rate to the total volumetric flow rate is defined as foam quality. Interfacial tension (IFT) is reduced by surfactants. IFT disappears in miscible gas injection which causes increasing displacement efficiency, resulting in incremental oil production (Li, 2016). Figure 2.11 shows a schematic of foam injection.

Viscous fingering and gravity segregation are problems for gas injection. High gas mobility compared to oil and water mobility is the reason for fingering and segregation. Driving fluid does not contact with large portion of reservoir which causes low sweep efficiency. Foaming gas reduces its mobility by immobilizing or trapping without decreasing efficiency. Foam effects oil recovery in two ways:

- Stabilize displacement process by increasing gas viscosity.

- Diverting gas toward upswept zones to touch remaining and trapped oil left behind the water flood

The aim of any recovery method is to increase oil production by increasing capillary number. This is possible with two ways: reducing mobility of displacing fluid (gas), for example increasing its viscosity and reducing IFT.

When N_2 reaches oil water contact, foam front is destroyed; this gives higher liquid saturation at oil water contact due to capillary effects. When foam is destroyed, its apparent viscosity decreases; hence, viscous forces stop being dominant over capillary forces and oil remains trapped (Farajzadeh, et al., 2010).

Chapter 3: Foam Models

In this chapter foam models will be presented with governing equations and mathematical models and differences from each other.

3.1 INTRODUCTION

There are two types of simulation models for foam EOR, which are population-balance model and implicit texture model. Population balance model treats foam texture or foam size explicitly. On the other hand, implicit texture model treats effect of foam texture implicitly through gas mobility reduction factor. In population models foam collapses as capillary pressure approaches Pc^*, while in implicit texture models foam collapse occurs when foam becomes too dry around Sw*. Falls et al. (1988), Friedmann et al. (1991), and Zitha (2006) models do not include foam coalescence at a limiting capillary pressure. Skoreyko et al. (2012) shows foam creation, foam corruption, and foam trapping by representing non reversible reactions by using Arrhenius type equations to calculate reaction rates. Their model does not make reference to foam coarsening at a capillary pressure which makes it different from other model which will be represented here.

Almost all foam models change only the transport properties of gas and assume that liquid mobility keeps the same function of saturations when no foam is present. Nonetheless, there are some experiments, which indicate foam has an effect on relative permeability of water. When there is foam in system, the gas trapped by settled lamellae reduces mobile gas saturation, blocks gas flow, changes gas flow channels, and consequently reduces gas relative permeability. On the other hand, moving lamellae experience a drag force while sliding along pore walls. That effect is similar to increase

in gas viscosity. However, viscosity of gas is not increased by foam, the effect of increased resistance to gas flow due to presence of lamellae is termed “apparent gas viscosity”. Many models merge the outcome of foam on gas relative permeability and apparent viscosity and decrease the gas mobility by a factor enforced to either the gas viscosity or the gas relative permeability.

3.2 IMPLICIT TEXTURE MODELS

In this section, the UT, STARS and Vassenden-Holt models are presented. Mathematical models of these models are provided in Table 3.1.

Table 3-1 Mathematical models for implicit texture models.

Model Description	Model Parameters
UT Model (1994) $k_{rg}^{f} = k_{rg}; S_w < S_w^* - \varepsilon \, or \, C_s < C_s^*$ $k_{rg}^{f} = \frac{k_{rg}}{(1+((R-1)(S_w - S_w^* + \varepsilon))/2\varepsilon)}; S_w^* - \varepsilon \le S_w \le S_w^* + \varepsilon \,\&\, C_s \ge C_s^*$ $k_{rg}^{f} = \frac{k_{rg}}{R}; S_w > S_w^* + \varepsilon \,\&\, C_s \ge C_s^*$ $R = R_{ref}\left(\frac{u_g}{u_{g_{ref}}}\right)^{\sigma-1}$	k_{rg}^{f} : foam relative permeability Cs: surfactant concentration C_s^* : threshold surfactant conc. S_w^* : limiting water saturation u_g : gas Darcy velocity $u_{g_{ref}}$: ref. gas Darcy velocity R: foam resistance factor ε : water saturation tolerance σ : power-low exponent σ =1, Newtonian σ <1, shear-thinning

Table 3-1 continued.

STARS MODEL $k_{rg}^{f} = k_{rg} \times FM$ $FM = \frac{1}{1 + fmmob(F_1 \times F_2 \times F_3 \times F_4 \times F_5 \times F_6)}$ $F_1 = (\frac{\text{MOLE FRACTION(ICPREL)}}{\text{FMSURF}})^{EPSURF}$ $F_2 = (\frac{\text{FMOIL - OIL SATURATION}}{\text{FMOIL-FLOIL}})^{EPOIL}$ $F_3 = (\frac{\text{FMCAP}}{\text{CAPILLARY NUMBER}})^{EPCAP}$ $F_4 = (\frac{\text{FMGCP - CAPILLARY NUMBER}}{\text{FMGCP}})^{EPGCP}$ $F_5 = (\frac{\text{FMOMF - OIL MOLE FR.(NUMX)}}{\text{FMOMF}})^{EPOMF}$ $F_6 = (\frac{\text{MOLE FRACTION(NUMW) -FLSALT}}{\text{FMSALT-FLSALT}})^{EPSALT}$	FM: mobility reduction factor fmmob: max. reduction factor fmsurf: Critical component mole fraction value fmcap: Reference rheology capillary number value fmoil: Critical oil saturation value fmgcp: Critical generation capillary number value fmomf: Critical oil mole fraction for component *numx* fmsalt: Critical salt mole fraction value (component *numw*)
Vassenden-Holt Model $k_{rg}^{f} = k_{rg} \times F$ $F = e^{(S_f - S_w)S_1} + (\frac{u_g}{u_{go}})^a F_o e^{(S_f - S_w)S_2}; S_w > S_f$ $F = 1; S_w \le S_f$	u_g : gas Darcy velocity u_{go} : ref. gas Darcy velocity F: foam mobility multiplier F_o : foam mobility multiplier at ref. gas velocity S_f : lowest water saturation for foam effect s_1 : slop of the gas relative permeability at high quality regime s_2 : slop of the gas relative permeability at low quality regime a : shear thinning exponent (for original model a =1)

3.2.1 UT Model

The UT display was initially in light of information of Persoff et al. (1991), which relies completely on the high quality regime. At settled gas superficial velocity, this model gives a precarious, straight increment in gas mobility as water saturation diminishes through a tight interim in the prompt region of Sw*, and a steady lessening in gas mobility for bigger estimations of Sw. The model takes into account non-Newtonian conduct in the low-quality regime by making the portability diminishment factor in the low-quality regime a power-law capacity of gas shallow speed. This model is as of now being used in compositional test system UT-DOECO2 and UTCHEM.

3.2.2 STARS Model

In the CMG-STARS demonstrate (Computer Modeling Group (CMG), 2012), when foam is available, the gas relative permeability is duplicated by a factor FM, which is capacity of a few variables. As in the UT display, foam mobility increments as Sw diminishes in the region of Sw*, named fmdry in the CMG-STARS demonstrate. Be that as it may, in the CMG-STARS demonstrate foam does not crumble totally at any water saturation. The capacity F5 takes into consideration shear-diminishing in the low-quality regime by making the portability lessening factor reliant on capillary number.

3.2.3 Vassenden-Holt Model

The simulation model proposed by Vassenden and Holt (1998) demonstrates that the gas mobility lessening factor, F, is the combining of two exponential elements of water saturation. For water saturation marginally more than Sf (equal to Sw*), foam portability diminishes steeply in view of the main exponential capacity; this compares to foam drying out and the high quality regime. The second function diminishes all the more

bit by bit for higher water saturation and controls foam conduct in the low-quality regime.

3.3 POPULATION BALANCE MODELS

Foam versatility is impacted by its composition. Froth composition is quantified based on lamellae numbers for every unit volume of gas. Froth for fine composition has additional lamellae in a provided volume gas and thus induces all the more imperviousness for gas stream. Population-balance models fuse foam composition explicitly to guess stream properties. An equalization mathematical statement for lamellae permits the test system on track froth composition dynamically. The rates about accumulation, convection, generation, and combination from claiming froth air pockets need aid consolidated under the air pocket balance, and, assuming that desired, rates of trapping and mobilization. Mathematical models of these models are provided in Table 3.2.

Table 3-2 Population Balance foam models.

Model Description	Model Parameters
Chen et al. (2010) **-generation rate** $r_g = k_l \lvert\vec{v}_w\rvert\lvert\vec{v}_f\rvert^{1/3}$ $k_l = k_l^o\left[1-(n_f / n^*)^{\omega}\right]$ **-coalescence rate** $r_c = k_{-l}\lvert\vec{v}_f\rvert n_f$ $k_{-l} = k_{-l}^o(\frac{P_c}{P_c^* - P_c})^2$ $P_c^* = P_{c,\max}^* \tanh(C_s / C_s^o)$ **-at local equilibrium** $n_f^{\omega} + \frac{n_f^{**} k_{-l}\lvert v_f\rvert^{2/3}}{k_l^o\lvert v_w\rvert} n_f - n^{**} = 0$ **-foam relative permeability** $k_{rf} = k_{rg}^o((1-X_t)S_{gD})^{n_g}$ $X_l = X_{l,\max}(\frac{\beta n_l}{1+\beta n_l})$ **-at local equilibrium** $n_l = n_f$	v_f : local gas velocity v_w : local water velocity k_l : generation coefficient k_l^o : model parameter (const.) n_f : flowing foam bubble density n^* : limiting (max.) bubble density ω : constant exponent k_{-l} : coalescence coefficient k_{-l}^o : model parameter (const.) P_c : capillary pressure P_c^* : limiting capillary pressure $P_{c,\max}^*$: limiting value of P_c^* C_s : surfactant concentration C_s^o : ref. surfactant concentration k_{rg}^o : gas endpoint relative permeability n_g : gas exponent relative permeability S_{gD} : dimensionless gas saturation X_l : trapping foam fraction $X_{l,\max}$: maximum trapping foam fraction n_l : trapping foam bubble density β : trapping parameter

Table 3-2 continued.

Kam et al. (2007) **-generation rate** $r_g = c_g S_w (\nabla p)^m$ **-coalescence rate** $r_c = c_c n_f (\frac{1}{S_w - S_w^*})^n$ **-at local equilibrium** $n_f = \frac{c_g}{c_c} S_w (S_w - S_w^*)^n (\nabla P)^m$	n_f : foam bubble density c_g : generation rate coefficient c_c : coalescence rate coefficient S_w^* : limiting water saturation ∇P : pressure gradient n: coalescence exponent m: model parameter
Kam (2008) **-generation rate** $r_g = \frac{c_g}{2}(erf(\frac{\nabla P - \nabla P_O}{\sqrt{2}}) - erf(\frac{-\nabla P_O}{\sqrt{2}}))$ **-coalescence rate** $r_c = c_c n_f (\frac{S_w}{S_w - S_w^*})^n$ **-at local equilibrium** $n_f = \begin{cases} \frac{c_g}{2c_c}(\frac{S_w - S_w^*}{S_w})^n (erf(\frac{\nabla P - \nabla P_O}{\sqrt{2}}) - erf(\frac{-\nabla P_O}{\sqrt{2}})); n_f < n_{\max} \\ n_{\max}; n_f \geq n_{\max} \end{cases}$	n_f : foam bubble density c_g : generation rate coefficient c_c : coalescence rate coefficient S_w^* : limiting water saturation ∇P : pressure gradient ∇P_O : model parameters related to minimum pressure gradient n: coalescence exponent $n_{\max}$: maximum (limiting) bubble density

3.3.1 Kovscek et al. (1994) Model, Modified by Chen et al. (2010)

Kovscek et al. (1994) considered Roof snap-off as the system of lamella creation. Their model utilizes a capillary-pressure-dependent kinetic expression for lamella mixture and furthermore a term to speak to the caught part of froth. The gas relative permeability is then lessened by the division of streaming gas to mirror the impact of gas catching. Lamella-era rate is taken as a power-law articulation, relative to the magnitude of the interstitial speed of surfactant arrangement and 1/3 energy of the interstitial gas

speed. Chen et al. (2010) presented a furthest farthest point for the focus of lamellae that is identified with pore size. The upper limit is accomplished by lessening the lamella-era rate as this point of confinement is drawn nearer; they found that this records for prior gas bubbles that possess froth era locales. They demonstrated that the LE type of this model can anticipate both low-and fantastic froth administration.

3.3.2 Kam et al. Model (2007)

Kam et al. (2007) exhibited a froth demonstrate in which lamella creation relies upon pressure gradient and furthermore on water saturation or capillary pressure, which represents the nearness of focal points or lamellae accessible to be prepared (Rossen and Gauglitz, 1990; Gauglitz et al., 2002). In particular, lamella era rate is relative to water saturation and a power-law articulation of pressure gradient. In this model, the lamella-era rate monotonically increments with the pressure gradient. The lamella blend rate is a power-law capacity of (Sw-Sw*), with the exponent of a flexible parameter. This model can speak to numerous froth states at the same superficial velocity and hops between those states and in addition the low and high administrations for strong foam.

3.3.3 Kam (2008)

The local pressure gradient has to be more than the minimum pressure gradient necessary for lamella mobilization and division for lamella creation. A new lamella production function was proposed that reaches a plateau at higher pressure gradient.

Chapter 4: Steam Foam History Matching

In this chapter the details of steam injection application of such a process are analyzed and discussed. The main purpose of this chapter is to conduct a simulation study in order to understand the mechanism behind steam foam approach and to see the effect of steam foam process on residual oil saturation and incremental oil production. First section of this chapter describes energy and steam equations. Next, a model for a core was created from an experiment conducted by H. C. Lau (2012) to evaluate the effect of steam foam on total oil recovery. Finally the discussion of the simulation results is presented.

STARS is CMG's new generation advanced processes reservoir simulator which includes options such as chemical/polymer flooding, thermal applications, steam injection, horizontal wells, dual porosity/permeability, directional permeabilities, flexible grids, fireflood, and many more. STARS was developed to simulate steam flood, steam cycling, steam-with-additives, dry and wet combustion, along with many types of chemical additive processes, using a wide range of grid and porosity models in both field and laboratory scale. However in this chapter we also discuss the detail of thermal governing equations to understand performance of temperature impact of mobility and behavior of multiphase flow.

4.1 Energy and Steam Equations

The conservation of energy in porous media is derived from the first law of thermodynamics. As Lashgari H. (2014) stated in his dissertation, this equation can be simplified by neglecting energy flux due to radiation and reactions and excluding kinetic

and potential energies. Therefore a statement of the energy balance or the first law of thermodynamics is suitable for this purpose. He used this statement as follows:

$$\left\{\begin{matrix} Accumulation\ rate \\ of\ \ energy\ in\ V \end{matrix}\right\} = \left\{\begin{matrix} Net\ rate\ of\ \ energy \\ transported\ of \\ \ energy\ \text{int}\, o\ V \end{matrix}\right\} + \left\{\begin{matrix} Energy\ \ production \\ rate\ of\ \ energy\ in\ V \end{matrix}\right\}$$

where V is an arbitrary volume. This can be written as

$$\int_V \frac{\partial}{\partial t}\left(\rho U + \frac{1}{2}\sum_{\ell=1}^{np} \rho_\ell \,|\, \vec{u}_\ell \,|^2 - \rho g D_z \right) dV + \int_V \nabla . \vec{E} dV - \dot{W} = 0 \qquad (4\text{-}1)$$

where U is an overall internal energy (total energy/total mass), and $\boldsymbol{\rho}$ is the overall density and the term $\frac{1}{2}\sum_{\ell=1}^{np} \rho_\ell \,|\, \vec{u}_\ell \,|^2$ represents total kinetic energy per unit bulk volume and $\boldsymbol{\rho g D_z}$ is total potential energy per unit bulk volume with reference to the depth below some horizontal plane; where $\vec{\boldsymbol{E}}$ represents energy flux and $\dot{\boldsymbol{W}}$ is work done and external heating source term in the system. The form of the first law of thermodynamics for open systems expressed in the above equation requires the $\dot{\boldsymbol{W}}$ term to be composed of work components only, in the absence of external heating sources. External heating sources can often be handled through boundary conditions. He considers only the rate of work done against a pressure field, although other types of work could be included. In this derivation, there is no compression or expansion work done on volume V since it is assumed to be constant.

$$\dot{W} = -\int_V \sum_{\ell=1}^{n_p} \nabla.\left(p_\ell \vec{u}_\ell \right) dV \tag{4-2}$$

This term is the work done by the force exerted by the pressure in phase ℓ . The energy flux term is made up of convective contributions from the flowing phases (internal, kinetic, and potential energy), conduction, and radiation as expressed as

$$\vec{E} = \sum_{l=1}^{n_p} \rho_\ell \vec{u}_\ell \left[U_\ell + \frac{1}{2} |\vec{v}_\ell|^2 + - gD_z \right] - \lambda_{eff} \nabla T + \vec{q}_r \tag{4-3}$$

For brevity, he neglects radiation in the following discussion, although this transport mechanism can be important in estimating heat losses from wells and in certain EOR processes and remediation that involve electromagnetic sources

$$\begin{aligned} &\frac{\partial}{\partial t}\left(\rho U + \frac{1}{2} \sum_{\ell=1}^{n_p} \rho_\ell |\vec{u}_\ell|^2 - \rho g D_z \right) + \nabla.\left(\sum_{\ell=1}^{n_p} \rho_\ell \vec{u}_\ell \left(U_\ell + \frac{1}{2} |\vec{v}_\ell|^2 + - gD_z \right) \right) \\ &-\nabla.\left(\lambda_{eff} \nabla T \right) + \sum_{\ell=1}^{n_p} \nabla.\left(p_\ell \vec{u}_\ell \right) = q \end{aligned} \tag{4-4}$$

The first sum in the energy flux and that in the pressure-volume work expression may be combined to give

$$\begin{aligned} &\frac{\partial}{\partial t}\left(\rho U + \frac{1}{2} \sum_{\ell=1}^{n_p} \rho_\ell |\vec{u}_\ell|^2 - \rho g D_z \right) + \nabla.\left(\sum_{\ell=1}^{n_p} \rho_\ell \vec{u}_\ell \left(H_\ell + \frac{1}{2} |\vec{v}_\ell|^2 + - gD_z \right) \right) \\ &-\nabla.\left(\lambda_{eff} \nabla T \right) = q \end{aligned} \tag{4-5}$$

where $H_\ell = U_\ell + p_\ell / \rho_\ell$ is defined as the enthalpy of phase ℓ per unit mass of ℓ. Neglecting the kinetic and potential energy in accumulation and transport of net rate of energy, the above expression can be written as

$$\frac{\partial}{\partial t}(\rho U) + \vec{\nabla}.\left(\sum_{\ell=1}^{n_p} \rho_\ell \vec{u}_\ell H_\ell\right) - \vec{\nabla}.(\lambda_{eff} \nabla T) = 0 \tag{4-6}$$

where $\rho U = (1-\phi)\rho_r U_r + \phi \sum_{\ell=1}^{n_p} \rho_\ell S_\ell U_\ell$ and by plugging this equation into the energy balance equation it can be written as

$$\frac{\partial}{\partial t}\left((1-\phi)\rho_r U_r + \phi \sum_{\ell=1}^{n_p} \rho_\ell S_\ell U_\ell\right) + \vec{\nabla}.\left(\sum_{\ell=1}^{n_p} \rho_\ell \vec{u}_\ell H_\ell\right) - \vec{\nabla}.(\lambda_{eff} \nabla T) = q \tag{4-7}$$

Since $\boldsymbol{H_r = U_r}$ and $H_\ell = U_\ell + \frac{p_\ell}{\rho_\ell}$, the above expression can be written as

$$(1-\phi)\rho_r \frac{\partial H_r}{\partial t} + \phi \sum_{\ell=1}^{n_p} \frac{\partial}{\partial t}(\rho_\ell S_\ell H_\ell - S_\ell p_\ell) + \vec{\nabla}.\left(\sum_{l=1}^{n_p} \rho_\ell \vec{u}_\ell H_\ell\right) - \vec{\nabla}.(\lambda_{eff} \nabla T) = q \tag{4-8}$$

If the pressure work is assumed to be negligible, $-\phi \sum_{\ell=1}^{n_p} \frac{\partial}{\partial t}(S_\ell p_\ell) = 0$ and the above equation can be written as

$$\begin{aligned} &(1-\phi)\rho_r \frac{\partial H_r}{\partial t} + \phi \sum_{\ell=1}^{n_p} \rho_\ell S_\ell \frac{\partial H_\ell}{\partial t} + \phi \sum_{\ell=1}^{n_p} H_\ell \frac{\partial}{\partial t}(\rho_\ell S_\ell) + \\ &\sum_{l=1}^{n_p} H_\ell \vec{\nabla}.(\rho_\ell \vec{u}_\ell) + \sum_{\ell=1}^{n_p} \rho_\ell \vec{u}_\ell . \vec{\nabla} H_\ell - \vec{\nabla}.(\lambda_{eff} \nabla T) = q \end{aligned} \tag{4-9}$$

If it is assumed only mass transfer can occur between water and steam, the mass equations for all phases can be written as

$$\frac{\partial}{\partial t}\left(\phi\rho_\ell S_\ell\right)+\vec{\nabla}.\left(\rho_\ell\vec{u}_\ell\right)=0 \quad \ell \neq water \ \ and \ \ steam \tag{4-10}$$

$$\frac{\partial}{\partial t}\left(\phi\rho_w S_w+\phi\rho_s S_s\right)+\vec{\nabla}.\left(\rho_w\vec{u}_w+\rho_s\vec{u}_s\right)=0 \tag{4-11}$$

or

$$\frac{\partial}{\partial t}\left(\phi\rho_w S_w\right)+\vec{\nabla}.\left(\rho_w\vec{u}_w\right)=-\frac{\partial}{\partial t}\left(\phi\rho_s S_s\right)-\vec{\nabla}.\left(\rho_s\vec{u}_s\right)$$

Thereby, energy fluxes in the reservoir occur by conduction and convection; thus the energy equation, considering all possible source terms, can be written as

$$\begin{aligned}&\frac{\partial}{\partial t}\left[\left(1-\phi\right)\rho_r U_r+\phi\sum_{\ell=1}^{n_p}\rho_\ell S_\ell U_\ell\right]+\vec{\nabla}\cdot\left(\sum_{\ell=1}^{n_p}\rho_\ell H_\ell\vec{u}_\ell\right)-\vec{\nabla}.\left(\lambda_{eff}\vec{\nabla}T\right)\\&=\mp q_H\pm q_L+q_{ele}\mp q_{instu}\end{aligned} \tag{4-12}$$

where U_r and U_ℓ are internal energy of rock and fluid phase l per unit mass, respectively, H_ℓ is enthalpy of phase per unit mass, u_ℓ is Darcy's velocity of fluid phase ℓ , ρ_r and ρ_ℓ are rock and mass density of phase ℓ , respectively. ϕ is porosity and S_ℓ is saturation of fluid phase ℓ . In Equation (1), n_p is the number of existing phases and λ_{eff} is an effective thermal conductivity. q_H is the enthalpy rate of source or sink term per bulk volume. A positive sign is assigned to q_H for a hot injection well and a negative sign is considered for a production well. q_L is the heat loss to overburden and underburden rocks. In the case of cold fluid injection where reservoir becomes colder than initial reservoir temperature, a positive sign is assigned to q_L (Lashgari, H., 2014). But in the case of hot fluid injection, which increases reservoir temperature compared to initial temperature, a negative sign for q_L is considered. q_{ele} is the electrical Joule heating as source term, which is always positive. q_{instu} is in-situ thermal generator source

that can be placed in the bottom hole of a well (Lashgari, H., 2014). A positive sign in front of q_{instu} is assigned for a heat source and a negative sign for a cold source. The following assumptions are made for simplification (Lake 1989):

- Neglect pressure-volume work ($H = U$) for all fluid phases.
- Neglect the dependency of enthalpies on pressure.
- Heat capacity is considered independent of temperature.
- Consider an effective thermal conductivity of all saturated fluids and rock as arithmetic-weighted average as expressed in Equation (4-3).
- Heat-loss to overburden and underburden, q_L is computed using Vinsome and Westerveld (1980) analytical method.

It is assumed that the mass transfer between water and steam phases occurs at the boiling point (saturated condition). The following equation must conserve energy during condensation and vaporization as

$$(1-\phi)\rho_r \frac{\partial H_r}{\partial t} + \phi \sum_{\ell=1}^{n_p} \rho_\ell S_\ell \frac{\partial H_\ell}{\partial t} + (\bar{H}_s - \bar{H}_w)\frac{\partial(\rho_s S_s)}{\partial t} + \left(\sum_{\ell=1}^{n_p} \rho_\ell u_\ell \vec{\nabla} H_\ell \right) + (\bar{H}_s - \bar{H}_w)\vec{\nabla}.(\rho_s \vec{u}_s) - \vec{\nabla}.\left(\lambda_{eff}\vec{\nabla}T\right) = \mp q_H \pm q_L + q_{ele} \mp q_{instu} \quad (4\text{-}13)$$

where $\bar{H}_s$ and $\bar{H}_w$ are steam and water enthalpy per unit mass; $\rho_s, \vec{u}_s$ and, S_s are density of steam phase, Darcy velocity of steam phase, and saturation of steam phase, respectively .Effective thermal conductivity is defined as

$$\lambda_{eff} = (1-\phi)\lambda_r + \phi \sum_{\ell=1}^{n_p} s_\ell \lambda_\ell \quad (4\text{-}14)$$

where λ_r is thermal conductivity of rock and λ_ℓ is thermal conductivity of phase ℓ (Lashgari, H., 2014). In addition, it is more convenient to substitute enthalpy with temperature functions based on the above assumptions. Using enthalpy definition of rock and fluid phases corresponding to reference temperature and enthalpy, (enthalpy reference of a reservoir is considered the initial temperature of reservoir in this work) it can be written as

$$\Delta H = \zeta_p \left(T - T_{ini}\right) \tag{4-15}$$

where ζ_p could be heat capacity of rock or fluid phases. Finally, the following energy equation becomes:

$$\begin{aligned} &\left(\left(1-\phi\right)\rho_r\zeta_{pr} + \phi\sum_{\ell=1}^{n_p}\rho_\ell S_\ell \zeta_{p\ell}\right)\frac{\partial T}{\partial t} + \left(\sum_{\ell=1}^{n_p}\rho_\ell \vec{u}_\ell \zeta_{p\ell}\vec{\nabla}T - \vec{\nabla}.\left(\lambda_{eff}\vec{\nabla}T\right)\right) + \\ &(\bar{H}_s - \bar{H}_w)\left(\frac{\partial(\rho_s S_s)}{\partial t} + \vec{\nabla}.(\rho_s \vec{u}_s)\right) = \mp q_H \pm q_L + q_{ele} \mp q_{instu} \end{aligned} \tag{4-16}$$

This equation consists of accumulation, convection, and conduction terms, respectively. The difference between steam and water enthalpy per unit mass $\left(\bar{H}_s - \bar{H}_w\right)$ is called latent heat of water vaporization. This term is a multiplier for mass equation of gas phase in Eq.(4-16). This equation can conserve energy in the presence of vaporization and condensation of water during mass transfer between water and steam. In order to solve this equation numerically, they consider only the latent heat term explicitly and other terms are solved implicitly (Delshad *et al.,* 1996).

In order to calculate phase behavior of steam and water, total enthalpy in equilibrium is obtained from energy balance equation and then steam quality is defined and written as

$$\alpha = \frac{H_{tot} - \bar{H}_w}{\bar{H}_s - \bar{H}_w} \tag{4-17}$$

These specific enthalpies, $\bar{H}_w$ and $\bar{H}_s$ of water and steam per unit mass that are calculated directly in phase behavior calculation from steam table as well as phase densities ρ_w and ρ_s , which are functions of pressure and temperature, are calculated from steam table in the steam/water phase behavior calculation. c_w and c_s are the volumetric concentrations of water and steam components, respectively. H_{tot} is total enthalpy of water and steam calculated as

$$H_{tot} = \frac{\rho_s c_s \zeta_{ps}(T - T_{ini}) + \rho_w c_w \zeta_{pw}(T - T_{ini})}{\rho_s c_s + \rho_w c_w} \tag{4-18}$$

where ζ_{pw} and ζ_{ps} are heat capacity of water and steam phases, and ρ_s and ρ_w are mass density of water and steam, respectively. Based on a simple definition of mass transfer between water and steam, mass quality of steam can be also defined as

$$\alpha = \frac{(\rho_s c_s)}{(\rho_s c_s + \rho_w c_w)} \tag{4-19}$$

Eqs. (4-17) and (4-19) express the same content but a difference in calculation. One is obtained from the energy balance equation and the second is computed from the mass balance equation. Therefore, mass quality can be calculated first; then, since mass must be conserved in Eq.(4-17), volume concentration of gas can be solved; then the mass balance equation is used to solve for water (Lashgari, H., 2014).

4.2 HEAT LOSS MODEL

Vinsome and Westerveld (1980) developed a semi-analytical approach to compute amount of heat loss in case of heat or cold injection into a reservoir layer that is surrounded between impermeable overburden or underburden layers. Their approach simplifies the heat conduction problem, while providing satisfactory accuracy. Vinsome and Westerveld considered that heat conduction perpendicular to the conductive boundary is more important than parallel to the boundary. Heat conduction tends to wipe out sharp temperature differences; they suggested that the temperature profile in the conductive domain may be approximated by means of a simple trial function that contains a few adjustable parameters. Lashgari used a similar model but he considers that the temperatures of overburden and underburden are not changed during heat loss from reservoir layer. Temperatures of overburden and underburden are set at the initial temperature of reservoir layer ($\boldsymbol{T_{OB} = T_{ij1}^{0}}$ and $\boldsymbol{T_{UB} = T_{ijN_z}^{0}}$).

$$q_{L,ijNz}^{n+1} = \lambda_{UB}\left(\frac{T_{ijNz}^{n+1} - T_{UB}}{d_{ijNz}} - \frac{\kappa\Delta t}{d_{ijNz}\left(3d_{ijNz}^{2} + \kappa\Delta t\right)}T_{ijNz}^{n+1} + \frac{\kappa\Delta t}{d_{ijNz}\left(3d_{ijNz}^{2} + \kappa\Delta t\right)}T_{UB}\right.$$
$$\left. - \frac{I_{ijNz}^{n}}{3d_{ijNz}^{2} + \kappa\Delta t} + \frac{d_{ijNz}^{3}}{\kappa\Delta t\left(3d_{ijNz}^{2} + \kappa\Delta t\right)}T_{ijNz}^{n+1} - \frac{d_{ijNz}^{3}}{\kappa\Delta t\left(3d_{ijNz}^{2} + \kappa\Delta t\right)}T_{ijNz}^{n}\right)\Delta x_{ijNz}\Delta y_{ijNz} \quad (4\text{-}20)$$

where $\boldsymbol{T_{OB}}$ is temperature of overburden, which is constant, $\boldsymbol{\lambda_{OB}}$ is thermal conductivity of overburden layer corresponding to grid block ($\boldsymbol{ij1}$) located at top layer and which is constant, $\boldsymbol{\lambda_{UB}}$ is thermal conductivity of overburden layer corresponding to grid block ($\boldsymbol{ijNz}$) located at bottom layer and $\boldsymbol{d_{ijNz}^{n}}$ is the underburden thermal diffusivity.

Brooks-Corey Relative Permeability Model

In 1954, Corey combined predictions of a tube-bundle model with his empirical expression for capillary pressure to obtain expressions for gas and oil relative permeability values. In 1964, Brooks and Corey extended Corey's results for capillary pressure to obtain the following expressions for oil and gas relative permeability values:

$$k_{ro} = \left(\frac{S_o - S_{or}}{1 - S_{or}}\right)^{\frac{2+3\lambda}{\lambda}} \tag{4-20}$$

$$k_{rg} = \left(\frac{1 - S_o}{1 - S_{or}}\right)^2 \left(1 - \left(\frac{S_o - S_{or}}{1 - S_{or}}\right)^{\frac{2+\lambda}{\lambda}}\right) \tag{4-212}$$

Eqs. (4-21) and (4-22) apply to a porous material that is initially fully saturated with oil and then invaded by gas. These equations do not allow for nonzero critical gas saturation.

For λ=2, Eqs. (4-22) and (4.23) reduce to the 1954 Corey expressions.

Brooks and Corey related the parameter λ to the distribution of pore sizes.

For narrow distributions, λ is greater than 2.

For wide distributions, λ is less than 2.

λ =7.30 for an unconsolidated pack of glass beads of uniform diameter.

For sandpacks with broader distributions of particle sizes, λ ranges from 1.8 to 3.7.

For a particularly homogeneous consolidated sandstone, they reported λ =4.17.

The following "power-law" relationships are often used to describe oil, water, and gas relative permeability values, respectively:

$$k_{ro} = k_{ro,\max}\left(\frac{S_o - S_{or}}{1 - S_{or} - S_{wc} - S_{gc}}\right)^{n_o} \quad (4\text{-}23)$$

$$k_{rw} = k_{rw,\max}\left(\frac{S_w - S_{wc}}{1 - S_{or} - S_{wc} - S_{gc}}\right)^{n_w} \quad (4\text{-}224)$$

$$k_{rg} = k_{rg,\max}\left(\frac{S_g - S_{gc}}{1 - S_{or} - S_{wc} - S_{gc}}\right)^{n_g} \quad (4\text{-}25)$$

The exponents *no, nw,* and *ng* range from 1 to 6.

The maximum relative permeability values, *kro, max, krw ,max,* and *krg, max,* are between 0 and 1.

These expressions are often referred to as modified Brooks-Corey relations, reflecting their similarity to the Brooks-Corey expression for oil relative permeability (Brooks, R.H. and Corey, A.T. 1964).

4.3 METHODOLOGY

Numerous case studies were experimentally done in order to understand how steam foam method affects residual and remaining oil saturation and oil recovery; to evaluate that effect; steam alone is used in cores and compared with steam foam cases under same conditions. However, there are not enough numerical simulation works done to investigate that effect of different parameters on the process efficiency. In addition to study effects of foam on oil recovery, we evaluated how to use steam alone and with foam changes incremental oil employing CMG-STARS. Relative permeability tables calculated from Brooks-Corey model are used for this study.

4.3.1 History Matching Case for Core Flood

A compositional reservoir simulator, CMG-STARS, was used to build the base case for 1D core model. STARS is CMG's new generation advanced processes reservoir simulator which includes options such as chemical/polymer flooding, thermal applications, steam injection, horizontal wells, dual porosity/permeability, directional permeability values, flexible grids, fireflood, and many more. CMG-STARS was developed to simulate steam flood, steam cycling, steam-with-additives, dry and wet combustion, along with many types of chemical additive processes, using a wide range of grid and porosity models in both field and laboratory scales.

In this procedure an experimental case conducted by H. C. Lau is simulated. The name of simulated case is "Alkaline Steam Foam: Concepts and Experimental Results" with SPE number of 144968. In this case Lau made 14 experiments on Ottowa sandpacks to study effect of Na_2CO_3 and ENORDET AOS 1618 on residual oil saturation. 1 ft long 1.5 in diameter F- 140 Ottowa sand cores were used. San Joaquin crude oil was used for these experiments and they flooded with distilled water until no oil was produced, which is 3 days long. Then fifty percent mass quality steam was injected with flow rate 3 bbl/day cold water equivalent for 0.903 days. This was followed by fifty percent mass quality steam for 1.355 days to see effect of steam without foam. Then for other cases instead of steam only base steam foam was injected with different water percentages of AOS, Na_2CO_3, and NaCl to see effect on residual oil saturation for this amount of time.

4.3.2 Case Model Properties

Grid block dimensions, initial reservoir conditions and reservoir rock and fluid properties are given in Table 4-1 and the input data file is provided in Appendix A.1.

Table 4-1 Core model properties.

Number of grid blocks	2x1x50
Grid block size	0.0625x0.0625x0.02 ft^3
Initial Temperature	212 ^oF
Initial pressure	15 psi
Number of wells	4 total wells 2 production wells 2 injection wells
Initial water saturation	0
Steam injection temperature	300 ^oF
Steam injection rate	3 bbl/Day
Steam injection quality	0.5
Oil viscosity	96 cp (180 ^oF and 82.2 ^oC)
Permeability $k_x = k_y = k_z$	4000 mD
Porosity	0.31

Table 4-2 Water-Oil Relative Permeability.

Sw	Krw	Krow
0.1	0.0000000	0.700000000
0.2	0.0002915	0.514285714
0.4	0.0078717	0.228571429
0.5	0.0186589	0.128571429
0.6	0.0364431	0.057142857
0.7	0.0629738	0.014285714
0.8	0.1000000	0.000000000

Table 4-3 Liquid-Gas Relative Permeability.

Sl	Krg	Krog
0.23	0.1	0
0.4	0.06878	0.016032215
0.5	0.05233	0.050966010
0.6	0.03744	0.112040629
0.7	0.02432	0.203758564
0.8	0.01324	0.330033759
0.9	0.00468	0.494376973
1	0.00000	0.700000000

In Table 4-2 *Sw*, *Krw*, and *Krow* represent water saturation, water relative permeability, and oil relative permeability to water respectively. In Table 4-3 *Sl*, *Krg*, and *Krog* are liquid saturation, gas relative saturation and gas relative permeability to gas

respectively. Capillary effect assumed is to be zero for both tables. Relative permeability graphs are given in Figure 4.1. In Table 4-4 viscosity table for oil and water are given with respect to temperature. Figure 4.2 gives the plots for water and oil viscosities with respect to temperature.

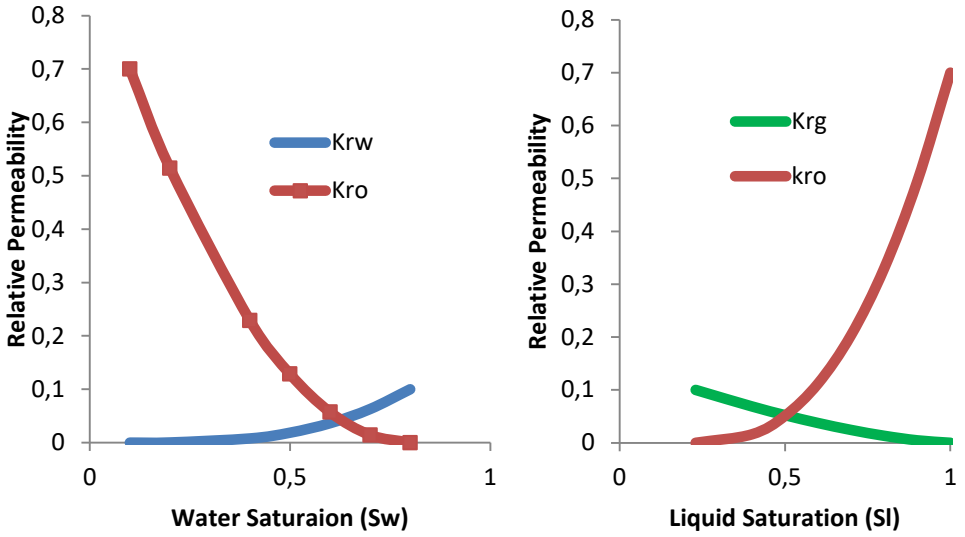

a) Oil water relative permeability b) Liquid gas relative permeability

Figure 4.1 Relative permeability of three phases used for simulation studies.

Table 4-4 Viscosity table.

Temperature (^{o}F)	Water (cp)	Oil (cp)
60	1.2	43400
100	0.682	2690
180	0.35	96
200	0.303	47
600	0.02094	10

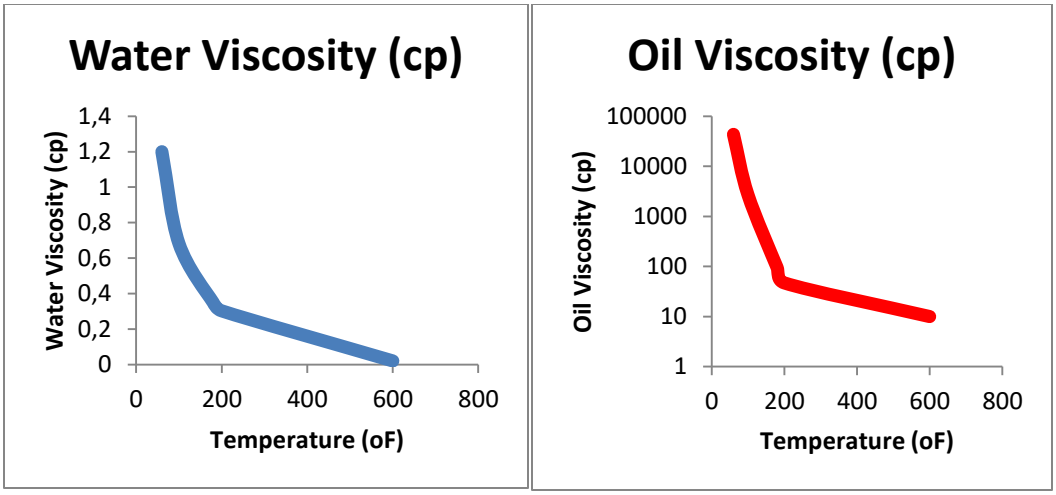

a) Water viscosity b) Oil viscosity

Figure 4.2 Water and oil viscosity plots respect to temperature.

4.4 RESULTS AND DISCUSSION

This section presents the simulation results for steam case after water flood alone and steam foam cases. Figure 4.3 gives a comparison of cumulative oil recovery between simulation result and history data. It can be said that results match very well. Figure 4.4 gives average pressure of core during the process. This graph indicates a decline and goes about steady until day 3. Since for the first 3 days the core is just flooded with distilled water, it is expected. After 3 days,, steam was injected and average pressure was increased. After 0.903 days average pressure decreased because steam foam started to be injected. Figure 4.5 illustrates average gas (with steam) saturation during core flood. For 3 days gas saturation is 0 as expected. When we start injecting steam, gas saturation increases to 45 percent and decreases to 25 percent. Figure 4.6 shows average temperature in core during the process. In this graph temperature goes steady for 3 days around 210 Fahrenheit, which is expected since we are injecting distilled water at same

temperature. When steam injection process is started, temperature increases to 330 ^{o}F and goes steady until steam foam process starts. Then temperature goes about 325 ^{o}F.

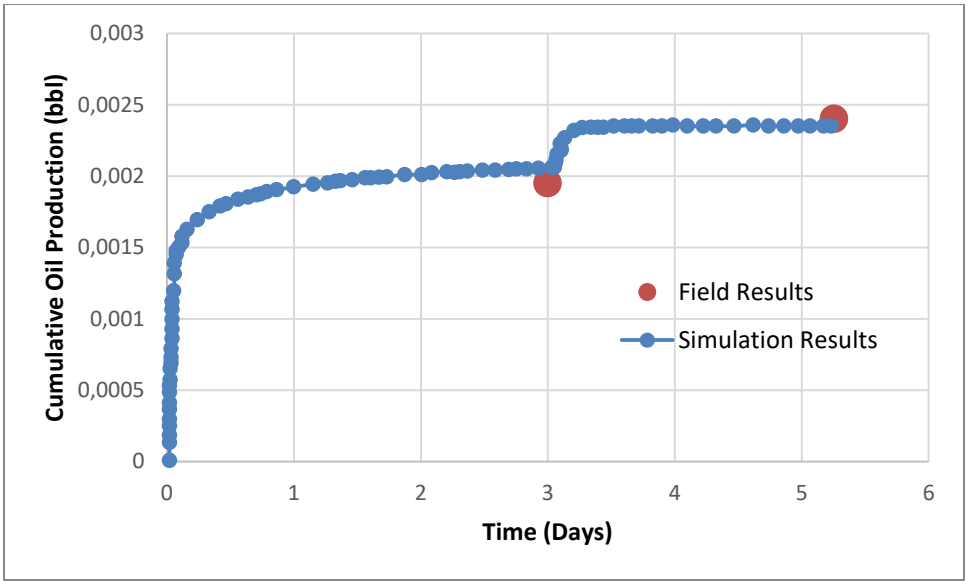

Figure 4.3 Comparison of cumulative oil recovery between simulation results and history data.

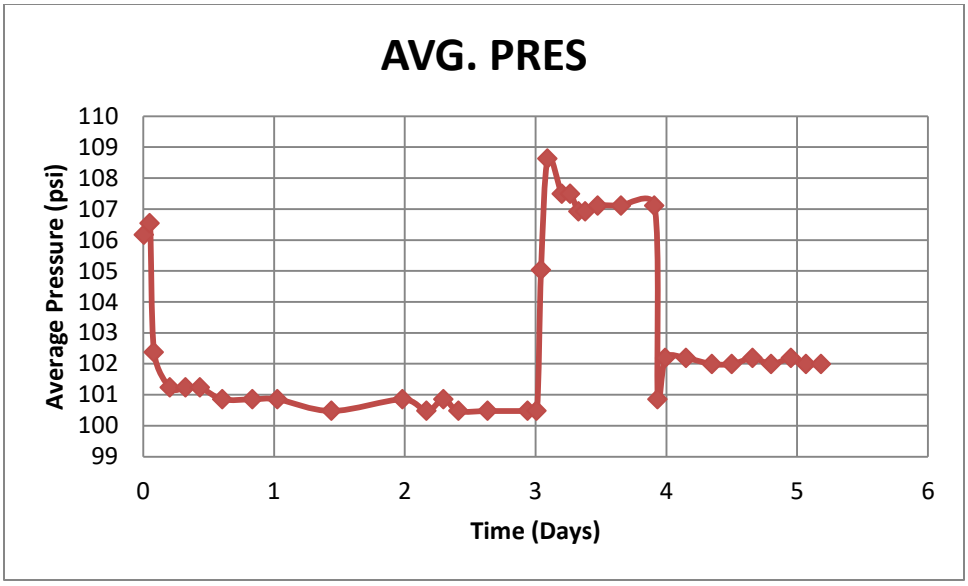

Figure 4.4 Average pressure of core.

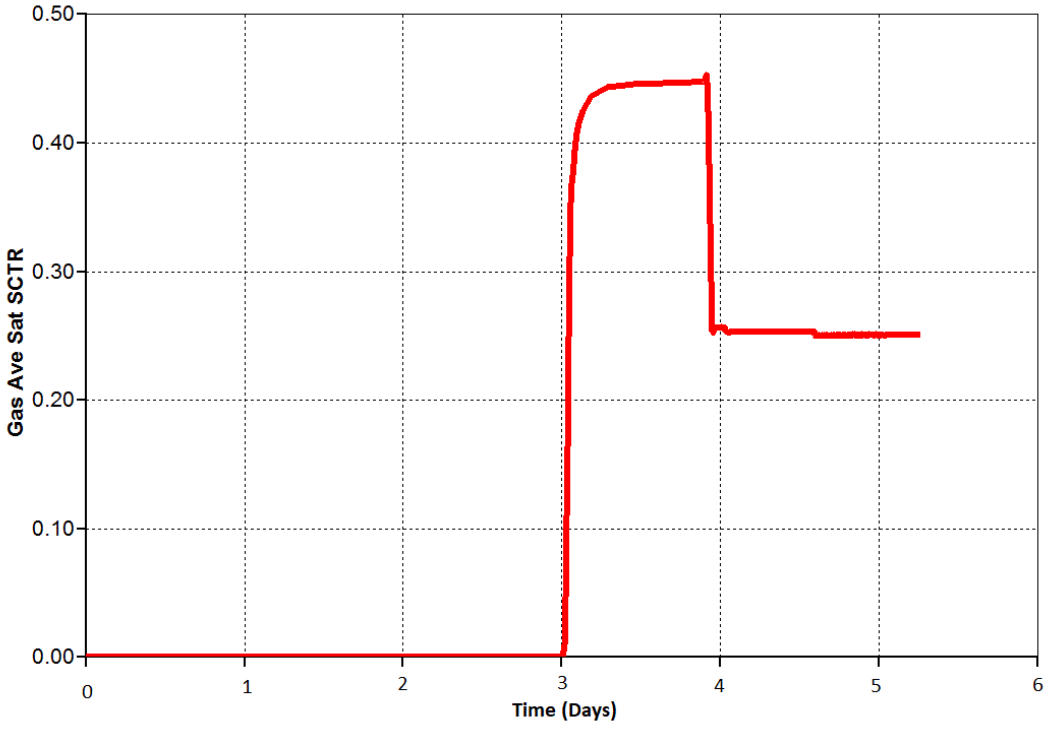

Figure 4.5 Average gas (with steam) saturation during core flood.

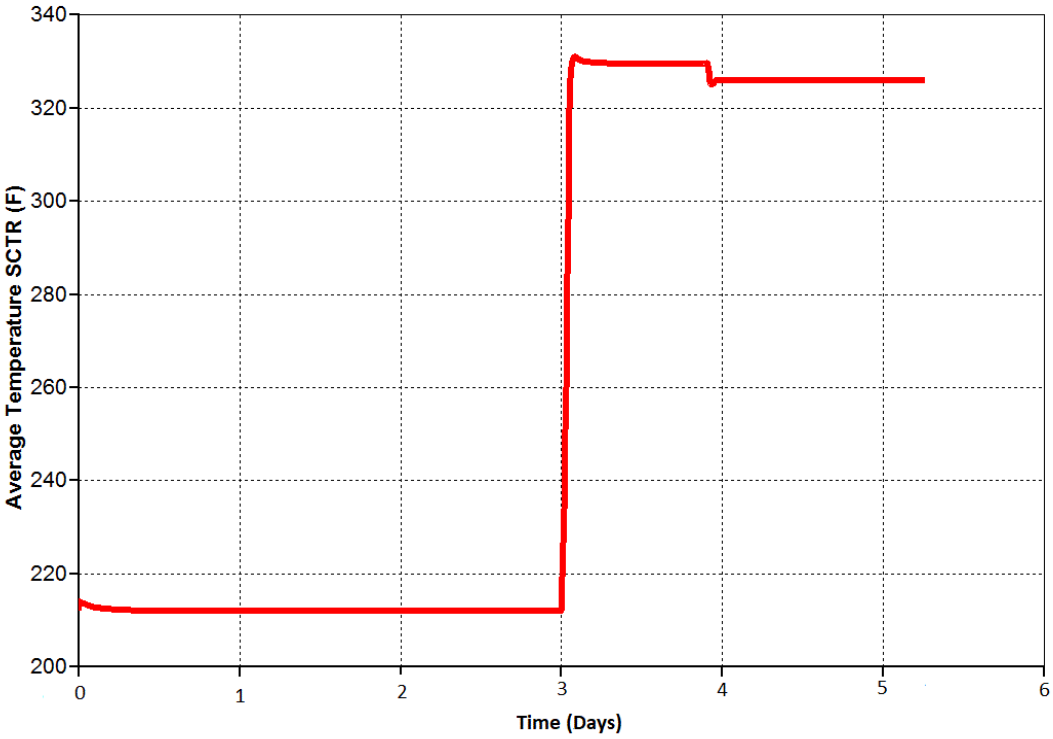

Figure 4.6 Average temperature in core.

Chapter 5: Sensitivity Analysis of Foam Parameters

In this chapter foam parameters' effect on oil recovery, reservoir temperature, average gas saturation, and average reservoir pressure are observed by changing each foam parameter one by one while keeping the other parameters fixed. The main purpose of this chapter is to understand how foam parameters may affect oil recovery and other simulation results.

5.1 METHODOLOGY

Numerous case studies were experimentally performed in order to understand how steam foam method affects residual oil saturation and oil recovery; moreover, to investigate these kinds of effects of steam injection, which was used in cores, and results are compared with steam foam cases under same conditions. However, there are not enough simulations conducted to investigate such effect on simulation results. In addition to study effects of foam on oil recovery, we evaluated how using steam alone and with foam changes incremental oil.

5.1.1 Case Model Properties

Grid block dimensions, initial reservoir conditions and reservoir rock and fluid properties are given in Table 5-1 and the input data file is provided in Appendix A.2. Reservoir shape is given in Figure 5.1.

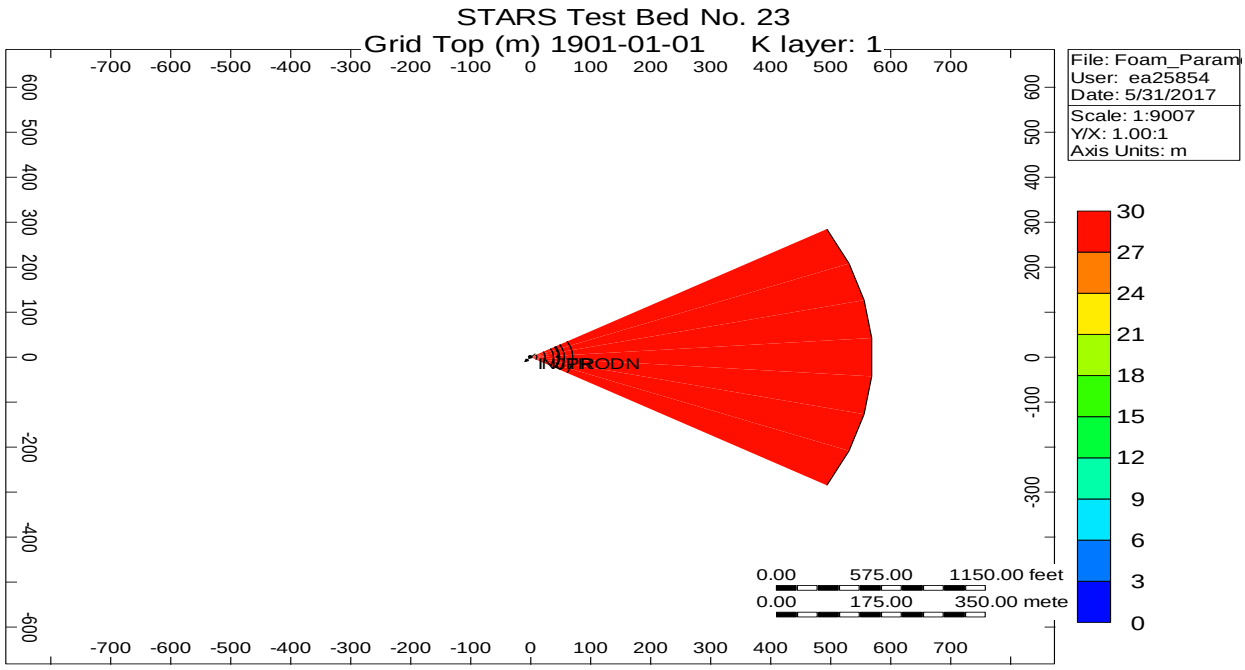

Figure 5.1 Reservoir model shape used for simulation study.

Table 5-1Reservoir model properties.

Number of grid blocks	9x1x3 (Radial)
Grid block size	570^2x3.1415 x(1/6) x15 m^3
Initial Temperature	50 ^oC
Initial pressure	700 kPa
Number of wells	2 total wells 1 production well 1 injection well
Initial gas saturation	0
Steam injection temperature	210 ^oC
Steam injection rate	150 m^3/Day
Steam injection quality	0.7
Oil viscosity	87 cp (121 ^oC)
Permeability $k_x = k_y = k_z$	1000 mD
Porosity	0.35

Table 5-2Water-Oil Relative Permeability values.

Sw	Krw	Krow
0.093000	0.0000000	1.00000
0.150000	1.7000E-4	0.8400000
0.200000	8.0000E-4	0.7100000
0.250000	0.0024000	0.5800000
0.300000	0.0061000	0.4650000
0.400000	0.0250000	0.2780000
0.500000	0.0760000	0.1360000
0.600000	0.1800000	0.0410000
0.650000	0.2600000	0.0130000
0.700000	0.3600000	0.0110000
0.800000	0.5700000	0.0060000
0.900000	0.7500000	0.0000000
1.000000	1.0000000	0.0000000

Table 5-3 Liquid-Gas Relative Permeability values.

Sl	Krg	Krog
0.1500000	1.0000000	0.0
0.4000000	0.9900000	1.0000E-4
0.4200000	0.9850000	8.0000E-4
0.4500000	0.9800000	0.0070000
0.5000000	0.8500000	0.0260000
0.5500000	0.6900000	0.0550000
0.6000000	0.5400000	0.0900000
0.7000000	0.2870000	0.1860000
0.8000000	0.1140000	0.3310000
0.9000000	0.0220000	0.5700000
0.9500000	0.0045000	0.7600000
1.00000	0.0000000	1.0000000

In Table 5-2, *Sw*, *Krw*, *Krow* are water saturation, water relative permeability, and oil relative permeability to water, respectively. In Table 5-3, *Sl*, *Krg*, and *Krog* are liquid saturation, gas relative saturation and gas relative permeability to gas, respectively. Capillary effect assumed to be zero for both tables. Relative permeability graphs are given in Figure 5.2. Foam parameters that are optimized in this study are explained in Table 5-4.

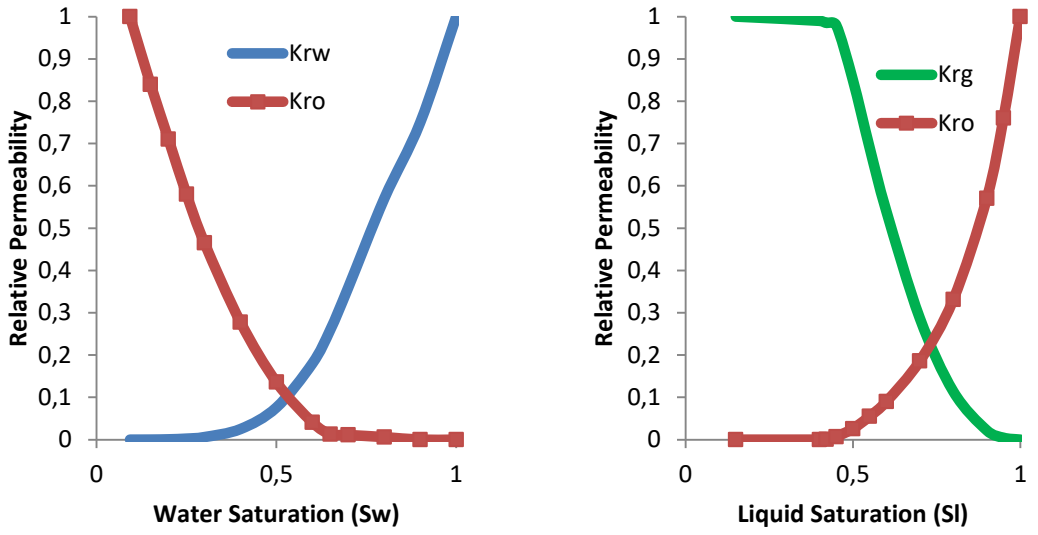

a) Oil-water relative permeability b) Liquid-gas relative permeability

Figure 5.2 Relative permeability of fluids.

Table 5-4 Optimized foam parameters in this study.

Parameter Name	Range
fmoil: Critical oil saturation value used in dimensionless foam interpolation calculation.	0 – 1
fmsurf: Critical component mole fraction value used in dimensionless foam interpolation calculation.	0 – 1
fmcap: Reference rheology capillary number value used in dimensionless foam interpolation calculation.	0 – 1
Epoil: Exponent for oil saturation contribution	0 – 5
Epsurf: Exponent for composition contribution to dimensionless foam interpolation calculation.	(-4) – 4
Epcap: Exponent for capillary number contribution to dimensionless foam interpolation calculation.	(-10) – 10
Fmmob: Reference foam mobility reduction factor used in dimensionless foam interpolation calculation.	0 – 100000

Table 5-5 Foam mathematical model.

$k_{rg}^{f} = k_{rg} \times FM$
$FM = \frac{1}{1 + fmmob(F_1 \times F_2 \times F_3 \times F_4 \times F_5 \times F_6)}$
$F_1 = \left(\frac{\text{MOLE FRACTION(ICPREL)}}{\text{FMSURF}}\right)^{EPSURF}$
$F_2 = \left(\frac{\text{FMOIL - OIL SATURATION}}{\text{FMOIL-FLOIL}}\right)^{EPOIL}$
$F_3 = \left(\frac{\text{FMCAP}}{\text{CAPILLARY NUMBER}}\right)^{EPCAP}$

Foam mathematical model is given in Table 5-5. That model has already been given in Chapter 3, but in Table 5-5 foam parameters which are changed are given. F4, F5, and F6 have not been changed in this study. FM, k_{rg}, and k_{rgf} are inverse mobility reduction factor, gas relative permeability without foam, and gas relative permeability with foam, respectively.

5.2 RESULTS AND CONCLUSION

This section presents the simulation results for layer 1, which is defined as 1 to 7 in X direction, 1 to 1 for Y direction, and 1 to 3 for Z direction, for changed foam parameters.

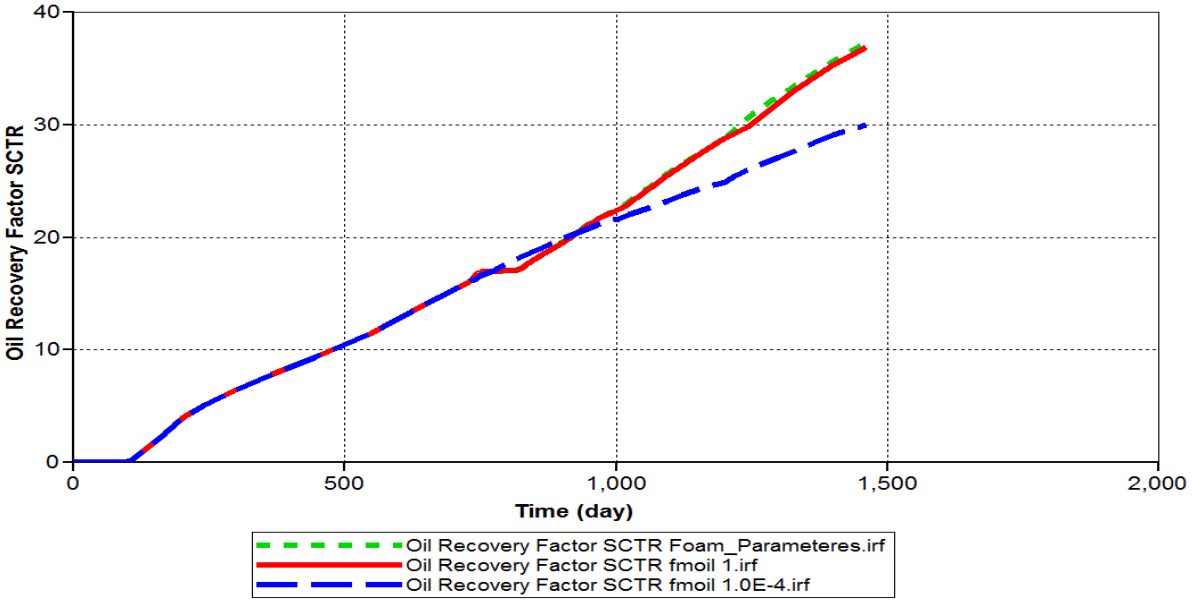

Figure 5.3 Oil recovery factor profiles for changing fmoil values.

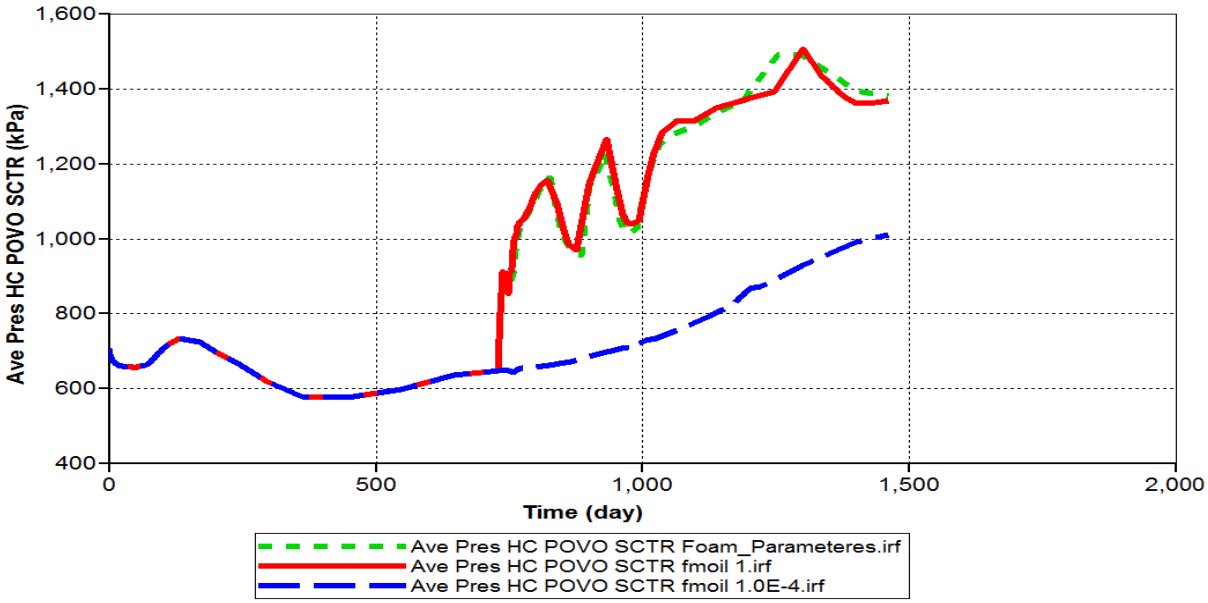

Figure 5.4 Average pressure profiles for changing fmoil values.

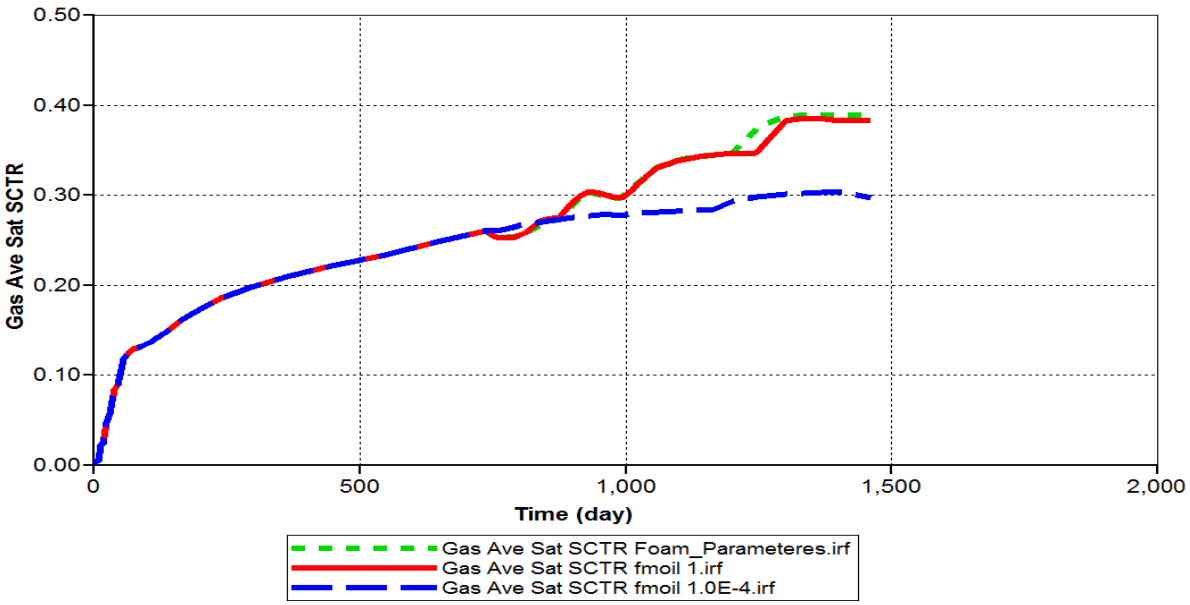

Figure 5.5 Average gas saturation profiles for changing fmoil values.

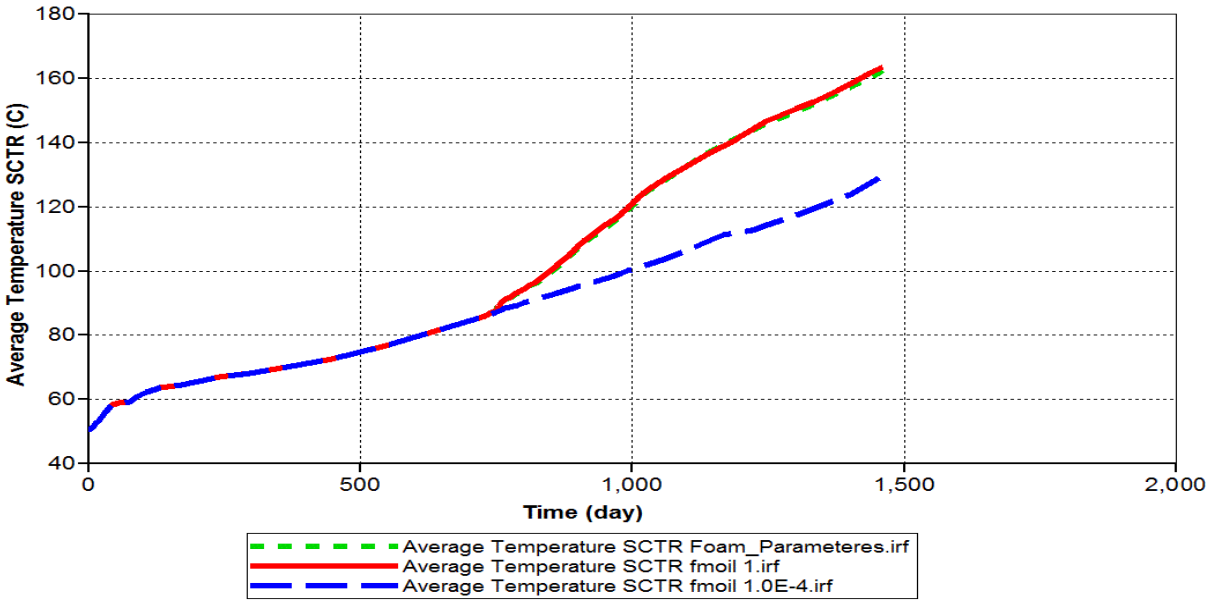

Figure 5.6 Average temperature profiles for changing fmoil values.

Fmoil for “foam parameters” case is 0.5. For other cases Fmoil values are 1 and 0.0004. Figure 5.3 gives oil recovery factor profiles for changing Fmoil values. For oil recovery there is not much difference between Fmoil 0.5 and 1. Fmoil 0.0004 gives less oil recovery. Figure 5.4 gives average pressure profiles for changing fmoil values. Pressure change caused by average gas saturation change. Figure 5.5 gives average gas saturation profiles for changing Fmoil values. When we decrease Fmoil value, gas mobility will be less. That causes more gas trapping and less gas saturation. Figure 5.6 gives average temperature profiles for changing fmoil values.

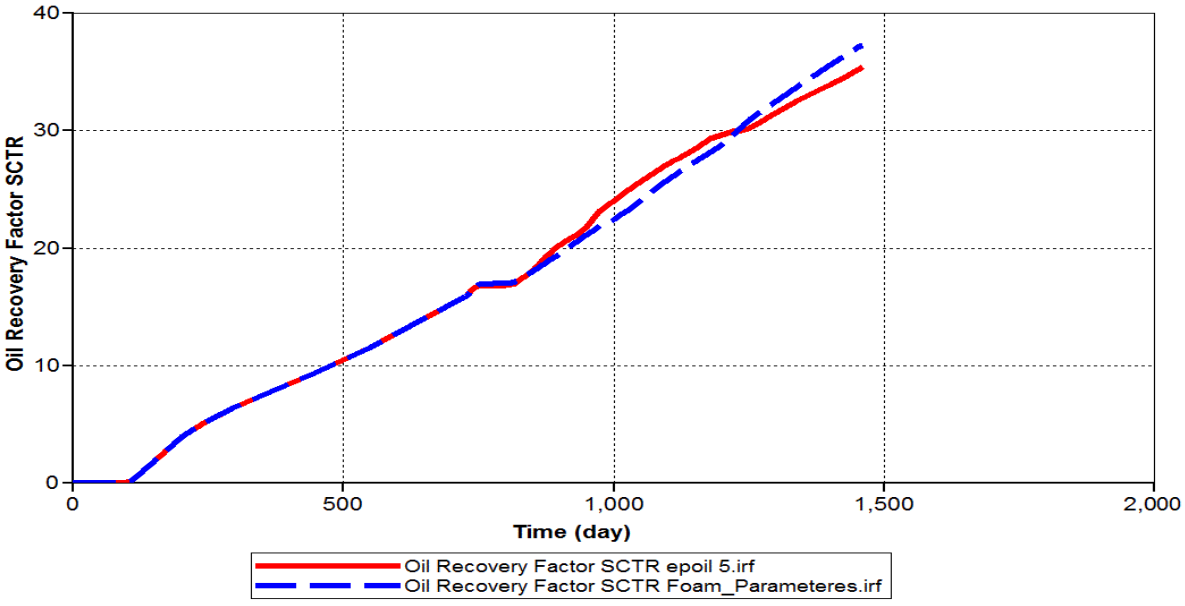

Figure 5.7 Oil recovery factor profiles for changing epoil values.

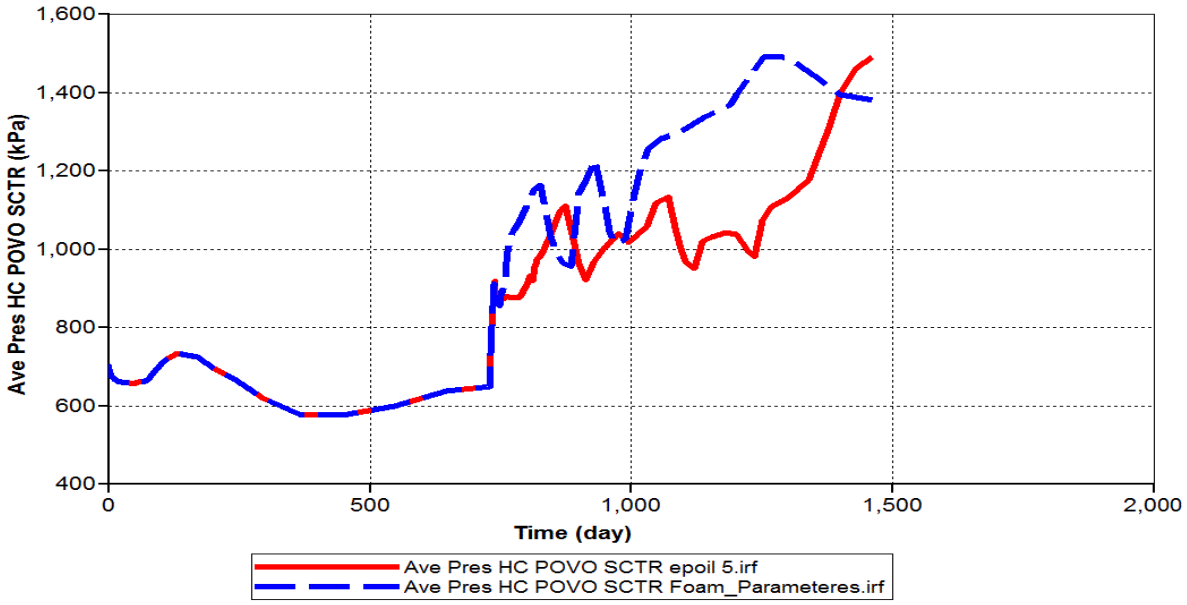

Figure 5.8 Average pressure profiles for changing epoil values.

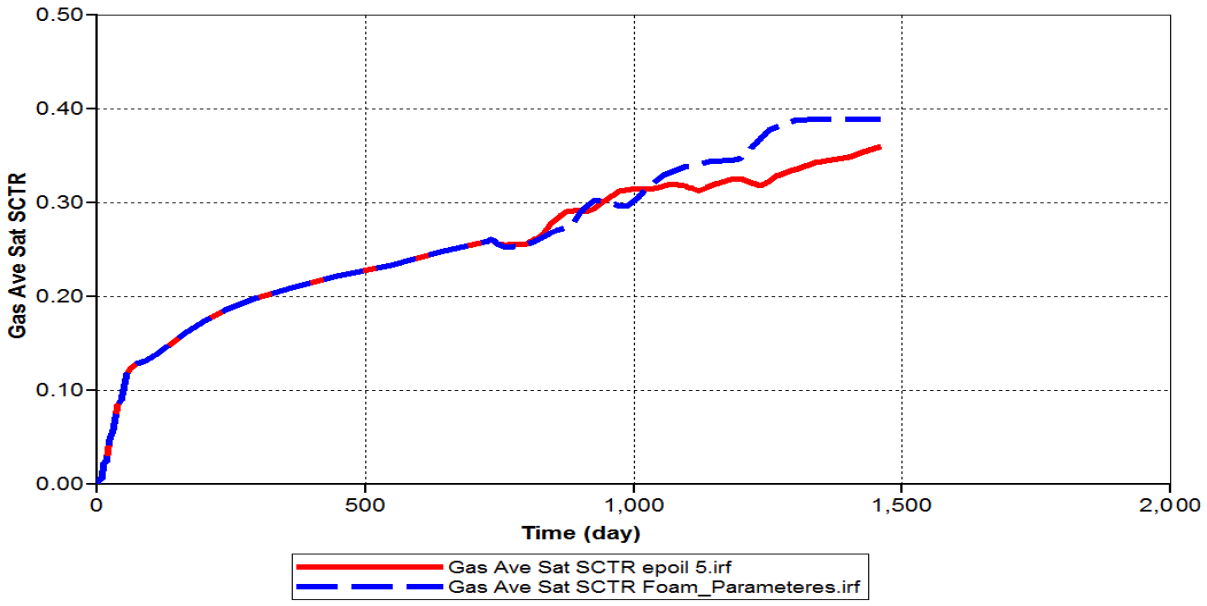

Figure 5.9 Average gas saturation profiles for changing epoil values.

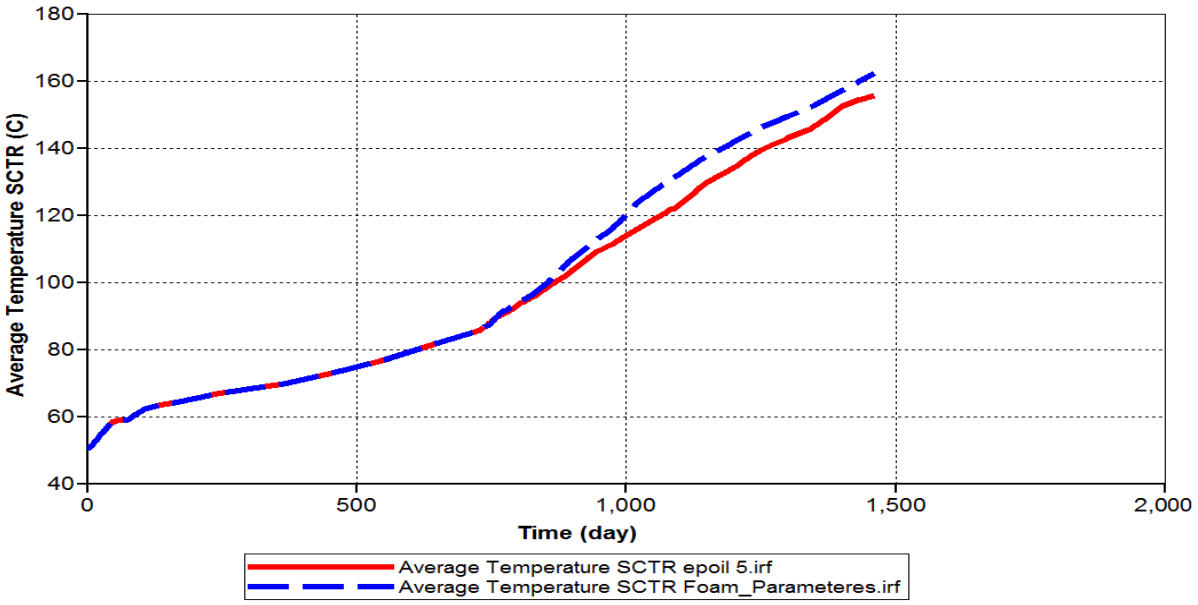

Figure 5.10 Average temperature profiles for changing epoil values.

In this case, "foam parameters" Epoil value is 1 while it is 5 in the other simulation. By changing Epoil values Figure 5.7, giving oil recovery factor, is obtained, and it is observed that there is a slight difference in oil recovery. Also Figures 5.8 and 5.9, which are average pressure and average gas saturation profiles respectively, are obtained by changing Epoil values. As Epoil value decreases, gas mobility increases, causing less gas trapping and triggering more gas saturation. Oil saturation is 0.734 and Floil has a value larger than 0.5 and less than 1. This is the reason that it does not give much change until Fmoil value of 0.0004. Figure 5.10 gives average temperature profiles for changing epoil values.

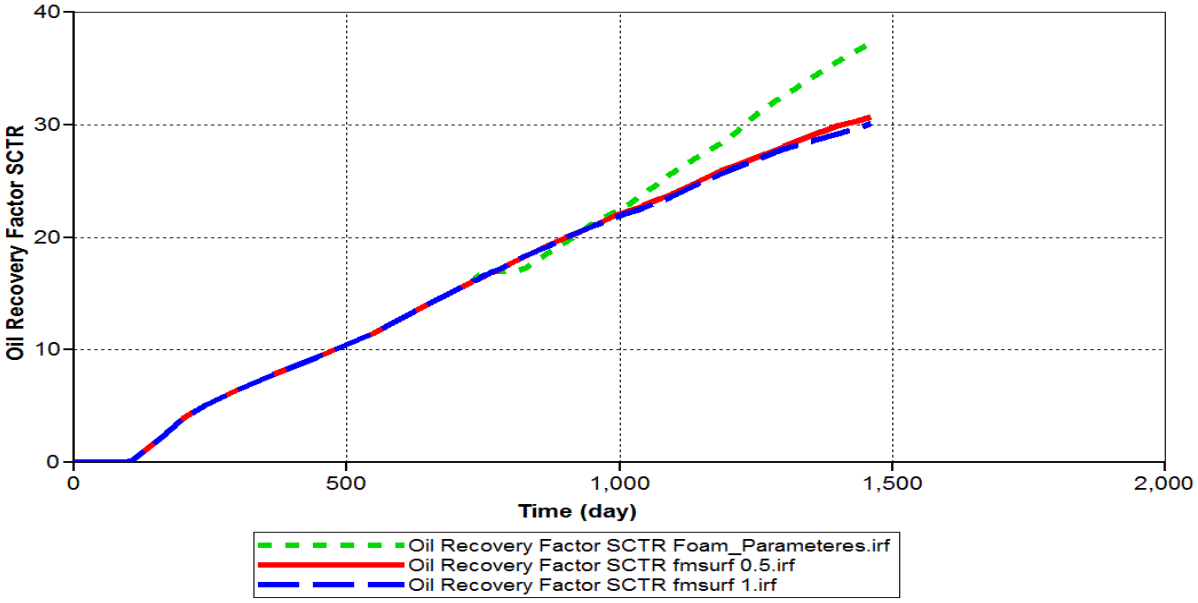

Figure 5.11 Oil recovery factor profiles for changing fmsurf values.

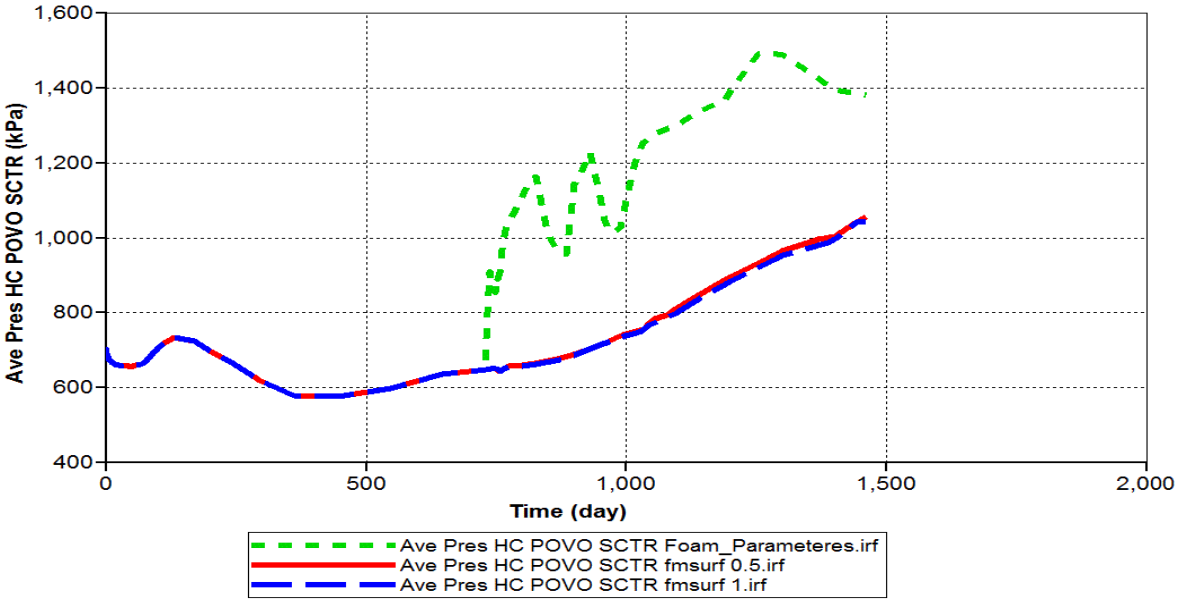

Figure 5.12 Average pressure profiles for changing fmsurf values.

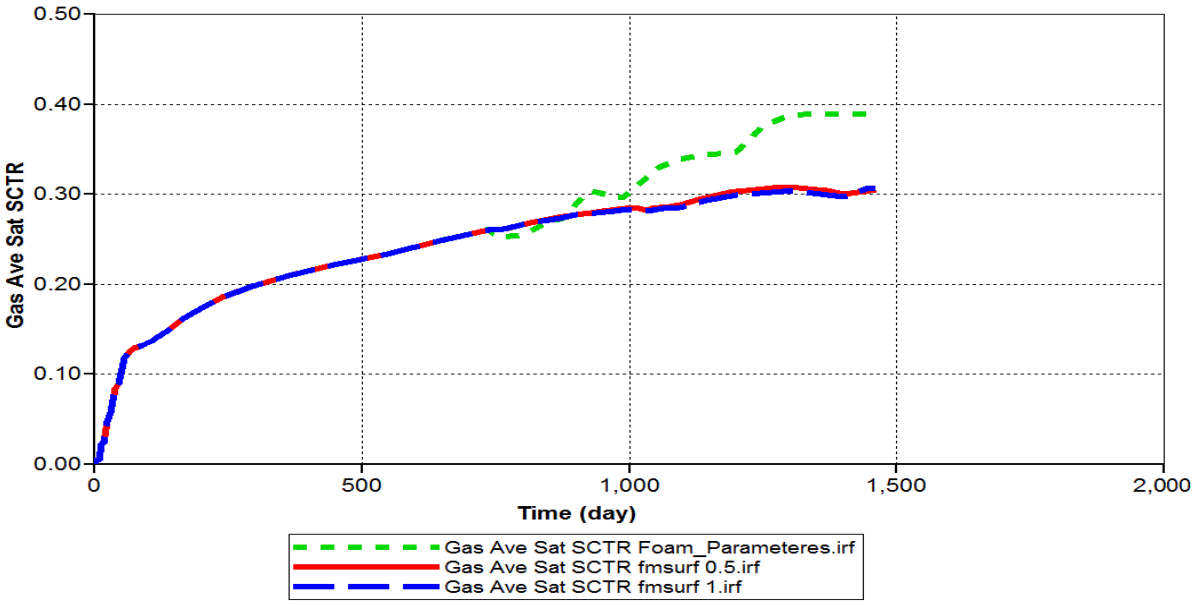

Figure 5.13 Average gas saturation profiles for changing fmsurf values.

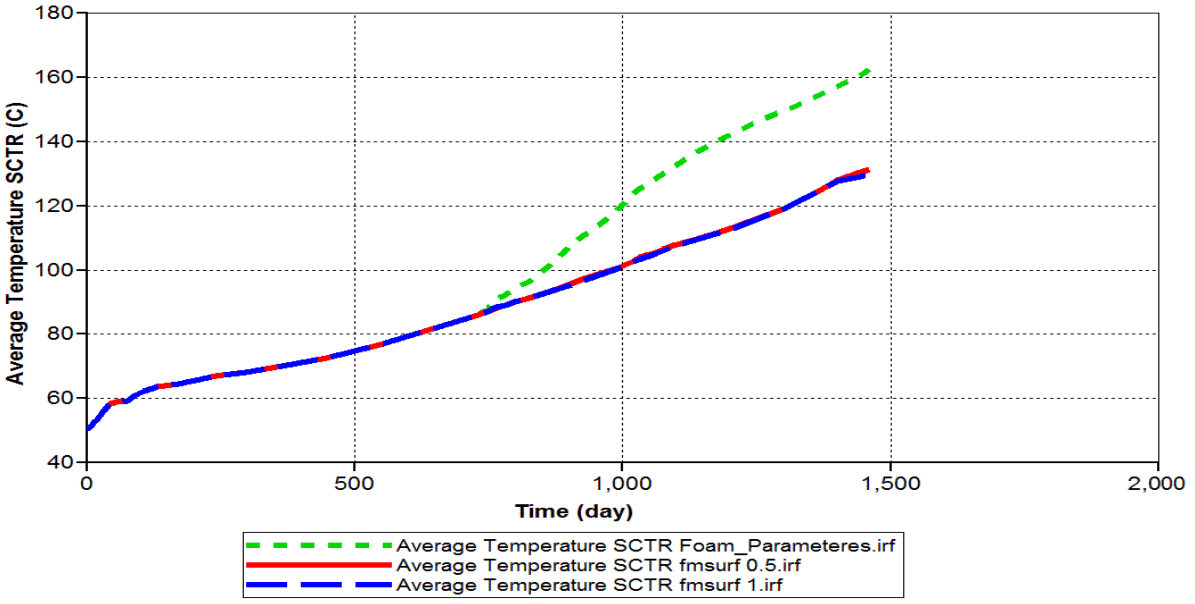

Figure 5.14 Average temperature profiles for changing fmsurf values.

Fmsurf for “foam parameters” case is 0.0001875 and for other cases, Fmsurf values are 0.5 and 1. Figure 5.11 gives oil recovery factor profiles for changing Fmsurf values. Oil recoveries are not remarkably different for 0.5 and 1 Fmsurf values. For Fmsurf 0.0001875 oil recovery is higher than others. Figures 5.12 and 5.13 give average pressure and average gas saturation profiles for changing Fmsurf values, respectively. Pressure change caused by average gas saturation changes. When we decrease Fmsurf value, gas mobility will be higher causing less gas trapping in effect causing more gas saturation. Figure 5.14 gives average temperature profiles for changing Fmsurf values.

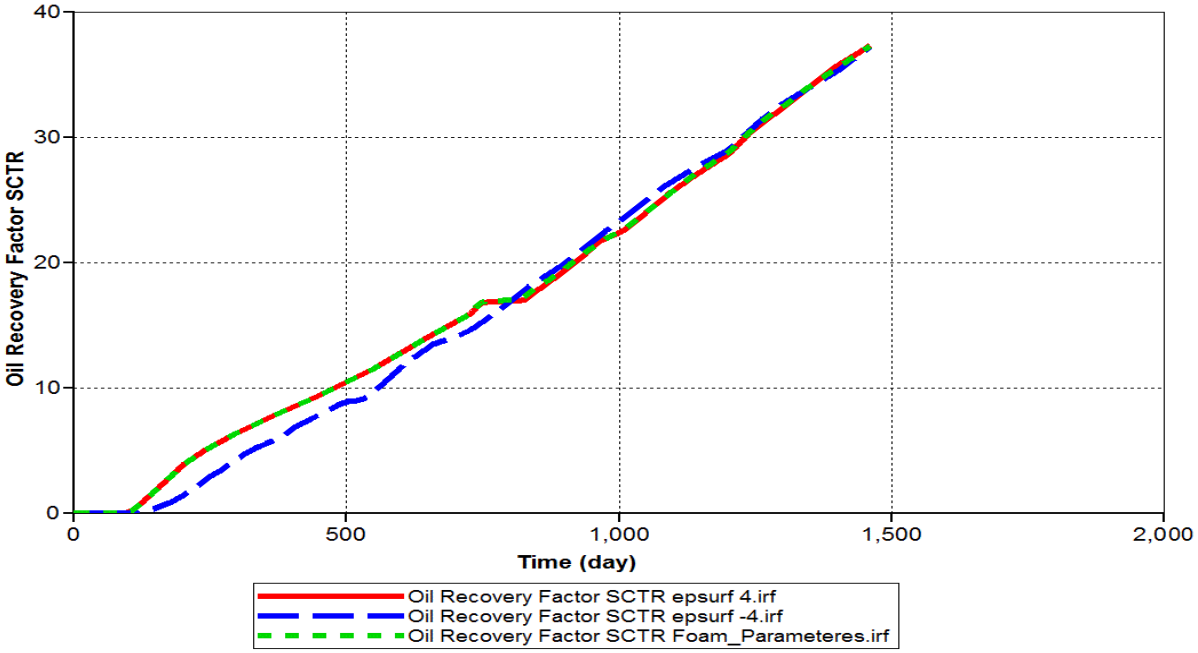

Figure 5.15 Oil recovery factor profiles for changing epsurf values.

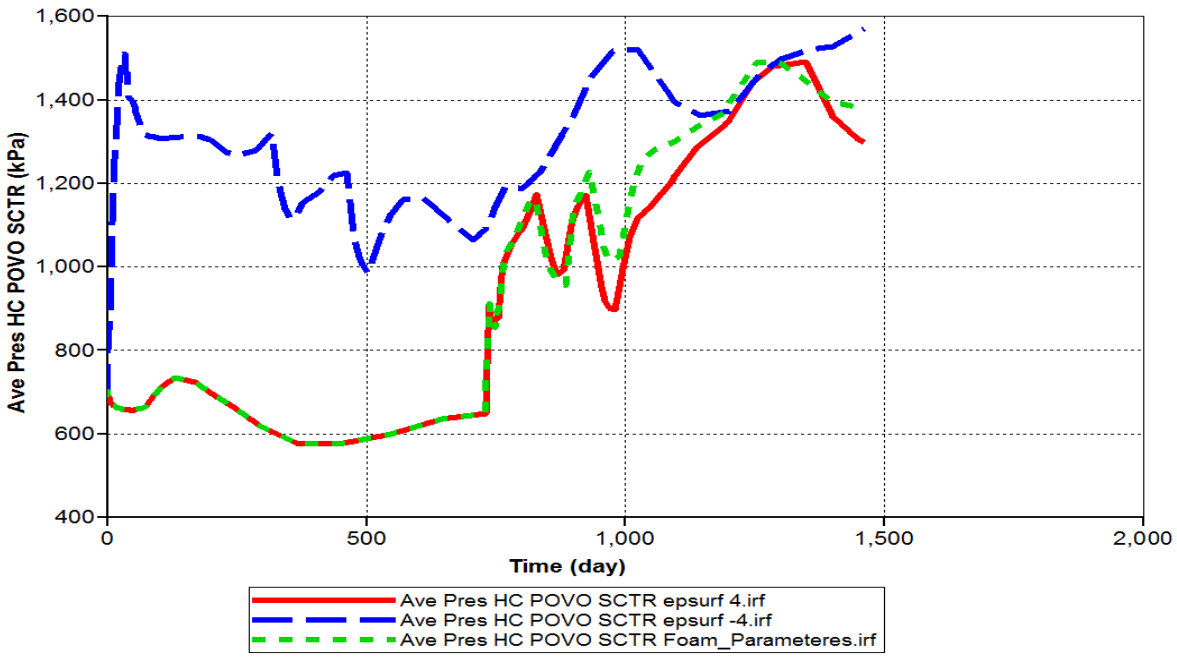

Figure 5.16 Average pressure profiles for changing epsurf values.

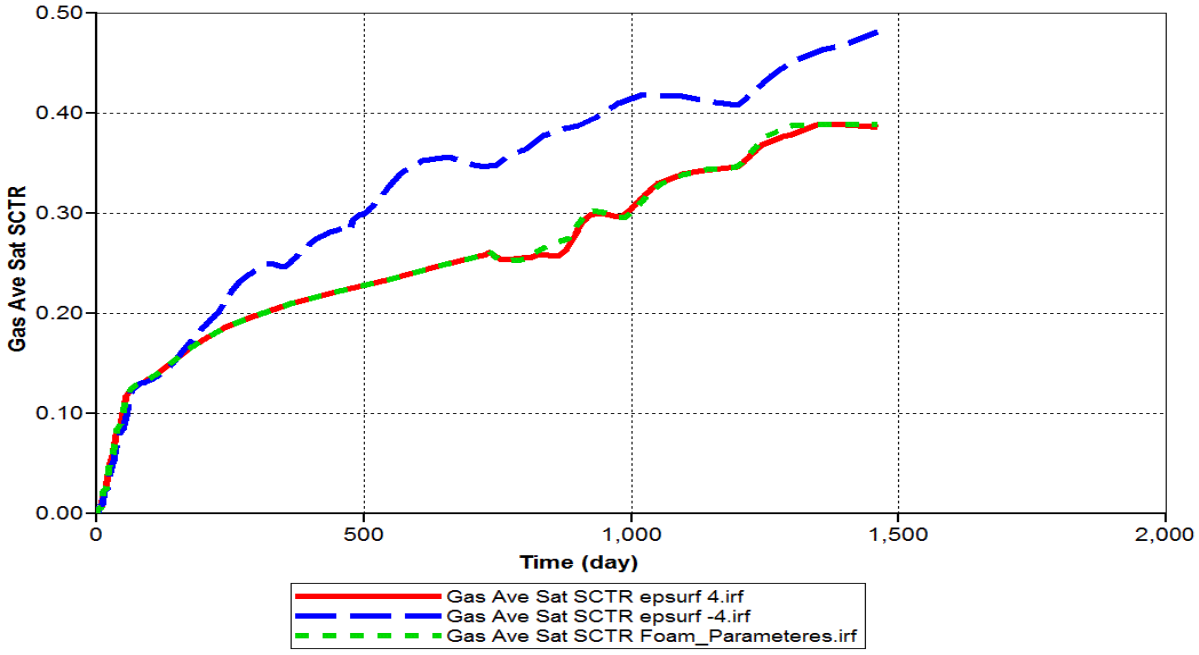

Figure 5.17 Average gas saturation profiles for changing epsurf values.

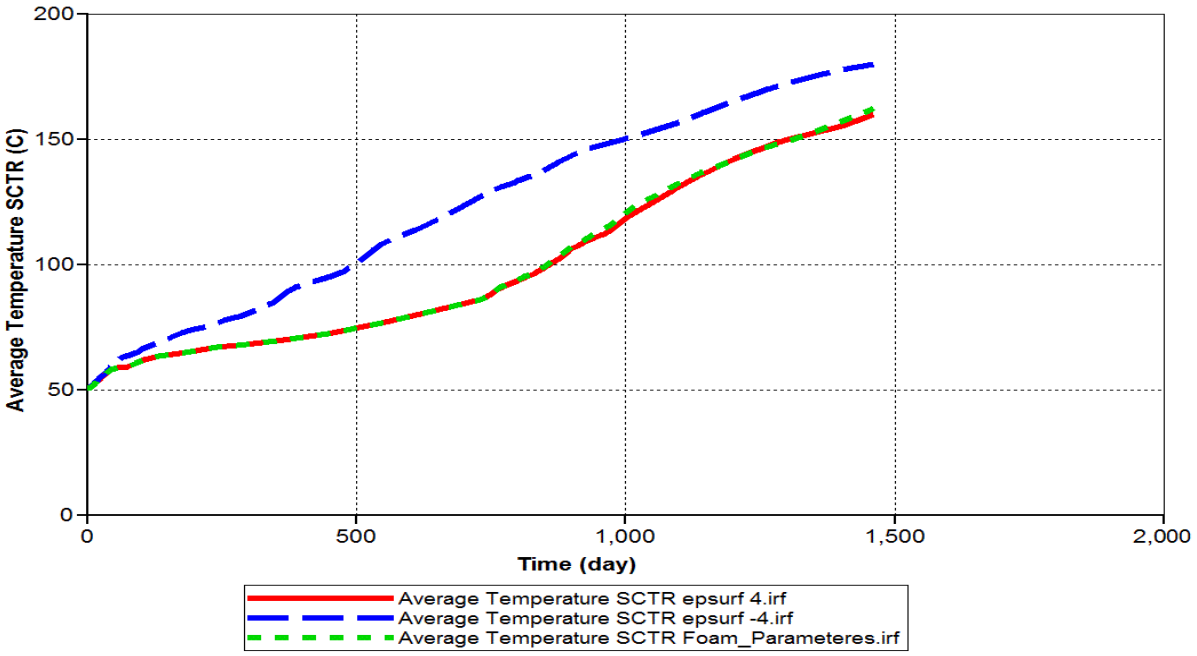

Figure 5.18 Average temperature profiles for changing epsurf values.

In the present case, Epsurf value is equal to 1 for "foam parameters" and equal to (-4) and 4 for other simulations. According to Figure 5.15, which gives oil recovery factor profiles for different Epsurf values, there is negligible difference between oil recovery factors. Based on Figures 5.16 and 5.17, giving average pressure and average gas saturation profiles for changing Epsurf values, respectively, the decrease in Epsurf value entails higher gas mobility. Subsequently, this increase in gas mobility causes less gas trapping and more gas saturation. Figure 5.18 gives average temperature profiles for changing Epsurf values.

When we decrease Fmsurf we expect F1 to increase which causes FM to decrease resulting strong foam. Strong foam causes more trapping and less gas saturation.

When we decrease Epsurf, F1 decreases and this causes FM to increase. This feature in effect causes weak foam, which results in less trapping and more gas saturation.

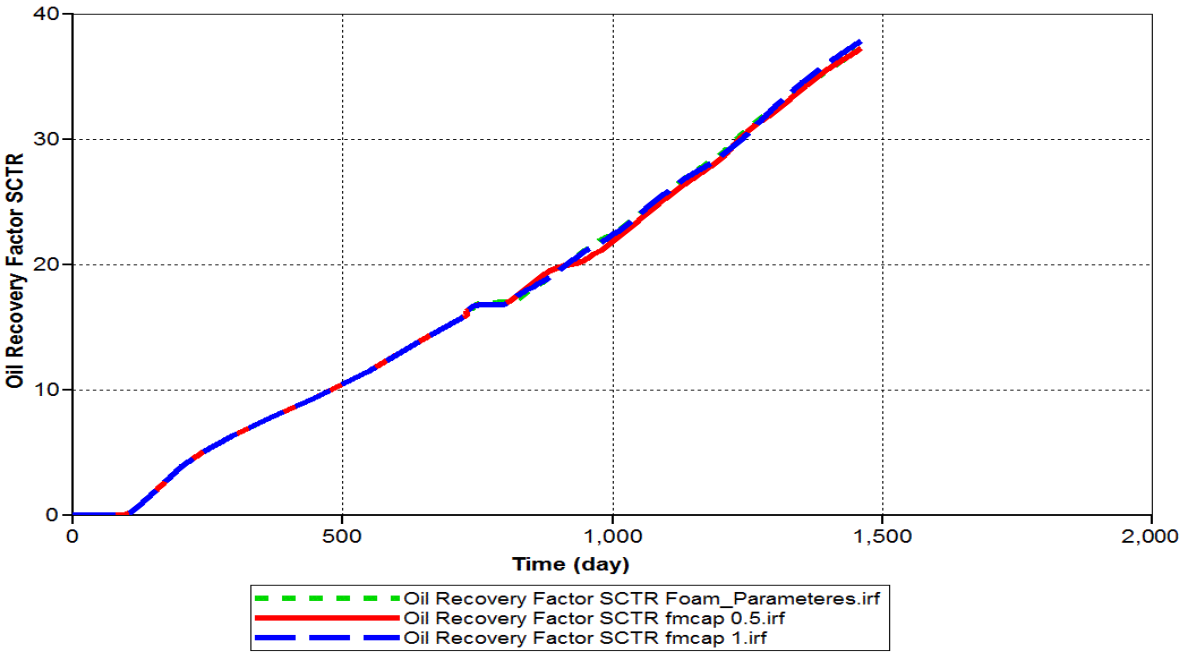

Figure 5.19 Oil recovery factor profiles for changing fmcap values.

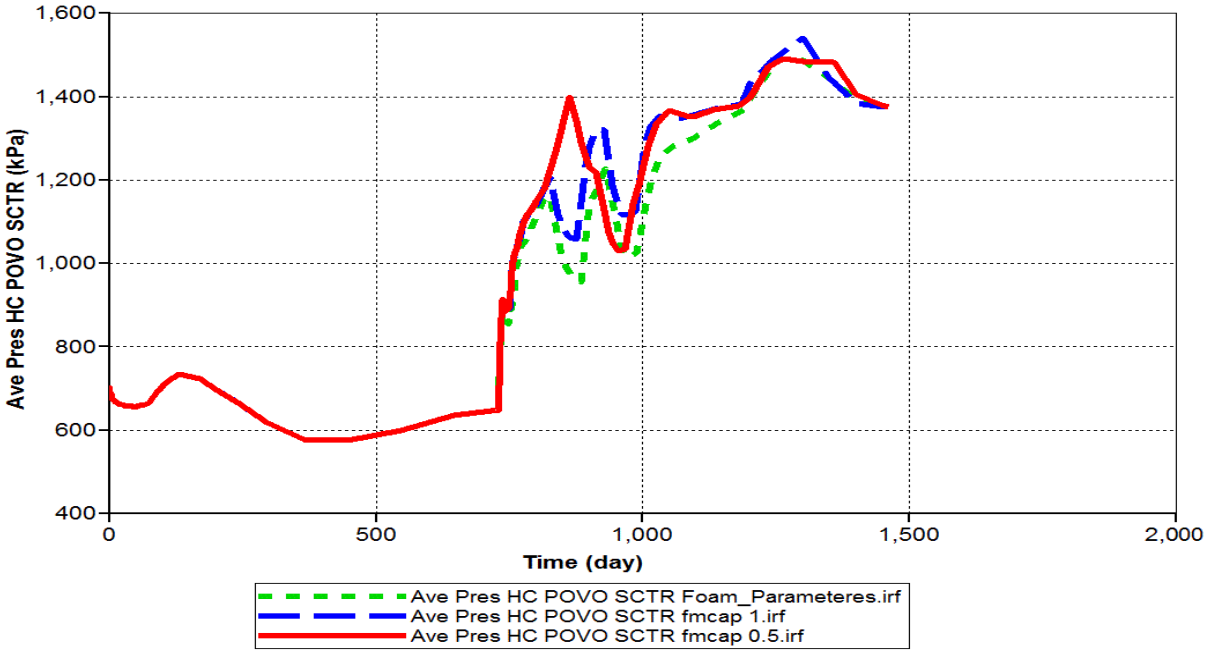

Figure 5.20 Average pressure profiles for changing fmcap values.

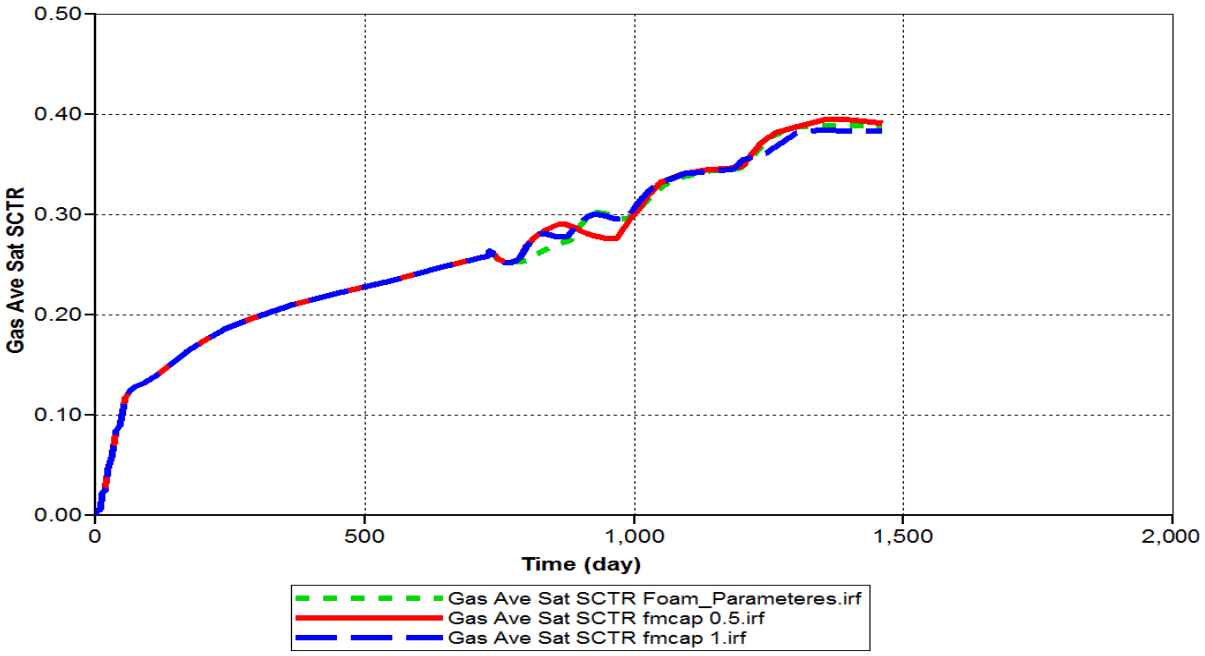

Figure 5.21 Average gas saturation profiles for changing fmcap values.

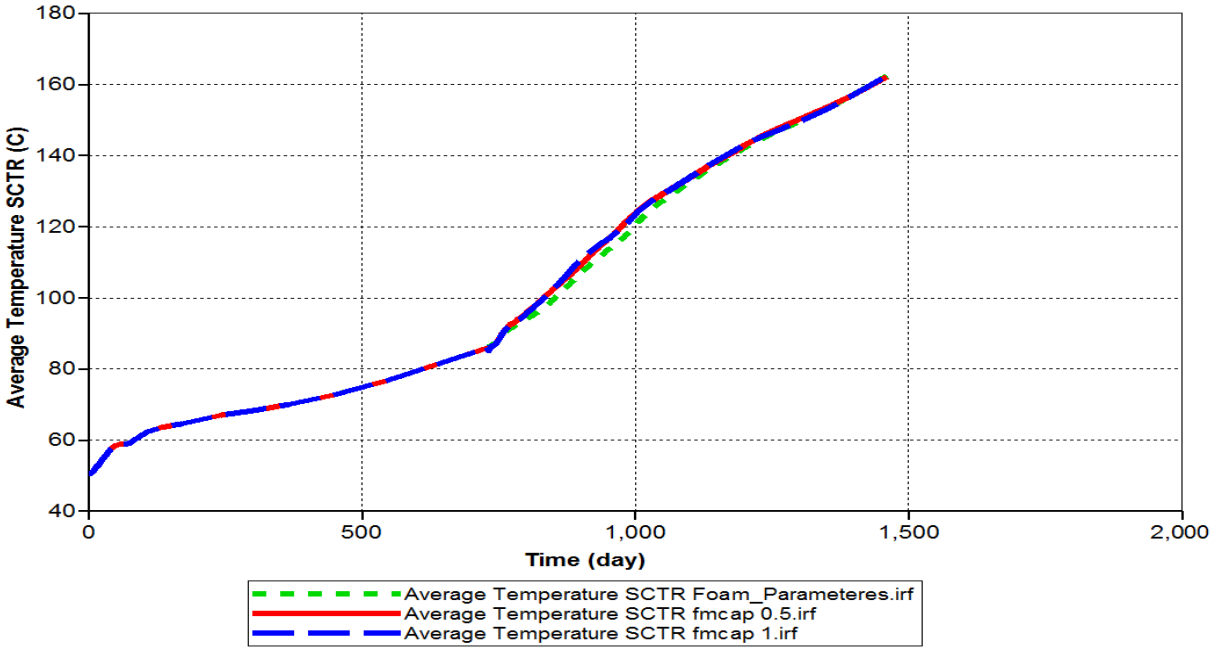

Figure 5.22 Average temperature profiles for changing fmcap values.

Fmcap for “foam parameters” case is 0.0004. For other cases, Fmcap values are 0.5 and 1. Figure 5.19 gives oil recovery factor profiles for changing Fmcap values. For oil recovery there is no difference. Figures 5.20 and 5.21 give average pressure and average gas saturation profiles for changing Fmcap values, respectively. Pressure and average gas saturation also follow the same trend. Based on the results obtained from these simulations Fmcap does not make much difference for foam. Figure 5.22 gives average temperature profiles for changing Fmcap values.

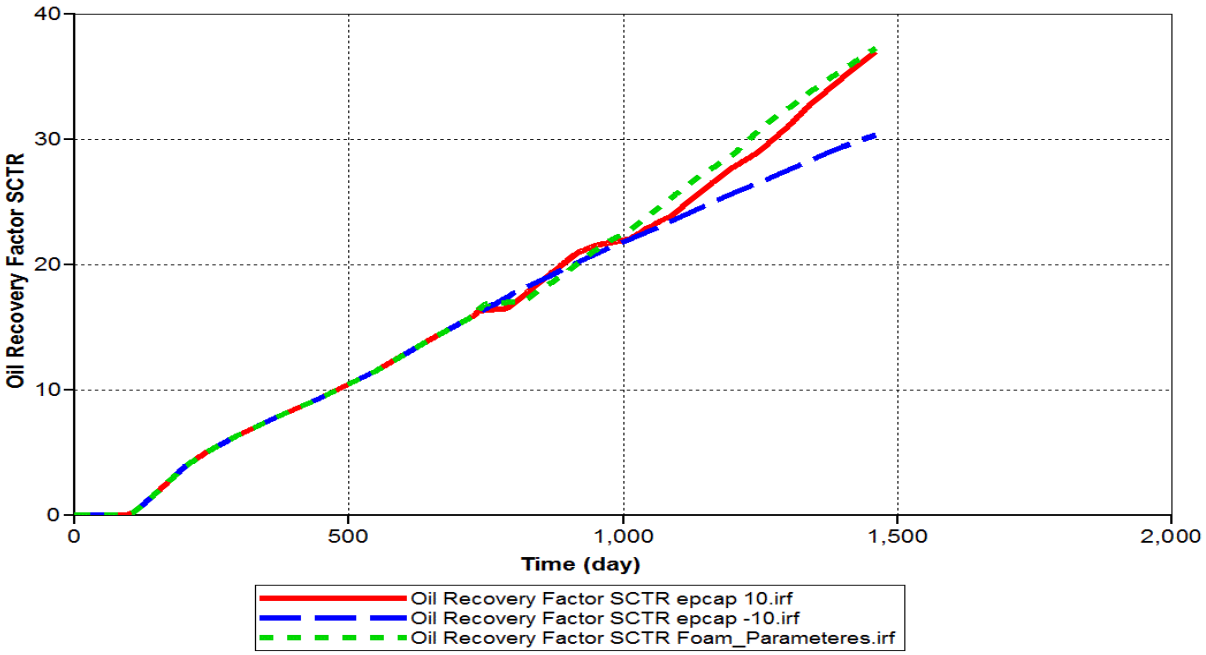

Figure 5.23 Oil recovery factor profiles for changing epcap values.

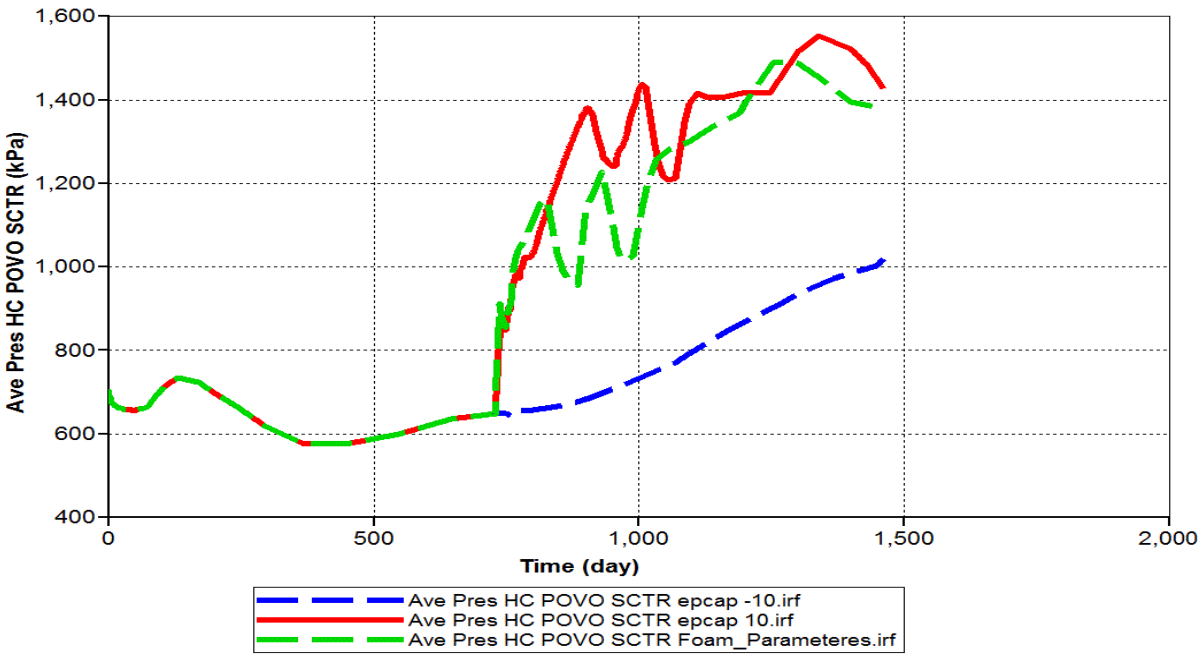

Figure 5.24 Average pressure profiles for changing epcap values.

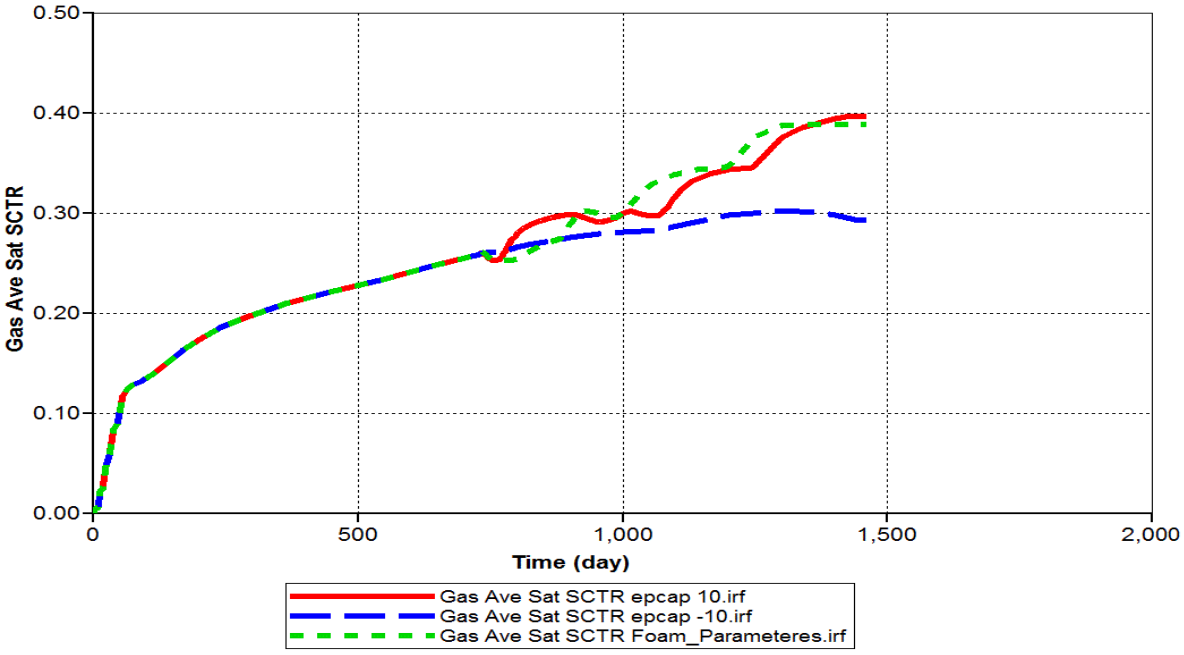

Figure 5.25 Average gas saturation profiles for changing epcap values.

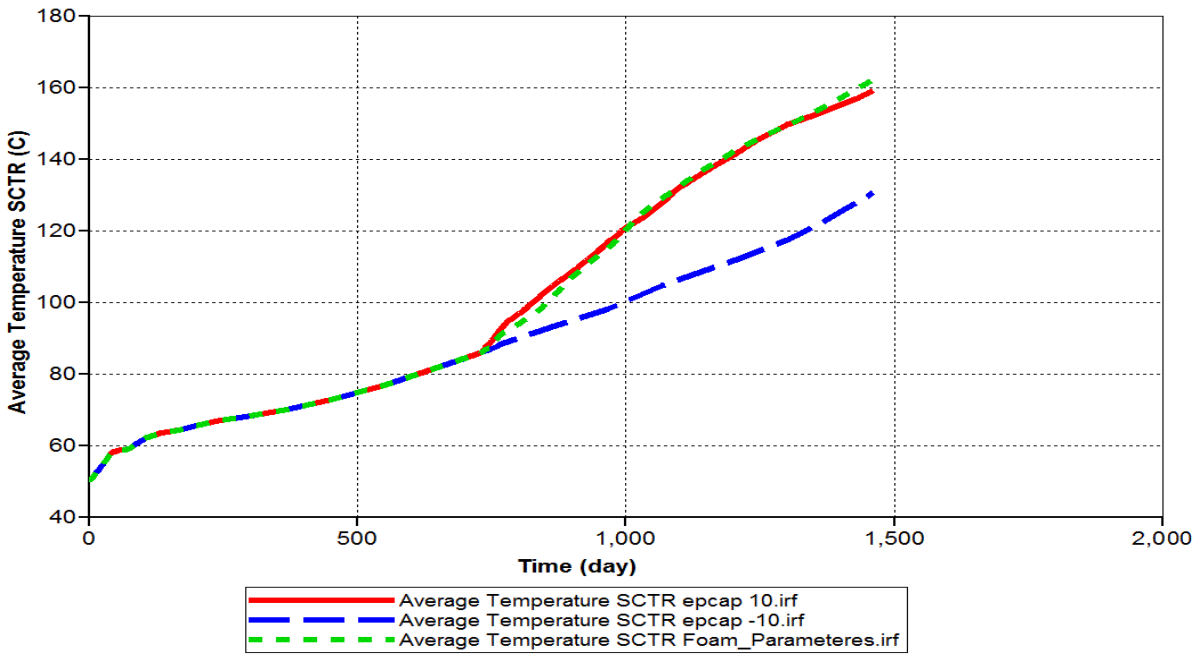

Figure 5.26 Average temperature profiles for changing epcap values.

Epcap value is 1 for "foam parameters" and (-10) and 10 for other simulations at this scenario. Figure 5.23, giving oil recovery factor profiles, illustrates that oil recovery factors are slightly different for different Epcap values; the highest recovery is attained while Epcap value is (-10). Figures 5.24 and 5.25, average pressure and average gas saturation profiles, respectively, demonstrate pressure change which caused by average gas saturation change. More gas trapping and less gas saturation are originated from low Epcap value, causing low gas mobility.

When we decrease Fmcap we expect F3 to decrease which causes FM to decrease because of a negative F value. However, it does not seem to affecting gas saturation or other results. This is because the Capillary number is much higher than the Fmcap value.

(Fmcap / Capillary Number) is less than 1. When we decrease Epcap it increases F3 and decreases FM. This decrease in FM causes strong foam and more gas trapping and less gas saturation. Figure 5.26 gives average temperature profiles.

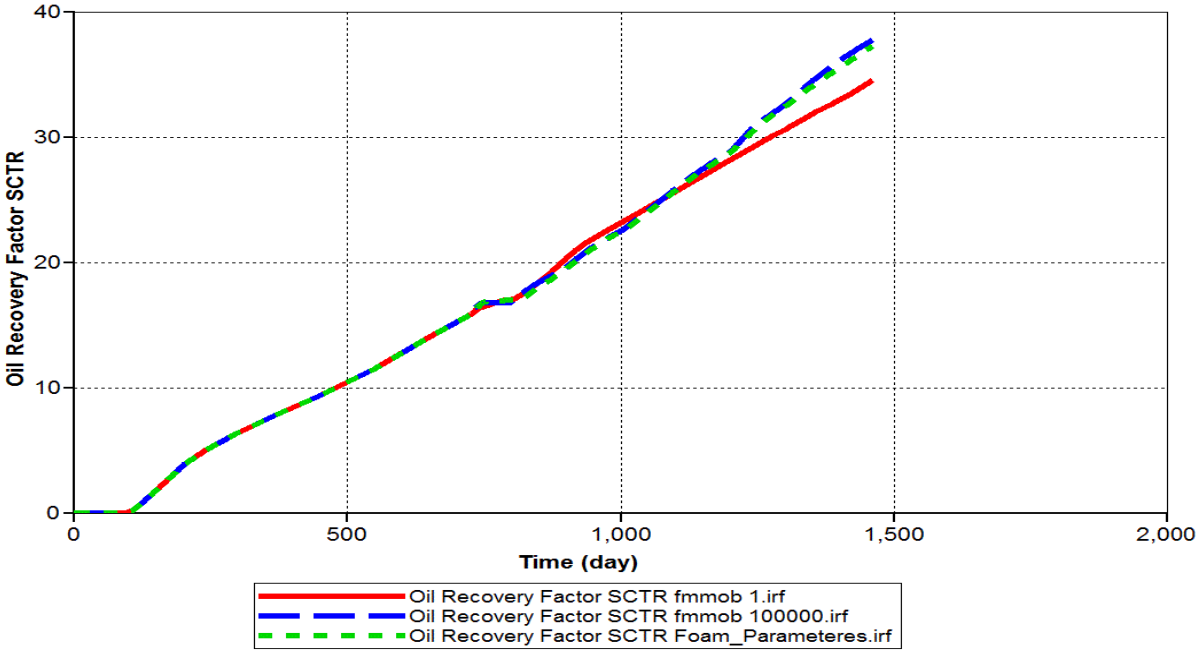

Figure 5.27 Oil recovery factor profiles for changing fmmob values.

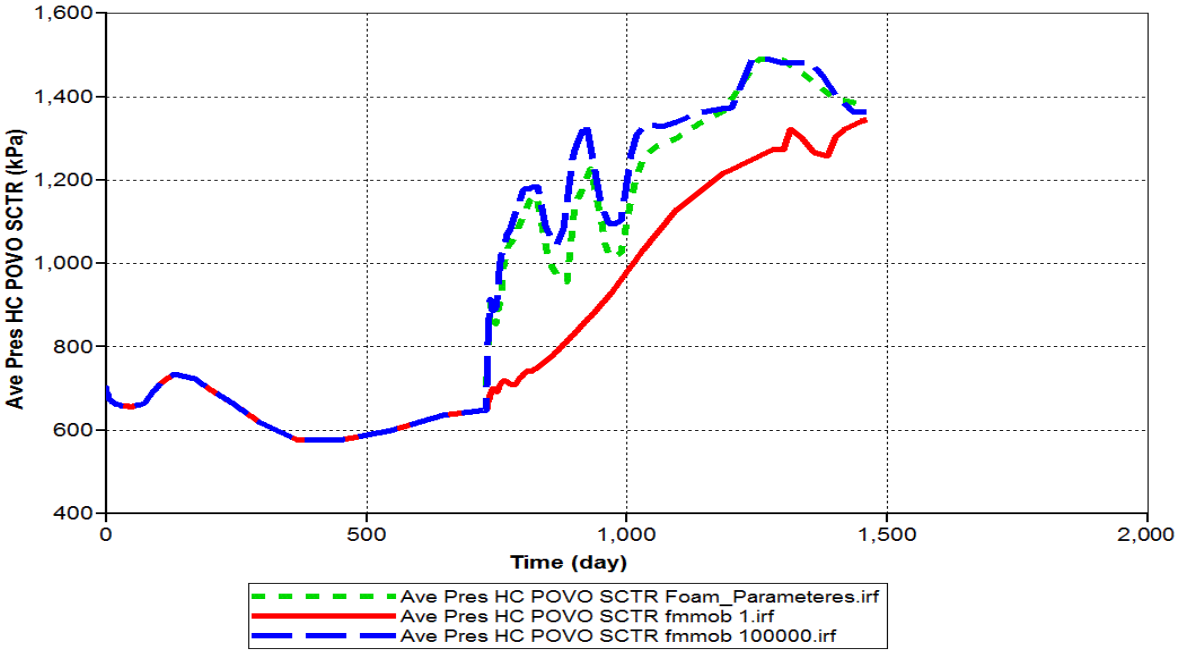

Figure 5.28 Average pressure profiles for changing fmmob values.

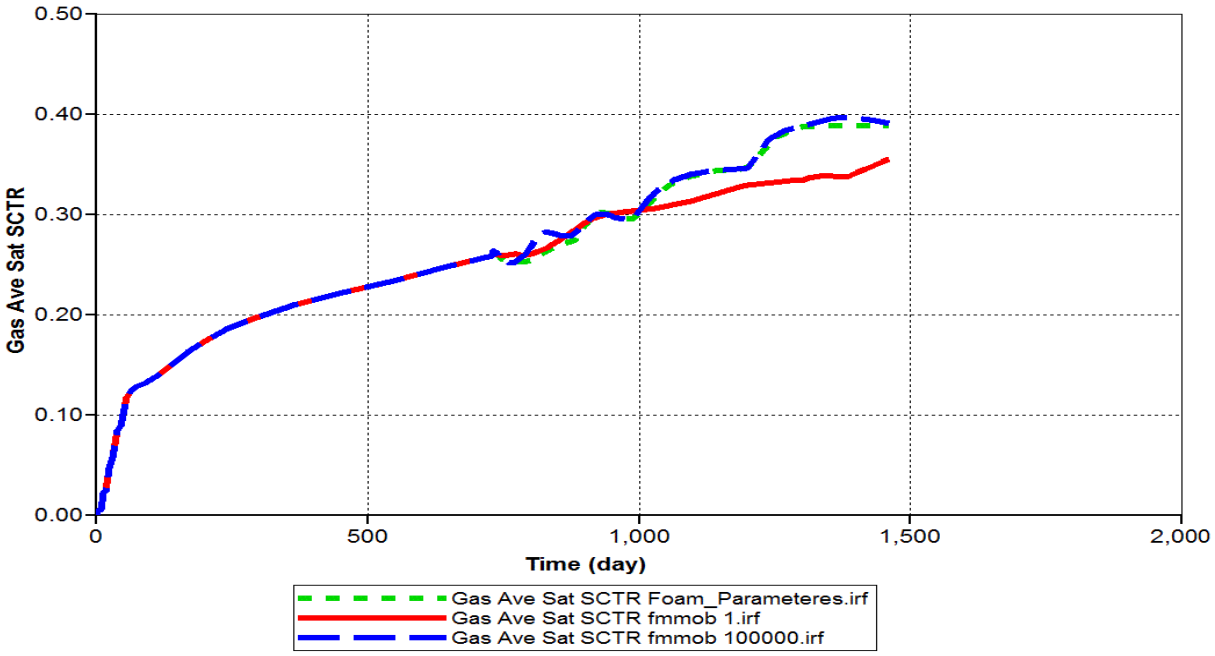

Figure 5.29 Average gas saturation profiles for changing fmmob values.

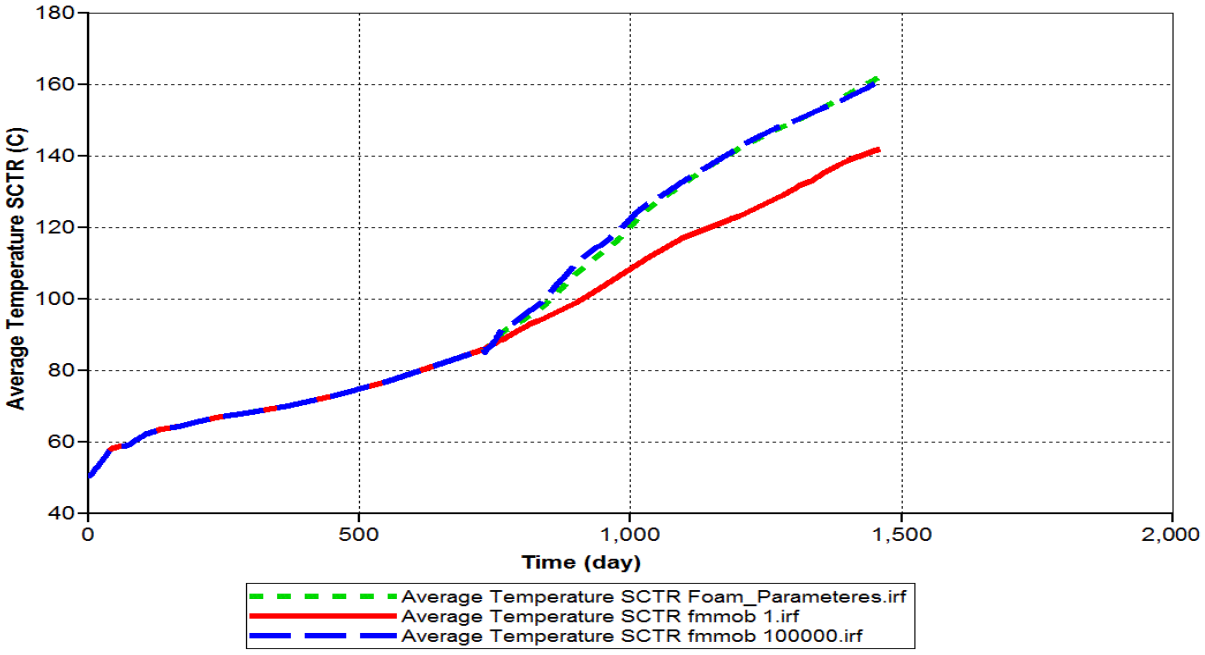

Figure 5.30 Average temperature profiles for changing fmmob values.

Here, Fmmob value for “foam parameters” is 50, and for other simulations, it is 1 and 100000. Figure 5.27 points out altering oil recovery factors by changing Fmmob values. For 100000 and 50 Fmmob values, oil recovery factors are about the same. While fmmob value is 1, oil recovery is low. Figures 5.28, average pressure profile, and Figure 5.29, average gas saturation profile, show low gas mobility for lower Fmmob values which causes more gas trapping and less gas saturation. Figure 5.30 demonstrates average temperature profiles.

Optimized case foam parameters have been chosen regarding results obtained from sensitivity analysis experiments. While parameters were chosen, the following topics were considered in the order of importance:

1) Oil recovery

2) Average Pressure

When comparing results from different values for parameters, the value which gives better oil recovery was picked primarily. For the cases in which oil recovery were the same, the one with lower average pressure was chosen. Based on these considerations, the values for each parameter are given below in Table 5-6:

Table 5-6 Selected foam parameter values.

Parameter	Value
Fmoil	0.5
Epoil	1
Fmsurf	0.0001875
Epsurf	4
Fmcap	0.0004
Epcap	1
Fmmob	50

Results for oil recovery, average pressure, average gas saturation, and average temperature for parameters optimized case and base case are compared below.

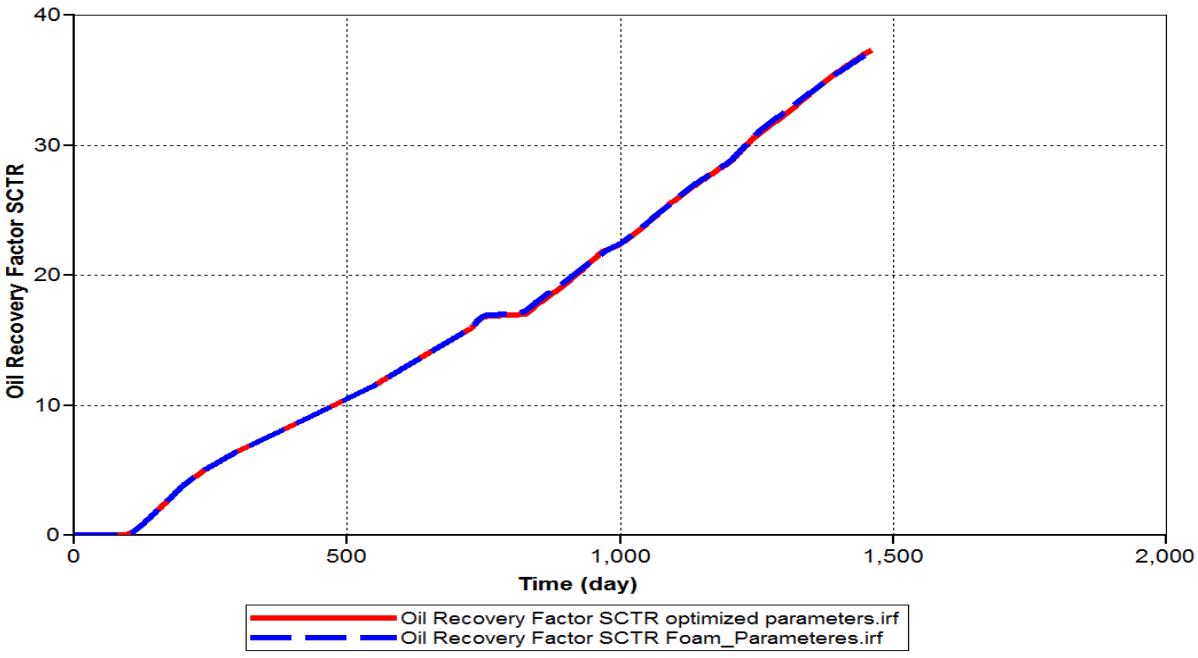

Figure 5.31 Oil recovery factor comparison between optimized and base cases.

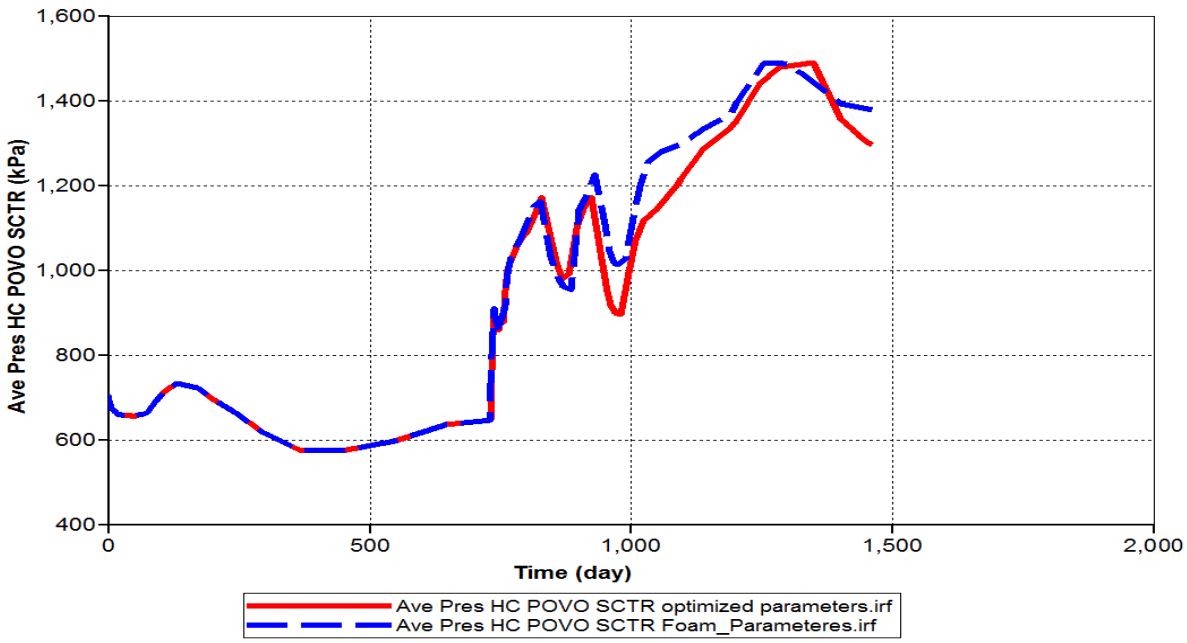

Figure 5.32 Average pressure comparison between optimized and base cases.

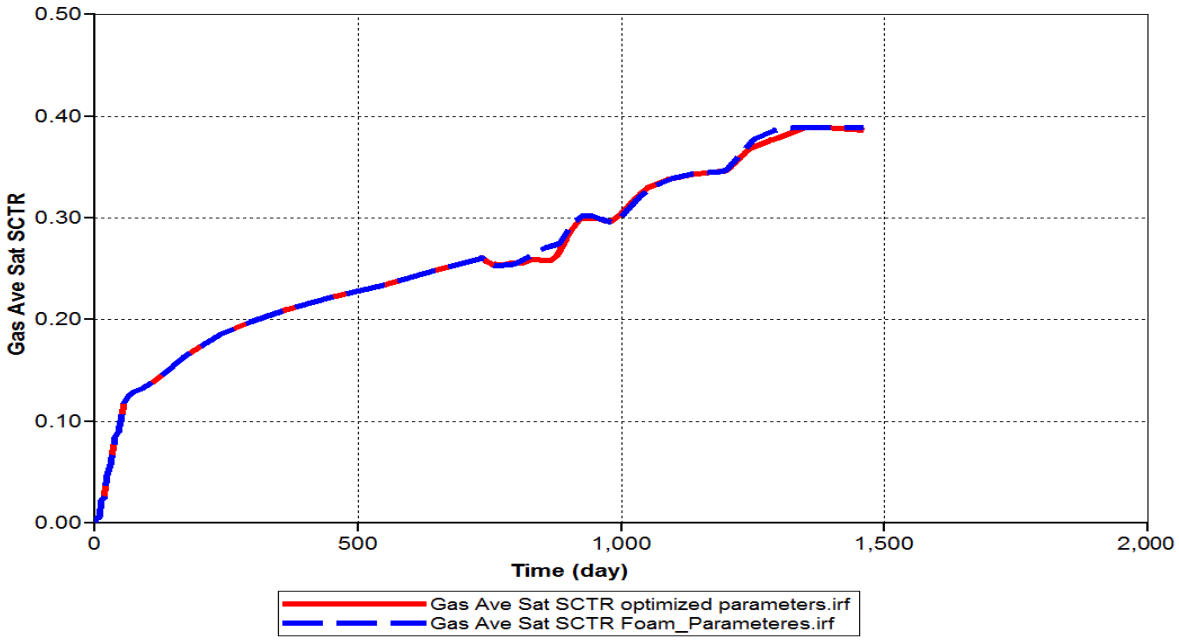

Figure 5.33 Average gas saturation comparison between optimized and base cases.

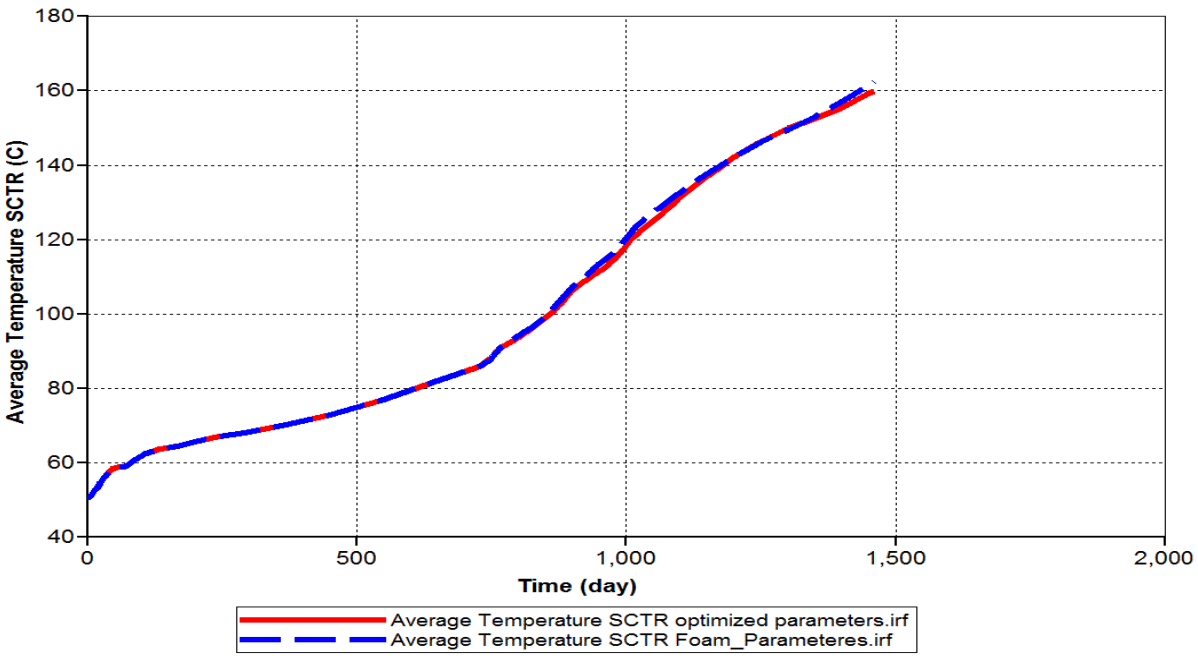

Figure 5.34 Average temperature comparison between optimized and base cases.

Figures 5.31 and 5.32 give oil recovery factor and average pressure comparison between optimized and base cases, respectively. There is not much difference for oil recovery in both cases because the values of parameters chosen for optimized case are close to the values of parameters of the base case. However, there is a difference in reservoir pressure for these 2 cases. Average pressure is less for the parameters optimized case which is favorable for the reservoir. This is because producing the same amount of oil in the same amount of time with lower average pressure is more favorable. Figures 5.33 and 5.34 give average gas saturation and average temperature comparison between optimized and base cases, respectively.

Chapter 6: Kern River Field Steam Foam History Matching

Patzek and Koinis in 1989 presented efficiency of steam foam injection into two different fields located in California. In the following session we summarize their work on the area of heavy oil recovery.

6.1 MECCA LEASE

The Kern River oil field is in the eastern San Joaquin Valley about 4 miles north of Bakersfield California. Two steam foam pilots were conducted in the Kern River field by Shell Company. One of them is Mecca lease (1980-1986) which is simulated in this work. The other one is Bishop Fee (1982-1986). Both fields are four contiguous inverted five spots and cover 12 and 14 acres respectively. Figure 6.1 shows pattern of these two fields.

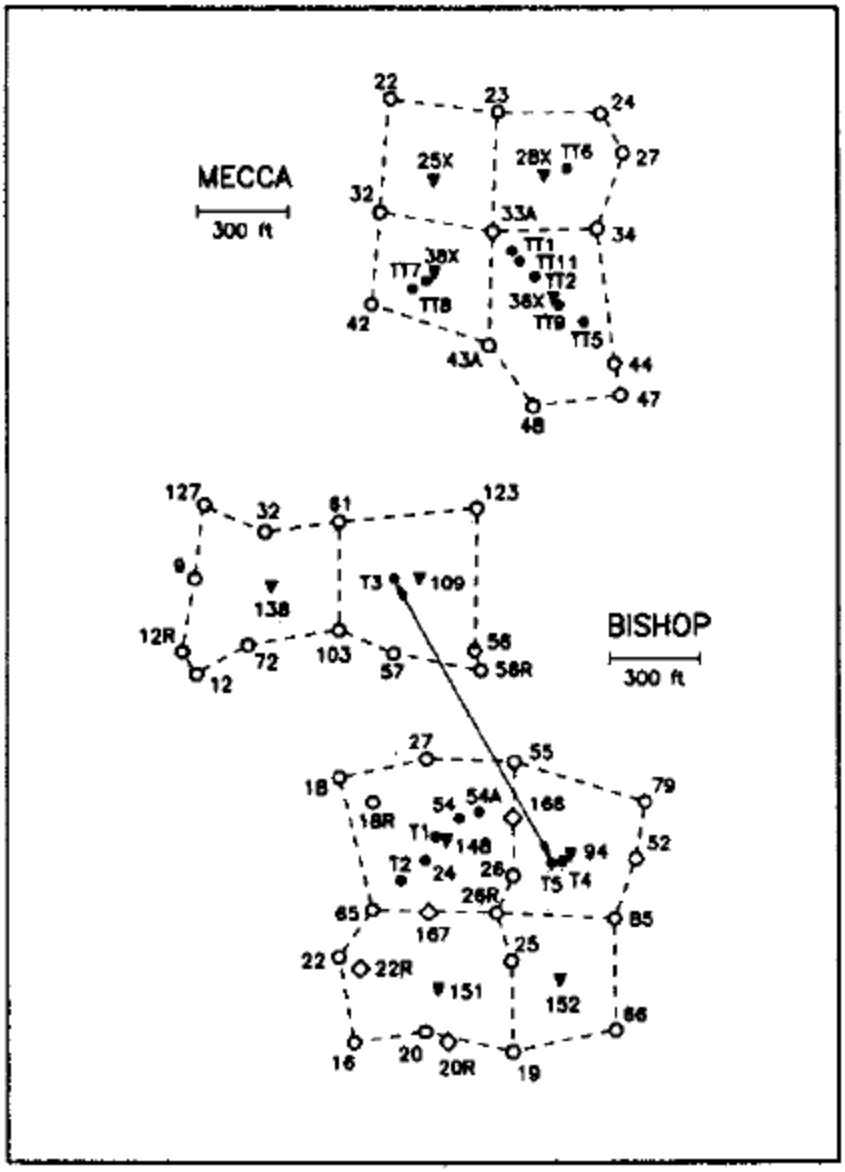

Figure 6.1 Kern River steam foam pilot location (Patzek and Koinis, 1990).

Sand M in the Mecca pilot is divided into Upper M which is 15 ft., Main M that is 40 ft., and Poor M which is 25 ft. There is a 3 ft thick silt layer between Upper M and Main M. We snapped the figure from the reference paper and plotted for further

modeling purpose. Figure 6.2 shows Mecca lease log including three layers which were discussed above.

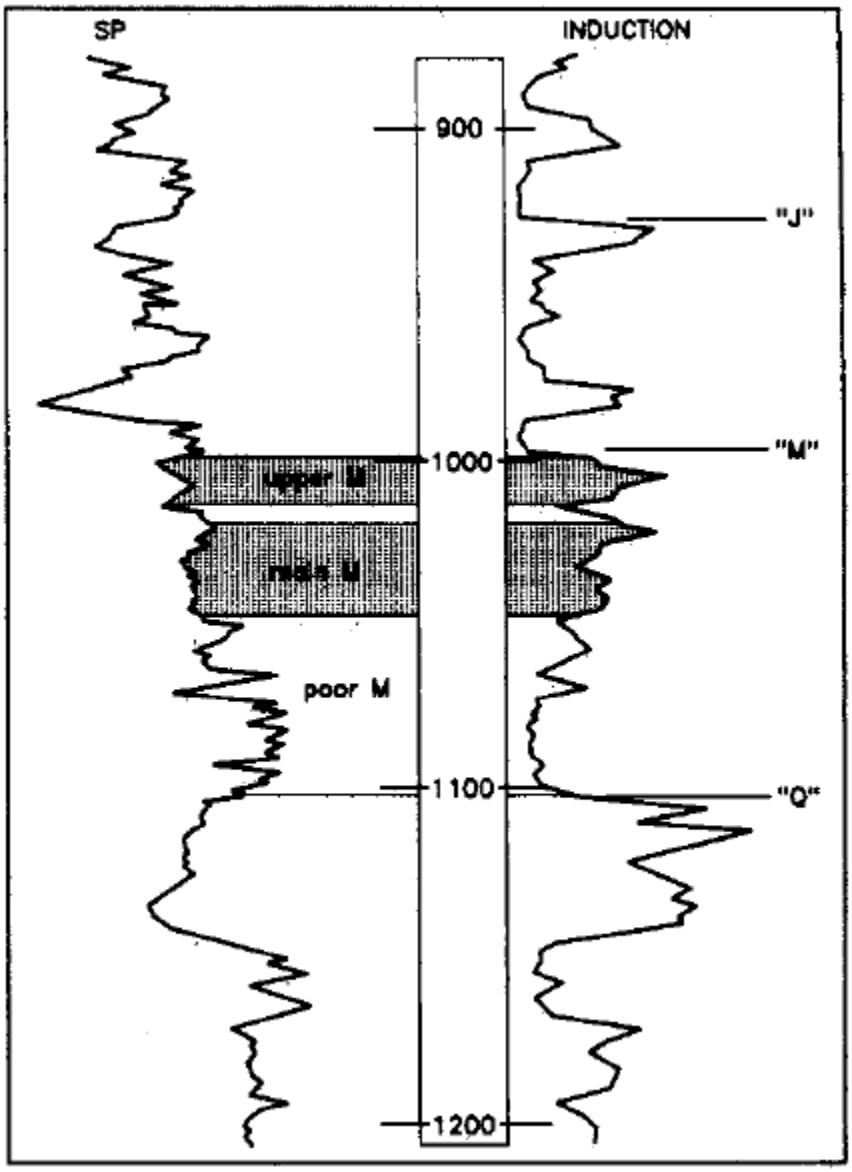

Figure 6.2 Mecca type log (Patzek, T.W., and Koinis, M. T., 1990).

The Kern River pilot for Mecca-Lease was designed to evaluate the steam foam performance when applied very late in steam drive which is 10 years. Table 6-1 illustrates reservoir descriptions for both Mecca and Bishop Pilots.

Table 6-1 Reservoir description of Mecca and Bishop Pilots (Patzek, T.W., and Koinis, M. T., 1990).

	Mecca Sand M	Bishop Sand Q
Depth, ft	1000	600
Dip, directional degrees	3 southwest	3 southwest
Gross thickness, ft	83	99
Good sands, ft	67	65
Poor sands, ft	7	19
Silt or clay, ft	9	15
Net pay, ft	67+7=74	65
***Soi*, %**	70	70
Porosity, %	30	30
Four-pattern area, acres	11.6	14
PV, thousand bbl	2000	2200
OOIP, thousand STB	1400	1500
API gravity, degrees	13	13
Barriers:		
-Continues within a pattern	1	0 to 3 random
-Discontinuous within a pattern	Random in lower one-third of Sand M	0 to 3 random
CEC, meq/100 g	8	9

During this work, focus was the incremental oil production resulting from steam foam. Oil production acceleration was disregarded. A significant oil production was observed after 2 years of steam foam injection. Figure 6.3 shows incremental oil production and cumulative incremental oil recovery.

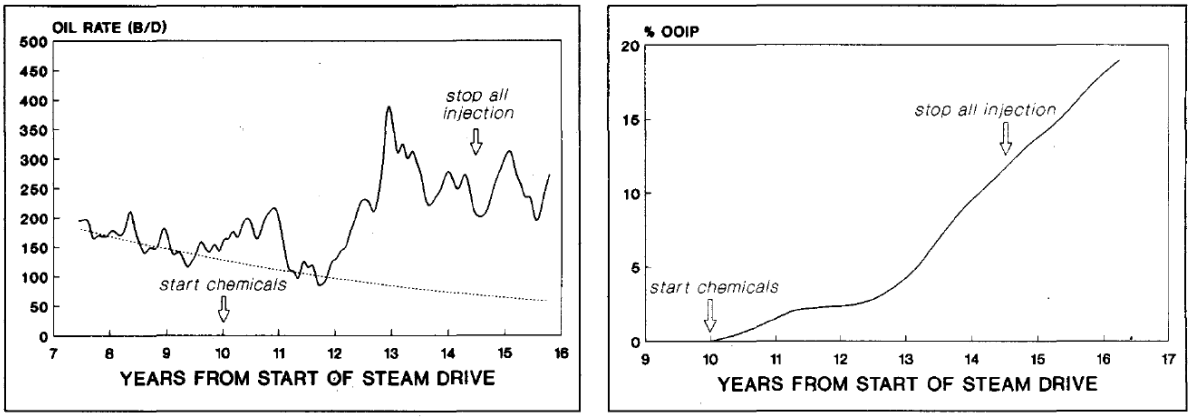

a) Incremental production b) Cumulative incremental oil recovery

Figure 6.3 Incremental production and cumulative oil recovery in Mecca steam foam pilot (Patzek, T.W., and Koinis, M. T., 1990).

Authors believe that a major reason maintaining the Mecca pilot's production was a slow release of stored energy in the foam zone. A basic explanation of the transient reaction to the foam injection shut-in says that it might take months to decline reservoir pressure if the foam does not collapse instantly. This happens because the heat stored in rock vaporizes water in the reservoir, which causes steam zone to extend and more oil to be extracted. Slow decline of temperature and bottom-hole pressures in observation and injection wells support that theory. All four injectors were used for measuring down-hole pressures between November 1983 and June 1985. Temperature surveys and gamma-ray-neutron logs were used to observe the steam foam effect on vertical sweep. Figure 6.4

indicates improved vertical sweep by steam foam in Mecca Observation Well TT2, 90 ft from injector.

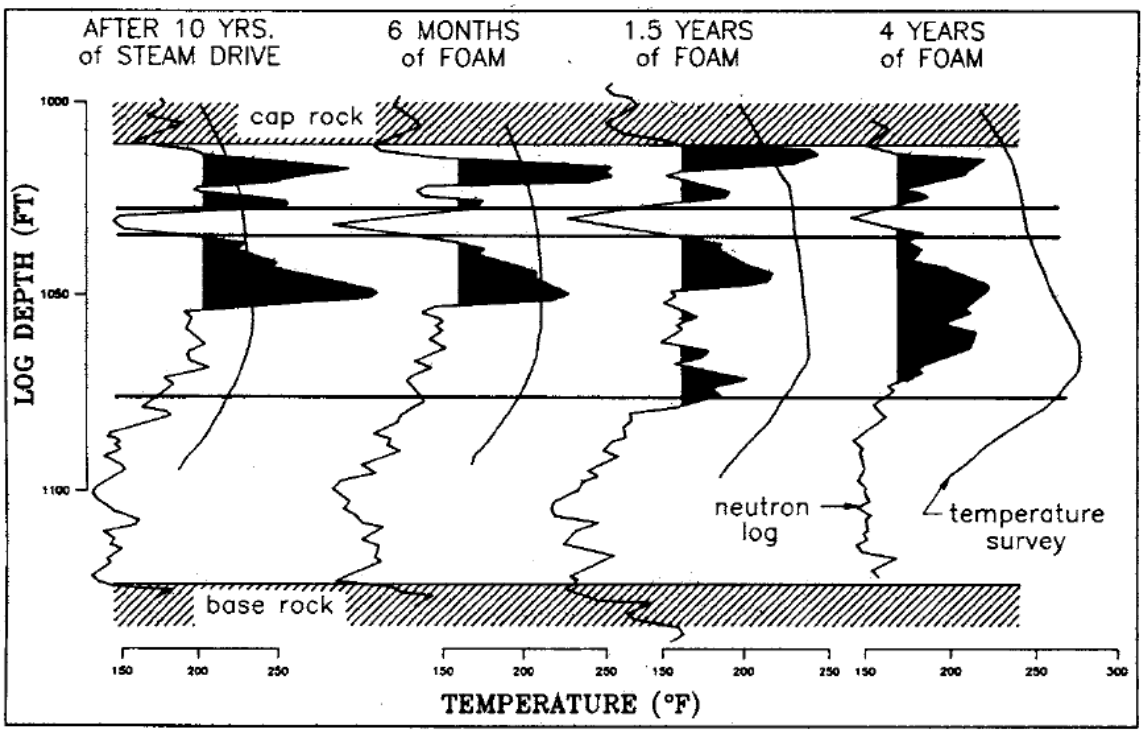

Figure 6.4 Improved vertical sweep by steam foam in Mecca Observation Well TT2, 90 ft from injector (Patzek, T.W., and Koinis, M. T., 1990).

Time laps evaluation of temperature surveys and neutron logs allowed calculating in-situ foam volume as a function of aqueous phase cumulative injection. Figure 6.5 illustrates injected pore volume of surfactant solution in field and mobility reduction factors. Table 6-2 shows events chronology at Mecca steam foam pilot. Injection and production histories for Mecca and Bishop Pilots are given in Table 6-3. Figure 6.6 illustrates schematic illustration of primary production and injection scenario to enhance oil recovery rate and the timing of processes from field results.

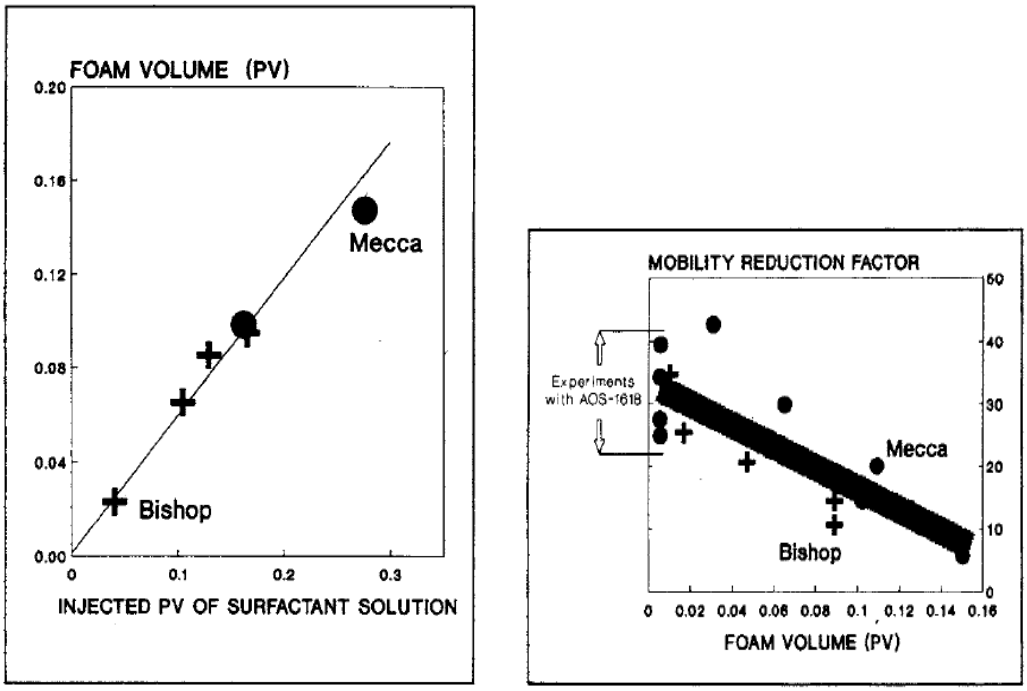

a) Injected pore volume of surfactant solution b) Mobility reduction factors

Figure 6.5 Injected pore volume of surfactant solution and mobility reduction factors (Patzek, T.W., and Koinis, M. T., 1990).

Table 6-2 Chronology of events at Mecca steam foam pilot (Patzek, T.W., and Koinis, M. T., 1990).

April 1970	**Drilled wells TT2 AND TT1, 90 and 185 ft northwest of well 36X; neither was perforated**
May 1970	Began steam drive pilot; average steam-injection rate 250 B/D CWE per injector, 50% quality; all injectors completed across bottom 16 to 18 ft of Main M

Table 6-2 continued.

Oct. 1976	Drilled well TT5, 110 ft southeast of well 36X; perforated at 1034 to 1050 ft to draw liquid samples and measure pressure Began 5 month steam-foam-injection test in Well 36X (see Dilgren et al.)
Aug. 1979	Drilled well TT6, 75 ft northeast of Well 28X
July 1980	Began steam-foam pilot with 0.5 wt% Siponate DS-10, 4 wt% brine, 250 B/D CWE per injector, 50% quality steam
Nov. 1980	Getty completed installation of steam drives north, west, and south of Mecca lease
Dec. 1980	Changed surfactant to Neodene 1618, 4% brine
Aug. 1981	Changed brine to 1%
Oct. 1981	Closed vents in plot procedures
Feb. 1982	Opened vents in plot procedures
March 1982	Changed surfactant to Siponate A-168, 4% brine
June 1982	Major oil-production response began

Table 6-2 continued.

Sept. 1983	Drilled and cored dual-completion Observation well TT9, 20 ft southwest of Well 36X, one tube perforated at 1033 to 1044 ft to measure pressure; oil saturation averaged over entire Upper and Main M was 9.2% Drilled and cored dual-completion Observation Well TT8, 70 ft southwest of Well 38X, perforated at 1077 to 1072 ft; oil saturation averaged over entire Upper and Main M was 16.7%
Dec. 1983	Doubled steam-injection rate in Wells 36X and 38X to 500 B/D; shut in Wells 25X and 28X
March 1984	Closed vents in selected pilot procedures
April 1984	Returned to 250 B/D CWE in all four injectors
July 1984	Returned to double injection rate in Wells 36X and 38X, shut in Wells 25X and 28X
Aug. 1984	Drilled Well TT11, 140 ft northwest of Well 36X, just outside predicted foam front; not perforated

Table 6-2 continued.

Nov. 1984	Squeezed or isolated perforations in Wells TT5 through TT9 to avoid interference from steam flow
Jan. 1985	Arrival of steam-foam front detected in Well TT11
Feb. 1985	Shut in steam and chemicals in the pilot; incremental oil recovery was 12% OOIP

Table 6-3 Injection and production histories for Mecca and Bishop Pilots (Patzek, T.W., and Koinis, M. T., 1990).

Item	Mecca
Primary oil produced	
Thousand bbl	**95**
% OOIP	**6.8**
Steam Soaks (Production Allocated)	
Years	9
Steam injected	
Thousand bbl CWE	475
PV CWE	0.24
Oil produced	
Thousand bbl	210
% OOIP	15
Gass production/injection	1.5
Cumulative OSR	0.44

Table 6-3 continued.

Steam Drive (Production Allocated)	
Years	10
Steam injected	
Thousand bbl CWE	4212
PV CWE	2.11
Oil produced	
Thousand bbl	402
% OOIP	28.7
Gass production/injection	0.4
Cumulative OSR	0.1
Total Oil Recovery Before Foam Injection	
Thousand bbl	707
% OOIP	50

Table 6-3 continued.

Foam Drive (Production Not Allocated)	
Years	4.5
Foam injected	
Thousand bbl CWE	1590
PV, CWE	0.8
Oil produced	
Thousand bbl	345
% OOIP	24.6
Surfactant injected, thousand bbl (100% active)	1390
Incremental oil after 5 years from start of foam	
Thousand bbl	
% OOIP	
lbm surfactant/bbl incremental oil	196
Gass production/injection	14
Delay of major oil response, years	7.1
Injected foam volume at major response	1.55
Thousand bbl CWE	2
PV CWE	
***With/without infill.**	730
OSR= oil/steam ratio.	0.37

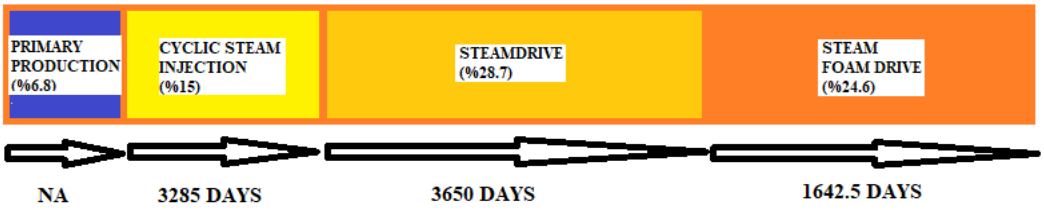

Figure 6.6 Schematic illustration of primary production and injection scenario to enhance oil recovery rate and timing of processes from field results.

6.2 MODELING AND SIMULATION

We use CMG-STARS simulator which is the undisputed industry standard in thermal reservoir simulation and advanced recovery processes. This simulator is fairly capable of simulating complicated enhanced oil recovery processes, such as thermal, chemical, gas floods as well as hybrid processes *e.g.* foam, steam foam, alkaline-surfactant-polymer injection processes.

To simulate all processes from primary production to steam injection, including cyclic steam injection and steam drive and then steam foam injection, several parameters are considered to capture different physics and phenomena to obtain all mechanisms behind steam and steam foam injection which are as follow:

- Heat loss model and parameters are discussed in the following.
- Surfactant adsorption, a very important factor that controls efficiency of foam injection along with steam. Langmuir model has been used for modeling purpose and consideration of surfactant adsorption.
- Relative permeability of three phase system obtained from history matching.

6.2.1 Heat Loss Model

As mentioned in Chapter 5, Lashgari H. (2014) dissertation, Vinsome and Westerveld (1980) developed a semi-analytical approach to compute the amount of heat-loss in case of heat or cold injection into a reservoir layer that is surrounded between impermeable overburden or underburden layers. Their approach simplifies the heat conduction problem, while providing satisfactory accuracy. Table 6-4 gives heat-loss model properties used in this study.

Table 6-4 Heat loss model properties

Parameter	Definition	Value
ROCKCP	Coefficients in the correlation (*rock_cp1* + *rock_cp2*·Tabs) for volumetric heat capacity of solid formation (rock) in the reservoir, where Tabs is absolute degrees.	2.347E+6
THCONR	Thermal conductivity of reservoir rock.	1.495E+5
THCONW	Thermal conductivity of the water phase.	5.35E+4
THCONO	Thermal conductivity of the oil phase.	1.15E+4
THCONG	Thermal conductivity of the gas phase.	4.5E+3
HLOSSPROP	Defines the heat-loss directions and over/underburden thermal properties for the semi-analytical infinite overburden heat loss model.	2.347E+6 1.495E+5 (Same for overburden and underburden)
HLOSST	Control the overburden temperature and critical temperature difference.	65.6

6.2.2 Langmuir Model for Surfactant Adsorption

Table 6-5 gives Langmuir model for surfactant adsorption. Table 6-6 shows Langmuir parameters and definitions.

Table 6-5 Langmuir model for surfactant adsorption

Formulation	Explanation	
$ad = \frac{(tad1 + tad2 \times xnacl) \times ca}{(1 + tad3 \times ca)}$	Adsorbed moles of component MM (Million) per unit pore volume	***Xnacl:*** salinity of the brine *ca*: the mole fraction of component name in phase described
(tad1 + tad2 *xnacl)/tad3	At high concentrations (large ca) the maximum adsorption	

Table 6-6 Langmuir Parameters

Parameter	Definition
Tad1	First parameter in the Langmuir expression for the adsorption isotherm (gmol/m^3 | lbmol/ft^3 | gmol/cm^3). It must be non-negative.
Tad2	Second parameter in the Langmuir expression for the adsorption isotherm associated with salt effects (gmol/m^3 | lbmol/ft^3 | gmol/cm^3).
Tad3	Third parameter in the Langmuir expression for the adsorption isotherm. It must be no less than 1e-15.

6.3 RESERVOIR MODEL

Mecca Lease field data utilized for simulation purpose in this study is reported by Patzek and Koinis in 1990, as was mentioned in the previous section. We follow the geology given in the reference paper with four layers and we tried to capture all model parameters. Same field volume was created in CMG STARS. Same rock and reservoir properties were applied to created reservoir. Oil recovery for each step was matched with minor differences.

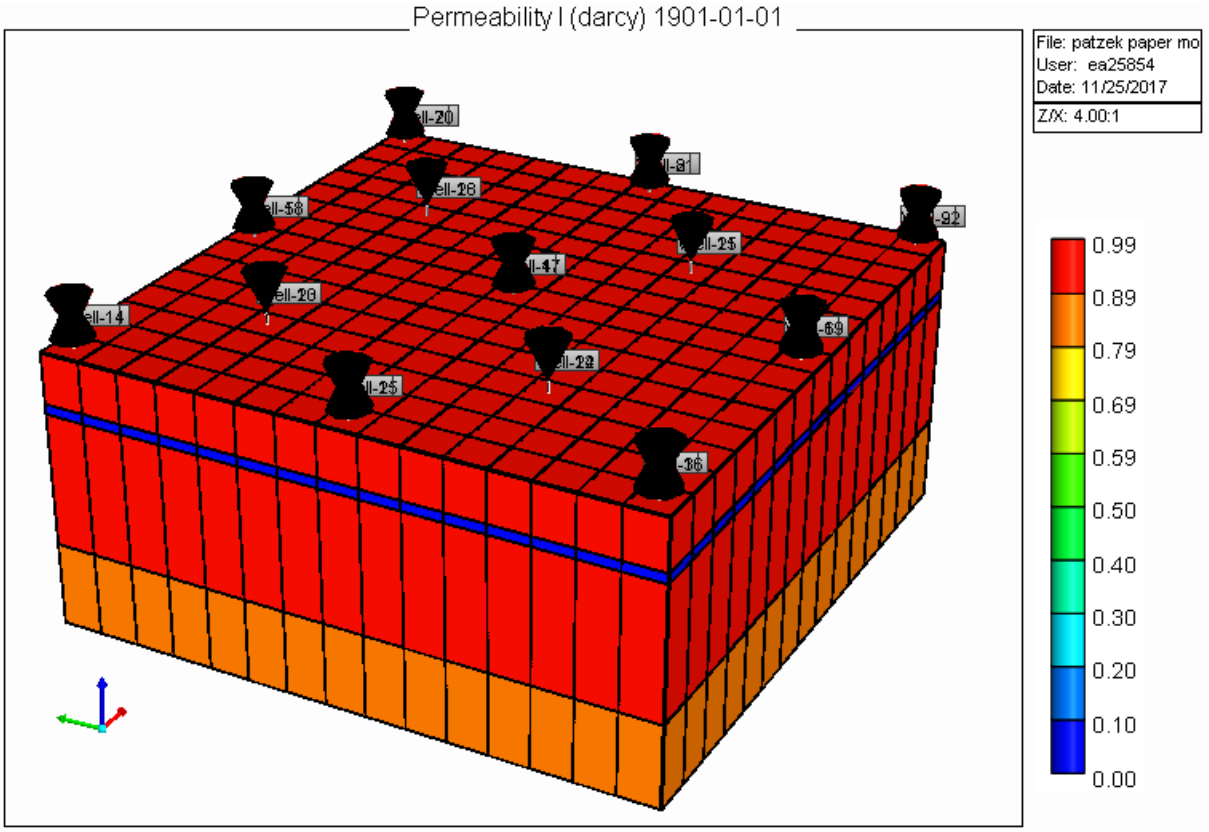

Figure 6.7 Reservoir model used in this study with four layers and 17 injection and 9 production wells.

We summarize the parameters modeled in this work in the following table. The reason we selected that sized grid blocks is for the simplicity and better computation.

Figure 6.7 shows reservoir model used in this study with four layers and 17 injection and 9 production wells. Table 6-7 gives reservoir model properties used for simulation study.

In this work we used heterogeneity because the layers given in Patzek and Koinis' paper were specified as upper M, silt, main M, and poor M.

Table 6-7 Reservoir model properties used for simulation study.

Number of grid blocks	15x15x4
Grid block size first layer	14.907x14.907x7.62 m3
Grid block size second layer	14.907x14.907x12.192 m3
Grid block size third layer	14.907x14.907x0.9144 m3
Grid block size forth layer	14.907x14.907x4.572 m3
Initial Temperature	65 ^{o}C

Table 6-7 continued.

Initial pressure respectively layer varied	
First Layer	3354 kpa
Second Layer	3277 kpa
Third Layer	3152.7 kpa
Forth Layer	3143.4 kpa
Initial water saturation	0.3
Oil viscosity	2200 cp @37.8 ^{o}C
Permeability $k_x = k_y = k_z$	
First Layer	800 Md
Second Layer	
Third Layer	990 Md
Forth Layer	
	0.001 Md (Clay)
	990 Md
Porosity	0.3

Table 6-7 continued.

Number of wells	26 9 production wells 17 injection wells

Figures 6.8 (a) and (b) show the production and injection well locations, respectively. Wells are located at the edges of reservoir and there is one well in the middle. Figure 6.8 (c) indicates well locations for steam drive and steam foam processes. In these processes, steam and steam foam are injected at the middle point of production wells to obtain better results.

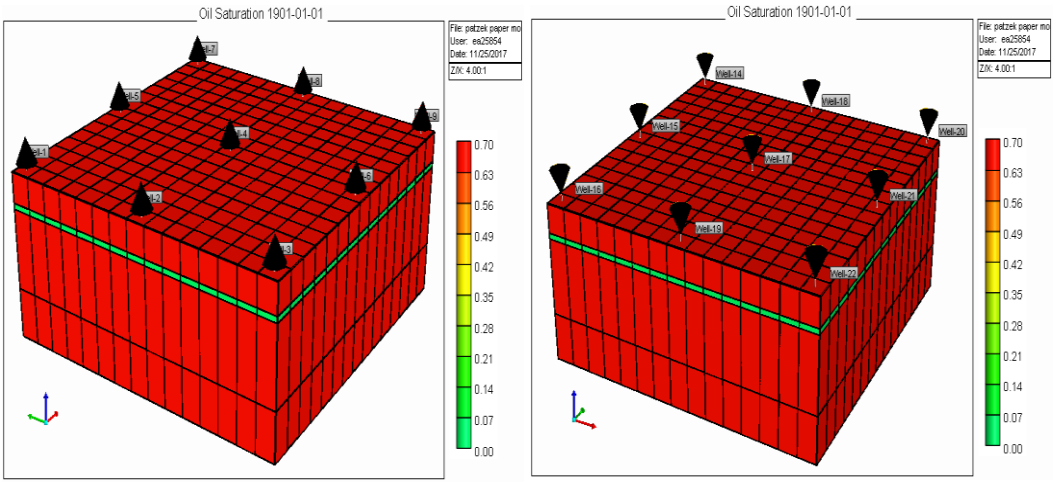

a) Production well locations b) Injection well locations during CSI

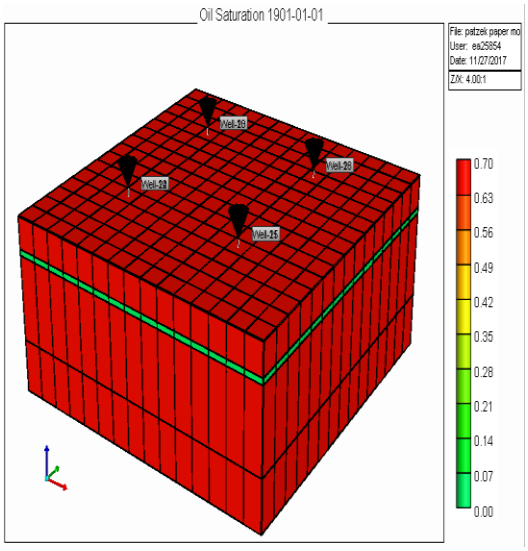

c) Injection well locations during steam drive and steam foam injection

Figure 6.8 Well locations.

Figure 6.9 (a) shows the relative permeability to water (*krw*) and relative permeability to oil (*kro*) versus water saturation (*Sw*) in the reservoir. Since the cross-over point is to the right half of the normalized water saturation and the relative permeability to oil approaches 100 percent at connate water saturation, the reservoir is considered to be "water-wet." Similarly, Figure 6.9 (b) exhibits the relative permeability of the gas-oil (*krg* and *krog*) versus liguid saturation (SL) in the reservoir. In this study, Figure 6.9 is taken from Patzek and Myhill' s paper. In that paper Patzek and Myhill (1989) simulated Bishop field steam foam pilots.

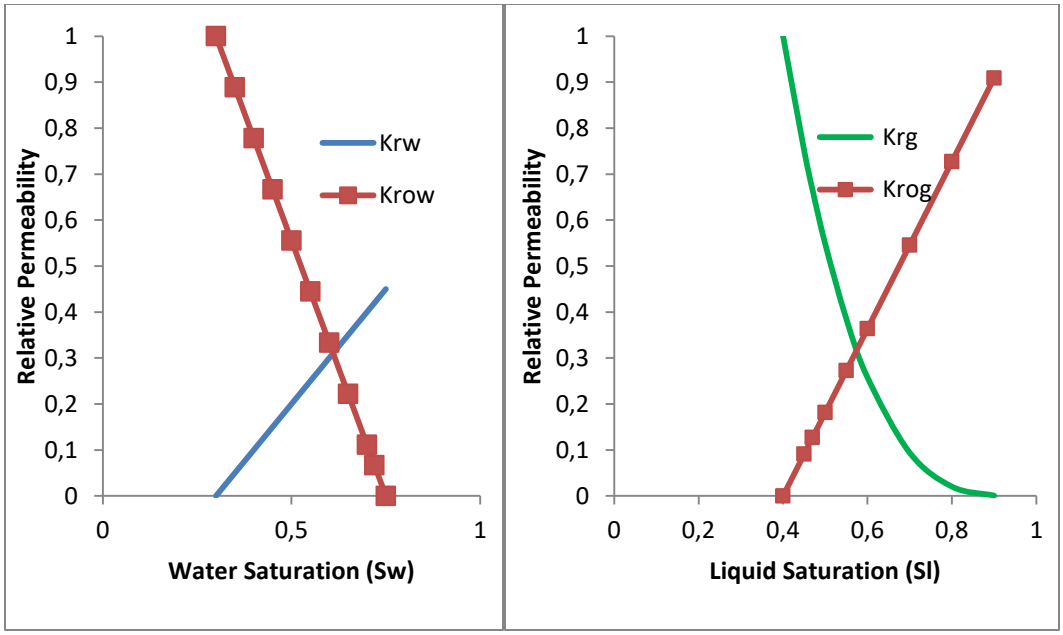

a) Oil water relative permeability b) Liquid gas relative permeability

Figure 6.9 Relative permeability of oil, gas (steam), and water.

Based on our work in Chapter 5, we used the same foam parameters to model the effect of foam in this part. Table 6-8 shows the foam parameter values used for this simulation. In Table 6-9, fluid and phase behavior parameters have been given for four components: water, surfactant, bitumen, and nitrogen gas. Surfactant adsorption parameters are given in Table 6-10. Langmuir adsorption parameters used in the simulation study for surfactant at different temperatures are given in Table 6-11.

Table 6-8 Foam parameter values

Parameter	Value
Fmoil	0.5
Epoil	1
Fmsurf	0.0001875
Epsurf	4
Fmcap	0.0004
Epcap	1
Fmmob	50

Table 6-9 Fluid and phase behavior parameters with four components

MODEL 4 4 3 2				
COMPONENT NAME	**WATER**	**SURFACTANT**	**BITUMEN**	**N2**
Molecular Weight (kg/gmole)	0.0182	0.48	0.5	0.028
Mole Density (gmole /m3)	55392	2020	1950	
Mass Density (kg/m3)	1008	969.6	975	
Compressibility (1/kPa)	4.570E-07	4e-6	4e-6	
Thermal Expansion (1/C)	3.583E-04	4.497E-04	4.497E-04	
Critical Pressure (kpa)	21760	1100	1100	3309
Critical Temperature (Cells)	371	494	494	-147
Vaporization enthalpy (J/gmol)	0	5500	5500	

Table 6-10 Surfactant adsorption parameters

Component	Molecular Weight (kg/gmole)	Mole Density (gmole/m3)	Mass Density (kg/m3)	Compressibility (1/kpa)	Thermal Expansion (1/C)
Adsorbed Surfactant	0.48	4.8E+04	2.3040E+04	0	0

Table 6-11 Langmuir adsorption parameters used in simulation study for surfactant at different temperatures

ADSCOMP 'SURFACT' WATER **Data for reversible aqueous surfactant adsorption				
ADMAXT 2.56				
ADSLANG TEMP				
51 °C	5.41e+6	0	2.1e+6	Langmuir concentration coefficients at T=51°C
151 °C	1.08e+6	0	9.3e+5	Langmuir concentration coefficients at T=151°C
250 °C	2.00e+5	0	5.3e+5	Langmuir concentration coefficients at T=250°C

In Table 6-12 oil recovery results are given that were obtained from the field. Table 6-13 shows our CMG-STARS simulation results. By comparing these two tables, it can be said that both results match very well.

Table 6-12 Oil recoveries from field results

Field Results From Patzek and Koinis Paper		
Process	Time	Recovery (%)
Primary Production	NA	6.8
Huff and Puff	9 years	15
Steam Drive	10 years	28.7
Steam Foam Drive	4.5 years	24.6

Table 6-13 Oil recoveries from simulation results

Simulation Results		
Process	**Time**	**Recovery (%)**
Primary Production	7.6 years	4.4
Huff n Puff	9 years	13.7
Steam Drive	10 years	32.5
Steam Foam Drive	4.5 years	25.9

6.4 SIMULATION RESULTS

In this section we present simulation results and then discuss history matching of simulation results with field data. Figure 6.10 gives a schematic illustration of process times and recoveries obtained from simulation results.

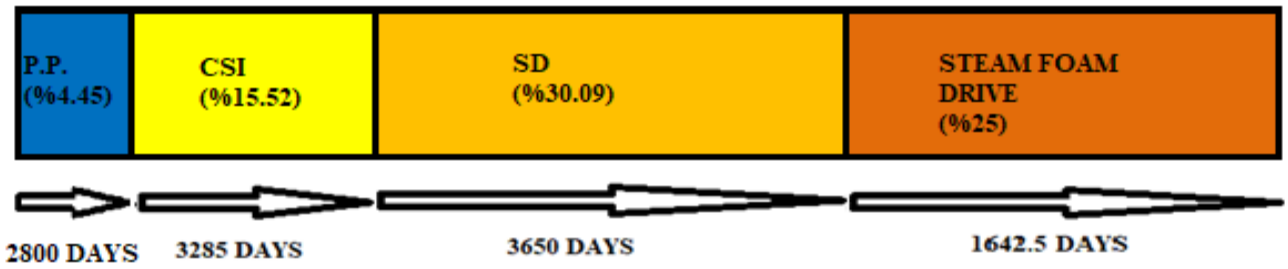

Figure 6.10 Schematic of primary production and injection scenario to enhance oil recovery rate and timing of processes from simulation results.

6.4.1 Natural Production Period

In this period, nine production wells are included. Figure 6.11 shows the wells used in primary production. There was no injection during that time and production is caused by natural pressure depletion of reservoir. Primary production time in Patzek and Koinis' work was not specified; in simulation program, we used 7.6 years for primary production to take place. This time is determined from the production graph, looking at the daily production rates. After that time, production rate was quite low; so we stopped production and started Cyclic Steam Injection.

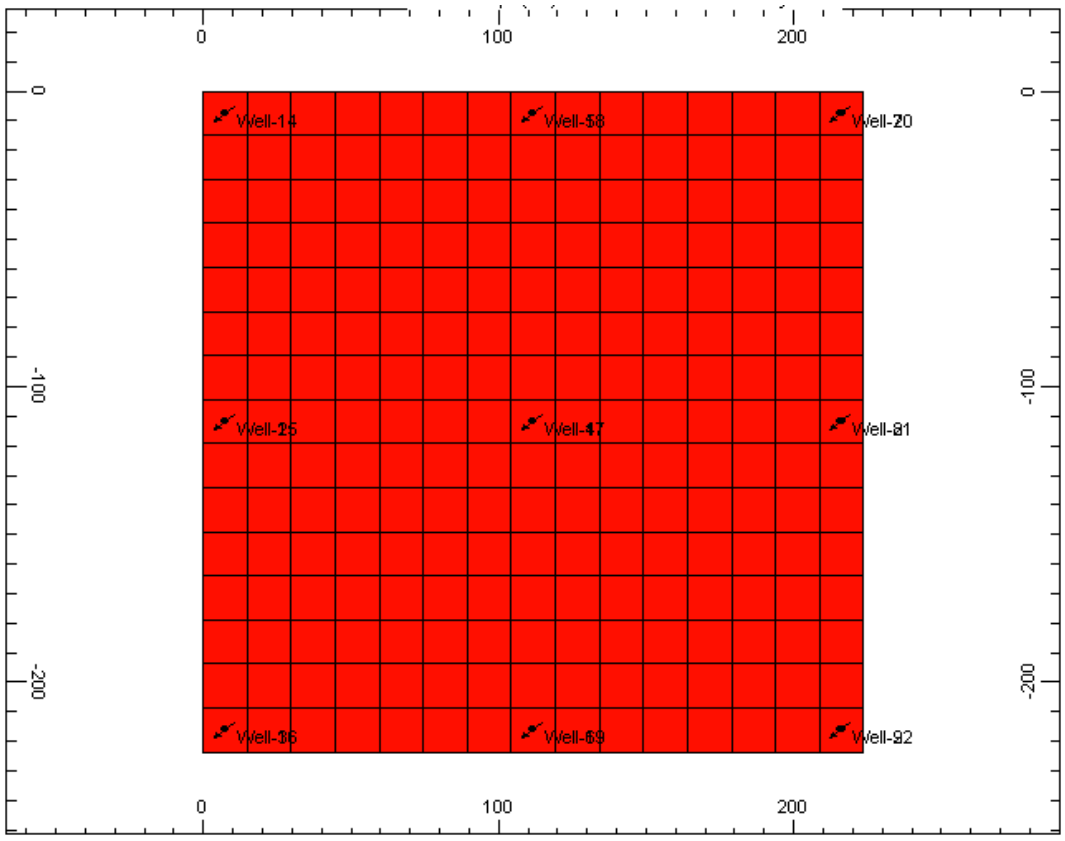

Figure 6.11 Wells used in primary production

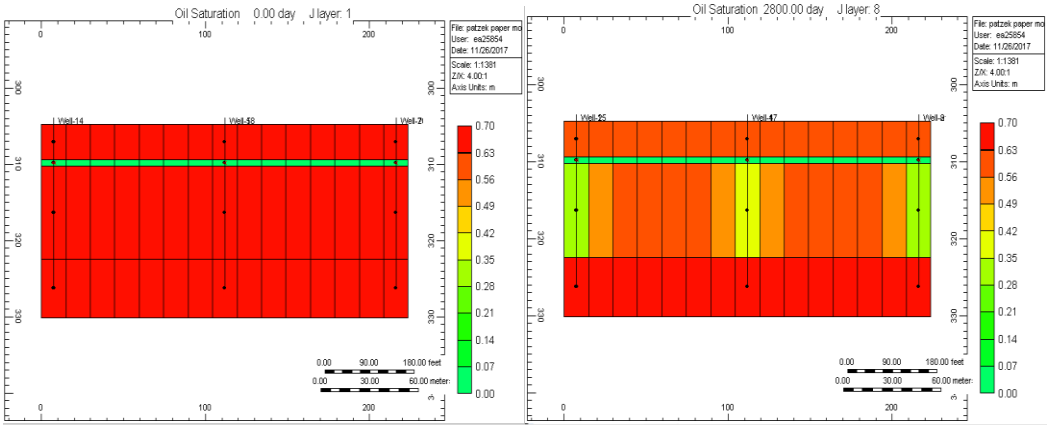

a) At the beginning of primary production b) At the end of primary production

Figure 6.12 Oil saturation profiles at the beginning and the end of primary production.

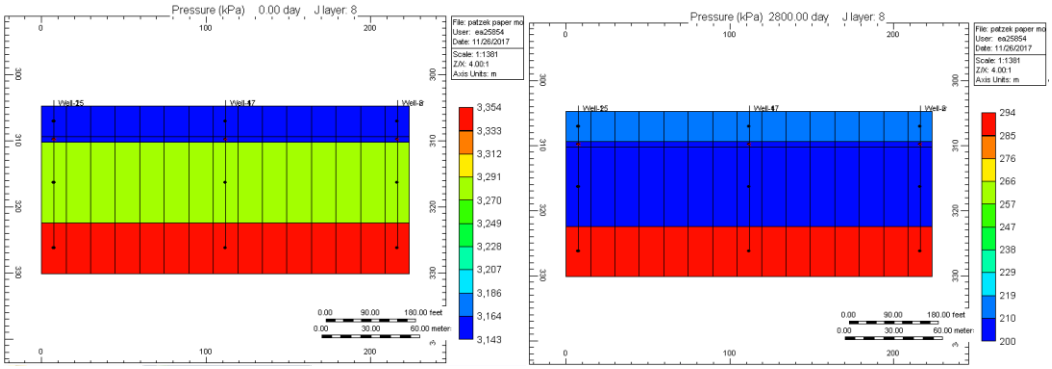

a) At the beginning of primary production b) At the end of primary production

Figure 6.13 Pressure profiles at the beginning and the end of primary production.

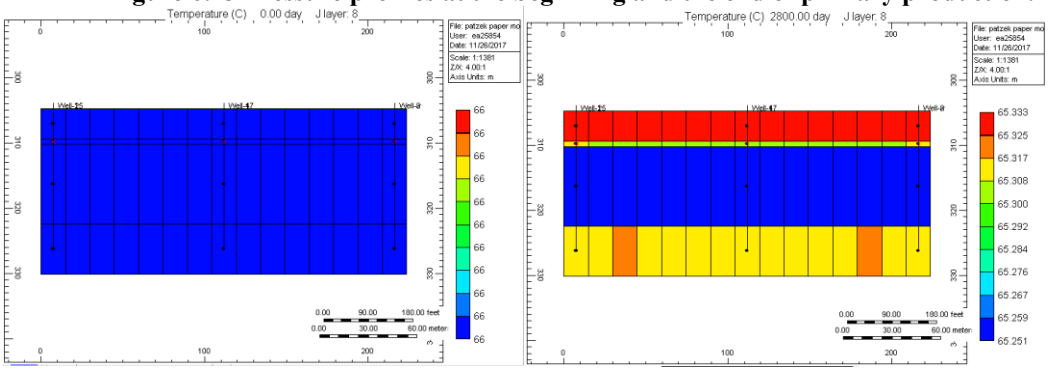

a) At the beginning of primary production b) At the end of primary production

Figure 6.14 Temperature profiles at the beginning and the end of primary production.

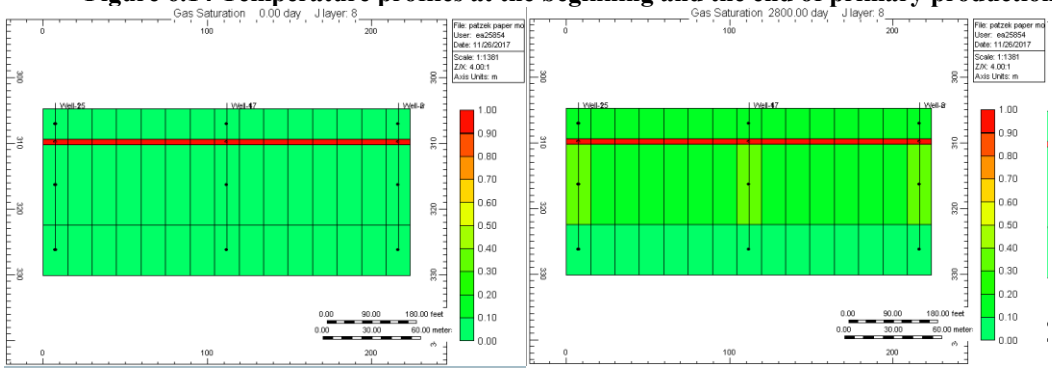

a) At the beginning of primary production b) At the end of primary production

Figure 6.15 Gas saturation profiles at the beginning and the end of primary production

Oil saturation, pressure, temperature, and gas saturation profiles are given for the beginning and the end of primary production process in the Figures 6.12, 6.13, 6.14, and 6.15. As can be seen in Figure 6.12, oil is extracted from near wellbore during this

process. This is expected, since it is heavy oil and viscosity is high at initial reservoir temperature. Since the driving force for this process is bottom-hole pressure, pressure drops to 294 psi from the initial pressure, which is around 3350 psi. This drop can be clearly seen in Figure 6.13. As expected from this process, Figure 6.14 indicates that there is no temperature change. Oil saturation does not change; we have a major decrease since pressure drive cannot extract a big amount of heavy oil.

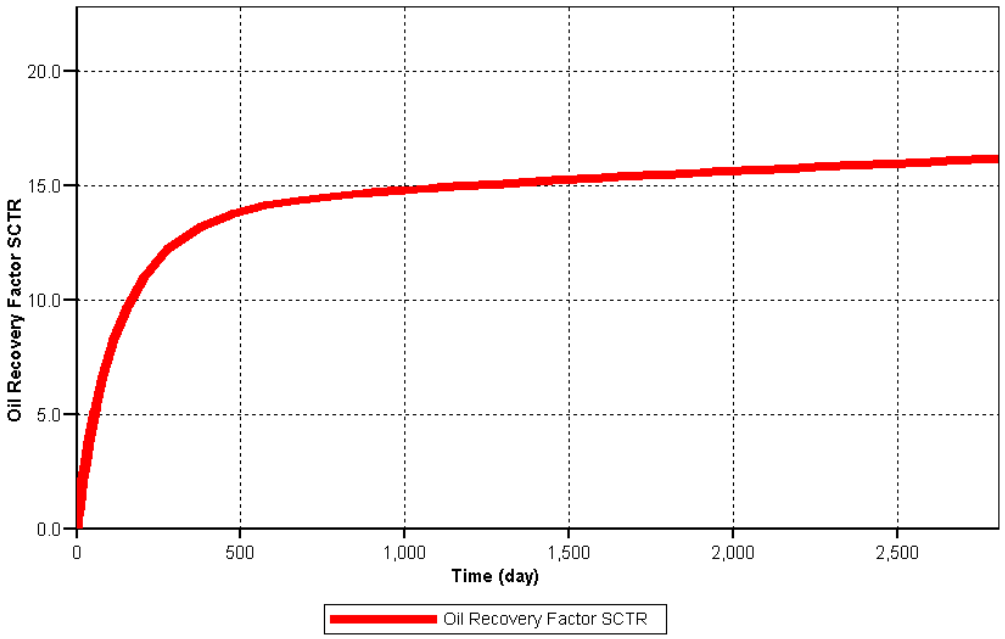

Figure 6.16 Simulation oil recovery factor for primary production.

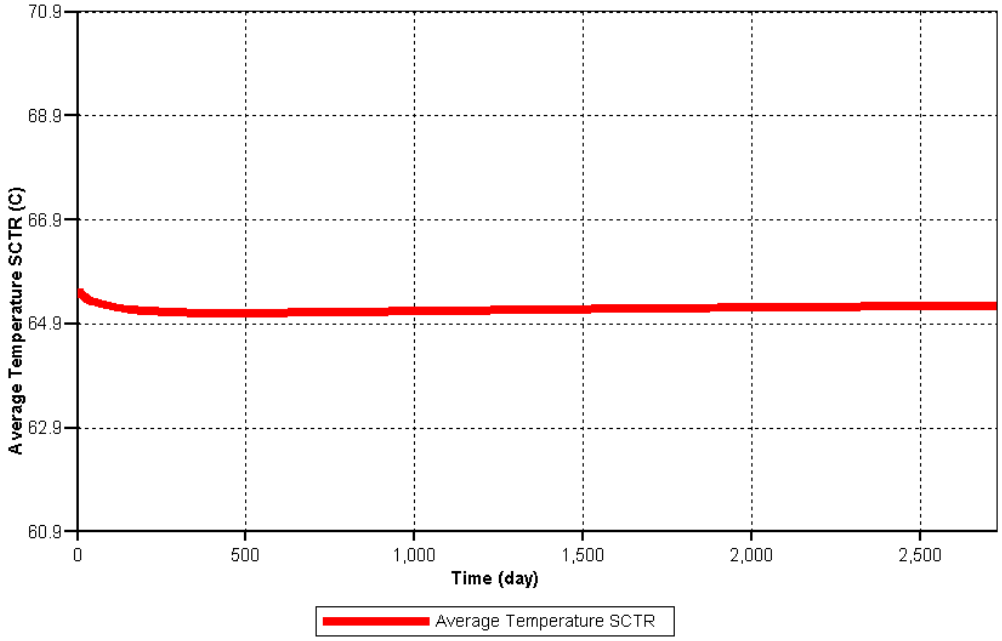

Figure 6.17 Reservoir average temperature for primary production from simulation study.

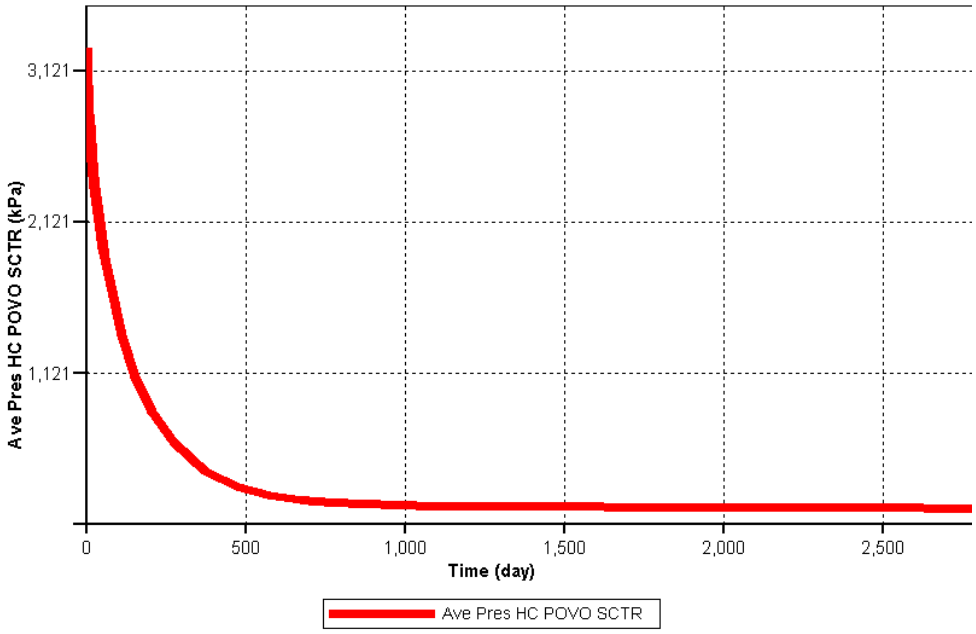

Figure 6.18 Reservoir average pressure for primary production.

In Figure 6.16 oil recovery shows an early pick and does not exhibit a major increase after that time because pressure is decreasing fast as can be seen in Figure 6.18. Those two graphs demonstrate a parallelism which also indicates that the driving force is pressure for this stage. Temperature stays steady in Figure 6.17 as expected.

6.4.2 Cyclic Steam Injection Period

Nine production wells and nine injection wells are included in this period and illustrated in Figure 6.19. Injection period of 30 days followed by 7 days of soak time and 328 days of production period for each cycle is applied. This cyclic steam process is repeated for a nine years period, as specified in Patzek and Koinis' paper. Oil saturation, pressure, temperature, and gas saturation profiles are given for the beginning and the end of cycles 1, 5, and 9 in Figures 6.20, 6.21, 6.22, and 6.23, respectively. As shown in Figure 6.20, the decrease in oil saturation for each cycle is accelerating towards the ninth

cycle. This situation can be explained with Figure 6.22 which demonstrates temperature profiles for cycles. In Figure 6.22 the temperature is increasing faster in each cycle because oil is produced and reservoir is filled with more steam. Pressure profiles in Figure 6.21 are parallel to other figures. Gas saturation is increasing in each cycle, as expected, which can be seen in Figure 6.23.

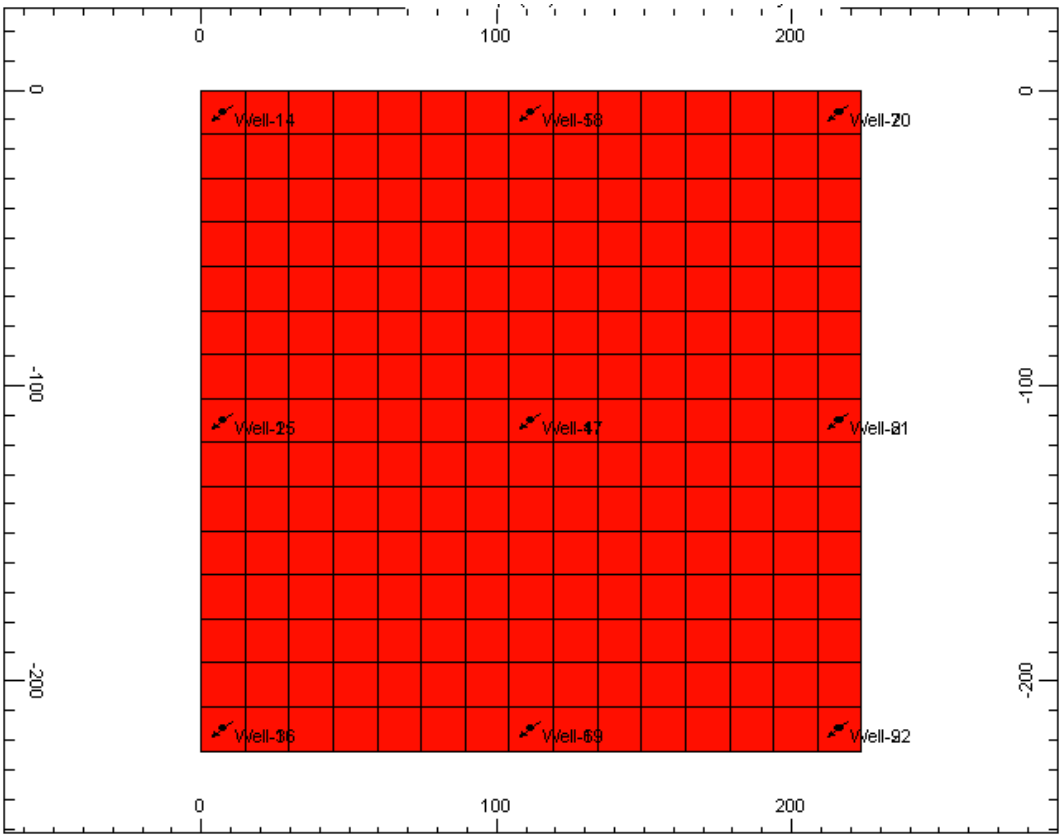

Figure 6.19 Wells used in cyclic steam injection period.

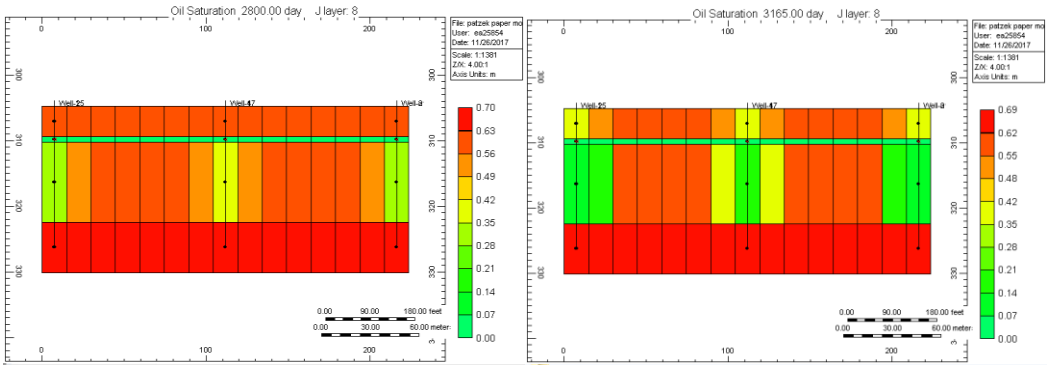

a) At the beginning of first cycle b) At the end of first cycle

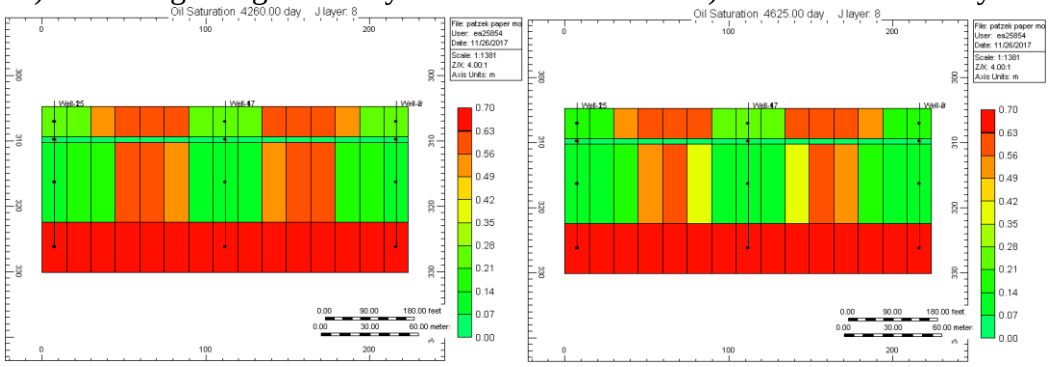

a) At the beginning of fifth cycle b) At the end of fifth cycle

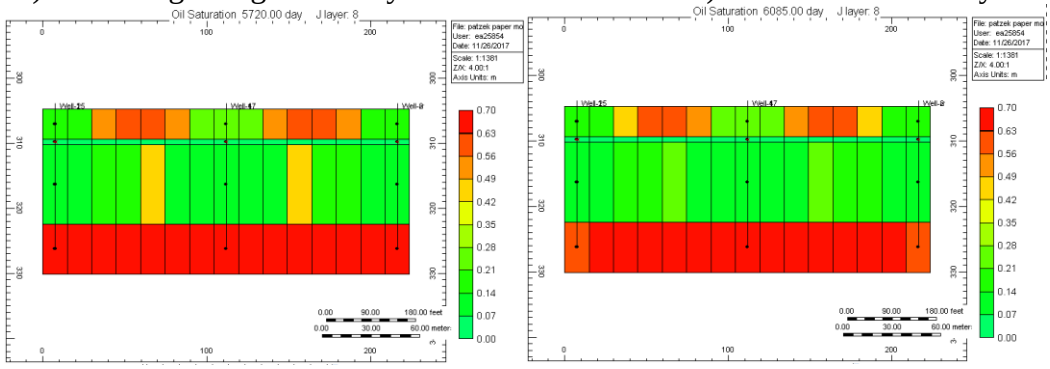

a) At the beginning of ninth cycle b) At the end of ninth cycle

Figure 6.20 Oil saturation profiles at the beginning and the end of cycles 1, 5 and 9.

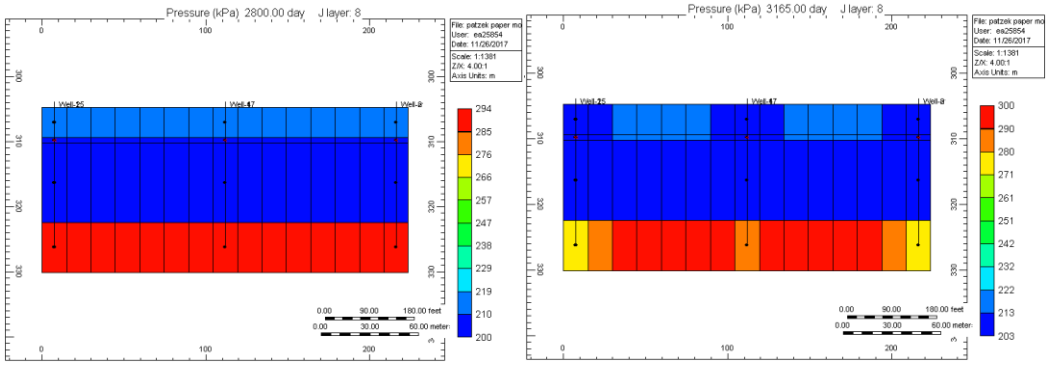

a) At the beginning of first cycle b) At the end of first cycle

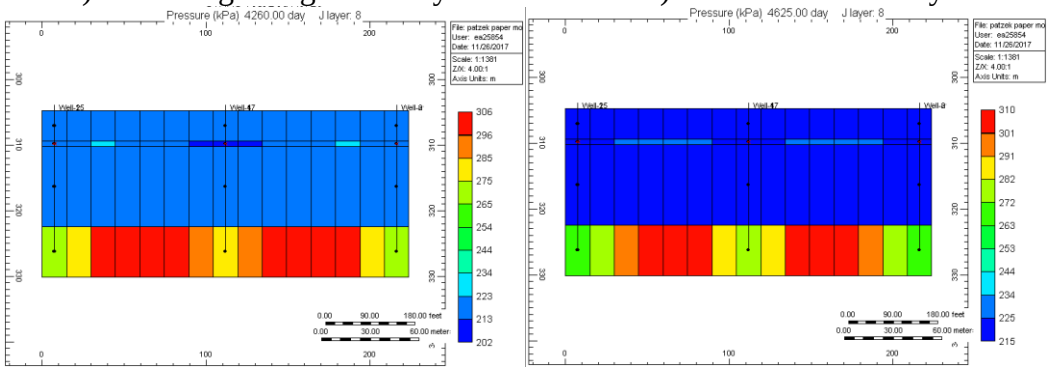

a) At the beginning of fifth cycle b) At the end of fifth cycle

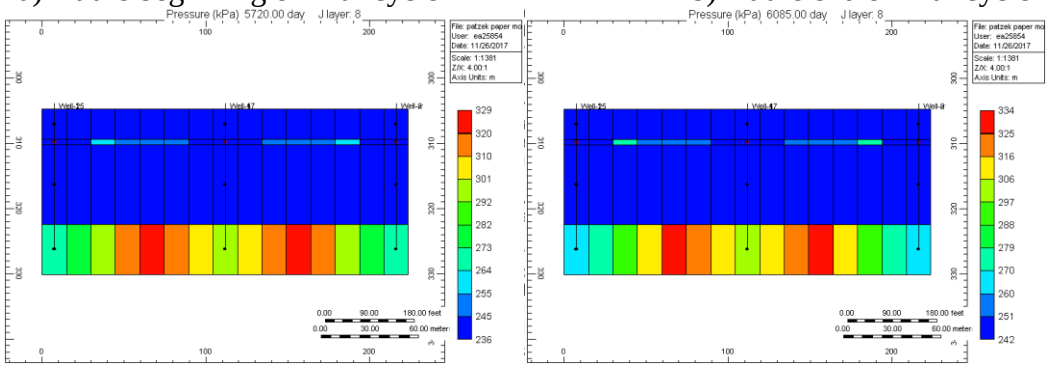

a) At the beginning of ninth cycle b) At the end of ninth cycle

Figure 6.21 Pressure profiles at the beginning and the end of cycles 1, 5 and 9.

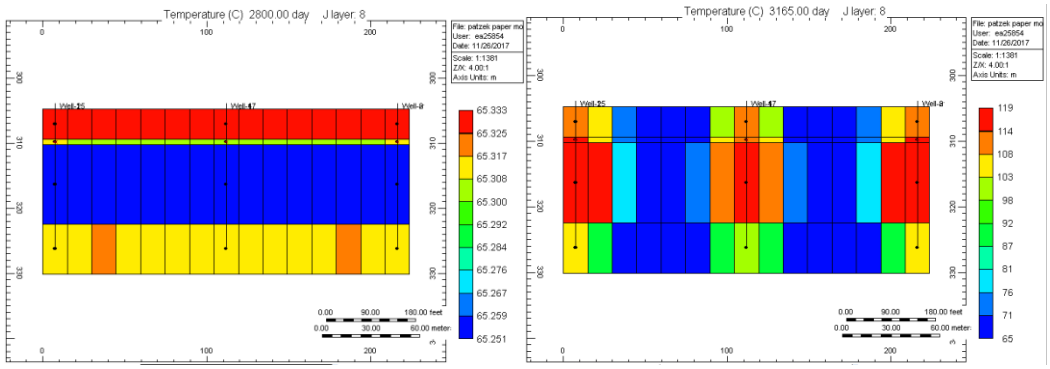

a) At the beginning of first cycle b) At the end of first cycle

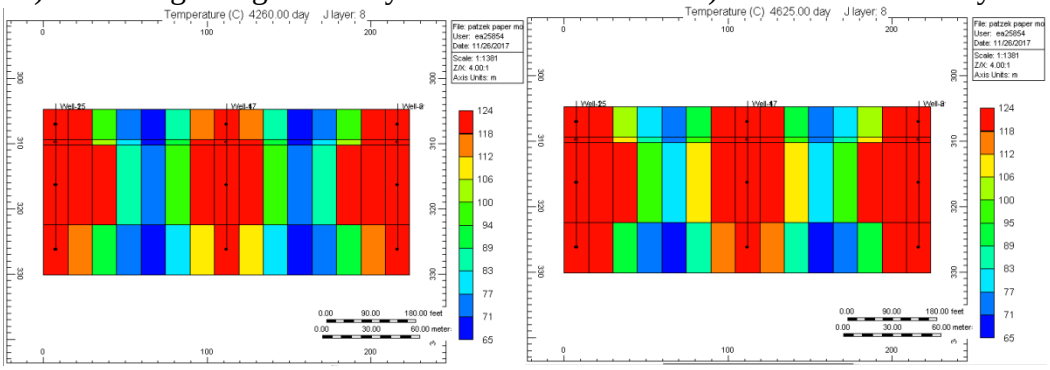

a) At the beginning of fifth cycle b) At the end of fifth cycle

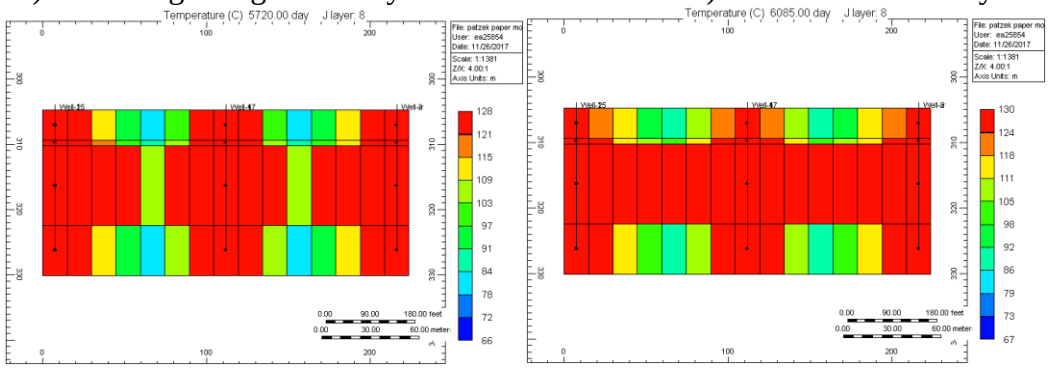

a) At the beginning of ninth cycle b) At the end of ninth cycle

Figure 6.22 Temperature profiles at the beginning and the end of cycles 1, 5 and 9.

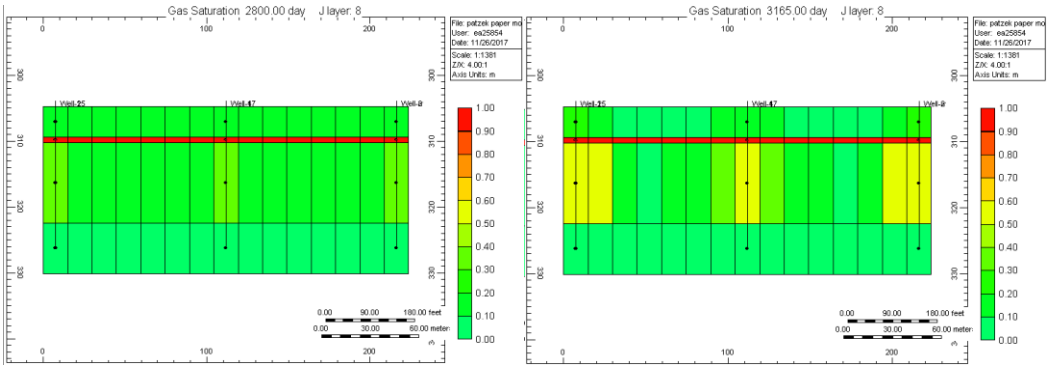

a) At the beginning of first cycle b) At the end of first cycle

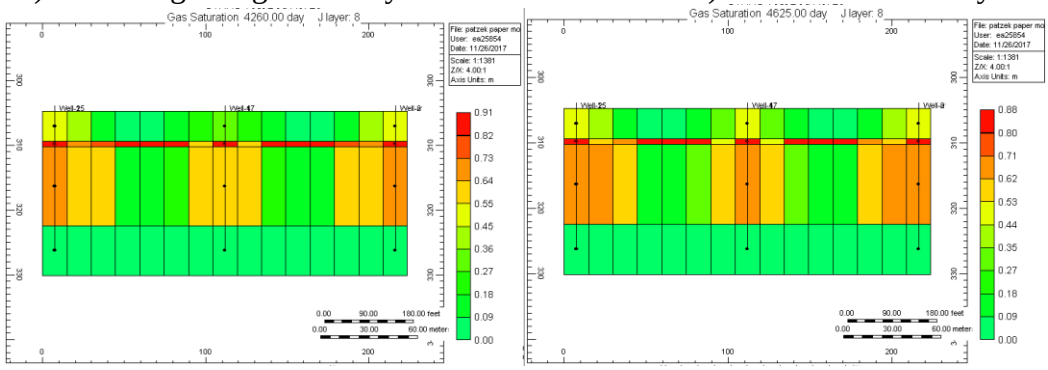

a) At the beginning of fifth cycle b) At the end of fifth cycle

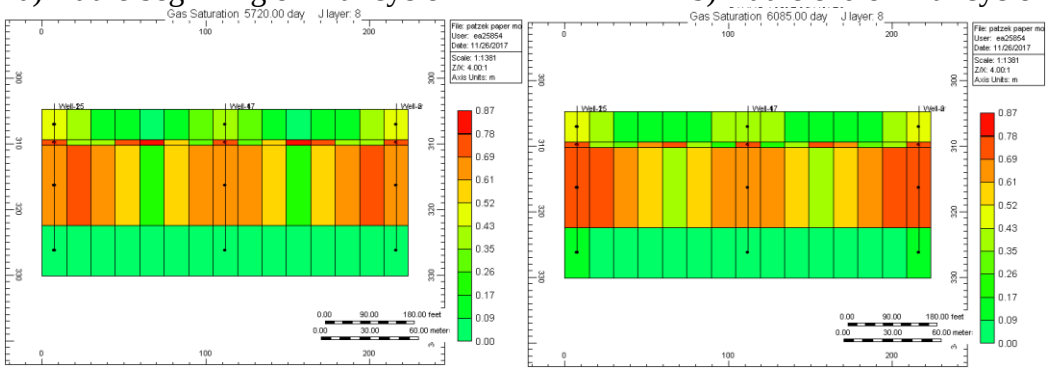

a) At the beginning of ninth cycle b) At the end of ninth cycle

Figure 6.23 Gas saturation profiles at the beginning and the end of cycles 1, 5 and 9.

Figure 6.24 displays the oil recovery factor for the cycles. The results indicate that oil recovery is increasing in good manner until the end of ninth cycle. Figure 6.25 shows average reservoir temperature for the cycles. At the end of each cycle reservoir, temperature is increasing. For each cycle during injection period, temperature is

increasing, as expected, and decreases for waiting time while it is spread along the reservoir. That decrease is mainly caused from heat loss. While average reservoir temperature is increasing gradually for each cycle, average reservoir pressure is staying about the same, which can be seen in Figure 6.26.

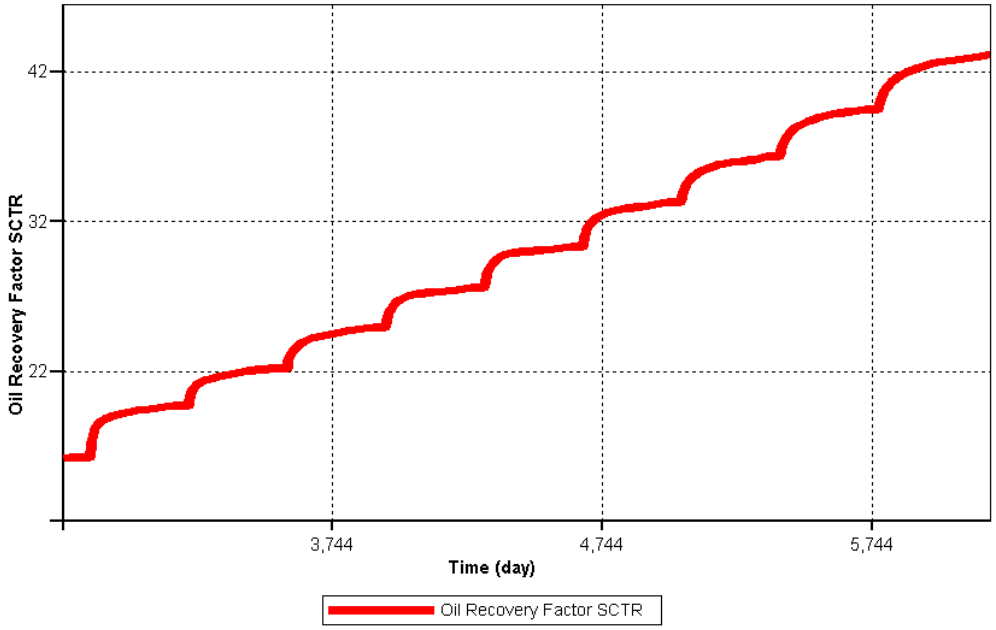

Figure 6.24 Oil recovery factor for cyclic steam injection process.

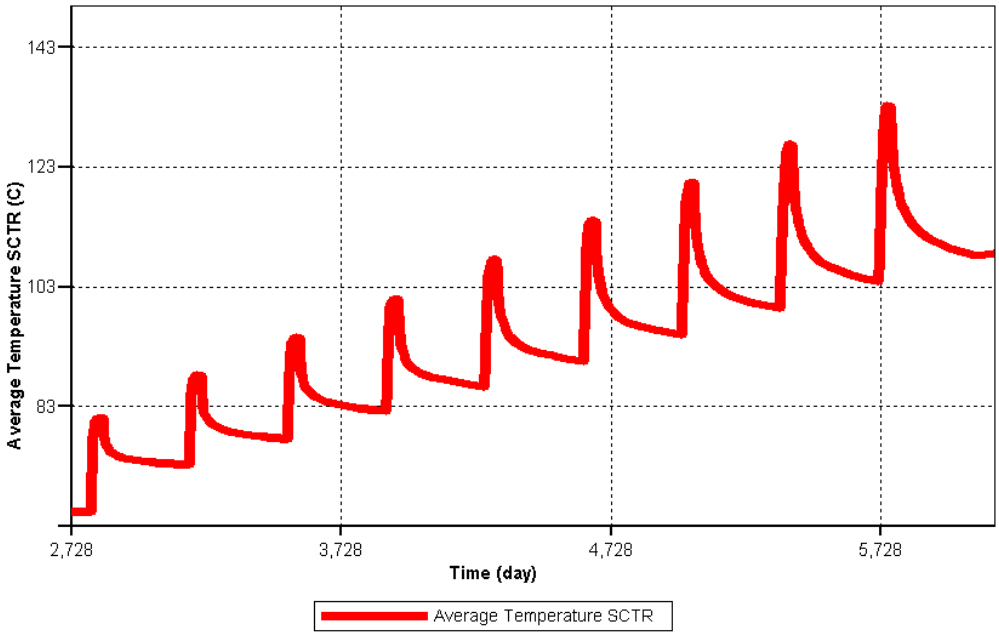

Figure 6.25 Average reservoir temperature for cyclic steam injection process.

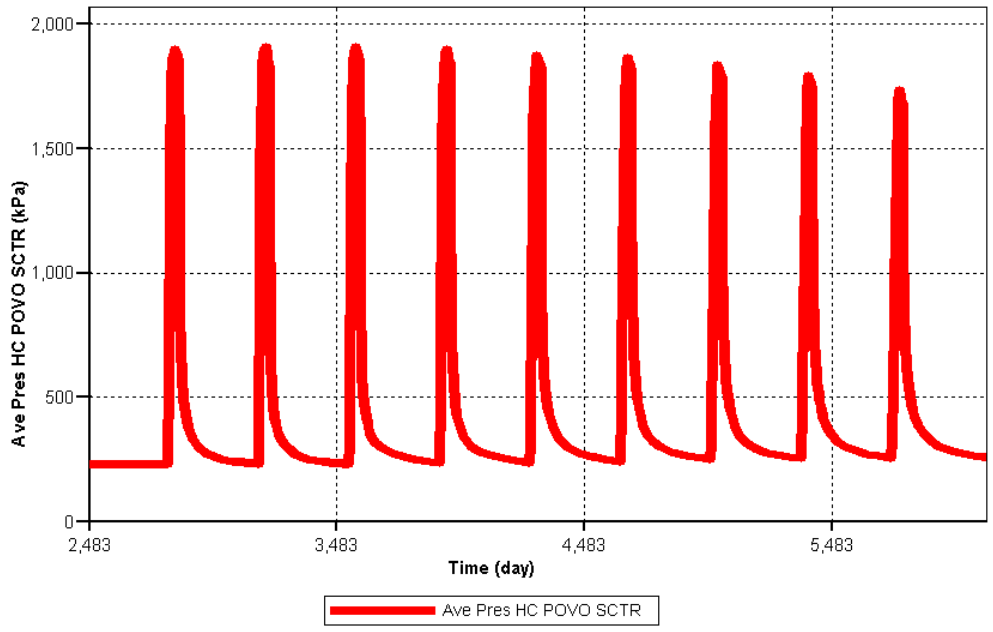

Figure 6.26 Average reservoir pressure for cyclic steam injection process.

6.4.3 Steam Drive Period

In this period, nine production wells are used to produce oil and four wells at the middle of each five spot pattern are used to inject 0.5 quality steams at 300 ^{o}C temperatures. Figure 6.27 shows wells used in the steam drive period. 10 years of steam drive process is applied as specified in Patzek and Koinis' paper. Figure 6.28, oil saturation profile, displays minor oil saturation change during the process. Figure 6.29, pressure profile, indicates a steady pressure profile. Figure 6.30, temperature profile, illustrates a more spread temperature along the reservoir. Gas saturation in figure 6.31 is not changing significantly during the process. These figures are given for the beginning, the middle, and the end time of steam drive process.

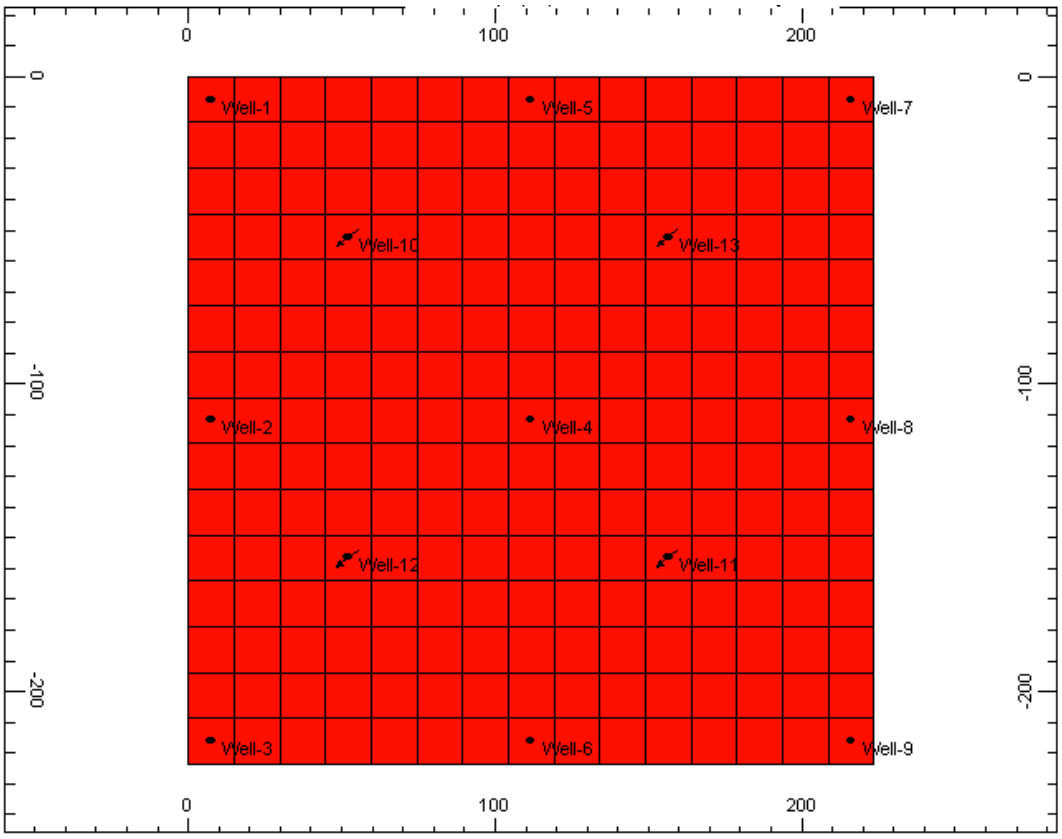

Figure 6.27 Wells used in steam drive period.

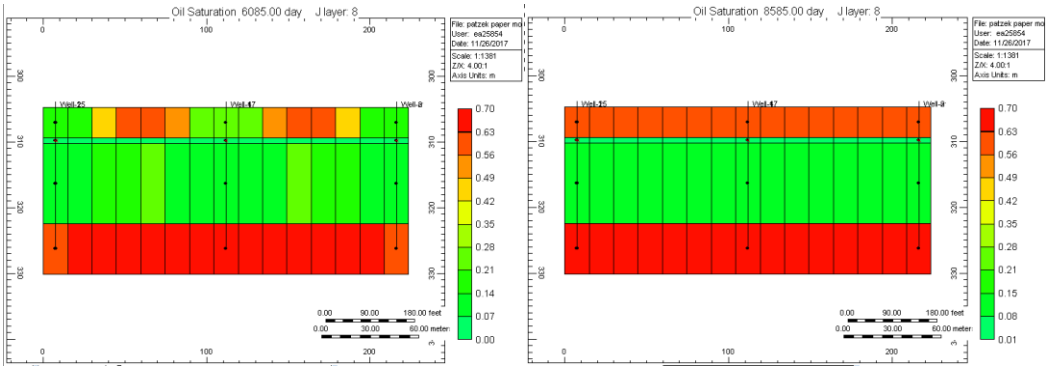

a) At the beginning of steam drive b) At the middle of steam drive

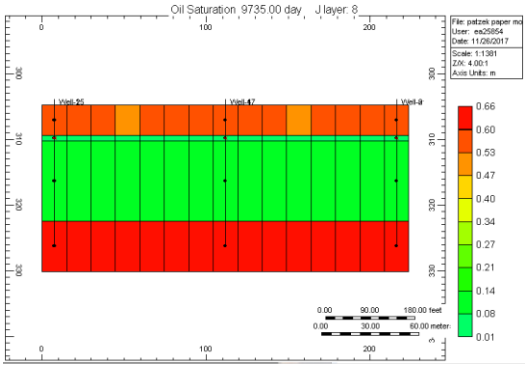

c) At the end of steam drive

Figure 6.28 Oil saturation profiles for beginning, middle, and end time of steam drive process.

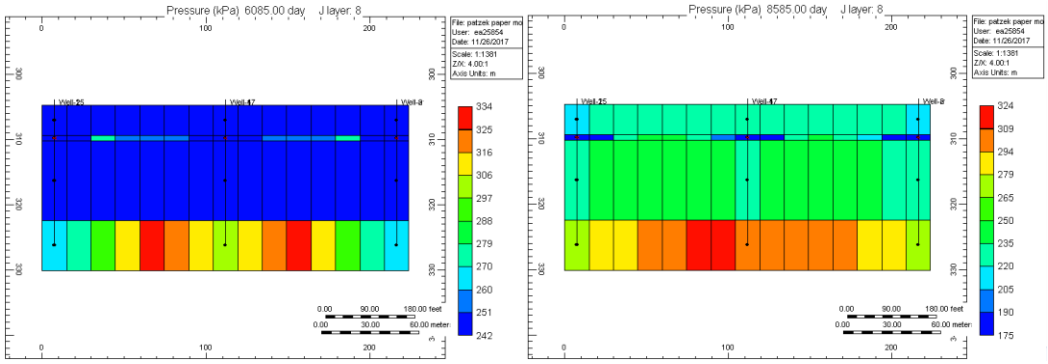

a) At the beginning of steam drive b) At the middle of steam drive

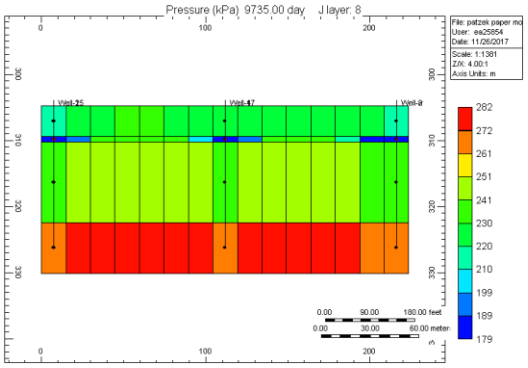

c) At the end of steam drive

Figure 6.29 Pressure profiles for beginning, middle, and end time of steam drive process.

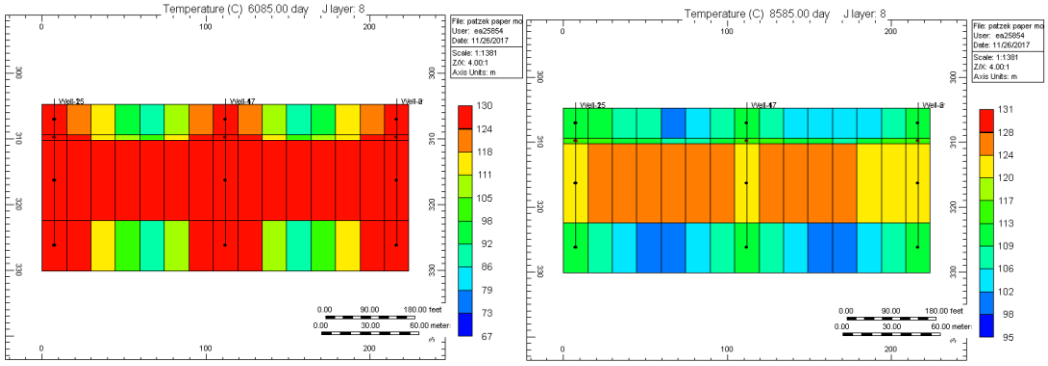

a) At the beginning of steam drive b) At the middle of steam drive

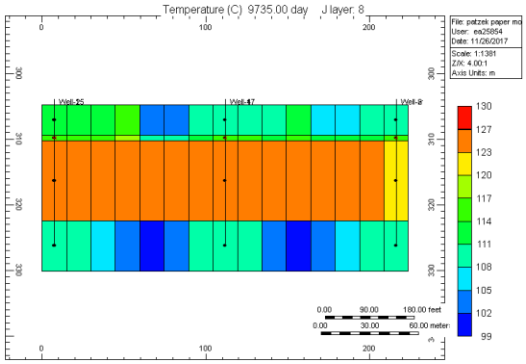

c) At the end of steam drive

Figure 6.30 Temperature profiles for beginning, middle, and end time of steam drive process.

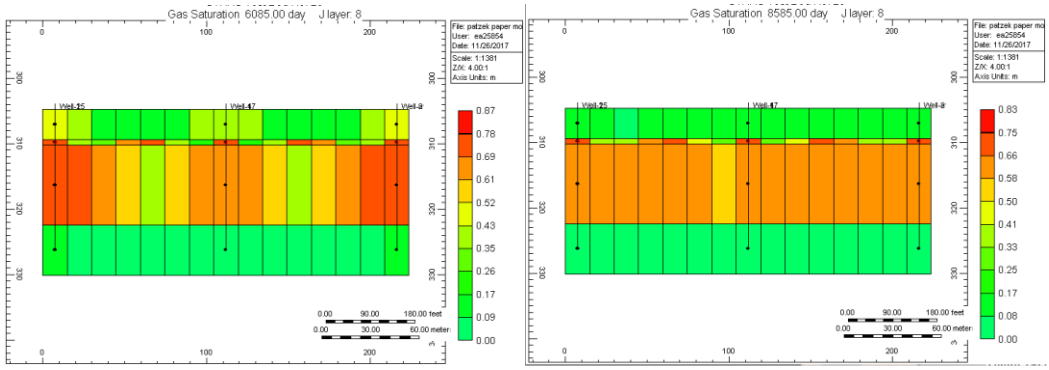

a) At the beginning of steam drive b) At the middle of steam drive

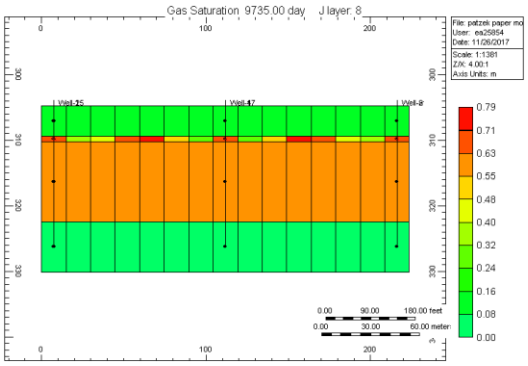

c) At the end of steam drive

Figure 6.31 Gas saturation profiles for beginning, middle, and end time of steam drive process.

As exhibited in Figure 6.32, the oil recovery is considerably increasing until the end of steam drive process. Figure 6.33 indicates the average reservoir temperature which is steadily increasing due to continuous steam injection during the entire process. Furthermore, Figure 6.34 displays that the average pressure remains steady since we are injecting and producing at the same time.

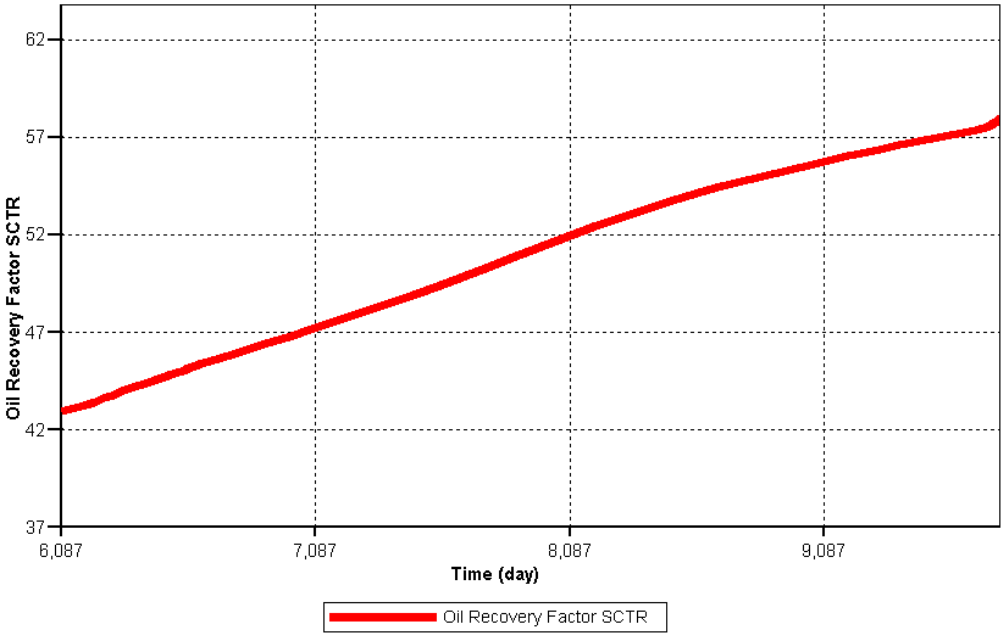

Figure 6.32 Oil recovery factor for steam drive process.

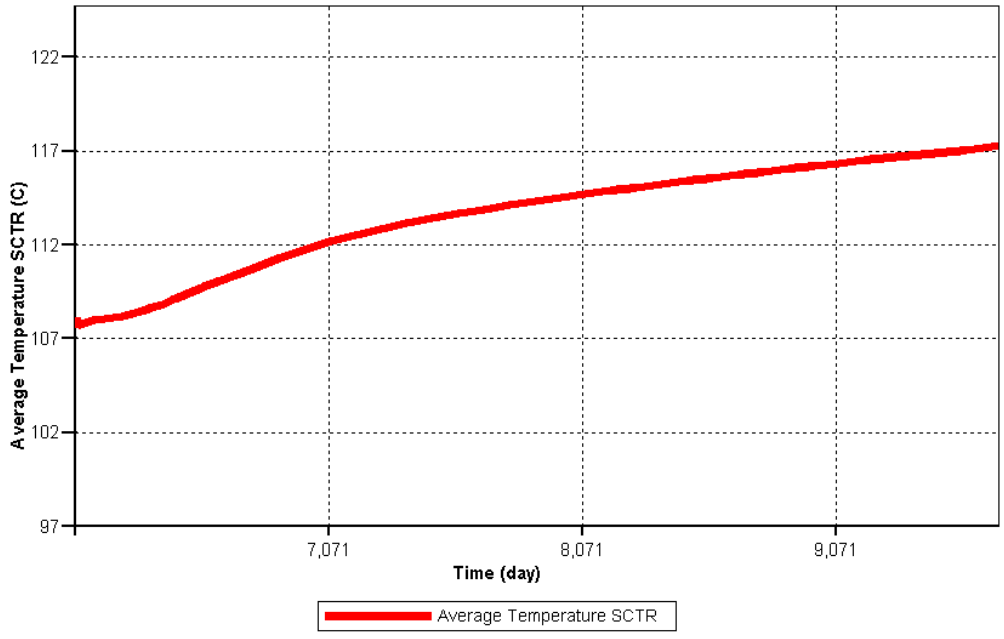

Figure 6.33 Average reservoir temperature for steam drive process.

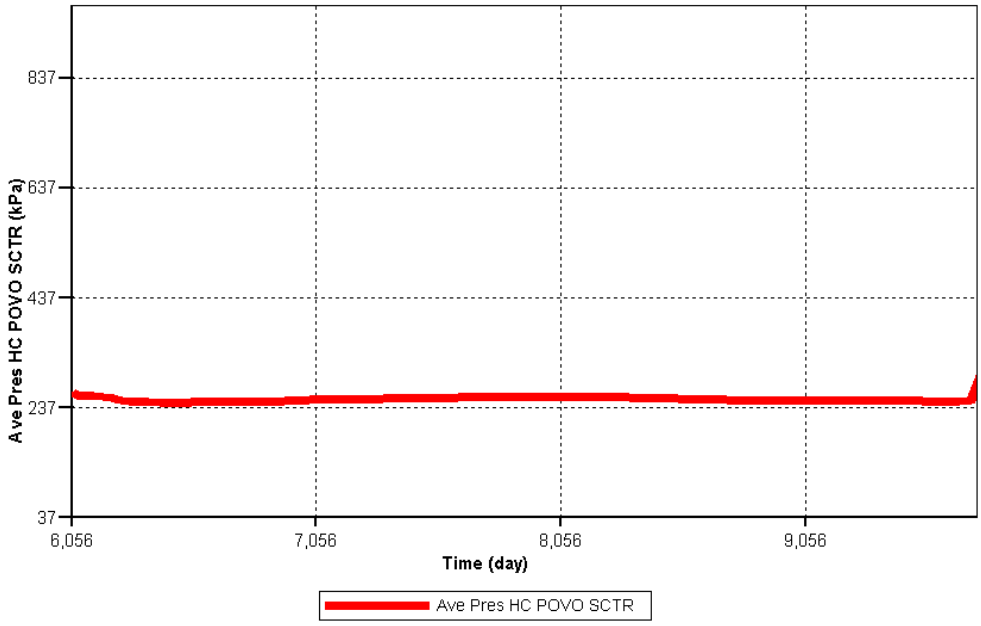

Figure 6.34 Average reservoir pressure for steam drive process.

6.4.4 Steam Foam Injection Period

In this fourth stage, oil was produced from nine different production wells and 0.5 quality steam foam was injected at 280 ^{o}C through four injection wells at the middle of each five spot pattern. Figure 6.35 shows the location of both production and injection wells. As designated in Patzek and Koinis' paper, four and a half years of steam foam injection process is applied. Oil saturation, pressure, temperature, and gas saturation profiles are illustrated for the beginning, middle, and end of steam foam injection process in the Figures 6.36, through 6.39. Surfactant adsorption profile at the end of steam foam injection process is demonstrated in Figure 6.40. Figure 6.36 exhibits a major oil saturation decrease during the process. Figure 6.37 indicates a major pressure difference between the beginning and the middle of this period and after the middle time, pressure

profile stays about steady. Figure 6.38 displays a major temperature difference between start of process and middle time, which is higher than the difference between the middle and end time of the process. Gas saturation in Figure 6.39 shows that the gas was spread along reservoir. Figure 6.40 displays a higher surfactant adsorption around well bore.

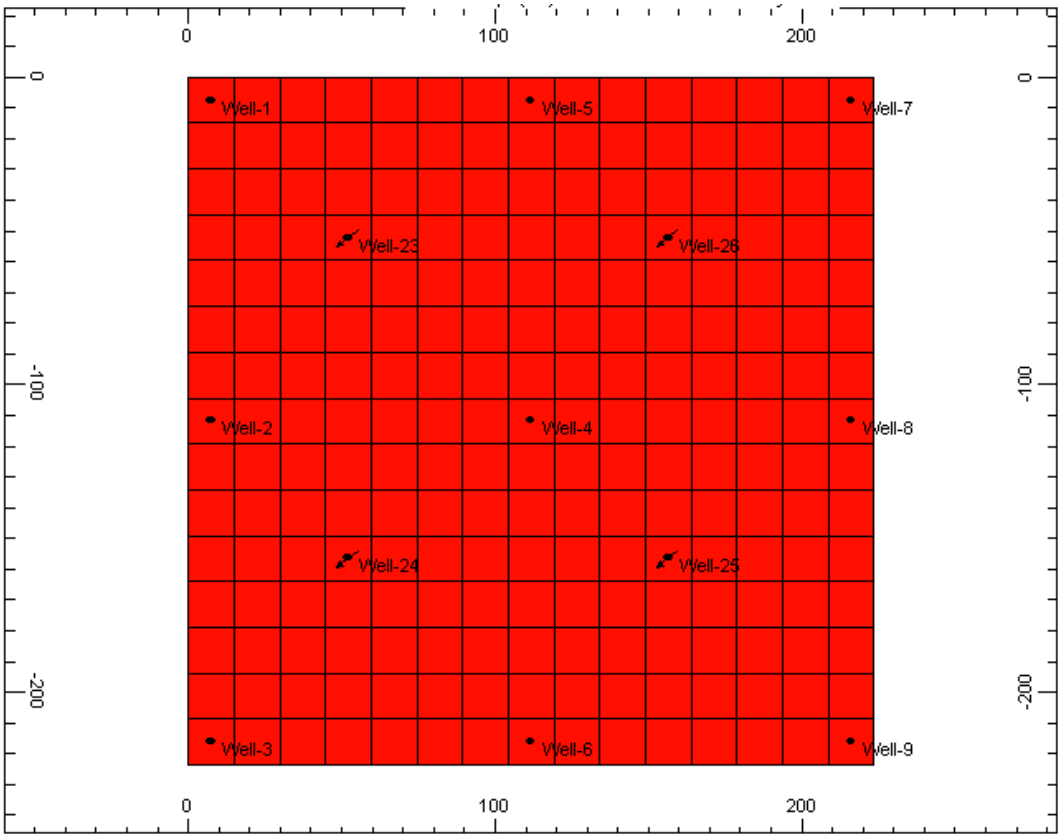

Figure 6.35 Wells used in steam foam injection period.

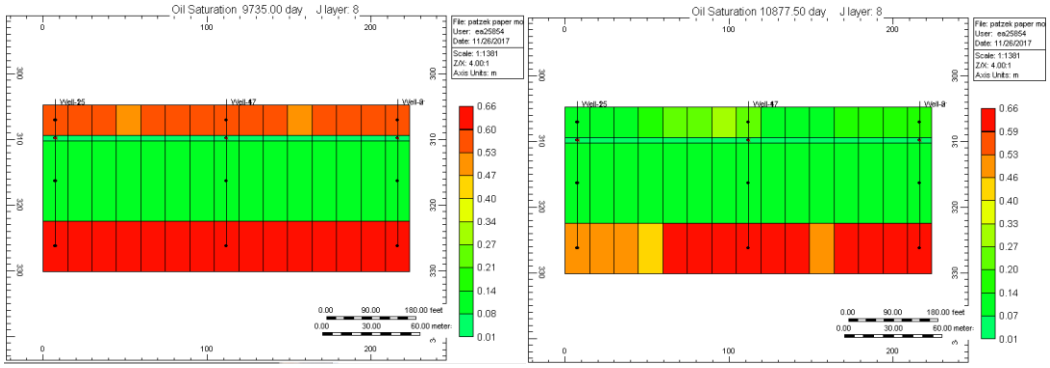

a) At the beginning of steam foam injection b) At the middle of steam foam injection

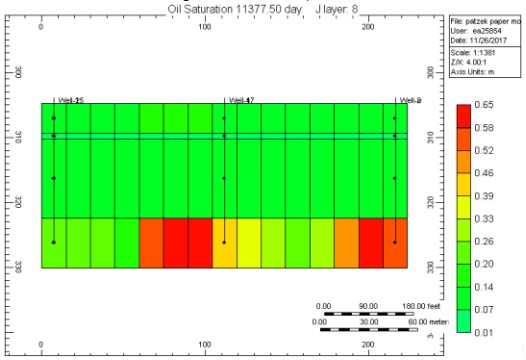

c) At the end of steam foam injection

Figure 6.36 Oil saturation profiles for beginning, middle, and end time of steam foam injection process.

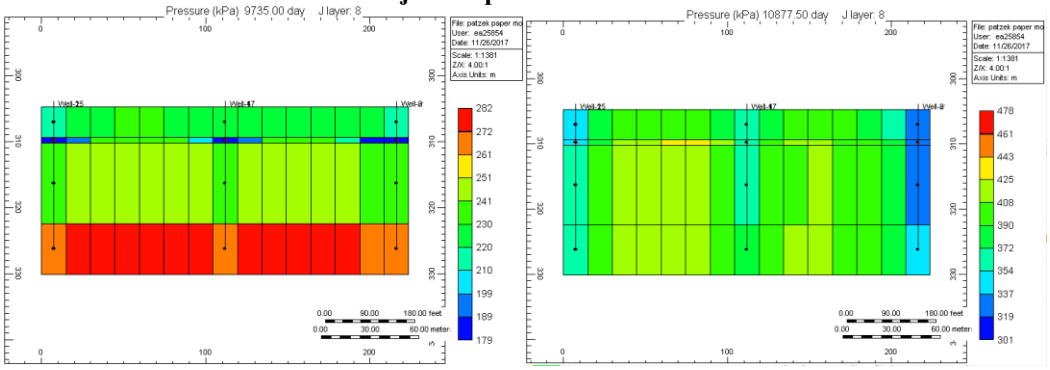

a) At the beginning of steam foam injection b) At the middle of steam foam injection

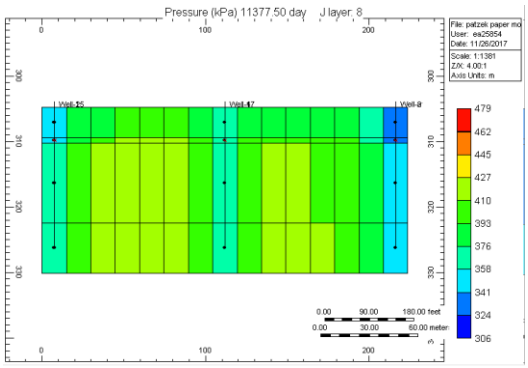

c) At the end of steam foam injection

Figure 6.37 Pressure profiles for beginning, middle, and end time of steam foam injection process.

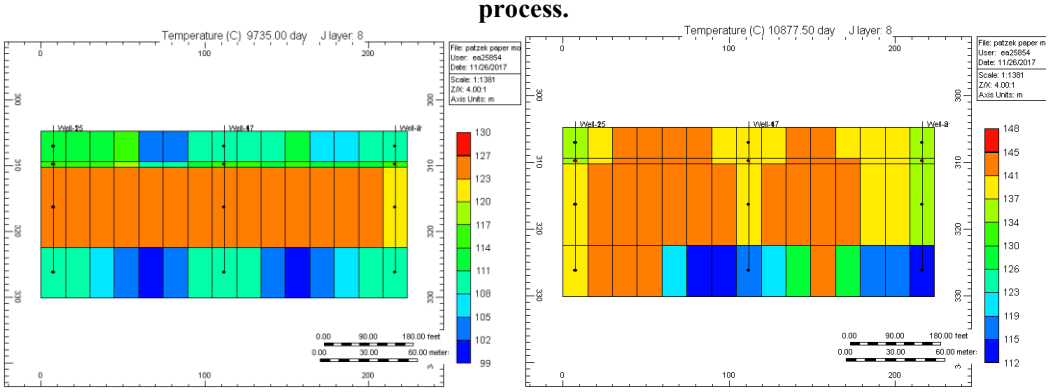

a) At the beginning of steam foam injection b) At the middle of steam foam injection

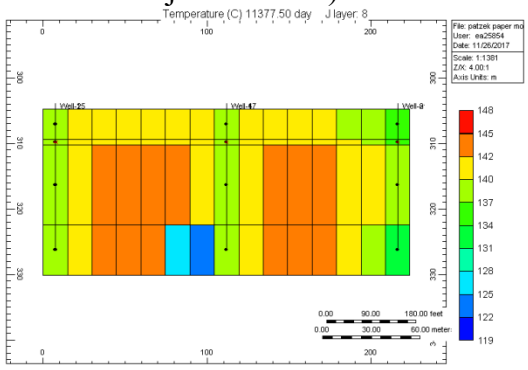

c) At the end of steam foam injection

Figure 6.38 Temperature profiles for beginning, middle, and end time of steam foam injection process.

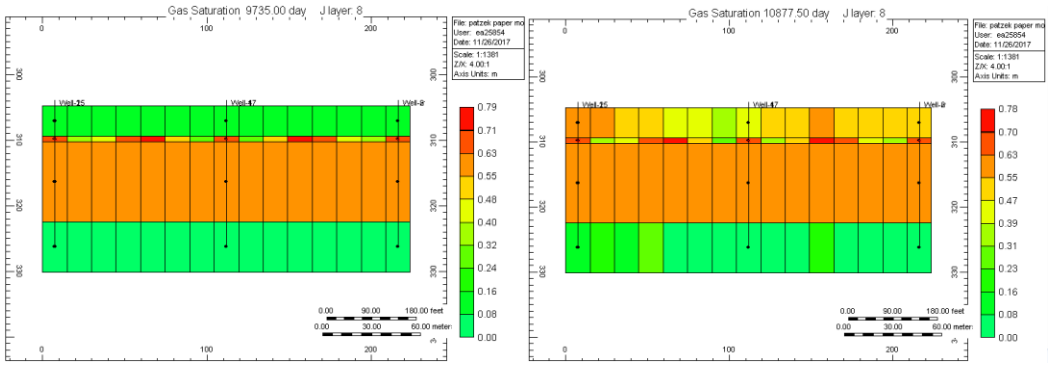

a) At the beginning of steam foam injection b) At the middle of steam foam injection

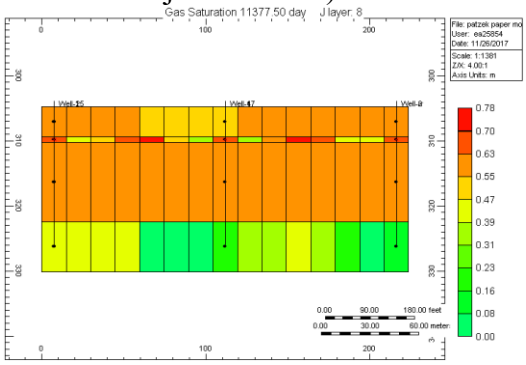

c) At the end of steam foam injection

Figure 6.39 Gas saturation profiles for beginning, middle, and end time of steam foam injection process.

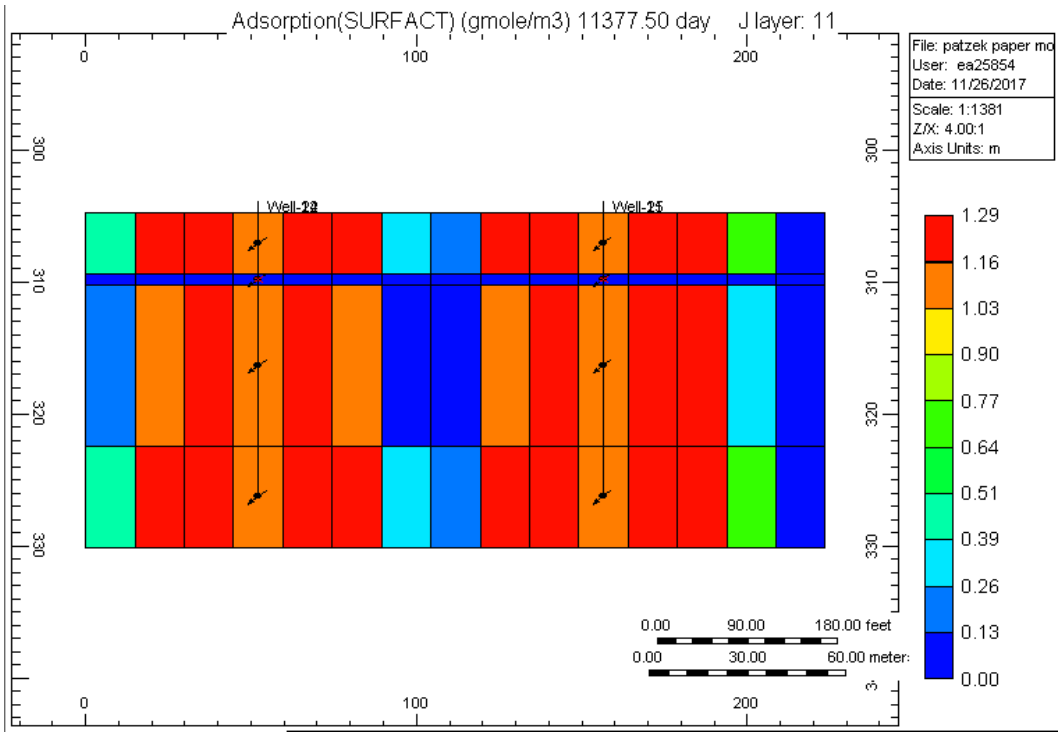

Figure 6.40 Surfactant adsorption profiles at the end time of steam foam injection process.

Figure 6.41, presenting the oil recovery factor, reveal that oil recovery is rising remarkably towards the end of steam foam drive. Underlying mechanism can be explained with the volumetric sweep efficiency of steam foam, controlling steam mobility and preventing gravity segregation as well as override. Thus, it results in improved oil recovery.

Injection of steam, during the whole process, brings about elevated reservoir temperature that is illustrated in Figure 6.42. In the average pressure profile, Figure 6.43, a steady average pressure is observed after a pick due to simultaneous injection and production processes.

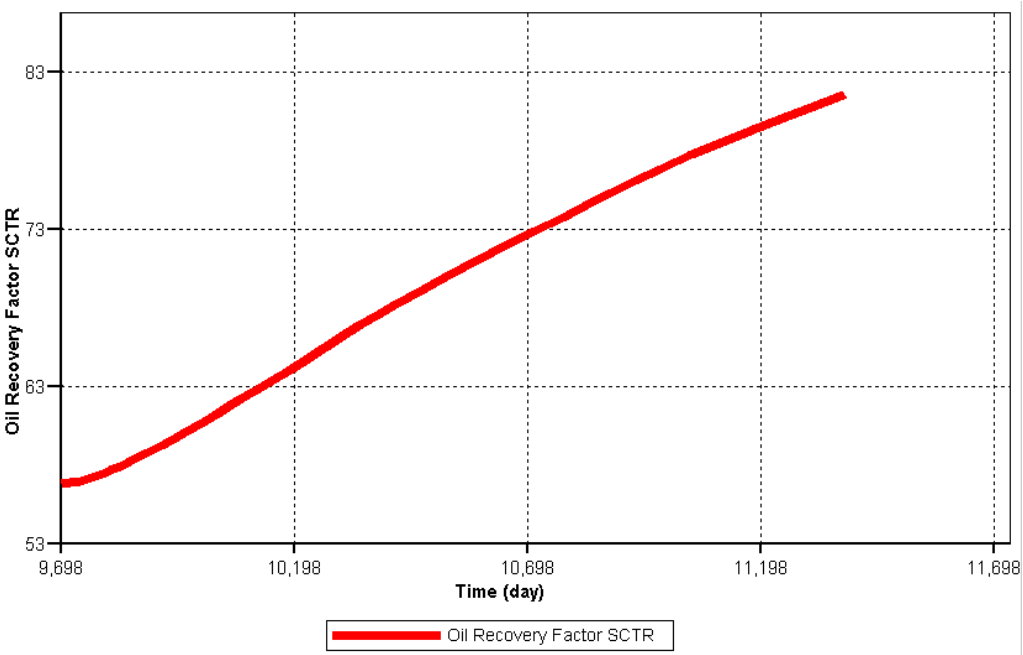

Figure 6.41 Oil recovery factor for steam foam injection process.

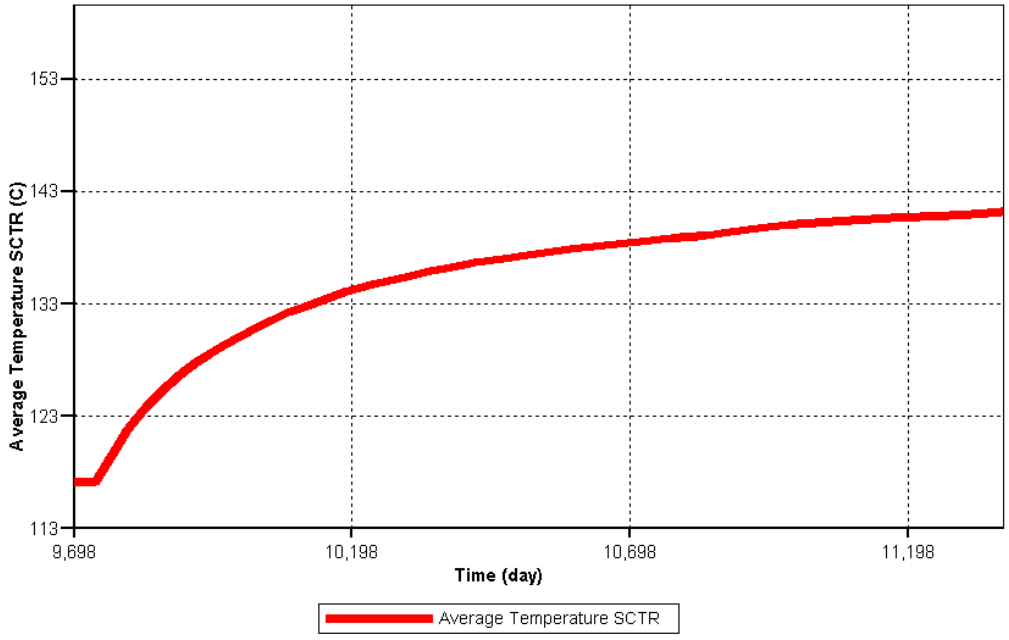

Figure 6.42 Average reservoir temperature for steam foam injection process.

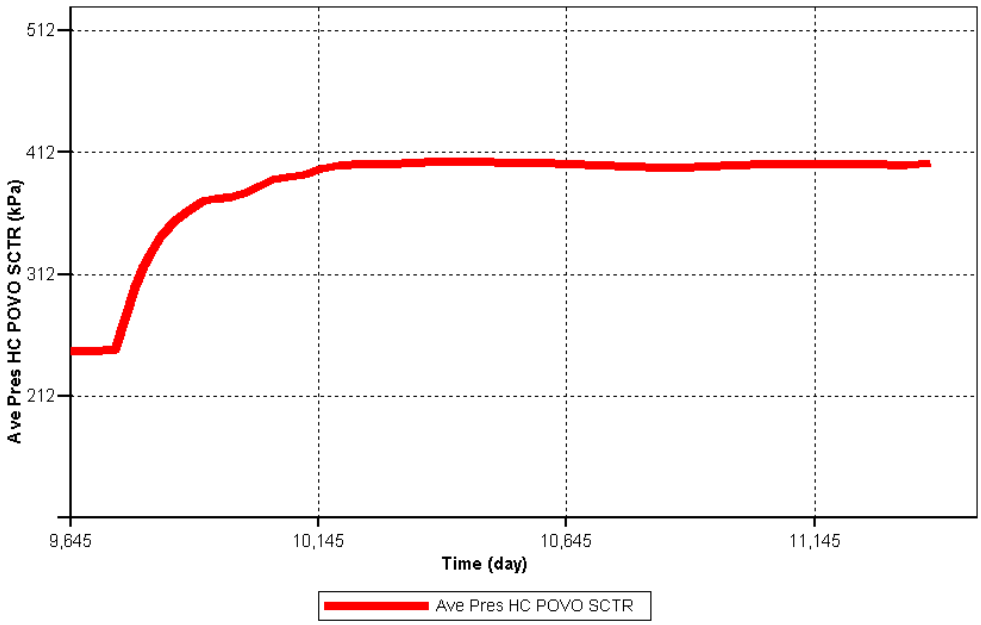

Figure 6.43 Average reservoir pressure for steam foam injection process.

6.4.5 General Results of All Combined Periods

Comparison of oil recovery factor between simulation results and field data are shown in the Figure 6.44. Simulation results are in good agreement with field data.

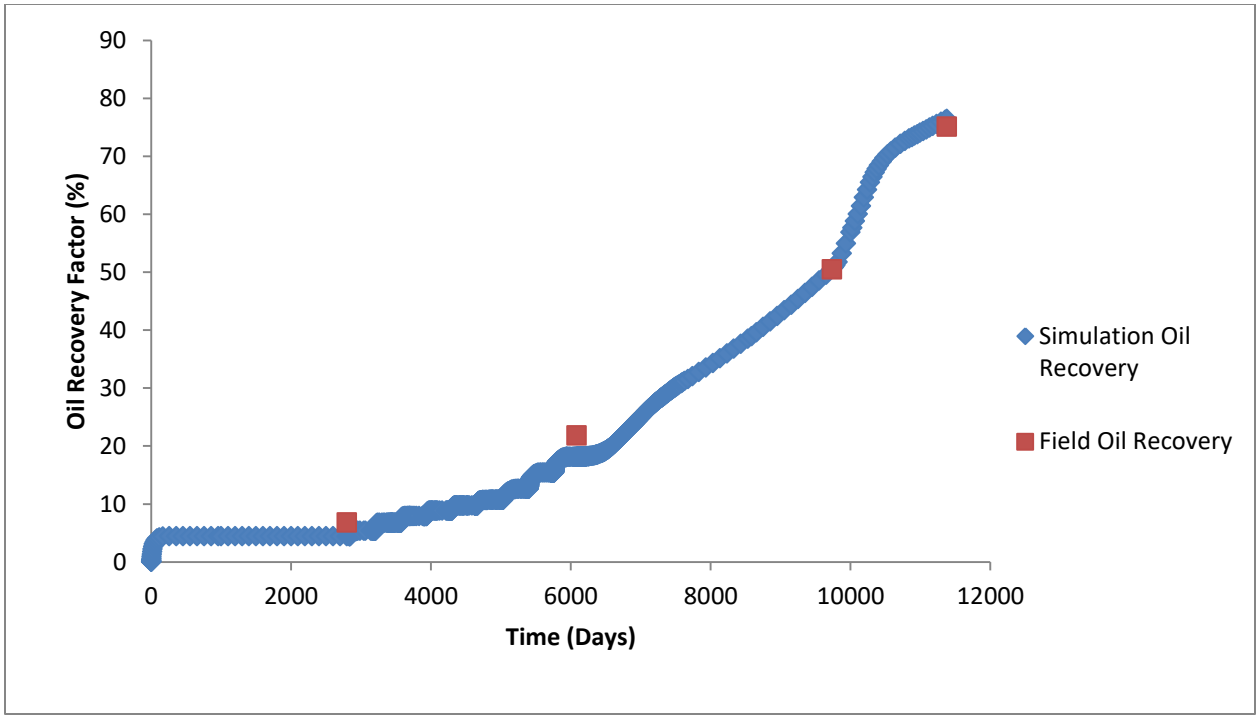

Figure 6.44 Oil recovery factor comparison between field data and simulation results.

As can be seen in Figure 6.45, initial reservoir temperature is 65.6 ^{o}C and it continues with the same temperature until 2800 days, which is the total primary production time. Starting from that time, cyclic steam injection started and an oscillating temperature can be seen. At the end of the cyclic steam injection process, which is 6085 days, steam drive process started and a relatively linear curve reached 115 ^{o}C. Starting from 9735 days, steam foam injection took place and increased the temperature to 135 ^{o}C. Figure 6.46 and Figure 6.47 show reservoir average pressure and cumulative oil steam ratio profiles, respectively.

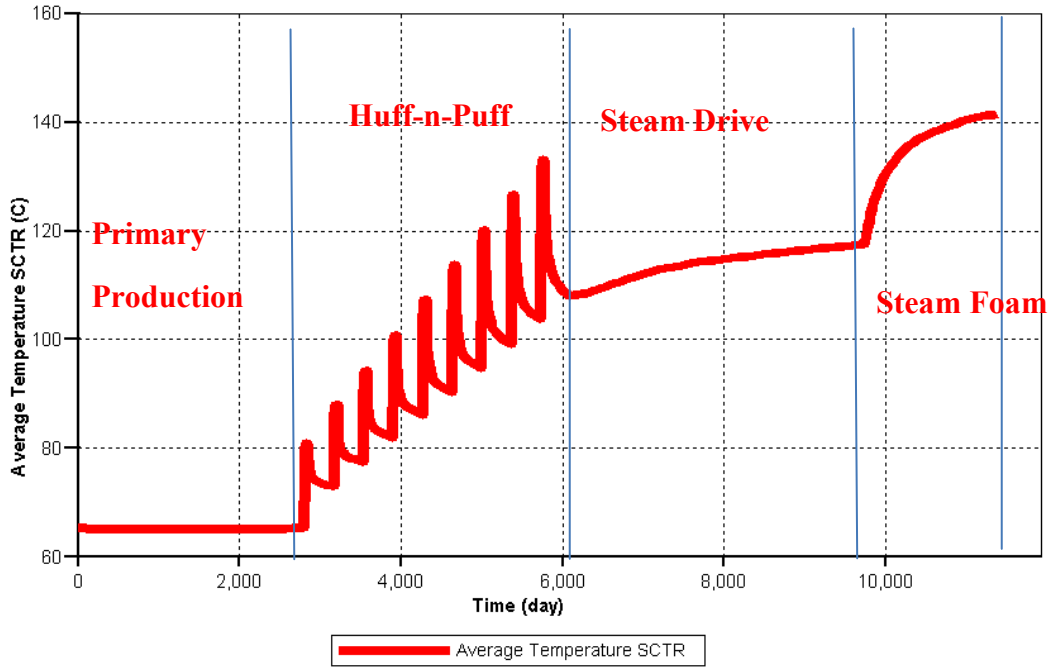

Figure 6.45 Reservoir average temperature profile.

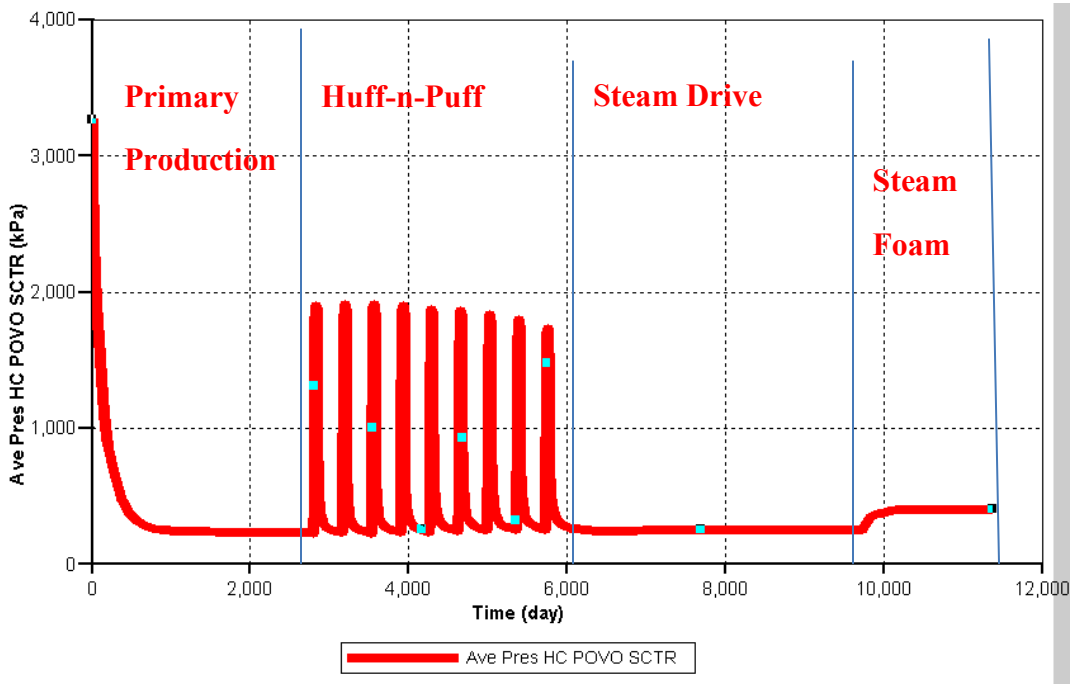

Figure 6.46 Reservoir average pressure profile.

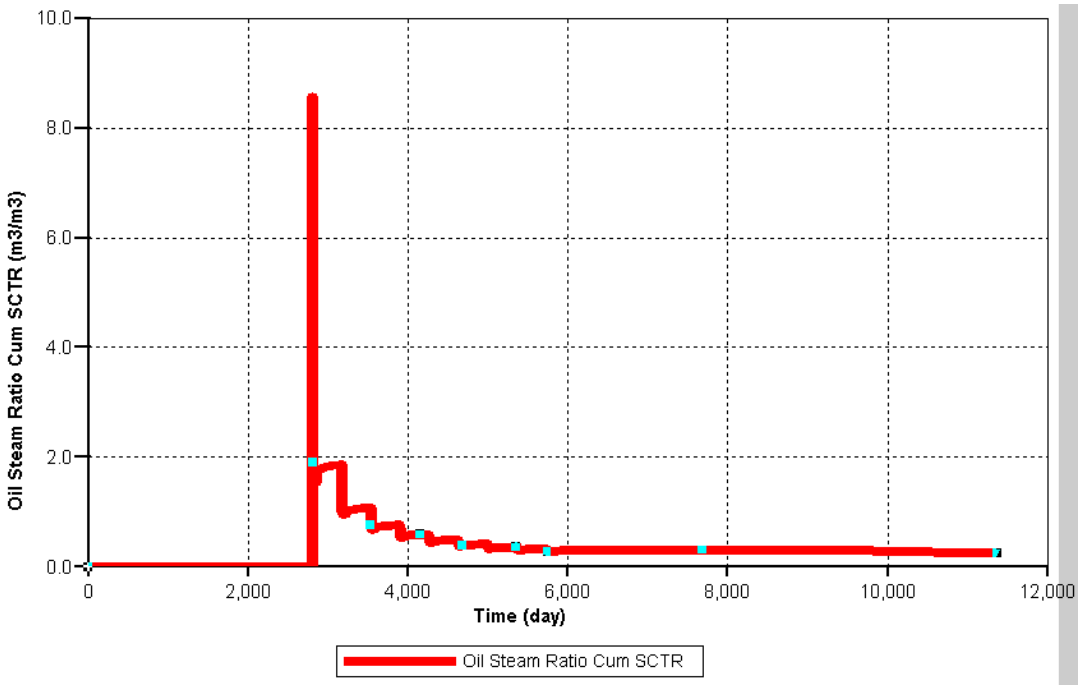

Figure 6.47 Cumulative oil steam ratio profile.

Chapter 7: Summary, Conclusions, and Recommendations

In this chapter, we summarize the tasks performed in this research and conclude the insights of this thesis and then several recommendations are made for future extension of this work.

7.1 SUMMARY

In this research the following tasks were performed:

- A simulation study was conducted in order to understand the mechanism behind steam foam approach and to see the effect of steam foam process on residual oil saturation and incremental oil production (Alkaline-steam core flood).
- A parameter optimization study was conducted for foam parameters on a reservoir. Based on CMG-STARS foam model some parameters changed and oil recovery, reservoir pressure, reservoir temperature, and average gas saturation were observed carefully for each case based on experimental data. Results analyzed then interpreted for different cases and influence of foam model on reservoir response tried to be observed.
- Production history data were matched for Mecca Lease, which is located in Kern River in Southern California by using similar reservoir geology given in Patzek and Koinis' work, which was presented in 1989 to construct numerical simulation model in order to evaluate steam foam process efficiency. We used geological information given in reference paper with four layers and tried to capture all model parameters. Same field volume was created in CMG-STARS. Same rock and reservoir properties were applied to build the reservoir model. Oil recovery for each step matched with

minor differences. In this work, steam-foam parameters that were obtained in Chapter 5 were used accordingly.

7.2 CONCLUSIONS

We conclude the following from this research:

- Oil recovery amounts were analyzed before and after alkaline steam foam injection on core scale and results were analyzed. Results are matching with field data and show 20 percent increase in cumulative oil production.
- Many cases were created using different relative permeability values and simulation results were successfully matched with the field results. During that study Brooks-Corey model was used in order to obtain relative permeability tables.
- Sensitivity analysis study was conducted using CMG-STARS simulator on field-scale in order to indicate the effect of each foam parameter on oil recovery by changing only one foam parameter at a time and keeping others fixed and optimum parameters were obtained.
- For Fmsurf, Epcap, and Epoil parameters, higher oil recovery factor was obtained at lower values of the parameters also changes in Fmoil and Fmmob parameters result in lower oil recovery for lower values. On the other hand, no difference in oil recovery factor was observed when varying Epsurf and Fmcap. Obtained foam parameter values were used in Chapter 6 for better results.
- Steam foam efficiency was tested by simulating the Patzek and Koinis' study conducted in Mecca Lease located in Kern River in Southern California. Results matched with field data and 24 percent oil recovery increase was obtained by applying steam foam. The study concluded that foam improves the volumetric sweep

efficiency by controlling steam mobility and preventing gravity segregation as well as override; therefore, it entails considerably increased oil recovery.

7.3 RECOMMENDATIONS FOR FUTURE WORK

Thermal and chemical EOR methods are quite complicated processes. Therefore, more research in this area is strongly recommended to develop a deeper conceptual understanding and to capture more physical mechanisms for field operations. During this research study, we observed the effect of steam foam process on heavy oil recovery. Recommendations for further study are listed as the following:

- Application of Alkaline steam foam should be studied in fractured reservoirs in order to ascertain the effect of enhanced oil recovery process.
- Similar modeling should be applied in other simulators such as UTCHEM and results of population balance-based models should be compared with other models for better understanding.
- More history matching applications should be studied in order to determine the accuracy of simulation results compared to field data.
- More parameter study should be conducted to ascertain the effect of other parameters not studied in this thesis.

Glossary

Fluid Flow Properties

k_{ro} = oil relative permeability

k_{rg} = gas relative permeability

$k_{ro,\max}$ = maximum relative permeability for oil in modified Brooks-Corey functions

$k_{rg,\max}$ = maximum relative permeability for gas in modified Brooks-Corey functions

$k_{rw,\max}$ = maximum relative permeability for water in modified Brooks-Corey functions

n_o = oil exponent for modified Brooks-Corey functions

n_g = gas exponent for modified Brooks-Corey functions

n_w = water exponent for modified Brooks-Corey functions

S_o = oil saturation, [L^3/L^3]

S_{or} = residual oil saturation, [L^3/L^3]

S_{wc} = residual water saturation, [L^3/L^3]

S_{gc} = residual gas saturation, [L^3/L^3]

λ = pore-size-distribution parameter in Corey functions

Foam Properties

c_g = generation rate coefficient

c_c = coalescence rate coefficient

C_s, C_s^* = surfactant and threshold surfactant concentration, respectively, [L^3/L^3]

C_s^o = reference surfactant concentration, [L^3/L^3]

epsurf = composition contribution exponent

epcap = capillary number contribution exponent

epoil = oil saturation contribution exponent

F = foam mobility multiplier

F_o = foam mobility multiplier at ref. gas velocity

FM = mobility reduction factor

fmmob = maximum reduction factor

fmsurf = critical component mole fraction value

fmcap = reference rheology capillary number value

fmoil = critical oil saturation value

fmgcp = critical generation capillary number value

fmomf = critical oil mole fraction for component numx

fmsalt = critical salt mole fraction value for component numw

k_{rg}^f = foam relative permeability

k_{rg}^o = gas endpoint relative permeability

k_l = generation coefficient

k_l^o = model parameter

k_{-l} = coalescence coefficient

k_{-l}^o = model parameter

m = model parameter

n = coalescence exponent

n_f = flowing foam bubble density, [m/L^3]

n^* = limiting (maximum) bubble density, [m/L^3]

n_g = gas exponent relative permeability

n_l = trapping foam bubble density, [m/L^3]

$n_{\max}$ = maximum (limiting) bubble density, [m/L^3]

P_c = capillary pressure, [m/Lt^2]

P_c^* = limiting capillary pressure, [m/Lt^2]

$P_{c,\max}^*$ = limiting value of P_c^*, [m/Lt^2]

∇P = pressure gradient, [m/Lt^2]

∇P_O = model parameters related to minimum pressure gradient, [m/Lt^2]

R = foam resistance factor

S_w^* = limiting water saturation, [L^3/L^3]

S_f = lowest water saturation for foam effect, [L^3/L^3]

s_1, s_2 = slop of the gas relative permeability at high quality regime and low quality regime, respectively

S_{gD} = dimensionless gas saturation

Tad1 = First parameter in the Langmuir expression for the adsorption isotherm, [mole/L^3]

Tad2 = Second parameter in the Langmuir expression for the adsorption isotherm associated with salt effects, [mole/L^3]

Tad3 = Third parameter in the Langmuir expression for the adsorption isotherm

u_g, u_{gref} = gas Darcy and reference gas Darcy velocity, [Lt^{-1}]

v_f = local gas velocity, [Lt^{-1}]

v_w = local water velocity, [Lt^{-1}]

X_l = trapping foam fraction

$X_{l,\max}$ = maximum trapping foam fraction

a = shear thinning exponent

β = trapping parameter

ε = water saturation tolerance

σ = power-low exponent

ω = constant exponent

Thermal Properties

Q = energy, [Q=M L^2t^{-2}]

M = mass, [M]

H = enthalpy [QM^{-1}]

U = internal energy [QM^{-1}]

$\bar{H}$ = specific enthalpy of phases [QM^{-1}]

q_H = enthalpy source or sink term rate [$QL^{-3}t^{-1}$]

q_L = heat loss rate to overburden and underburden rocks [$QL^{-3}t^{-1}$]

q_{instu} = insitu thermal conduction source rate [$QL^{-3}t^{-1}$]

λ = thermal conductivity of phases [$Qt^{-1}L^{-1}T^{-1}$]

c_w = volume concentration of steam component [L3/L3]

c_s = volume concentration of water component [L3/L3]

ζ_{pw} = heat capacity of water, [$QM^{-1}T^{-1}$]

ζ_{ps} = heat capacity of aqueous, [$QM^{-1}T^{-1}$]

α = steam mass quality [M/M]

μ = viscosity, [ML^{-1} t^{-1}]

T = temperature [T]

P = pressure [$ML^{-1}\ t^{-2}$]

u = Darcy velocity for each phase [Lt^{-1}]

Subscripts:

h = component number, where 1 = water; 2 = oil; 3 = surfactant; 4 = polymer;5 = anion; 6 = cation; 7 = alcohol; 8 = gas

l = phase number, where 1 = water (aqueous); 2 = oil (oleic); 3 = micro emulsion; 4 = gas

Appendix A: Sample Input Data

A.1 STEAM AND STEAM FOAM INJECTION CASE (CASE-1)

The following is the input data file for CMG STARS simulator. We used this case in Chapter 4 for oil recovery factor comparison between steam injection only model and steam foam injection model.

```
:
**  ==============  INPUT/OUTPUT CONTROL  ======================

RESULTS SIMULATOR STARS

*INTERRUPT *STOP

*TITLE1 'STARS Test Bed No. 6'
*TITLE2 'Fourth SPE Comparative Solution Project'
*TITLE3 'Problem 1A:  2-D CYCLIC STEAM INJECTION'

*INUNIT *FIELD   ** output same as input

*OUTPRN *GRID *PRES *SW *SO *SG *TEMP *Y *X *W *SOLCONC *OBHLOSS *VISO *VISG
*OUTPRN *WELL *ALL
*WRST 200
*WPRN *GRID 200
*WPRN *ITER 200

outsrf special blockvar pres 2,1,2
            blockvar so 2,1,2
            blockvar sg 2,1,2
            blockvar temp 2,1,2
            blockvar cchloss 1,1,4
            blockvar cchloss 7,1,4
            matbal well 'OIL'    ** cumulative oil production
            matbal well 'Water'  ** cumulative water production
            cchloss              ** cumulative heat loss/gain
*OUTSRF *GRID *PRES *SO *SG *TEMP




**  ==============  GRID AND RESERVOIR DEFINITION  ==================


*GRID *RADIAL 1 1 50 *RW    0     ** Zero inner radius matches previous treatment

**  Radial blocks:  small near well;  outer block is large
```

```
*DI *IVAR  0.125

*DJ *CON   360     **  Full circle

*DK *KVAR 50*0.02

*POR *CON 0.31
*PERMI *CON 4000
*PERMJ *EQUALSI
*PERMK *EQUALSI

*END-GRID

*CPOR 5e-4
*PRPOR 75
*ROCKCP 35
*THCONR 24
*THCONW 24
*THCONO 24
*THCONG 24
*HLOSSPROP  *OVERBUR 35 24  *UNDERBUR 35 24



**  ==============  FLUID DEFINITIONS  ======================


*MODEL 4 4 4 2   ** Components are water and dead oil.  Most water
            ** properties are defaulted (=0).  Dead oil K values
            ** are zero, and no gas properties are needed.

*COMPNAME       'Water'    'SURFACT'     'OIL'                       'N2'
**              -----    -------   ------------          ----
    *CMM        18.02      480         600                     28
    *PCRIT      3206.2     160               160                       480             ** These four properties
    *TCRIT      705.4      921               921                       -232.6          ** are for the gas phase.
    *AVG        1.13e-5    0                 0                                         ** The dead oil component does
    *BVG        1.075      0                 0                                         ** not appear in the gas phase.
    *MOLDEN     0        0.202       0.10113
    *CP         0        5.e-6         5.e-6
    *CT1        0        3.8e-4        3.8e-4
    *CPL1       0        300           300
*****************************************************************************

*PRSR 14.7
*TEMR 60
*PSURF 14.7
*TSURF 100

**  ==============  ROCK-FLUID PROPERTIES  ======================

*SOLID_DEN 'SURFACT' 23040 0 0  ** Mass density based on 48000 gmole/m3
*SOLID_CP 'SURFACT' 17 0

*VISCTABLE
```

```
**    Temp

 60.0                          1.20000        1.0              43400.0
 100.0000     0.68200 1.0  2690
 180.0000     0.35000 1.0  96.0
 200.0000     0.30300 1.0  47.0
  600.000     0.02094 1.0  10.00000

**  Gas/liq K values  are defaulted correlation
**  Liq/liq K values  are entered as tables
*LIQLIQKV
*KVTABLIM 100.0 8000.0  15 550
*KVTABLE 'WATER'
   0    0
   0    0
*KVTABLE 'SURFACT'
  .2   .2
  .2   .2
*KVTABLE  'BITUMEN'
   0    0
   0    0

** Reference conditions
*PRSR 100.0
*TEMR 15.5
*PSURF 100.0
*TSURF 15.5

**  reaction describes surfactant decomposition
**  first order decay rate is assumed (valid for basic pH)

*STOREAC    0           1       0
*STOPROD    26.37       0       0
*RPHASE     0           1       0
*RORDER     0           1       0
*FREQFAC  34.7
*EACT 32500
*RENTH 0
*O2CONC


*ROCKFLUID

**  ==============  ROCK-FLUID PROPERTIES  ======================

**  This simulation incorporates foam mobility reduction in
**  relative permeability effects which are region dependent.
**  ------------------------------------------------------------

*KRTYPE *CON       1   ** Standard bed permeability
  *MOD 1  1 1:2 =  2   ** Higher perm commumication path
       6  1 1:2 =  2   ** Higher perm commumication path
     1:9  1   3 =  2   ** Higher perm commumication path

*RPT 1    ** First rock type for standard permeability zones
**  ------------------------------------------------------------
```

```
**  Interpolation between 3 sets: zero, weak and strong foam curves
**  Capillary number calculation is based on aqueous SURFACT IFT
**  specified at 2 temperatures and 2 SURFACT concentrations.

*INTCOMP 'SURFACT' *WATER
*INTLIN

*IFTTABLE    ** aq mole frac      IFT
    *TEMP  10.0
                0.0           13.
                0.3           13.
    *TEMP 320.0
                0.0           13.
                0.3           13.

*FMSURF 1.875E-4
*FMCAP 1.0E-4
*FMOIL 0.5
*FMMOB 50
*EPSURF 1.0
*EPCAP 1.0
*EPOIL 1.0

**  Set #1:  No foam, corresponding to no SURFACT
**  ---------------------------------------------

*KRINTRP 1

*DTRAPW  1.0  ** no mobility reduction

*SWT   **  Water-oil relative permeabilities

**   Sw         Krw       Krow
**  -----     -------    -------
 0.0930000       0.0   1.00000       0.0
 0.1500000 1.7000E-4 0.8400000       0.0
 0.2000000 8.0000E-4 0.7100000       0.0
 0.2500000 0.0024000 0.5800000       0.0
 0.3000000 0.0061000 0.4650000       0.0
 0.4000000 0.0250000 0.2780000       0.0
 0.5000000 0.0760000 0.1360000       0.0
 0.6000000 0.1800000 0.0410000       0.0
 0.6500000 0.2600000 0.0130000       0.0
 0.7000000 0.3600000 0.0110000       0.0
 0.8000000 0.5700000 0.0060000       0.0
 0.9000000 0.7500000       0.0       0.0
   1.00000   1.00000       0.0       0.0

*SLT  *NOSWC   **  Liquid-gas relative permeabilities

**   Sl         Krg       Krog
**  ----      -------    ------
 0.1500000   1.00000       0.0       0.0
 0.4000000 0.9900000 1.0000E-4       0.0
 0.4200000 0.9850000 8.0000E-4       0.0
 0.4500000 0.9800000 0.0070000       0.0
```

```
 0.5000000 0.8500000 0.0260000       0.0
 0.5500000 0.6900000 0.0550000       0.0
 0.6000000 0.5400000 0.0900000       0.0
 0.7000000 0.2870000 0.1860000       0.0
 0.8000000 0.1140000 0.3310000       0.0
 0.9000000 0.0220000 0.5700000       0.0
 0.9500000 0.0045000 0.7600000       0.0
   1.00000       0.0   1.00000       0.0

**  Override critical saturations on table
*SWR 0.0
*SORW 0.00
*SGR 0
*SORG 0


**  Set #2:  Weak foam, corresponding to intermediate SURFACT concentration
**  ---------------------------------------------------------------------------

*KRINTRP 2 *COPY 1 1    ** copy from first set, then overwrite

*DTRAPW 0.4  ** weak foam inverse mobility reduction factor (MRF=2.5)

**  Override critical saturations on table
*SWR 0.15
*SORW 0.00
*SGR 0.05
*SORG 0.16
*KRGCW 0.4

**  Set #3:  Strong foam, corresponding to high SURFACT concentration
**  ---------------------------------------------------------------------

*KRINTRP 3 *COPY 1 1    ** copy from first set, then overwrite

*DTRAPW 0.02  ** strong foam inverse mobility reduction factor (MRF=50)

**  Override critical saturations on table
*SWR 0.15
*SORW 0.00
*SGR 0.05
*SORG 0.16
*KRGCW 0.02

*RPT 2    ** Second rock type for high permeability zones
**  ---------------------------------------------------------------------
**  Interpolation between 3 sets: zero, weak and strong foam curves
**  Capillary number calculation is based on aqueous SURFACT IFT
**  specified at 2 temperatures and 2 SURFACT concentrations.

*INTCOMP 'SURFACT' *WATER
*INTLIN

*IFTTABLE    ** aq mole frac      IFT
    *TEMP  10.0
                0.0           13.
```

```
                0.3           13.
    *TEMP 320.0
                0.0           13.
                0.3           13.

*FMSURF 1.875E-4
*FMCAP 1.0E-4
*FMOIL 0.5
*FMMOB 50
*EPSURF 1.0
*EPCAP 1.0
*EPOIL 1.0

**  Set #1:  No foam, corresponding to no SURFACT
**  ---------------------------------------------

*KRINTRP 4

*DTRAPW  1.0  ** no mobility reduction

*SWT   **  Water-oil relative permeabilities

**   Sw         Krw       Krow
**  -----     -------    -------
      0.0       0.0   1.00000       0.0
 0.2000000 0.2000000 0.8000000       0.0
 0.4000000 0.4000000 0.6000000       0.0
 0.6000000 0.6000000 0.4000000       0.0
 0.8000000 0.8000000 0.2000000       0.0
  1.00000   1.00000       0.0       0.0

*SLT  *NOSWC   **  Liquid-gas relative permeabilities

**   Sl         Krg       Krog
**  ----      -------    ------
      0.0   1.00000       0.0       0.0
 0.2000000 0.8000000 0.2000000       0.0
 0.4000000 0.6000000 0.4000000       0.0
 0.6000000 0.4000000 0.6000000       0.0
 0.8000000 0.2000000 0.8000000       0.0
  1.00000       0.0   1.00000       0.0

**  Override critical saturations on table
*SWR 0.15
*SORW 0.01
*SGR 0.05
*SORG 0.16


**  Set #2:  Weak foam, corresponding to intermediate SURFACT concentration
**  ---------------------------------------------------------------------

*KRINTRP 5 *COPY 2 1    ** copy from first set, then overwrite

*DTRAPW 0.4  ** weak foam inverse mobility reduction factor (MRF=2.5)
```

```
**  Override critical saturations on table
*SWR 0.15
*SORW 0.01
*SGR 0.05
*SORG 0.16
*KRGCW 0.4

**  Set #3:  Strong foam, corresponding to high SURFACT concentration
**  ------------------------------------------------------------------

*KRINTRP 6 *COPY 2 1    ** copy from first set, then overwrite

*DTRAPW 0.02  ** strong foam inverse mobility reduction factor (MRF=50)

**  Override critical saturations on table
*SWR 0.15
*SORW 0.01
*SGR 0.05
*SORG 0.16
*KRGCW 0.02


**  Adsorption Data
**  ---------------

*ADSCOMP 'SURFACT' *WATER   **Data for reversible aqueous surfactant adsorption
*ADMAXT 2.56   ** no mobility effects
*ADSLANG *TEMP
     51.0 5.41e+6 0 2.1e+6   ** Langmuir concentration coefficients at T=51
    151.0 1.08e+6 0 9.3e+5   ** Langmuir concentration coefficients at T=151
    250.0 2.00e+5 0 5.3e+5   ** Langmuir concentration coefficients at T=250



**  ==============  INITIAL CONDITIONS  ======================


*INITIAL

** Automatic static vertical equilibrium
*VERTICAL *DEPTH_AVE
*REFPRES 75
*REFBLOCK 1 1 4

*TEMP *CON 212



**  ==============  NUMERICAL CONTROL  ======================


*NUMERICAL   ** All these can be defaulted.  The definitions
             ** here match the previous data.

*SDEGREE GAUSS
*DTMAX 90
```

```
*NORM     *PRESS 200  *SATUR 0.2   *TEMP 180  *Y 0.2   *X 0.2


*RUN


**  ==============  RECURRENT DATA  ======================

**    The injection and production phases of the single cycling well
**  will be treated as two distinct wells which are in the same
**  location but are never active at the same time.  In the well data
**  below, both wells are defined immediately, but the producer is
**  shut in, to be activated for the drawdown.
*RUN

*DATE 1973 01 01

   *DTWELL 1

   ** INJECTOR:  Constant pressure steam injection type

   *WELL 1 'Injector 1'
   *INJECTOR *MOBWEIGHT 'Injector 1'
   *INCOMP WATER  1.0  0.0  0.0
   *TINJW 100
   QUAL .0
   *OPERATE *STW  0.03     **  water rate is 0.03 BPD
  **$          rad  geofac  wfrac  skin
    GEOMETRY  K   0.01  0.235  1.  0.
  PERF  GEO  'Injector 1'
  **$ UBA    ff  Status  Connection
      1     1    50   1  OPEN    FLOW-FROM  'SURFACE'  REFLAYER



   ** PRODUCER:  Constant liquid rate type

   *WELL 2 'Producer 1'
   *PRODUCER 'Producer 1'
   *OPERATE     *STL    0.03    ** Starting liquid rate is 0.03 BPD
     GEOMETRY  K   0.01  0.235  1.  0.
     PERF  GEO  'Producer 1'
     **$ UBA    ff  Status  Connection
    1     1    1   1   OPEN    FLOW-FROM ‘SURFACE’  REFLAYER

   *OUTSRF *GRID  *REMOVE *SO
*TIME 1.5
*TIME 3



   *DTWELL .1

*SHUTIN 'Producer 1'   ** Shut in producer 1
```

```
*SHUTIN 'Injector 1'   ** Shut in Injector 1

*WELL 3 'Injector 2'
  *INJECTOR *MOBWEIGHT 'Injector 2'
  *INCOMP WATER  1.0  0.0 0.0
  *TINJW 300
  QUAL .5

  *OPERATE  *STW   0.03    **  water rate is 0.03 BPD
 **$          rad  geofac  wfrac  skin
 GEOMETRY  K  0.01  0.235  1.  0.
 PERF  GEO  'Injector 2'
 **$ UBA    ff  Status  Connection
   1     1    1  1  OPEN    FLOW-FROM  'SURFACE'  REFLAYER



*WELL 4 'Producer 2'
  *PRODUCER 'Producer 2'
  *OPERATE     *STL    0.03    ** Starting liquid rate is 0.03 BPD


 **$          rad  geofac  wfrac  skin
 GEOMETRY  K  0.01   0.235  1.  0.
 PERF  GEO 'Producer 2'
 **$ UBA    ff  Status  Connection
   1     1    50    1   OPEN    FLOW-FROM  'SURFACE'  REFLAYER


  *OUTSRF *GRID *NONE

*TIME 3.45
*TIME 3.903

 *DTWELL .1

*WELL 3 'Injector 2'
*INJECTOR *MOBWEIGHT 'Injector 2'
*INCOMP *WATER 0.994 0.0 0.0 0.006
  *TINJW 300
  QUAL .5
*OPERATE *STW 0.03
 **$          rad  geofac  wfrac  skin
 GEOMETRY K 0.01   0.235 1.  0.
 PERF GEO ‘Injector 2'
 **$ UBA    ff Status Connection
   1     1    1    1   OPEN    FLOW-FROM ‘SURFACE’ REFLAYER


 *WELL 4 'Producer 2'
  *PRODUCER 'Producer 2'
  *OPERATE     *STL    0.03    ** Starting liquid rate is 0.03 BPD
  *OPERATE *BHP    100        ** 100 PSI backpresuure

 **$          rad  geofac  wfrac  skin
```

```
  GEOMETRY K   0.01   0.235 1.  0.
  PERF GEO 'Producer 2'
  **$ UBA    ff Status Connection
    1     1    50     1    OPEN    FLOW-FROM 'SURFACE' REFLAYER


    *OUTSRF *GRID *SG *TEMP

*TIME 4.58
TIME 5.258
STOP
```

A.2 SENSITIVITY ANALYSIS OF FOAM PARAMETERS (CASE-2)

The following are the input data files for CMG-STARS simulator. We used this case in Chapter 5 to see effect of foam parameters on production, average temperature, and average pressure in reservoir.

CMG-STARS

```
**  ==============  INPUT/OUTPUT CONTROL  ======================

RESULTS SIMULATOR STARS

*INTERRUPT *STOP

*TITLE1 'STARS Test Bed No. 23'
*TITLE2 'Steam History Match & Foam Forecast'

*INUNIT  *SI  *EXCEPT 6 1  ** darcy instead of millidarcy

*OUTPRN *GRID *PRES *SW *SG *SO *TEMP *OBHLOSS *KRG *KRO *KRW
        *ADSORP *KRINTER *CAPN *VISO
        *MOLFR *ADSPCMP  ** special adsorption component (mole fr)
        *PPM   *RLPMCMP  ** special rel perm component (in ppm)

*OUTPRN *WELL ALL
*OUTPRN *ITER *NEWTON

*WRST 300
*WPRN *GRID 300
*WPRN *ITER 1

*OUTSRF GRID  *PRES *SW *SO *SG *TEMP *ADSORP
        *MOLFR *ADSPCMP  ** special adsorption component (mole fr)
        *PPM   *RLPMCMP  ** special rel perm component (in ppm)

WPRN GRID TIME
OUTPRN GRID POREVOL
OUTPRN RES NONE
OUTPRN WELL ALL
OUTPRN ITER NEWTON
WPRN ITER 1
WRST TIME
OUTSRF SPECIAL AVGVAR DATUMPRES
OUTSRF WELL MASS COMPONENT ALL
OUTSRF WELL MOLE COMPONENT ALL
**OUTSRF WELL LAYER ALL
WSRF SECTOR 1
WPRN SECTOR TIME


**  ==============  GRID AND RESERVOIR DEFINITION  ==================
```

```
*GRID *RADIAL 9 1 3  *RW 0.0   ** Two-dimensional radial crossection grid
                       ** Zero inner radius matches previous treatment

*DI *IVAR 2 8 14 14 8 2 8 14 500
*DJ *CON 60
*DK *CON 15.0
**DJ *CON 0.3333  *DK *CON 15.0

*POR *CON 0.35

*PERMI *CON 1           ** Standard bed permeability
  *MOD 1  1 1:2 =  10   ** Higher perm commumication path
       6  1 1:2 =  10   ** Higher perm commumication path
     1:9  1   3 =  10   ** Higher perm commumication path
*PERMJ *EQUALSI
*PERMK *EQUALSI
*SECTOR 'Layer 1' 1:7 1 1:3
*END-GRID

*PRPOR 1200.0

*CPOR 1E-5
*CTPOR 3.84E-5
*ROCKCP 2.347E+6
*THCONR 1.495E+5
*THCONW 5.35E+4
*THCONO 1.15E+4
*THCONG 4.5E+3
*HLOSSPROP  *OVERBUR 2.347E+6 1.495E+5  *UNDERBUR 2.347E+6 1.495E+5
*HLOSST 15.5

**  ==============  FLUID DEFINITIONS  ======================


*MODEL 3 3 3 2   ** Two aqueous and a dead oil components

*COMPNAME  'WATER' 'SURFACT'  'BITUMEN'
**          -----   --------   --------
*CMM        0.0182     0.480     0.500
*MOLDEN       0.0      2020      2020
*CP             0      4e-6      4e-6
*CT1            0      4e-4      4e-4
*CT2            0     1.6e-7    1.6e-7
*PCRIT      21760       1100      1100
*TCRIT      371.0      494.0     494.0

*CPG1       0          125.6     125.6
*CPG2       0            0         0
*CPL1       0         1047.0    1047.0
*CPL2       0            0         0
*HVAPR      0         5500.0    5500.0

*SOLID_DEN 'SURFACT' 23040 0 0  ** Mass density based on 48000 gmole/m3
*SOLID_CP 'SURFACT' 17 0
```

```
*VISCTABLE

**    Temp
  10.00000    0.0   1.00000  3.0000E+6
  23.90000    0.0   1.00000  1.5000E+6
  37.80000    0.0   1.00000    30000.0
  65.60000    0.0   1.00000   2000.000
  93.30000    0.0   1.00000    300.000
   121.000    0.0   1.00000   87.00000
   148.900    0.0   1.00000   31.00000
   204.400    0.0   1.00000    9.00000
   260.000    0.0   1.00000    4.30000
   315.600    0.0   1.00000    2.90000

**  Gas/liq K values  are defaulted correlation
**  Liq/liq K values  are entered as tables
*LIQLIQKV
*KVTABLIM 100.0 8000.0  15 550
*KVTABLE 'WATER'
    0    0
    0    0
*KVTABLE 'SURFACT'
   .2   .2
   .2   .2
*KVTABLE  'BITUMEN'
    0    0
    0    0

** Reference conditions
*PRSR 100.0
*TEMR 15.5
*PSURF 100.0
*TSURF 15.5

**  reaction describes surfactant decomposition
**  first order decay rate is assumed (valid for basic pH)

*STOREAC    0           1       0
*STOPROD    26.37       0       0
*RPHASE     0           1       0
*RORDER     0           1       0
*FREQFAC  34.7
*EACT 32500
*RENTH 0
*O2CONC


*ROCKFLUID

**  ==============  ROCK-FLUID PROPERTIES  ======================

**  This simulation incorporates foam mobility reduction in
**  relative permeability effects which are region dependent.
**  ------------------------------------------------------------
```

```
*KRTYPE *CON       1   ** Standard bed permeability
  *MOD 1  1 1:2 =  2   ** Higher perm commumication path
       6  1 1:2 =  2   ** Higher perm commumication path
     1:9  1   3 =  2   ** Higher perm commumication path
*RPT 1    ** First rock type for standard permeability zones
**  ---------------------------------------------------------------------
**  Interpolation between 3 sets: zero, weak and strong foam curves
**  Capillary number calculation is based on aqueous SURFACT IFT
**  specified at 2 temperatures and 2 SURFACT concentrations.

*INTCOMP 'SURFACT' *WATER
*INTLIN

*IFTTABLE    ** aq mole frac      IFT
    *TEMP  10.0
                0.0           13.
                0.3           13.
    *TEMP 320.0
                0.0           13.
                0.3           13.

*FMSURF 1.875E-4
*FMCAP 1.0E-4
*FMOIL 0.5
*FMMOB 50
*EPSURF 1.0
*EPCAP 10.0
*EPOIL 1.0

**  Set #1:  No foam, corresponding to no SURFACT
**  ------------------------------------------------

*KRINTRP 1

*DTRAPW  1.0  ** no mobility reduction

*SWT   **  Water-oil relative permeabilities

**   Sw         Krw       Krow
**  -----     -------    -------
 0.0930000       0.0   1.00000       0.0
 0.1500000 1.7000E-4 0.8400000       0.0
 0.2000000 8.0000E-4 0.7100000       0.0
 0.2500000 0.0024000 0.5800000       0.0
 0.3000000 0.0061000 0.4650000       0.0
 0.4000000 0.0250000 0.2780000       0.0
 0.5000000 0.0760000 0.1360000       0.0
 0.6000000 0.1800000 0.0410000       0.0
 0.6500000 0.2600000 0.0130000       0.0
 0.7000000 0.3600000 0.0110000       0.0
 0.8000000 0.5700000 0.0060000       0.0
 0.9000000 0.7500000       0.0       0.0
   1.00000   1.00000       0.0       0.0

*SLT  *NOSWC   **  Liquid-gas relative permeabilities
```

```
**  Sl         Krg       Krog
**  ----       -------   ------
 0.1500000   1.00000       0.0       0.0
 0.4000000 0.9900000 1.0000E-4       0.0
 0.4200000 0.9850000 8.0000E-4       0.0
 0.4500000 0.9800000 0.0070000       0.0
 0.5000000 0.8500000 0.0260000       0.0
 0.5500000 0.6900000 0.0550000       0.0
 0.6000000 0.5400000 0.0900000       0.0
 0.7000000 0.2870000 0.1860000       0.0
 0.8000000 0.1140000 0.3310000       0.0
 0.9000000 0.0220000 0.5700000       0.0
 0.9500000 0.0045000 0.7600000       0.0
   1.00000       0.0   1.00000       0.0

**  Override critical saturations on table
*SWR 0.15
*SORW 0.00
*SGR 0.05
*SORG 0.16


**  Set #2:  Weak foam, corresponding to intermediate SURFACT concentration
**  ------------------------------------------------------------------------

*KRINTRP 2 *COPY 1 1    ** copy from first set, then overwrite

*DTRAPW 0.4  ** weak foam inverse mobility reduction factor (MRF=2.5)

**  Override critical saturations on table
*SWR 0.15
*SORW 0.00
*SGR 0.05
*SORG 0.16
*KRGCW 0.4

**  Set #3:  Strong foam, corresponding to high SURFACT concentration
**  ------------------------------------------------------------------

*KRINTRP 3 *COPY 1 1    ** copy from first set, then overwrite

*DTRAPW 0.02  ** strong foam inverse mobility reduction factor (MRF=50)

**  Override critical saturations on table
*SWR 0.15
*SORW 0.00
*SGR 0.05
*SORG 0.16
*KRGCW 0.02

*RPT 2    ** Second rock type for high permeability zones
**  ----------------------------------------------------------------
**  Interpolation between 3 sets: zero, weak and strong foam curves
**  Capillary number calculation is based on aqueous SURFACT IFT
**  specified at 2 temperatures and 2 SURFACT concentrations.
```

```
*INTCOMP 'SURFACT' *WATER
*INTLIN

*IFTTABLE    ** aq mole frac      IFT
    *TEMP  10.0
                0.0           13.
                0.3           13.
    *TEMP 320.0
                0.0           13.
                0.3           13.

*FMSURF 1.875E-4
*FMCAP 1.0E-4
*FMOIL 0.5
*FMMOB 50
*EPSURF 1.0
*EPCAP 10.0
*EPOIL 1.0

**  Set #1:  No foam, corresponding to no SURFACT
**  ---------------------------------------------

*KRINTRP 4

*DTRAPW  1.0  ** no mobility reduction

*SWT   **  Water-oil relative permeabilities

**   Sw         Krw       Krow
**  -----     -------    -------
      0.0       0.0   1.00000       0.0
 0.2000000 0.2000000 0.8000000       0.0
 0.4000000 0.4000000 0.6000000       0.0
 0.6000000 0.6000000 0.4000000       0.0
 0.8000000 0.8000000 0.2000000       0.0
   1.00000   1.00000       0.0       0.0

*SLT  *NOSWC   **  Liquid-gas relative permeabilities

**   Sl         Krg       Krog
**  ----      -------    ------
      0.0   1.00000       0.0       0.0
 0.2000000 0.8000000 0.2000000       0.0
 0.4000000 0.6000000 0.4000000       0.0
 0.6000000 0.4000000 0.6000000       0.0
 0.8000000 0.2000000 0.8000000       0.0
   1.00000       0.0   1.00000       0.0

**  Override critical saturations on table
*SWR 0.15
*SORW 0.01
*SGR 0.05
*SORG 0.16


**  Set #2:  Weak foam, corresponding to intermediate SURFACT concentration
```

```
**  ------------------------------------------------------------------------

*KRINTRP 5 *COPY 2 1    ** copy from first set, then overwrite

*DTRAPW 0.4  ** weak foam inverse mobility reduction factor (MRF=2.5)

**  Override critical saturations on table
*SWR 0.15
*SORW 0.01
*SGR 0.05
*SORG 0.16
*KRGCW 0.4

**  Set #3:  Strong foam, corresponding to high SURFACT concentration
**  ------------------------------------------------------------------

*KRINTRP 6 *COPY 2 1    ** copy from first set, then overwrite

*DTRAPW 0.02  ** strong foam inverse mobility reduction factor (MRF=50)

**  Override critical saturations on table
*SWR 0.15
*SORW 0.01
*SGR 0.05
*SORG 0.16
*KRGCW 0.02


**  Adsorption Data
**  ---------------

*ADSCOMP 'SURFACT' *WATER   **Data for reversible aqueous surfactant adsorption
*ADMAXT 2.56   ** no mobility effects
*ADSLANG *TEMP
     51.0 5.41e+6 0 2.1e+6   ** Langmuir concentration coefficients at T=51
    151.0 1.08e+6 0 9.3e+5   ** Langmuir concentration coefficients at T=151
    250.0 2.00e+5 0 5.3e+5   ** Langmuir concentration coefficients at T=250



*INITIAL



**  ==============  INITIAL CONDITIONS  ======================


*PRES *KVAR               800.0 688.0 532.0
*SW   *CON 0.15           **Standard bed permeability
     *MOD 1  1 1:2 =  .5   ** Higher perm commumication path
         6  1 1:2 =  .5   ** Higher perm commumication path
        1:9  1   3 =  .5   ** Higher perm commumication path

*TEMP *CON 15.5           **Standard bed permeability
     *MOD 1  1 1:2 =  110  ** Higher perm commumication path
         6  1 1:2 =  110  ** Higher perm commumication path
```

```
      1:9  1   3 =  110  ** Higher perm commumication path

*mfrac_wat 'WATER' *con 1

*NUMERICAL



**  ==============  NUMERICAL CONTROL  ======================


** All these can be defaulted.  The definitions
** here match the previous data.

*TFORM *SXY

*DTMAX 100.0
*SDEGREE 1
*SORDER *RCMRB
*UPSTREAM *KLEVEL

*NORM      *PRESS 500  *SATUR .2   *TEMP 45  Y .2  *W .2


*RUN



**  ==============  RECURRENT DATA  ======================


*TIME 0

  *DTWELL 0.1

  *WELL 1 'INJTR'  *FRAC .1667    ** Well list
  *WELL 2 'PRODN'  *FRAC .5000

  *PRODUCER 'PRODN'
  *OPERATE *STL 30.0
  *PERF 'PRODN'   **  i j k  wi
            6 1 1 2345.49 ** 200

  *INJECTOR *MOBWEIGHT 'INJTR'
  *INCOMP  *WATER  1.0  0.0  0.0
  *TINJW 210
  *QUAL .7
  *OPERATE *STW 150

  *PERF 'INJTR'   ** i j k  wi
          1 1 1 469.098 ** 40

** Obtain printouts and results at the following times
  *TIME  365
  *TIME  730
  *DTWELL  1.0
```

```
  *INJECTOR MOBWEIGHT 'INJTR'

  *INCOMP *WATER .9998125   1.875E-4  0         ** inj surfactant (1.0wt%)
  *TINJW 210
  *QUAL .7
  *OPERATE *STW 150

  *PERF 'INJTR'   ** i j k  wi
          1 1 1 469.098 ** 40

*OUTSRF *GRID *SG *TEMP
*TIME 800
*TIME 900
*TIME 1095
*TIME 1200
*TIME 1300
*TIME 1400

*TIME 1460.0
*STOP
```

A.3 KERN RIVER FIELD STEAM FOAM HISTORY MATCH CASE (CASE-3)

The following are the input data files for CMG-STARS simulator. We used this case in Chapter 6 to see steam foam effect on incremental oil.

```
  ********************************************************************************
  ** CMG STARS                                                                  **
  ********************************************************************************
  ********************************************************************************
** ==============  INPUT/OUTPUT CONTROL  =======================
** 2017-09-29, 11:03:29 AM, ea25854
RESULTS SIMULATOR STARS 201110


*INTERRUPT *STOP

*TITLE1 'STARS Test Bed No. 23'
*TITLE2 'Steam History Match & Foam Forecast'

*INUNIT  *SI  *EXCEPT 6 1  ** darcy instead of millidarcy

*OUTPRN *GRID *PRES *SW *SG *SO *TEMP *OBHLOSS *KRG *KRO *KRW
          *ADSORP *KRINTER *CAPN *VISO
          *MOLFR *ADSPCMP  ** special adsorption component (mole fr)
          *PPM   *RLPMCMP  ** special rel perm component (in ppm)

*OUTPRN *WELL ALL
*OUTPRN *ITER *NEWTON

*WRST 300
*WPRN *GRID 300
*WPRN *ITER 1
** special adsorption component (mole fr)
** special rel perm component (in ppm)
OUTSRF GRID ADSORP MOLFR ADSPCMP PRES PPM RLPMCMP SG SO SW TEMP

WPRN GRID TIME
OUTPRN GRID POREVOL
OUTPRN RES NONE
OUTPRN WELL ALL
OUTPRN ITER NEWTON
WPRN ITER 1
WRST TIME
OUTSRF SPECIAL AVGVAR DATUMPRES
OUTSRF WELL MASS COMPONENT ALL
OUTSRF WELL MOLE COMPONENT ALL
**OUTSRF WELL LAYER ALL
WSRF SECTOR 1
WPRN SECTOR TIME


**  ==============  GRID AND RESERVOIR DEFINITION  ==================
```

```
GRID VARI 15 15 4
KDIR UP
DI IVAR
 15*14.907
DJ JVAR
 15*14.907
DK ALL
 225*7.62 225*12.192 225*0.9144 225*4.572
DTOP
 225*304.8
**$ Property: NULL Blocks  Max: 1  Min: 1
**$  0 = null block, 1 = active block
NULL CON            1


*POR *CON 0.3

*PERMI *CON 0.99           ** Standard bed permeability
  *MOD 1:15  1:15 3 =  0.001   ** lower perm commumication path
       1:15  1:15 1 =  0.8     ** lower perm commumication path
*PERMJ *EQUALSI
*PERMK *EQUALSI
**$ Property: Pinchout Array  Max: 1  Min: 1
**$  0 = pinched block, 1 = active block
PINCHOUTARRAY CON            1
*END-GRID
ROCKTYPE 1

*PRPOR 1200.0

*CPOR 1E-5
*CTPOR 3.84E-5
*ROCKCP 2.347E+6
*THCONR 1.495E+5
*THCONW 5.35E+4
*THCONO 1.15E+4
*THCONG 4.5E+3
*HLOSSPROP  *OVERBUR 2.347E+6 1.495E+5  *UNDERBUR 2.347E+6 1.495E+5
*HLOSST 65.6

**  ==============  FLUID DEFINITIONS  ======================


*MODEL 4 4 3 2   ** Two aqueous and a dead oil components

*COMPNAME  'WATER' 'SURFACT'  'BITUMEN'        'N2'
**          -----   --------   --------                  -----
*CMM        0.0182     0.480     0.500       0.028
*MOLDEN       0.0      2020      1950
*CP             0      4e-6      4e-6
*CT1            0      4e-4      4e-4
*CT2            0    1.6e-7    1.6e-7
*PCRIT      21760      1100      1100        3309
*TCRIT      371.0     494.0     494.0        -147.0

*CPG1       0         125.6     125.6           31.15
```

```
*CPG2       0            0       0               0
*CPL1       0        1047.0    1047.0          1047.0
*CPL2       0            0       0               0
*HVAPR      0        5500.0    5500.0

*SOLID_DEN 'SURFACT' 23040 0 0  ** Mass density based on 48000 gmole/m3
*SOLID_CP 'SURFACT' 17 0

*VISCTABLE

**    Temp
  10.00000    0.0   1.31000  3.0000E+6
  26.70000    0.0   0.86200  1.5000E+6
  37.80000    0.0   0.68200   2200.0
  65.60000    0.0   0.43000    87.000
  93.30000    0.0   0.30300    31.000
   121.000    0.0   0.01306    9.0000
   148.900    0.0   0.01410    4.30000
   204.400    0.0   0.01600    2.90000
   260.000    0.0   0.01860    1.00000
   315.600    0.0   0.02094    1.00000

**  Gas/liq K values  are defaulted correlation
**  Liq/liq K values  are entered as tables
*LIQLIQKV
*KVTABLIM 50.0 8000.0  15 550
*KVTABLE 'WATER'
    0    0
    0    0
*KVTABLE 'SURFACT'
   .2   .2
   .2   .2
*KVTABLE  'BITUMEN'
    0    0
    0    0

** Reference conditions
*PRSR 100.0
*TEMR 37.7
*PSURF 100.0
*TSURF 37.7

**  reaction describes surfactant decomposition
**  first order decay rate is assumed (valid for basic pH)

*STOREAC    0                1       0       1
*STOPROD    27.91208791208      0       0               0
*RPHASE     0                1       0       3
*RORDER     0                1       0       1
*FREQFAC  34.7
*EACT 32500
*RENTH 0
*O2CONC


*ROCKFLUID
```

```
**  ==============  ROCK-FLUID PROPERTIES  ======================

**  This simulation incorporates foam mobility reduction in
**  relative permeability effects which are region dependent.
**  ------------------------------------------------------------

*KRTYPE *CON       1   ** Standard bed permeability


*RPT 1    ** First rock type for standard permeability zones
**  ------------------------------------------------------------
**  Interpolation between 3 sets: zero, weak and strong foam curves
**  Capillary number calculation is based on aqueous SURFACT IFT
**  specified at 2 temperatures and 2 SURFACT concentrations.

*INTCOMP 'SURFACT' *WATER
*INTLIN

*IFTTABLE    ** aq mole frac      IFT
    *TEMP  10.0
                0.0           13.
                0.3           13.
    *TEMP 320.0
                0.0           13.
                0.3           13.

*FMSURF 1.875E-4
*FMCAP 1.0E-4
*FMOIL 0.5
*FMMOB 50
*EPSURF 4.0
*EPCAP 1.0
*EPOIL 1.0

**  Set #1:  No foam, corresponding to no SURFACT
**  ------------------------------------------------

*KRINTRP 1

*DTRAPW  1.0  ** no mobility reduction

*SWT   **  Water-oil relative permeabilities

**   Sw         Krw       Krow
**  -----     -------    -------
0.3               0.0000000    1                              0
0.35              0.0500000    0.8888888889 0
0.4               0.1000000    0.7777777778 0
0.45              0.1500000    0.6666666667 0
0.5               0.2000000    0.5555555556 0
0.55              0.2500000    0.4444444444 0
0.6               0.3000000    0.3333333333 0
0.65              0.3500000    0.2222222222 0
0.7               0.4000000    0.1111111111 0
0.72              0.4200000    0.0666666667 0
```

```
0.75            0.4500000   0                           0




*SLT   **  Liquid-gas relative permeabilities

**   Sl        Krg       Krog
**  ----      -------    ------
0.4             1.00000     0                           0
0.45            0.75131     0.0909090910
0.47            0.66472     0.1272727270
0.5             0.54771     0.1818181820
0.55            0.38467     0.2727272730
0.6             0.25770     0.3636363640
0.7             0.09391     0.5454545450
0.8             0.02029     0.7272727270
0.9             0.00075     0.9090909090
0.95            0.00000     1                           0

**  Override critical saturations on table
*SWR 0.3
*SORW 0.25
*SGR 0.05
*SORG 0.1


**  Set #2:  Weak foam, corresponding to intermediate SURFACT concentration
**  ------------------------------------------------------------------------

*KRINTRP 2 *COPY 1 1    ** copy from first set, then overwrite

*DTRAPW 0.4  ** weak foam inverse mobility reduction factor (MRF=2.5)

**  Override critical saturations on table
*SWR 0.3
*SORW 0.25
*SGR 0.05
*SORG 0.1
*KRGCW 0.4

**  Set #3:  Strong foam, corresponding to high SURFACT concentration
**  ------------------------------------------------------------------------

*KRINTRP 3 *COPY 1 1    ** copy from first set, then overwrite

*DTRAPW 0.02  ** strong foam inverse mobility reduction factor (MRF=50)

**  Override critical saturations on table
*SWR 0.3
*SORW 0.25
*SGR 0.05
SORG 0.1
```

```
**  Adsorption Data
**  ---------------

*ADSCOMP 'SURFACT' *WATER   **Data for reversible aqueous surfactant adsorption
*ADMAXT 2.56   ** no mobility effects
*ADSLANG *TEMP
     51.0 5.41e+6 0 2.1e+6   ** Langmuir concentration coefficients at T=51
    151.0 1.08e+6 0 9.3e+5   ** Langmuir concentration coefficients at T=151
    250.0 2.00e+5 0 5.3e+5   ** Langmuir concentration coefficients at T=250



*INITIAL
VERTICAL OFF

INITREGION 1



**  ==============  INITIAL CONDITIONS  ======================


*PRES *KVAR                3354 3277 3152.7 3143.4
*SW   *CON 0.3             **Standard bed permeability
*SO   *CON 0.7

*TEMP *CON 65.6            **Standard bed permeability



*NUMERICAL



**  ==============  NUMERICAL CONTROL  ======================


** All these can be defaulted.  The definitions
** here match the previous data.

*TFORM *SXY

*DTMAX 100.0
*SDEGREE 1
*SORDER *RCMRB
*UPSTREAM *KLEVEL
NORM PRESS 500 SATUR 0.2 TEMP 45 Y 0.2 W 0.2


*RUN



**  ==============  RECURRENT DATA  ======================
```

```
*TIME 0

  *DTWELL 0.1

**       ** Well list
**
**    *WELL 1 'Well-1'  *FRAC .5000
**$
WELL  'Well-1'  FRAC  0.5
**    *WELL 2 'Well-2'  *FRAC .5000
**$
WELL  'Well-2'  FRAC  0.5
**    *WELL 3 'Well-3'  *FRAC .5000
**$
WELL  'Well-3'  FRAC  0.5
**    *WELL 4 'Well-4'  *FRAC .5000
**$
WELL  'Well-4'  FRAC  0.5
**    *WELL 5 'Well-5'  *FRAC .5000
**$
WELL  'Well-5'  FRAC  0.5
**    *WELL 6 'Well-6'  *FRAC .5000
**$
WELL  'Well-6'  FRAC  0.5
**    *WELL 7 'Well-7'  *FRAC .5000
**$
WELL  'Well-7'  FRAC  0.5
**    *WELL 8 'Well-8'  *FRAC .5000
**$
WELL  'Well-8'  FRAC  0.5
**    *WELL 9 'Well-9'  *FRAC .5000
**$
WELL  'Well-9'  FRAC  0.5
**    *WELL 10 'Well-10'  *FRAC .1667
**$
WELL  'Well-10'  FRAC  0.1667
**    *WELL 11 'Well-11'  *FRAC .1667
**$
WELL  'Well-11'  FRAC  0.1667
**    *WELL 12 'Well-12'  *FRAC .1667
**$
WELL  'Well-12'  FRAC  0.1667
**    *WELL 13 'Well-13'  *FRAC .1667
**$
WELL  'Well-13'  FRAC  0.1667
**    *WELL 14 'Well-14'  *FRAC .1667

WELL  'Well-14'  FRAC  0.1667
**    *WELL 15 'Well-15'  *FRAC .1667

WELL  'Well-15'  FRAC  0.1667
**    *WELL 16 'Well-16'  *FRAC .1667

WELL  'Well-16'  FRAC  0.1667
```

```
**    *WELL 17 'Well-17'  *FRAC .1667

WELL  'Well-17'  FRAC  0.1667
**    *WELL 18 'Well-18'  *FRAC .1667

WELL  'Well-18'  FRAC  0.1667
**    *WELL 19 'Well-19'  *FRAC .1667

WELL  'Well-19'  FRAC  0.1667
**    *WELL 20 'Well-20'  *FRAC .1667

WELL  'Well-20'  FRAC  0.1667
**    *WELL 21 'Well-21'  *FRAC .1667

WELL  'Well-21'  FRAC  0.1667
**    *WELL 22 'Well-22'  *FRAC .1667

WELL  'Well-22'  FRAC  0.1667

PRODUCER 'Well-1'
  *OPERATE *MIN *BHP    250
**$         rad  geofac  wfrac  skin
GEOMETRY  K  0.086  0.249  1.  0.
PERF  GEOA  'Well-1'
**$ UBA     ff  Status  Connection
   1 1 1  1.  OPEN    FLOW-TO  'SURFACE'  REFLAYER
   1 1 2  1.  OPEN    FLOW-TO  1
   1 1 3  1.  OPEN    FLOW-TO  2
   1 1 4  1.  OPEN    FLOW-TO  3

PRODUCER 'Well-2'
  *OPERATE *MIN *BHP    250
**$         rad  geofac  wfrac  skin
GEOMETRY  K  0.086  0.249  1.  0.
PERF  GEOA  'Well-2'
**$ UBA     ff  Status  Connection
   1 8 1  1.  OPEN    FLOW-TO  'SURFACE'  REFLAYER
   1 8 2  1.  OPEN    FLOW-TO  1
   1 8 3  1.  OPEN    FLOW-TO  2
   1 8 4  1.  OPEN    FLOW-TO  3


PRODUCER 'Well-3'
  *OPERATE *MIN *BHP    250
**$         rad  geofac  wfrac  skin
GEOMETRY  K  0.086  0.249  1.  0.
PERF  GEOA  'Well-3'
**$ UBA     ff  Status  Connection
   1 15 1  1.  OPEN    FLOW-TO  'SURFACE'  REFLAYER
   1 15 2  1.  OPEN    FLOW-TO  1
   1 15 3  1.  OPEN    FLOW-TO  2
   1 15 4  1.  OPEN    FLOW-TO  3


PRODUCER 'Well-4'
  *OPERATE *MIN *BHP    250
```

```
**$        rad  geofac  wfrac  skin
GEOMETRY  K  0.086  0.249  1.  0.
PERF  GEOA  'Well-4'
**$ UBA    ff  Status  Connection
   8 8 1  1.  OPEN    FLOW-TO  'SURFACE'  REFLAYER
   8 8 2  1.  OPEN    FLOW-TO  1
   8 8 3  1.  OPEN    FLOW-TO  2
   8 8 4  1.  OPEN    FLOW-TO  3


PRODUCER 'Well-5'
  *OPERATE *MIN *BHP    250
**$        rad  geofac  wfrac  skin
GEOMETRY  K  0.086  0.249  1.  0.
PERF  GEOA  'Well-5'
**$ UBA    ff  Status  Connection
   8 1 1  1.  OPEN    FLOW-TO  'SURFACE'  REFLAYER
   8 1 2  1.  OPEN    FLOW-TO  1
   8 1 3  1.  OPEN    FLOW-TO  2
   8 1 4  1.  OPEN    FLOW-TO  3


PRODUCER 'Well-6'
  *OPERATE *MIN *BHP    250
**$        rad  geofac  wfrac  skin
GEOMETRY  K  0.086  0.249  1.  0.
PERF  GEOA  'Well-6'
**$ UBA    ff  Status  Connection
   8 15 1  1.  OPEN    FLOW-TO  'SURFACE'  REFLAYER
   8 15 2  1.  OPEN    FLOW-TO  1
   8 15 3  1.  OPEN    FLOW-TO  2
   8 15 4  1.  OPEN    FLOW-TO  3



PRODUCER 'Well-7'
  *OPERATE *MIN *BHP    250
**$        rad  geofac  wfrac  skin
GEOMETRY  K  0.086  0.249  1.  0.
PERF  GEOA  'Well-7'
**$ UBA    ff  Status  Connection
   15 1 1  1.  OPEN    FLOW-TO  'SURFACE'  REFLAYER
   15 1 2  1.  OPEN    FLOW-TO  1
   15 1 3  1.  OPEN    FLOW-TO  2
   15 1 4  1.  OPEN    FLOW-TO  3

PRODUCER 'Well-8'
  *OPERATE *MIN *BHP    250
**$        rad  geofac  wfrac  skin
GEOMETRY  K  0.086  0.249  1.  0.
PERF  GEOA  'Well-8'
**$ UBA    ff  Status  Connection
   15 8 1  1.  OPEN    FLOW-TO  'SURFACE'  REFLAYER
   15 8 2  1.  OPEN    FLOW-TO  1
   15 8 3  1.  OPEN    FLOW-TO  2
   15 8 4  1.  OPEN    FLOW-TO  3
```

```
PRODUCER 'Well-9'
  *OPERATE *MIN *BHP    250
**$         rad  geofac  wfrac  skin
GEOMETRY  K  0.086  0.249  1.  0.
PERF  GEOA  'Well-9'
**$ UBA      ff  Status  Connection
    15 15 1  1.  OPEN    FLOW-TO  'SURFACE'  REFLAYER
    15 15 2  1.  OPEN    FLOW-TO  1
    15 15 3  1.  OPEN    FLOW-TO  2
    15 15 4  1.  OPEN    FLOW-TO  3

INJECTOR UNWEIGHT 'Well-10'
  *INCOMP  *WATER  1.0  0.0  0.0
  *TINJW 300
  *QUAL .5
 *OPERATE      *BHP   395     ** Starting BHP is 1000 kpa
**$         rad  geofac  wfrac  skin
GEOMETRY  K  0.086  0.249  1.  0.
PERF  GEOA  'Well-10'
**$ UBA    ff  Status  Connection
    4 4 1  1.  OPEN    FLOW-FROM  'SURFACE'  REFLAYER
    4 4 2  1.  OPEN    FLOW-FROM  1
    4 4 3  1.  CLOSED  FLOW-FROM  2
    4 4 4  1.  OPEN    FLOW-FROM  3


INJECTOR UNWEIGHT 'Well-11'
  *INCOMP  *WATER  1.0  0.0  0.0
  *TINJW 300
  *QUAL .5
 *OPERATE      *BHP   395     ** Starting BHP is 1000 kpa
**$         rad  geofac  wfrac  skin
GEOMETRY  K  0.086  0.249  1.  0.
PERF  GEOA  'Well-11'
**$ UBA      ff  Status  Connection
    11 11 1  1.  OPEN    FLOW-FROM  'SURFACE'  REFLAYER
    11 11 2  1.  OPEN    FLOW-FROM  1
    11 11 3  1.  CLOSED  FLOW-FROM  2
    11 11 4  1.  OPEN    FLOW-FROM  3


INJECTOR UNWEIGHT 'Well-12'
  *INCOMP  *WATER  1.0  0.0  0.0
  *TINJW 300
  *QUAL .5
 *OPERATE      *BHP   395     ** Starting BHP is 1000 kpa
**$         rad  geofac  wfrac  skin
GEOMETRY  K  0.086  0.249  1.  0.
PERF  GEOA  'Well-12'
**$ UBA     ff  Status  Connection
    4 11 1  1.  OPEN    FLOW-FROM  'SURFACE'  REFLAYER
    4 11 2  1.  OPEN    FLOW-FROM  1
    4 11 3  1.  CLOSED  FLOW-FROM  2
    4 11 4  1.  OPEN    FLOW-FROM  3
```

```
INJECTOR UNWEIGHT 'Well-13'
  *INCOMP  *WATER  1.0  0.0  0.0
  *TINJW 300
  *QUAL .5
 *OPERATE     *BHP   395    ** Starting BHP is 1000 kpa
**$         rad  geofac  wfrac  skin
GEOMETRY  K  0.086  0.249  1.  0.
PERF  GEOA  'Well-13'
**$ UBA     ff  Status  Connection
   11 4 1  1.  OPEN    FLOW-FROM  'SURFACE'  REFLAYER
   11 4 2  1.  OPEN    FLOW-FROM  1
   11 4 3  1.  CLOSED  FLOW-FROM  2
   11 4 4  1.  OPEN    FLOW-FROM  3


INJECTOR UNWEIGHT 'Well-14'
  *INCOMP  *WATER  1.0  0.0  0.0
  *TINJW 300
  *QUAL 0.6
 *OPERATE     *BHP   2000    ** Starting BHP is 1000 kpa
**$         rad  geofac  wfrac  skin
GEOMETRY  K  0.086  0.249  1.  0.
PERF  GEOA  'Well-14'
**$ UBA     ff  Status  Connection
   1 1 1  1.  OPEN    FLOW-FROM  'SURFACE'  REFLAYER
   1 1 2  1.  OPEN    FLOW-FROM  1
   1 1 3  1.  CLOSED  FLOW-FROM  2
   1 1 4  1.  OPEN    FLOW-FROM  3

INJECTOR UNWEIGHT 'Well-15'
  *INCOMP  *WATER  1.0  0.0  0.0
  *TINJW 300
  *QUAL 0.6
 *OPERATE     *BHP   2000    ** Starting BHP is 1000 kpa
**$         rad  geofac  wfrac  skin
GEOMETRY  K  0.086  0.249  1.  0.
PERF  GEOA  'Well-15'
**$ UBA     ff  Status  Connection
   1 8 1  1.  OPEN    FLOW-FROM  'SURFACE'  REFLAYER
   1 8 2  1.  OPEN    FLOW-FROM  1
   1 8 3  1.  CLOSED  FLOW-FROM  2
   1 8 4  1.  OPEN    FLOW-FROM  3


INJECTOR UNWEIGHT 'Well-16'
  *INCOMP  *WATER  1.0  0.0  0.0
  *TINJW 300
  *QUAL 0.6
 *OPERATE     *BHP   2000    ** Starting BHP is 1000 kpa
**$         rad  geofac  wfrac  skin
GEOMETRY  K  0.086  0.249  1.  0.
PERF  GEOA  'Well-16'
**$ UBA     ff  Status  Connection
   1 15 1  1.  OPEN    FLOW-FROM  'SURFACE'  REFLAYER
```

```
   1 15 2  1.  OPEN    FLOW-FROM  1
   1 15 3  1.  CLOSED  FLOW-FROM  2
   1 15 4  1.  OPEN    FLOW-FROM  3

INJECTOR UNWEIGHT 'Well-17'
  *INCOMP  *WATER  1.0  0.0  0.0
  *TINJW 300
  *QUAL 0.6
 *OPERATE     *BHP   2000    ** Starting BHP is 1000 kpa
**$         rad  geofac  wfrac  skin
GEOMETRY  K  0.086  0.249  1.  0.
PERF  GEOA  'Well-17'
**$ UBA    ff  Status  Connection
   8 8 1  1.  OPEN    FLOW-FROM  'SURFACE'  REFLAYER
   8 8 2  1.  OPEN    FLOW-FROM  1
   8 8 3  1.  CLOSED  FLOW-FROM  2
   8 8 4  1.  OPEN    FLOW-FROM  3


INJECTOR UNWEIGHT 'Well-18'
  *INCOMP  *WATER  1.0  0.0  0.0
  *TINJW 300
  *QUAL 0.6
  *OPERATE     *BHP   2000    ** Starting BHP is 1000 kpa
**$         rad  geofac  wfrac  skin
GEOMETRY  K  0.086  0.249  1.  0.
PERF  GEOA  'Well-18'
**$ UBA    ff  Status  Connection
   8 1 1  1.  OPEN    FLOW-FROM  'SURFACE'  REFLAYER
   8 1 2  1.  OPEN    FLOW-FROM  1
   8 1 3  1.  CLOSED  FLOW-FROM  2
   8 1 4  1.  OPEN    FLOW-FROM  3


INJECTOR UNWEIGHT 'Well-19'
  *INCOMP  *WATER  1.0  0.0  0.0
  *TINJW 300
  *QUAL 0.6
 *OPERATE     *BHP   2000    ** Starting BHP is 1000 kpa
**$         rad  geofac  wfrac  skin
GEOMETRY  K  0.086  0.249  1.  0.
PERF  GEOA  'Well-19'
**$ UBA    ff  Status  Connection
   8 15 1  1.  OPEN    FLOW-FROM  'SURFACE'  REFLAYER
   8 15 2  1.  OPEN    FLOW-FROM  1
   8 15 3  1.  CLOSED  FLOW-FROM  2
   8 15 4  1.  OPEN    FLOW-FROM  3


INJECTOR UNWEIGHT 'Well-20'
  *INCOMP  *WATER  1.0  0.0  0.0
  *TINJW 300
  *QUAL 0.6
 *OPERATE     *BHP   2000    ** Starting BHP is 1000 kpa
**$         rad  geofac  wfrac  skin
GEOMETRY  K  0.086  0.249  1.  0.
```

```
PERF  GEOA  'Well-20'
**$ UBA     ff  Status  Connection
    15 1 1  1.  OPEN    FLOW-FROM  'SURFACE'  REFLAYER
    15 1 2  1.  OPEN    FLOW-FROM  1
    15 1 3  1.  CLOSED  FLOW-FROM  2
    15 1 4  1.  OPEN    FLOW-FROM  3

INJECTOR UNWEIGHT 'Well-21'
  *INCOMP  *WATER  1.0  0.0  0.0
  *TINJW 300
  *QUAL 0.6
 *OPERATE     *BHP   2000     ** Starting BHP is 1000 kpa
**$         rad  geofac  wfrac  skin
GEOMETRY  K  0.086  0.249  1.  0.
PERF  GEOA  'Well-21'
**$ UBA     ff  Status  Connection
    15 8 1  1.  OPEN    FLOW-FROM  'SURFACE'  REFLAYER
    15 8 2  1.  OPEN    FLOW-FROM  1
    15 8 3  1.  CLOSED  FLOW-FROM  2
    15 8 4  1.  OPEN    FLOW-FROM  3


INJECTOR UNWEIGHT 'Well-22'
  *INCOMP  *WATER  1.0  0.0  0.0
  *TINJW 300
  *QUAL 0.6
 *OPERATE     *BHP   2000     ** Starting BHP is 1000 kpa
**$         rad  geofac  wfrac  skin
GEOMETRY  K  0.086  0.249  1.  0.
PERF  GEOA  'Well-22'
**$ UBA     ff  Status  Connection
    15 15 1  1.  OPEN    FLOW-FROM  'SURFACE'  REFLAYER
    15 15 2  1.  OPEN    FLOW-FROM  1
    15 15 3  1.  CLOSED  FLOW-FROM  2
    15 15 4  1.  OPEN    FLOW-FROM  3

WELL  'Well-23'
INJECTOR MOBWEIGHT IMPLICIT 'Well-23'
INCOMP  WATER-GAS  0.99919  0.00021  0.  0.0006
TINJW  280.
QUAL  0.5
OPERATE   STF  55.  CONT
**$         rad  geofac  wfrac  skin
GEOMETRY  K  0.086  0.249  1.  0.
PERF  GEOA  'Well-23'
**$ UBA    ff  Status  Connection
    4 4 1  1.  OPEN    FLOW-FROM  'SURFACE'  REFLAYER
    4 4 2  1.  OPEN    FLOW-FROM  1
    4 4 3  1.  CLOSED  FLOW-FROM  2
    4 4 4  1.  OPEN    FLOW-FROM  3

**$
WELL  'Well-24'
INJECTOR MOBWEIGHT IMPLICIT 'Well-24'
INCOMP  WATER-GAS  0.99919  0.00021  0.  0.0006
TINJW  280.
```

```
QUAL  0.5
OPERATE   STF  55.  CONT
**$         rad  geofac  wfrac  skin
GEOMETRY  K  0.086  0.249  1.  0.
PERF  GEOA  'Well-24'
**$ UBA     ff  Status  Connection
   4 11 1  1.  OPEN    FLOW-FROM  'SURFACE'  REFLAYER
   4 11 2  1.  OPEN    FLOW-FROM  1
   4 11 3  1.  CLOSED  FLOW-FROM  2
   4 11 4  1.  OPEN    FLOW-FROM  3

**$
WELL  'Well-25'
INJECTOR MOBWEIGHT IMPLICIT 'Well-25'
INCOMP  WATER-GAS  0.99919  0.00021  0.  0.0006
TINJW  280.
QUAL  0.5
OPERATE   STF  55.  CONT
**$         rad  geofac  wfrac  skin
GEOMETRY  K  0.086  0.249  1.  0.
PERF  GEOA  'Well-25'
**$ UBA     ff  Status  Connection
   11 11 1  1.  OPEN    FLOW-FROM  'SURFACE'  REFLAYER
   11 11 2  1.  OPEN    FLOW-FROM  1
   11 11 3  1.  CLOSED  FLOW-FROM  2
   11 11 4  1.  OPEN    FLOW-FROM  3

**$
WELL  'Well-26'
INJECTOR MOBWEIGHT IMPLICIT 'Well-26'
INCOMP  WATER-GAS  0.99919  0.00021  0.  0.0006
TINJW  280.
QUAL  0.5
OPERATE   STF  55.  CONT
**$         rad  geofac  wfrac  skin
GEOMETRY  K  0.086  0.249  1.  0.
PERF  GEOA  'Well-26'
**$ UBA     ff  Status  Connection
   11 4 1  1.  OPEN    FLOW-FROM  'SURFACE'  REFLAYER
   11 4 2  1.  OPEN    FLOW-FROM  1
   11 4 3  1.  CLOSED  FLOW-FROM  2
   11 4 4  1.  OPEN    FLOW-FROM  3


  **  primary production

  *SHUTIN 'Well-10'   ** Shut in injector
  *SHUTIN 'Well-11'   ** Shut in injector
  *SHUTIN 'Well-12'   ** Shut in injector
  *SHUTIN 'Well-13'   ** Shut in injector
  *SHUTIN 'Well-14'   ** Shut in injector
  *SHUTIN 'Well-15'   ** Shut in injector
  *SHUTIN 'Well-16'   ** Shut in injector
  *SHUTIN 'Well-17'   ** Shut in injector
  *SHUTIN 'Well-18'   ** Shut in injector
  *SHUTIN 'Well-19'   ** Shut in injector
```

```
   *SHUTIN 'Well-20'   ** Shut in injector
   *SHUTIN 'Well-21'   ** Shut in injector
   *SHUTIN 'Well-22'   ** Shut in injector
   *SHUTIN 'Well-23'   ** Shut in injector
   *SHUTIN 'Well-24'   ** Shut in injector
   *SHUTIN 'Well-25'   ** Shut in injector
   *SHUTIN 'Well-26'   ** Shut in injector

OUTSRF GRID ADSORP MOLFR ADSPCMP PRES PPM RLPMCMP SG SW TEMP

*TIME 1000
*TIME 1900
*TIME 2800


    ** Cycle No. 1  -  Injection

    *SHUTIN 'Well-1'   ** Shut in PRODUCER
    *SHUTIN 'Well-2'   ** Shut in producer
    *SHUTIN 'Well-3'   ** Shut in producer
    *SHUTIN 'Well-4'   ** Shut in producer
    *SHUTIN 'Well-5'   ** Shut in producer
    *SHUTIN 'Well-6'   ** Shut in producer
    *SHUTIN 'Well-7'   ** Shut in producer
    *SHUTIN 'Well-8'   ** Shut in producer
    *SHUTIN 'Well-9'   ** Shut in producer

  *OPEN 'Well-14'   ** Turn on injector
  *OPEN 'Well-15'   ** Turn on injector
  *OPEN 'Well-16'   ** Turn on injector
  *OPEN 'Well-17'   ** Turn on injector
  *OPEN 'Well-18'   ** Turn on injector
  *OPEN 'Well-19'   ** Turn on injector
  *OPEN 'Well-20'   ** Turn on injector
  *OPEN 'Well-21'   ** Turn on injector
  *OPEN 'Well-22'   ** Turn on injector
 OUTSRF GRID ADSORP MOLFR ADSPCMP PRES PPM RLPMCMP SG SW TEMP


 *TIME 2830.00

    *DTWELL 7

    ** Cycle No. 1  -  Soak

    *SHUTIN 'Well-14'   ** Shut in injector
    *SHUTIN 'Well-15'   ** Shut in injector
    *SHUTIN 'Well-16'   ** Shut in injector
    *SHUTIN 'Well-17'   ** Shut in injector
    *SHUTIN 'Well-18'   ** Shut in injector
    *SHUTIN 'Well-19'   ** Shut in injector
    *SHUTIN 'Well-20'   ** Shut in injector
    *SHUTIN 'Well-21'   ** Shut in injector
    *SHUTIN 'Well-22'   ** Shut in injector
 OUTSRF GRID ADSORP MOLFR ADSPCMP PPM RLPMCMP SG SW TEMP PRES
```

```
*TIME 2838.00
*TIME 2845.00

  *DTWELL 1

  ** Cycle No. 1  -  Production

  *OPEN 'Well-1'   ** Turn on producer
  *OPEN 'Well-2'   ** Turn on producer
  *OPEN 'Well-3'   ** Turn on producer
  *OPEN 'Well-4'   ** Turn on producer
  *OPEN 'Well-5'   ** Turn on producer
  *OPEN 'Well-6'   ** Turn on producer
  *OPEN 'Well-7'   ** Turn on producer
  *OPEN 'Well-8'   ** Turn on producer
  *OPEN 'Well-9'   ** Turn on producer
OUTSRF GRID PRES

*TIME 3065
*TIME 3165

  *DTWELL 2

  ** Cycle No. 2  -  Injection

  *SHUTIN 'Well-1'   ** Shut in PRODUCER
  *SHUTIN 'Well-2'   ** Shut in producer
  *SHUTIN 'Well-3'   ** Shut in producer
  *SHUTIN 'Well-4'   ** Shut in producer
  *SHUTIN 'Well-5'   ** Shut in producer
  *SHUTIN 'Well-6'   ** Shut in producer
  *SHUTIN 'Well-7'   ** Shut in producer
  *SHUTIN 'Well-8'   ** Shut in producer
  *SHUTIN 'Well-9'   ** Shut in producer

 *OPEN 'Well-14'   ** Turn on injector
 *OPEN 'Well-15'   ** Turn on injector
 *OPEN 'Well-16'   ** Turn on injector
 *OPEN 'Well-17'   ** Turn on injector
 *OPEN 'Well-18'   ** Turn on injector
 *OPEN 'Well-19'   ** Turn on injector
 *OPEN 'Well-20'   ** Turn on injector
 *OPEN 'Well-21'   ** Turn on injector
 *OPEN 'Well-22'   ** Turn on injector
OUTSRF GRID PRES


*TIME 3195

  *DTWELL 7

  ** Cycle No. 2  -  Soak


  *SHUTIN 'Well-14'   ** Shut in injector
  *SHUTIN 'Well-15'   ** Shut in injector
```

```
   *SHUTIN 'Well-16'   ** Shut in injector
   *SHUTIN 'Well-17'   ** Shut in injector
   *SHUTIN 'Well-18'   ** Shut in injector
   *SHUTIN 'Well-19'   ** Shut in injector
   *SHUTIN 'Well-20'   ** Shut in injector
   *SHUTIN 'Well-21'   ** Shut in injector
   *SHUTIN 'Well-22'   ** Shut in injector
OUTSRF GRID PRES

*TIME 3203
*TIME 3210

   *DTWELL 1

   ** Cycle No. 2  -  Production

   *OPEN 'Well-1'   ** Turn on producer
   *OPEN 'Well-2'   ** Turn on producer
   *OPEN 'Well-3'   ** Turn on producer
   *OPEN 'Well-4'   ** Turn on producer
   *OPEN 'Well-5'   ** Turn on producer
   *OPEN 'Well-6'   ** Turn on producer
   *OPEN 'Well-7'   ** Turn on producer
   *OPEN 'Well-8'   ** Turn on producer
   *OPEN 'Well-9'   ** Turn on producer
OUTSRF GRID PRES

*TIME 3430
*TIME 3530


   *DTWELL 2

  ** Cycle No. 3  -  Injection

   *SHUTIN 'Well-1'   ** Shut in PRODUCER
   *SHUTIN 'Well-2'   ** Shut in producer
   *SHUTIN 'Well-3'   ** Shut in producer
   *SHUTIN 'Well-4'   ** Shut in producer
   *SHUTIN 'Well-5'   ** Shut in producer
   *SHUTIN 'Well-6'   ** Shut in producer
   *SHUTIN 'Well-7'   ** Shut in producer
   *SHUTIN 'Well-8'   ** Shut in producer
   *SHUTIN 'Well-9'   ** Shut in producer

  *OPEN 'Well-14'   ** Turn on injector
  *OPEN 'Well-15'   ** Turn on injector
  *OPEN 'Well-16'   ** Turn on injector
  *OPEN 'Well-17'   ** Turn on injector
  *OPEN 'Well-18'   ** Turn on injector
  *OPEN 'Well-19'   ** Turn on injector
  *OPEN 'Well-20'   ** Turn on injector
  *OPEN 'Well-21'   ** Turn on injector
  *OPEN 'Well-22'   ** Turn on injector
OUTSRF GRID PRES
```

```
*TIME 3560


  *DTWELL 7

  ** Cycle No. 3  -  Soak

  *SHUTIN 'Well-14'   ** Shut in injector
  *SHUTIN 'Well-15'   ** Shut in injector
  *SHUTIN 'Well-16'   ** Shut in injector
  *SHUTIN 'Well-17'   ** Shut in injector
  *SHUTIN 'Well-18'   ** Shut in injector
  *SHUTIN 'Well-19'   ** Shut in injector
  *SHUTIN 'Well-20'   ** Shut in injector
  *SHUTIN 'Well-21'   ** Shut in injector
  *SHUTIN 'Well-22'   ** Shut in injector
OUTSRF GRID PRES

*TIME 3568
*TIME 3575

  *DTWELL 1

  ** Cycle No. 3  -  Production


  *OPEN 'Well-1'   ** Turn on producer
  *OPEN 'Well-2'   ** Turn on producer
  *OPEN 'Well-3'   ** Turn on producer
  *OPEN 'Well-4'   ** Turn on producer
  *OPEN 'Well-5'   ** Turn on producer
  *OPEN 'Well-6'   ** Turn on producer
  *OPEN 'Well-7'   ** Turn on producer
  *OPEN 'Well-8'   ** Turn on producer
  *OPEN 'Well-9'   ** Turn on producer
OUTSRF GRID PRES

*TIME 3795
*TIME 3895

  *DTWELL 2

 ** Cycle No. 4  -  Injection

  *SHUTIN 'Well-1'   ** Shut in PRODUCER
  *SHUTIN 'Well-2'   ** Shut in producer
  *SHUTIN 'Well-3'   ** Shut in producer
  *SHUTIN 'Well-4'   ** Shut in producer
  *SHUTIN 'Well-5'   ** Shut in producer
  *SHUTIN 'Well-6'   ** Shut in producer
  *SHUTIN 'Well-7'   ** Shut in producer
  *SHUTIN 'Well-8'   ** Shut in producer
  *SHUTIN 'Well-9'   ** Shut in producer

 *OPEN 'Well-14'   ** Turn on injector
```

```
 *OPEN 'Well-15'   ** Turn on injector
 *OPEN 'Well-16'   ** Turn on injector
 *OPEN 'Well-17'   ** Turn on injector
 *OPEN 'Well-18'   ** Turn on injector
 *OPEN 'Well-19'   ** Turn on injector
 *OPEN 'Well-20'   ** Turn on injector
 *OPEN 'Well-21'   ** Turn on injector
 *OPEN 'Well-22'   ** Turn on injector
OUTSRF GRID PRES


*TIME 3925

   *DTWELL 7

   ** Cycle No. 4  -  Soak

   *SHUTIN 'Well-14'   ** Shut in injector
   *SHUTIN 'Well-15'   ** Shut in injector
   *SHUTIN 'Well-16'   ** Shut in injector
   *SHUTIN 'Well-17'   ** Shut in injector
   *SHUTIN 'Well-18'   ** Shut in injector
   *SHUTIN 'Well-19'   ** Shut in injector
   *SHUTIN 'Well-20'   ** Shut in injector
   *SHUTIN 'Well-21'   ** Shut in injector
   *SHUTIN 'Well-22'   ** Shut in injector
OUTSRF GRID PRES

*TIME 3933
*TIME 3940

   *DTWELL 1

   ** Cycle No. 4  -  Production

   *OPEN 'Well-1'   ** Turn on producer
   *OPEN 'Well-2'   ** Turn on producer
   *OPEN 'Well-3'   ** Turn on producer
   *OPEN 'Well-4'   ** Turn on producer
   *OPEN 'Well-5'   ** Turn on producer
   *OPEN 'Well-6'   ** Turn on producer
   *OPEN 'Well-7'   ** Turn on producer
   *OPEN 'Well-8'   ** Turn on producer
   *OPEN 'Well-9'   ** Turn on producer
OUTSRF GRID PRES

*TIME 4160
*TIME 4260

   *DTWELL 2

  ** Cycle No. 5  -  Injection

   *SHUTIN 'Well-1'   ** Shut in PRODUCER
   *SHUTIN 'Well-2'   ** Shut in producer
   *SHUTIN 'Well-3'   ** Shut in producer
```

```
   *SHUTIN 'Well-4'   ** Shut in producer
   *SHUTIN 'Well-5'   ** Shut in producer
   *SHUTIN 'Well-6'   ** Shut in producer
   *SHUTIN 'Well-7'   ** Shut in producer
   *SHUTIN 'Well-8'   ** Shut in producer
   *SHUTIN 'Well-9'   ** Shut in producer

  *OPEN 'Well-14'   ** Turn on injector
  *OPEN 'Well-15'   ** Turn on injector
  *OPEN 'Well-16'   ** Turn on injector
  *OPEN 'Well-17'   ** Turn on injector
  *OPEN 'Well-18'   ** Turn on injector
  *OPEN 'Well-19'   ** Turn on injector
  *OPEN 'Well-20'   ** Turn on injector
  *OPEN 'Well-21'   ** Turn on injector
  *OPEN 'Well-22'   ** Turn on injector
OUTSRF GRID PRES


*TIME 4290

   *DTWELL 7

   ** Cycle No. 5  -  Soak

   *SHUTIN 'Well-14'   ** Shut in injector
   *SHUTIN 'Well-15'   ** Shut in injector
   *SHUTIN 'Well-16'   ** Shut in injector
   *SHUTIN 'Well-17'   ** Shut in injector
   *SHUTIN 'Well-18'   ** Shut in injector
   *SHUTIN 'Well-19'   ** Shut in injector
   *SHUTIN 'Well-20'   ** Shut in injector
   *SHUTIN 'Well-21'   ** Shut in injector
   *SHUTIN 'Well-22'   ** Shut in injector
OUTSRF GRID PRES

*TIME 4298
*TIME 4305

   *DTWELL 1

   ** Cycle No. 5  -  Production

   *OPEN 'Well-1'   ** Turn on producer
   *OPEN 'Well-2'   ** Turn on producer
   *OPEN 'Well-3'   ** Turn on producer
   *OPEN 'Well-4'   ** Turn on producer
   *OPEN 'Well-5'   ** Turn on producer
   *OPEN 'Well-6'   ** Turn on producer
   *OPEN 'Well-7'   ** Turn on producer
   *OPEN 'Well-8'   ** Turn on producer
   *OPEN 'Well-9'   ** Turn on producer
OUTSRF GRID PRES

*TIME 4525
*TIME 4625
```

```
   *DTWELL 2

  ** Cycle No. 6  -  Injection

   *SHUTIN 'Well-1'   ** Shut in PRODUCER
   *SHUTIN 'Well-2'   ** Shut in producer
   *SHUTIN 'Well-3'   ** Shut in producer
   *SHUTIN 'Well-4'   ** Shut in producer
   *SHUTIN 'Well-5'   ** Shut in producer
   *SHUTIN 'Well-6'   ** Shut in producer
   *SHUTIN 'Well-7'   ** Shut in producer
   *SHUTIN 'Well-8'   ** Shut in producer
   *SHUTIN 'Well-9'   ** Shut in producer


  *OPEN 'Well-14'   ** Turn on injector
  *OPEN 'Well-15'   ** Turn on injector
  *OPEN 'Well-16'   ** Turn on injector
  *OPEN 'Well-17'   ** Turn on injector
  *OPEN 'Well-18'   ** Turn on injector
  *OPEN 'Well-19'   ** Turn on injector
  *OPEN 'Well-20'   ** Turn on injector
  *OPEN 'Well-21'   ** Turn on injector
  *OPEN 'Well-22'   ** Turn on injector
OUTSRF GRID PRES

*TIME 4655


   *DTWELL 7

   ** Cycle No. 6  -  Soak

   *SHUTIN 'Well-14'   ** Shut in injector
   *SHUTIN 'Well-15'   ** Shut in injector
   *SHUTIN 'Well-16'   ** Shut in injector
   *SHUTIN 'Well-17'   ** Shut in injector
   *SHUTIN 'Well-18'   ** Shut in injector
   *SHUTIN 'Well-19'   ** Shut in injector
   *SHUTIN 'Well-20'   ** Shut in injector
   *SHUTIN 'Well-21'   ** Shut in injector
   *SHUTIN 'Well-22'   ** Shut in injector
OUTSRF GRID PRES

*TIME 4663
*TIME 4670

   *DTWELL 1

   ** Cycle No. 6  -  Production

   *OPEN 'Well-1'   ** Turn on producer
   *OPEN 'Well-2'   ** Turn on producer
   *OPEN 'Well-3'   ** Turn on producer
   *OPEN 'Well-4'   ** Turn on producer
```

```
   *OPEN 'Well-5'   ** Turn on producer
   *OPEN 'Well-6'   ** Turn on producer
   *OPEN 'Well-7'   ** Turn on producer
   *OPEN 'Well-8'   ** Turn on producer
   *OPEN 'Well-9'   ** Turn on producer
OUTSRF GRID PRES

*TIME 4890
*TIME 4990

   *DTWELL 2

   ** Cycle No. 7  -  Injection


   *SHUTIN 'Well-1'   ** Shut in PRODUCER
   *SHUTIN 'Well-2'   ** Shut in producer
   *SHUTIN 'Well-3'   ** Shut in producer
   *SHUTIN 'Well-4'   ** Shut in producer
   *SHUTIN 'Well-5'   ** Shut in producer
   *SHUTIN 'Well-6'   ** Shut in producer
   *SHUTIN 'Well-7'   ** Shut in producer
   *SHUTIN 'Well-8'   ** Shut in producer
   *SHUTIN 'Well-9'   ** Shut in producer

 *OPEN 'Well-14'   ** Turn on injector
 *OPEN 'Well-15'   ** Turn on injector
 *OPEN 'Well-16'   ** Turn on injector
 *OPEN 'Well-17'   ** Turn on injector
 *OPEN 'Well-18'   ** Turn on injector
 *OPEN 'Well-19'   ** Turn on injector
 *OPEN 'Well-20'   ** Turn on injector
 *OPEN 'Well-21'   ** Turn on injector
 *OPEN 'Well-22'   ** Turn on injector
OUTSRF GRID PRES


*TIME 5020

   *DTWELL 7

   ** Cycle No. 7  -  Soak


   *SHUTIN 'Well-14'   ** Shut in injector
   *SHUTIN 'Well-15'   ** Shut in injector
   *SHUTIN 'Well-16'   ** Shut in injector
   *SHUTIN 'Well-17'   ** Shut in injector
   *SHUTIN 'Well-18'   ** Shut in injector
   *SHUTIN 'Well-19'   ** Shut in injector
   *SHUTIN 'Well-20'   ** Shut in injector
   *SHUTIN 'Well-21'   ** Shut in injector
   *SHUTIN 'Well-22'   ** Shut in injector
OUTSRF GRID PRES

*TIME 5028
```

```
*TIME 5035

  *DTWELL 1

  ** Cycle No. 7  -  Production

  *OPEN 'Well-1'   ** Turn on producer
  *OPEN 'Well-2'   ** Turn on producer
  *OPEN 'Well-3'   ** Turn on producer
  *OPEN 'Well-4'   ** Turn on producer
  *OPEN 'Well-5'   ** Turn on producer
  *OPEN 'Well-6'   ** Turn on producer
  *OPEN 'Well-7'   ** Turn on producer
  *OPEN 'Well-8'   ** Turn on producer
  *OPEN 'Well-9'   ** Turn on producer
OUTSRF GRID PRES

*TIME 5255
*TIME 5355

  *DTWELL 2

  ** Cycle No. 8  -  Injection


  *SHUTIN 'Well-1'   ** Shut in PRODUCER
  *SHUTIN 'Well-2'   ** Shut in producer
  *SHUTIN 'Well-3'   ** Shut in producer
  *SHUTIN 'Well-4'   ** Shut in producer
  *SHUTIN 'Well-5'   ** Shut in producer
  *SHUTIN 'Well-6'   ** Shut in producer
  *SHUTIN 'Well-7'   ** Shut in producer
  *SHUTIN 'Well-8'   ** Shut in producer
  *SHUTIN 'Well-9'   ** Shut in producer

 *OPEN 'Well-14'   ** Turn on injector
 *OPEN 'Well-15'   ** Turn on injector
 *OPEN 'Well-16'   ** Turn on injector
 *OPEN 'Well-17'   ** Turn on injector
 *OPEN 'Well-18'   ** Turn on injector
 *OPEN 'Well-19'   ** Turn on injector
 *OPEN 'Well-20'   ** Turn on injector
 *OPEN 'Well-21'   ** Turn on injector
 *OPEN 'Well-22'   ** Turn on injector
OUTSRF GRID PRES


*TIME 5385

  *DTWELL 7

  ** Cycle No. 8  -  Soak

  *SHUTIN 'Well-14'   ** Shut in injector
  *SHUTIN 'Well-15'   ** Shut in injector
  *SHUTIN 'Well-16'   ** Shut in injector
```

```
   *SHUTIN 'Well-17'   ** Shut in injector
   *SHUTIN 'Well-18'   ** Shut in injector
   *SHUTIN 'Well-19'   ** Shut in injector
   *SHUTIN 'Well-20'   ** Shut in injector
   *SHUTIN 'Well-21'   ** Shut in injector
   *SHUTIN 'Well-22'   ** Shut in injector
OUTSRF GRID PRES

*TIME 5393
*TIME 5400

   *DTWELL 1

   ** Cycle No. 8  -  Production

   *OPEN 'Well-1'   ** Turn on producer
   *OPEN 'Well-2'   ** Turn on producer
   *OPEN 'Well-3'   ** Turn on producer
   *OPEN 'Well-4'   ** Turn on producer
   *OPEN 'Well-5'   ** Turn on producer
   *OPEN 'Well-6'   ** Turn on producer
   *OPEN 'Well-7'   ** Turn on producer
   *OPEN 'Well-8'   ** Turn on producer
   *OPEN 'Well-9'   ** Turn on producer
OUTSRF GRID PRES

*TIME 5620
*TIME 5720

   *DTWELL 2

  ** Cycle No. 9  -  Injection

   *SHUTIN 'Well-1'   ** Shut in PRODUCER
   *SHUTIN 'Well-2'   ** Shut in producer
   *SHUTIN 'Well-3'   ** Shut in producer
   *SHUTIN 'Well-4'   ** Shut in producer
   *SHUTIN 'Well-5'   ** Shut in producer
   *SHUTIN 'Well-6'   ** Shut in producer
   *SHUTIN 'Well-7'   ** Shut in producer
   *SHUTIN 'Well-8'   ** Shut in producer
   *SHUTIN 'Well-9'   ** Shut in producer

  *OPEN 'Well-14'   ** Turn on injector
  *OPEN 'Well-15'   ** Turn on injector
  *OPEN 'Well-16'   ** Turn on injector
  *OPEN 'Well-17'   ** Turn on injector
  *OPEN 'Well-18'   ** Turn on injector
  *OPEN 'Well-19'   ** Turn on injector
  *OPEN 'Well-20'   ** Turn on injector
  *OPEN 'Well-21'   ** Turn on injector
  *OPEN 'Well-22'   ** Turn on injector
OUTSRF GRID PRES


*TIME 5750
```

```
   *DTWELL 7

   ** Cycle No. 9  -  Soak


   *SHUTIN 'Well-14'   ** Shut in injector
   *SHUTIN 'Well-15'   ** Shut in injector
   *SHUTIN 'Well-16'   ** Shut in injector
   *SHUTIN 'Well-17'   ** Shut in injector
   *SHUTIN 'Well-18'   ** Shut in injector
   *SHUTIN 'Well-19'   ** Shut in injector
   *SHUTIN 'Well-20'   ** Shut in injector
   *SHUTIN 'Well-21'   ** Shut in injector
   *SHUTIN 'Well-22'   ** Shut in injector
OUTSRF GRID PRES

*TIME 5758
*TIME 5765

   *DTWELL 1

   ** Cycle No. 9  -  Production

   *OPEN 'Well-1'   ** Turn on producer
   *OPEN 'Well-2'   ** Turn on producer
   *OPEN 'Well-3'   ** Turn on producer
   *OPEN 'Well-4'   ** Turn on producer
   *OPEN 'Well-5'   ** Turn on producer
   *OPEN 'Well-6'   ** Turn on producer
   *OPEN 'Well-7'   ** Turn on producer
   *OPEN 'Well-8'   ** Turn on producer
   *OPEN 'Well-9'   ** Turn on producer
OUTSRF GRID PRES

*TIME 5985
*TIME 6085

               *OPEN 'Well-10'   ** Turn on injector
               *OPEN 'Well-11'   ** Turn on injector
               *OPEN 'Well-12'   ** Turn on injector
               *OPEN 'Well-13'   ** Turn on injector

*TIME 6585
*TIME 7585
*TIME 8585
*TIME 9735

   *SHUTIN 'Well-10'   ** Shut in injector
   *SHUTIN 'Well-11'   ** Shut in injector
   *SHUTIN 'Well-12'   ** Shut in injector
   *SHUTIN 'Well-13'   ** Shut in injector

               *OPEN 'Well-23'   ** Turn on injector
               *OPEN 'Well-24'   ** Turn on injector
               *OPEN 'Well-25'   ** Turn on injector
```

```
                *OPEN 'Well-26'   ** Turn on injector

*TIME 10377.5
*TIME 10877.5
*TIME 11377.5
*STOP                                                   *
```

References

(n.d.). Retrieved December 01, 2016, from https://www.sec.gov/Archives/edgar/data/34088/000095012311031215/d80379exv99.htm.

Briggs, P. J., Baron, P. R., Fulleylove, R. J., & Wright, M. S.: "Development of Heavy-Oil Reservoirs," Journal of Petroleum Technology, V. 40, pp.206-214. 1988.

Bryan, J. L., & Kantzas, A.: "Enhanced Heavy-Oil Recovery by Alkali-Surfactant Flooding," Paper SPE 110738 presented at Annual Technical Conference and Exhibition of the Society of the Petroleum Engineers, Anaheim, California, November 2007.

Butler, R. M.: "Some Recent Developments in SAGD," Journal of Canadian Petroleum Technology 40, No.1:18-22. 2001. PETSOC-01-01-DAS

Cinar, M.: "Kinetics of Crude Oil Combustion in Porous Media Interpreted Using Isoconversional Methods," Ph. D. Thesis, Stanford University, California, 2011.

Cristofari, J., Castanier, L. M., & Kovscek, A. R.: "Laboratory Investigation of the Effect of Solvent Injection on In-Situ Combustion," Society of Petroleum Engineers Journal 13, No.2, June 2008.

Das, S. K.: "Vapex: An Efficient Process for the Recovery of Heavy Oil and Bitumen," Society of Petroleum Engineers Journal 3, No.3, September 1998.

Farouq Ali, S.: "Non-Thermal Heavy Oil Recovery Methods," Paper SPE 5893 presented at the Rocky Mountain Regional Meeting of the Society of the Petroleum Engineers, Casper, Wyoming, May 1976.

Farouq Ali, S.M.: "Heavy Oil—evermore Mobile," Journal of Petroleum Science and Engineering 37, No.1–2 5–9, February 2003.

Hiraski, G. J.: "The Steam-Foam Process," Journal of Petroleum Technology, V. 41, pp.449-456. 1989.

Jiang, T., Jia, X., Zeng, F., & Gu, Y.: "A Novel Solvent Injection Technique for Enhanced Heavy Oil Recovery : Cyclic Production with Continuous Solvent Injection," Paper SPE 165455 presented at SPE Heavy Oil Conference, Calgary, Canada, June 2013.

JPT staff: “Cold Production of Heavy Oil,” Journal of Petroleum Technology, V. 49, pp.1125-1126. 1997.

Kaneko, F., Nakano, M., Imai, M., & Nishioka, I.: “How Heavy Gas Solvents Reduce Heavy Oil Viscosity?,” Paper SPE 165451 presented at SPE Heavy Oil Conference, Calgary, Canada, June 2013.

Karajgikar, A.: “Thermal Recovery of Heavy Oil Using Pressure Pulses of Injected Syngas,” MS. Thesis, University of Calgary, 2015.

Karimi G., Samimi A. K.: “In-Situ Combustion Process, One of IOR Methods Livening The Reservoirs,” NOIC-Research Institue of Petroleum Industry, 2010.

Lagasca, J.: “Alberta Grosmont Carbonates: The Next Frontier in Oilsands,” Course Notes, Stanford University, December 2012.

Lashgari, H. R.: “, Development of a Four-Phase Thermal-Chemical Reservoir Simulator for Heavy Oil,” PhD Dissertation, University of Texas at Austin, December 2014.

Li, K.: “The Effects of Oil on CO2 Foam Flooding under Miscible Conditions,” MS. Thesis, Delft University of Technology, 2016.

Liu, Q., M. Dong, Ma, S.: “Alkaline/Surfactant Flood Potential in Western Canadian Heavy Oil Reservoirs,” SPE-Paper 99791-MS. SPE/DOE Symposium on Improved Oil Recovery, Tulsa, Oklahoma, USA, April 22-26, 2006.

Ma, K.: "Transport of Surfactant and Foam in Porous Media for Enhanced Oil Recovery Processes," PhD dissertation, Rice University, September 2013.

Ma, K., Lopez-Salinas, J. L., Biswal, S. L., & Hirasaki, G. J.: “Estimation of parameters for simulation of steady state,” presented at Conference, Wyoming, USA, February 2012.

Mai, A., and Kantzas, A.: “Heavy Oil Water flooding: Effects of Flow Rate and Oil Viscosity,” Journal of Canadian Petroleum Technology 48, No. 3, March 2009.

Memon, A., Gao, J., Taylor, S., Engel, T., and Jia N.: “A Systematic Workflow Process for Heavy Oil Characterization: Experimental Techniques and Challenges,” Society of Petroleum Engineers, 2010.

Naeem, W.: “Modeling Sand Production and Wormhole Growth using Pressure and Stress Continuity at Wormhole Tip,” Course Notes, University of Calgary.

Nasr, T., and Ayodele, O.: “Thermal Techniques for the Recovery of Heavy Oil and Bitumen,” Society of Petroleum Engineers, 2005.

Nasr, T. N., Beaulieu, G., Golbeck, H., & Heck, G.: “Of Steam and Solvent,” Society of Petroleum Engineers, 2001.

Patzek, T.W., Koinis, M.T.: “Kern River Steam-Foam Pilots,” Journal of Petroleum Technology 42, No.4: 496 – 503, 1990. SPE-17380.

Patzek, T.W., Myhill, N.A.: “Simulation of the Bishop Steam Foam Pilot,” Paper SPE-18786, California Regional Meeting, Bakersfield, California, April 5-7, 1989.

Pitts, M. J., Wyatt, K., & Surkalo, H.: “Alkaline-Polymer Flooding of the David Pool, Lloydminster Alberta,” SPE-Paper 89386-MS. SPE/DOE Symposium on Improved Oil Recovery, Tulsa, Oklahoma, USA, April 17-21, 2004.

Pope, G.A., Nelson, R.C.: “A Chemical Flooding Compositional Simulator,” Society of Petroleum Engineers Journal 18(05): 339 – 354, 1978. SPE-6725-PA

Prats,M.: “A Current Appraisal of Thermal Recovery,” Journal of Petroleum Technology. 30(08):1129-1136. SPE-7044, 1978.

National Research Council: "Induced Seismicity Potential in Energy Technologies," Washington, USA, 2013.

Sarathi, P. S., Olsen, D. K.: “Practical Aspects of Steam Injection Processes,” A Handbook For Independent Operators, Bartlesville, Oklohama, 1992.

Sawatzky, R. P., Lillico, D. A., London, M. J., Tremblay, B. R., & Coates, R. M.: “Tracking Cold Production Footprints,” Paper- PETSOC-2002-086. Canadian International Petroleum Conference, Calgary, Alberta, Canada, 11-13 June, 2002.

Szasz, E.: “Oil recovery by thermal methods,” Paper presented at World Petroleum Congress, Frankfurt, Germany, 1963.

Taghavifar, M., Fortenberry R.P., DeRouffignac E., Sepehrnoori, K., Pope, G.A., “Hybrid Thermal-Chemical Processes (HTCP) for Heavy-Oil and Oil-Sand Recovery” Paper SPE 170161. SPE Heavy Oil Conference-Canada, 10-12 June, Alberta, Canada, 2014

Thomas, S., Farouq Ali, S., Scoular, J., and Verkoczy, B.: “Chemical Methods for Heavy Oil Recovery," Journal of Canadian Petroleum Technology 40, No. 3, March 2001.

Wang, J., Dong, M.: “Simulation of O/W Emulsion Flow in Alkaline/Surfactant Flood for Heavy Oil Recovery,” SPE Paper- PETSOC-2009-066. Canadian International Petroleum Conference, Calgary, Alberta, Canada, June 16-18, 2009.

Zerkalov, G.: “Steam Injection for Enhanced Oil Recovery,” Course Notes, Stanford University, December 2015.

Zhong, L., Szecsody, J. E., Zhang, F., & Mattigod, S. V.: “Foam Delivery of Amendments for Vadose Zone Remediation: Propagation Performance in Unsaturated Sediments,” Vadose Zone Journal 9, No. 3, August 2010.